Analysis and degradation mechanisms of enamels, *grisailles* and silver stains on *modernist* stained glass

Martí Beltrán, November 2020

Directed by:

Dr. Trinitat Pradell

Departament de Física
Programa de Doctorat en Física Computacional i Aplicada

Analysis and degradation mechanisms of enamels, *grisailles* and silver stains on *modernist* stained glass

Martí Beltrán González

Directed by

Trinitat Pradell Cara

A thesis presented for the degree of Doctor at the

Universitat Politècnica de Catalunya

Barcelona, November 2020

Acknowledgements

I want to acknowledgment my thesis director, Dr. Trinitat Pradell, for her patience, efforts and guidance in the development of this work. I'm profoundly indebted for her invaluable help and for the opportunity to do this research in the characterization of materials group. I also want to extend my grateful to all the members of the Physics department, which have help so many times on the course of the thesis. Especially thanks to Drs. Daniel Crespo, Eloi Pineda and Glòria Molina, who introduced me to the ancient materials research group.

I'm grateful to all the J.M. Bonet Vitralls S.L. team of work, and particularly to Jordi Bonet, who kindly supplied all the materials from the *Rigalt, Granell & cia* workshop as well as historic enameled glasses, so many pictures and explanations about the origin of the different samples.

I want to give special thanks to Drs. Nati Salvadó, Salvador Butí and Victòria Beltran for its advice on the FTIR measurements at the beginning of the research. Special thanks are also given to Drs. Maite Garcia Vallès and Mariona Tarragó for their help with the HSM measurements and the preparation of synthetic glasses. I'm also indebt with Drs. Andrew Shortland and Fiona Brock at Cranfield Forensic Institute, and also to Drs. Nadine Schibille and Bernard Gratuze at Institut de Recherche sur les Archéomatériaux Centre Enert Babelon CNRS; for their advice with LA-ICP-MS measurements. I'm also so grateful to the Alba staff, and especially to Oriol Vallcorba, for the collaboration with the SR-μ-XRD measurements performed at BM4-MSPD beamline at Alba synchrotron facility. The project was made with the funds received from Ministerio de Ciencia e Innovación (Spain) project MAT2016-N0748719-R and Generalitat de Catalunya project 2017 SGR 00042.

Finally, I want to express my gratefulness to my parents, family, friends, and especially to my partner Aina Martín, for its patience with all this amounts of work and tension moments and for all its love.

Abstract

Materials and methods used in the production of *modernist* (late 19th and early 20th century) stained glass from the city of Barcelona with special regards to the degradation mechanisms of enamels, *grisailles* and silver stains have been studied. Coloured enamels from the raw materials used in the *Rigalt, Granell & cia* modernist workshops from Barcelona were produced and compared to those found in the buildings and belonging to the private collection of J.M. Bonet workshop to explore the reason for the reduced stability of the blue and green enamels. The chemical composition has been determined (and pigments identified) by means of Laser Ablation Inductively-Coupled Plasma Mass Spectrometry (LA-ICP-MS), X-Ray Diffraction (XRD) and UV-Vis-NIR spectroscopy, and the thermal properties of the enamels measured by Differential Scanning Calorimetry (DSC) and Hot Stage Microscopy (HSM). The enamels are made of a lead-zinc borosilicate glass characterised by its low sintering temperatures and high stability against chemical corrosion, in particular to water corrosion. However, the relatively narrow range of firing temperatures necessary for correct adherence of the enamels to the contemporary glass base may have required the addition of a high lead borosilicate flux, which would have increased the lead content of the enamel, decreasing the firing temperature but also its stability. The historical enamels show a lead, boron and zinc depleted silica rich amorphous glass, with precipitated lead and calcium sulphates or carbonates, characteristic of extensive atmospheric corrosion. The blue and green enamels show a heterogeneous layered microstructure more prone to degradation which is augmented by a greater heating and thermal stress affectation produced by the enhanced Infrared absorbance of blue tetrahedral cobalt colour centres and copper ions dissolved in the glass and, in particular, of the cobalt spinel particles.

Keywords: lead zinc borosilicate glass, colourant, pigments, microstructure, Modernist enamels, chemical stability, softening temperature, atmospheric corrosion

Resum

S'han estudiat els materials i mètodes utilitzats en la producció dels vitralls modernistes (finals del segle XIX i començaments del segle XX) de la ciutat de Barcelona, especialment en relació als mecanismes de degradació d'esmalts, grisalles i grocs de plata. S'han produït i estudiat els esmalts de color a partir de les matèries primeres utilitzades pel taller *Rigalt, Granell & cia* de Barcelona, per comparar amb mostres originals pertanyents a la col·lecció privada del taller J.M. Bonet vitralls per així estudiar la raó de la reduïda estabilitat dels esmalts blaus i verds. La composició química i els pigments han estat identificats per LA-ICP-MS, espectroscòpia d'UV-Vis-NIR i XRD, i les propietats tèrmiques dels esmalts han estat mesurades amb DSC i HSM. Els esmalts són vidres borosilicats de plom i zinc caracteritzats per baixes temperatures de sinterització i una gran estabilitat contra la corrosió química, especialment respecte a la corrosió de l'aigua. No obstant, el relativament estret marge de temperatures necessari per una correcta adherència dels esmalts al vidre base de l'època podria haver requerit l'addició d'un fundent amb un alt tant per cent de plom i bor, que podria haver augmentat la proporció de plom a l'esmalt disminuint la temperatura de treball juntament amb la seva estabilitat. Els esmalts històrics presenten una composició alterada a on plom, bor i zinc han disminuït en front a un augment de la proporció de silici a la fase vítria, amb l'aparició de precipitats de sulfats o carbonats de plom i calci, característics de l'efecte de la corrosió atmosfèrica. Els esmalts blaus i verds presenten una microestructura en capes heterogènies que són més susceptibles a la degradació, la qual augmenta degut a la calor i l'estrès tèrmic respecte al vidre base que provoca una major absorbància a la regió de l'infraroig proper deguda a la presència d'estructures tetraèdriques dels ions de cobalt i coure dissoltes a la fase vítria, i en particular de les partícules d'espinel·les de cobalt.

Paraules clau: vidre borosilicat de plom i zinc, colorants, pigments, microestructura, esmalts modernistes, estabilitat química, temperatures d'estovament, corrosió atmosfèrica.

Resumen

Se han estudiado los materiales y métodos utilizados en la producción de los vitrales modernistas (finales del siglo XIX y principios del siglo XX) de la ciudad de Barcelona, especialmente en relación a los mecanismos de degradación de esmaltes, grisallas y amarillos de plata. Se han producido y estudiado los esmaltes de color a partir de las materias primas utilizadas por el taller *Rigalt, Granell & cia* de Barcelona, para luego comparar con muestras originales de la colección privada del taller J.M. Bonet vitralls y así estudiar la razón de la reducida estabilidad de los esmaltes azules y verdes. La composición química y los pigmentos han sido identificados por LA-ICP-MS, espectroscopía UV-Vis-NIR, y las propiedades térmicas de los esmaltes han sido medidas con DSC y HSM. Los esmaltes son vidrios borosilicatos de plomo y zinc caracterizados por bajas temperaturas de sinterizado y una gran estabilidad contra la corrosión química, especialmente contra la corrosión del agua. No obstante, el relativamente estrecho margen de temperaturas necesario para una correcta adherencia de los esmaltes al vidrio base de la época podría haber requerido la adición de un fundente con un alto tanto por ciento de plomo y boro, que podría haber aumentado la proporción de plomo en el esmalte disminuyendo la temperatura de trabajo junto con su estabilidad. Los esmaltes históricos presentan una composición alterada donde plomo, boro y zinc han disminuido a favor de un aumento de la proporción de silicio en la fase vítrea, con la aparición de precipitados de sulfatos o carbonatos de plomo y calcio, característicos del efecto de la corrosión atmosférica. Los esmaltes azules y verdes presentan una microestructura en capas heterogéneas que es mas susceptible a la degradación, que aumenta debido a la temperatura y al estrés térmico respecto al vidrio base que provoca una mayor absorbancia en la región del infrarrojo cercano debido a la presencia de estructuras tetraédricas de los iones de cobalto y cobre disueltos en la fase vítrea, así como a la presencia de partículas de espinelas de cobalto.

Palabras clave: vidrio borosilicato de plomo y zinc, colorantes, pigmentos, microestructura, esmaltes modernistas, estabilidad química, temperaturas de reblandecimiento, corrosión atmosférica.

Contents

List of Figures

Figures:

Chapter 2:

Chapter 3:

Chapter 4:

List of Tables

Tables:

The following papers have been published as a result of this work:

Papers in International Journals:

M. Beltrán, F. Brock, T. Pradell, Thermal properties and stability of Catalan Modernist blue and green enamels, Int. J. Appl. Glass Sci. 10 (2019) 414–425.
DOI: 10.1111/ijag.13098

M. Beltrán, N. Schibille, F. Brock, B. Gratuze, O. Vallcorba, T. Pradell, Modernist enamels: Composition, microstructure and stability, J. Europ. Ceram. Soc. 40 (2020) 1753-1766.
DOI:/10.1016/j.jeurceramsoc.2019.11.038

M. Beltrán, N. Schibille, B. Gratuze, O. Vallcorba, J. Bonet, T. Pradell, Composition, microstructure and corrosion mechanisms of Catalan Modernist enamelled glass, J. Europ. Ceram. Soc. (in press)
DOI: 10.1016/j.jeurceramsoc.2020.10.041

Conference Proceedings:

M. Beltran, J. Bonet, T. Pradell, Enamel Deterioration: The Thermal Properties of the modernist enamels and stain glasses from the city of Barcelona. Art at the Surface. Creation, Recognition, Conservation. Transactions of the 10th forum for the conservation and Technology on Stained Glass. Ed. S Brown, C Loiset, A Rabaut, I Rauch, S Strobl and S Wolf, ISCCSG, Press Green York (2017) 102-112.
ISBN: 1527212319 9781527212312. ISBN-13: 978-1527212312

M. Beltrán, J. Bonet, T. Pradell, The Thermal Properties of the modernist enamels and stain glasses rom the city of Barcelona. Proceedings of the 5th GLASSAC International Conference ed. I Coutinho, T. Palomar, S. Coentro, A Machado and M. Vilarigues, NOVA FCT Lisboa (2017) 26-28.
https://eventos.fct.unl.pt/glassac2017/files/actas_glassac.pdf

Results have also been presented in the following international conferences:

Poster “Thermal properties of the modernist enamels and stain glasses from the city of Barcelona” on 5th GLASSAC International Conference, Lisbon, 2017.

Oral “Propiedades térmicas y estabilidad de los esmaltes modernistas catalanes verdes y azules” in V Congreso Hispano-Luso de Cerámica y Vidrio y LVI Congreso de la SECV, Barcelona, 2018.

Poster “Colour Enamels in the Modernist Catalan stained glasses from Barcelona” in IX AUSE Conference and 4th ALBA User’s Meeting, Cerdanyola, 2019

Oral “Colour Enamels in the Modernist Catalan stained glasses from Barcelona” in Cultural and Natural Heritage Workshop, ESRF-EBS, Grenoble, 22-24 January 2020.

Chapter 1

Introduction

Chapter 1

Introduction

A stained glass panel is made of small pieces of coloured glass which are held together by strips of lead and arranged to form patterns and pictures. It was initially used to cover windows, mainly of churches and religious and official buildings, but later to decorate house windows, skylights, indoors panels and even produce three-dimensional objects. Painted designs of transparent and translucent enamels (thin colour glass layer fired to be fixed over a transparent substrate glass), *grisailles* (iron oxide based dark opaque paint used to draw contour lines and produce the effect of volumes and shadows), *carnations* (iron oxide based reddish partly opaque paint used to imitate flesh) and silver stains (metallic silver nanoparticles diffused in the glass surface) were also widely used to facilitate the recreation of paintings.

The object of the thesis is the study of the materials, painting and firing techniques used as well as the alterations shown by the enamelled glass produced during the *Modernist* period. This chapter is devoted to summarise the stained glass historical background (section 1.1), the *Modernist* movement and workshops in Barcelona (section 1.2), the materials used for the production of stained glass and the innovations introduced in the *Modernist* period (section 1.3), the state of preservation of the *Modernist* stained glass (section 1.4), finishing with a summary of the objectives and milestones of this thesis (section 1.5).

1.1. Historical background

Stained glass was first produced during the Romanesque period in France (earliest remaining stained glass windows date back to the 11th century), although some archaeological evidences, the Ravena fragments, set its origins back to the 6th century. However, it is not until the Gothic period, a style which included large windows to maximise light into the church, that stained glass had its period of splendour. The Abbot Suger was one of the most decisive figures for the development of the Gothic art. On his

account, the 1140's restoration of the Abbey Church of Saint Denis provided one of the first depictions of stained glass, incorporating allegorical figures in the panels (**Fig. 1.1**), creating images changing the colour of the light and "*Una quarum de materialibus ad immaterialia exitans*" (urging us onward from the material to the immaterial) [1]. Biblical scenes and artist paintings were cut in glass and mounted in large window panels between the 12th and the 16th century. At the end the 16th century, the Protestant movements active in central Europe generated a decay of the religious demand. At the beginning of the 17th century, the development of the Baroque style suppressed stained glass from the churches. Nevertheless, stained glass continued decorating private houses and official buildings but without the splendour of the Gothic period until the great emergence of the decorative arts at the end of the 19th century.

Fig. 1.1. Stained glass (c. 1140) Christ between Ecclesia and Synagogue, Anagogical window, chapel of Saint Peregrine, Basilica of Saint Denis, Paris, France. Pict.: Vassil-wikicommons.

The period between 1880-1920 was characterised by the emergence of decorative and fine arts. Originality and artistic value were identity signs of this movement [2] which extended all over Europe and America. This new style, linked to the emergence of the decorative arts was called *Art Nouveau* in France, *Modern style* in the British islands,

Jugendstil in Germany, *Sezessionsstil* in Austria, *Stile Liberty* in Italy, *Tyffany style* in the United States and was named *Modernisme* in Catalonia [3-4]. The movement was particularly innovative and extremely important for the creation of the Catalan identity at the end of the century with figures of international value such as the architect Antoni Gaudí. The movement had an early reference in the Arts and Crafts movement by the writer and designer William Morris, who set the ground to the revaluation of the manual arts opposite to the industrial revolution. William Morris influence in the *Art Nouveau* was important as a source of inspiration for the Catalan designers [3].

Modernisme[1] (ca.1885-1920) was a universal style reflected in the architecture, sculpture, painting, literature, music, furniture and all the decorative arts. A new urban project for the expansion of the city of Barcelona designed by Ildefons Cerdà i Sunyer and known as *Eixample de Barcelona* was approved in 1859 providing a great landscape for architects and artists. New churches, palaces, mansions and private houses designed by the most recognised architects as Lluís Domènech i Montaner, Josep Puig i Cadafalch or Antoni Gaudí i Cornet are examples of some of the most spectacular buildings of this time (**Fig. 1.2**).

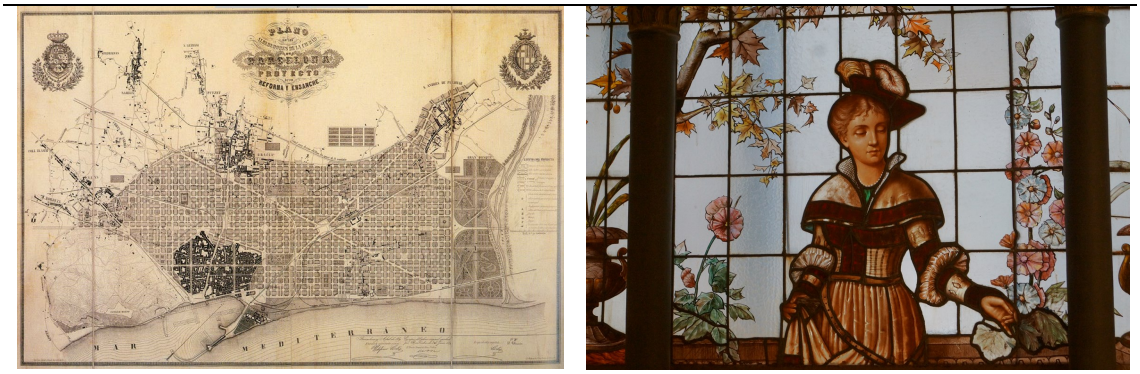

Fig 1.2. (**Left**) The original design of the *Barcelona Eixample* by Ildefons Cerdà. Pict.: Ildefons Cerdà i Sunyer, Eixample Project, Barcelona: Museu d'Història de la Ciutat, 1859.

(**Right**) A modernist stained glass panel located in a private house from *Eixample* made by *Rigalt i Granell*. Pict.: J.M. Bonet workshop.

The *Modernist* artists were strongly influenced by the beauty of the large medieval and renaissance stained glasses that decorate the walls of some of the most important churches

[1] In advance we will use the term *Modernism* or *modernist* in reference to the *Modernisme*.

[2]. Under its inspiration artists in collaboration with stained glass makers worked together to recreate the techniques of the past designing some of the most beautiful works of art of the period. Stained glasses were an important part of the aesthetics of the *Modernisme* and almost every house had its windows decorated. In the period between 1885 and 1920, thousands of enamelled windows, skylights and panels of doors, lifts and folding screens were produced in the glass workshops of Barcelona [2-3]. The new style combined the use of glasses either coloured or transparent of different textures including blown, rolled and moulded glass, which was flashed, coloured and stained. Transparent and translucent enamels, *grisailles*, *carnations* and silver stains were also quite extensively used to boost the artistic expression. Due to the high demand, numerous workshops for stained glass production established in the city of Barcelona, and are responsible for a rich heritage that today is preserved in museums, churches and private houses.

The stained glass produced during the *Modernist* period in Catalonia, and in particular in the city of Barcelona is object of this study. The quantity and quality of the stained glass produced in the city is beyond doubt. However, after a hundred years, it has suffered from neglect and destruction due to accidents, distastefulness and wars. In the last four or five decades, aesthetic appreciation and valorisation of *Modernisme* has boosted up the documentation and restauration of this magnificent collection of stained glass. This study is framed within a long-term research project carried out by scholars, glazier workshops and scientist in order to avoid more destruction and preserve the city cultural Heritage.

1.2. *Modernist* Catalan stained glass workshops

Stained glasses in Catalonia boosted in the last years of the 19th Century, in a context of economical flourishment and expansion of the city, in a similar way to what happened throughout the whole European continent and the United States during the period known as the *Belle Époque*. The new materials discovered and commercialised by many companies of the time, among which we have to highlight the French company *Lacroix* [3], and the techniques developed by the *Modernist* stained glass workshops were of great importance in the creation of a new aesthetics. The article published in l'*Art Décorative* about the stained glasses exhibited in the 1900 Universal Exhibition of Paris gives a

sample of this movement and the artists that were working to decorate the new buildings with stained glass [4].

Unfortunately, the art history literature on the 19th and 20th century Catalan stained glasses is not so abundant. A few volumes are dedicated to the *Modernist* stained glass; among which two classical books: *Vidrieras de un gran jardín de vidrios* by Manuel García-Martín [5] and *Els Vitrallers de la Barcelona Modernista* by Joan Vila-Grau and Francesc Rodon [3]. Some general history books with some chapters and excerpts dedicated to *Modernist* artists give also some details about stained glass. Information can also be found in the catalogues of *Modernist* Art exhibitions and some releases regarding restoration of some art works [2,6].

Most importantly, Nuria Gil Farré, a researcher on the art history of stained glass has published several works on the subject, among which we have to highlight her PhD these *El taller de vitralls modernista Rigalt, Granell & cia. (1890-1931)*, dedicated to the history and works of the *Rigalt & Granell* workshop, and which includes also information about some contemporary stained glass workshops [7]. As in this thesis we will be studying stained glasses from some of the most important workshops from the period in Barcelona, most of the historical information has been obtained from her work.

Fig. 1.3. (**Left**) 1911 picture of *Palau de Justicia de Barcelona* designed by the architect Enric Sagnier-Domenech Estapà. Pict.: AA.VV., Sagnier. Arquitecte, Barcelona 1858-1931, Barcelona: Ed. Antonio Sagnier, 2007.

(**Right**) The stained glass skylight made by *Rigalt, Granell & cia* workshop. Pict.: J.M. Bonet workshop.

One of the most important stained glass workshops active in the period in Barcelona was *Rigalt, Granell & cia* located in the 46, Enric Granados St. in Barcelona. *Rigalt, Granell & cia* was founded in 1890 by Antoni Rigalt i Blanch (1850-1914) and Jeroni F. Granell i Manresa (1868-1931), its name changed to *Granell & cia* in 1923 and continued active until 1931. They produced some of the most important pieces of stained glass of the *modernist* style such as those installed at the *Palau de la Música Catalana*, *Lleó Morera* house, *Palau de Justícia (High court Palace)* (**Fig. 1.3**) and *Seu del Districte de Sants-Montjuic (Town hall of Sants-Montjuic district)*, all of them located in Barcelona. At the end of the nineteenth century, Antoni Rigalt was probably at the forefront of the technical and aesthetic renovation of Catalan stained glass and was almost the only one who wrote his thoughts regarding materials, conservation and craftmanship. Before closing the company, the materials were acquired by *J.M. Bonet Vitralls S.L.*, a company dedicated since 1923 to the production and restoration of stained glass [7].

Texts wrote by A. Rigalt give some insights to the workshop techniques and the materials used. One of the most interesting texts is a dissertation wrote in 1897 and entitled *Presentación de algunas muestras de vidrieras de color y explicación de los procedimientos seguidos para pintar y construir las mismas, desde la aplicación de este arte hasta nuestros días, por el académico numerario D. Antonio Rigalt*. The discourse discusses the procedures for making stained glass, among them it highlights the importance of applying enamel and *grisaille* on the same side of the glass, in the same way that the Dutch workshops did and contrarily to the French workshops, with the aim to obtain better artistic results avoiding the misfit between the coloured areas and the contour designs. The text gives also some recipes for the making of different colour enamels, and which are more or less coincident with the formulations developed by *Lacroix* [3].

The *Rigalt, Granell & cia.* workshop was also indebted to instruct some of the new glazier masters of the period, such as, Antoni Bordalba (?-1925) who founded in 1901 *Casa Bordalba* together with Lluís Buxeres and Antoni Codorniu. Antoni Bordalba worked in some important commissions and has been only briefly studied by art historians [7,8]. He is the author of the stained glasses located at *Cercle del Liceu* private club, probably his most important work, and at some private houses of Barcelona, such as, the residence of the Francesc Burés i Borràs family (**Fig. 1.4**) built in 1900 by the architect Francesc Berenguer i Mestres. In 1905 *Buxeres i Codorniu* was founded from a scission of *casa*

Bordalba, and in collaboration with Joan Busquet made some important stained glass panels for the *Exposición Internacional de Barcelona* of 1907.

The *Amigó* workshop was one of the most important *pre-modernist* and *modernist* stained glass workshops from Barcelona. The studio was created by Eudald Ramón Nonat Amigó i Dou (1818-85) and introduced many technical innovations. The workshop was very prolific during the second half of the 19th century with important works, among which we can highlight the stained glasses of the city parishes *Santa Maria del Mar*, *Santa Maria del Pi* or the cathedral of Barcelona. This studio has often been mentioned for the weakness and instability of the paints (enamels and *grisailles*). The workshop changed its commercial name several times and during the last years of the 19th century was known as *Hijos de Eudaldo Ramon Amigó* which closed in 1920; afterwards, the workshop continued under the name *Artes del Vidrio A. Oriach* [7,9].

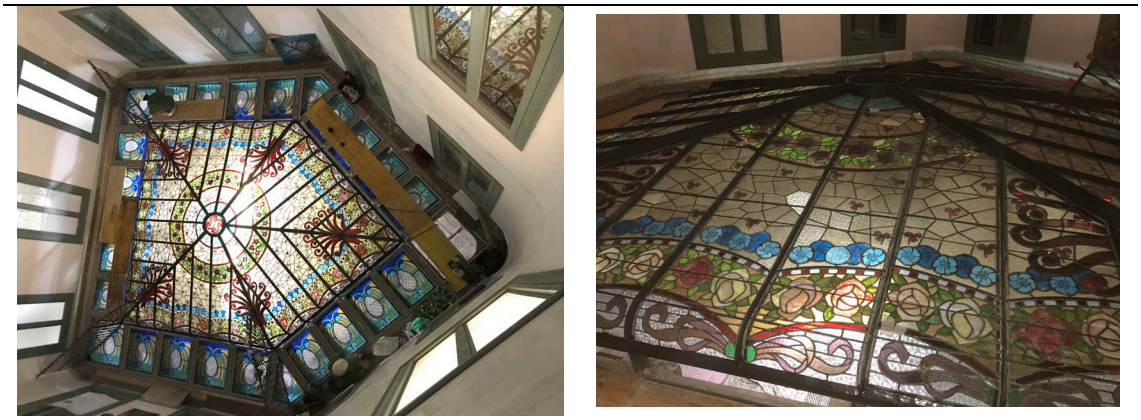

Fig 1.4. Stained glass skylight from the *Burés* family house made by *Casa Bordalba* workshop. Pict.: J.M. Bonet workshop.

The *Maumejean* workshop was founded in 1860 by the stained glass maker Jules Pierre Maumejean in the French village of Pau. The workshop was projected as an industry and soon started to open workshops at different cities among which, Madrid, Paris, San Sebastián or Barcelona. The Barcelona *Maumejean* stained glass workshop was located at number 120 Rambla de Catalunya and opened its doors in 1907. Designed as an industry, the stained glasses from the *Maumejean* had a solid technical background. Some of its most important works in Catalonia were the stained glasses of the *Caixa d'Estalvis de Sabadell* (1909), projected by the architect Jeroni Martorell i Terrats and the stairway

at the *Casa Pérez Samanillo* (1910) located in Barcelona and designed by the architect Joan Josep Hervàs [7,10].

Ludwig Dietrich von Bearn (1860-1935) was an Alsatian stained glass maker established in Barcelona in 1900 [7] and who founded a dynasty of glaziers. Little information is kept about him, apart from the fact that he is the author of one of the most iconic *modernist* stained glass assemblage in Catalonia, *Les Dames de Cerdanyola* (**Fig. 1.5**), conserved in the *Museu de Cerdanyola* [3].

The demand of stained glass was not only satisfied by the local companies, as sometimes private customers ordered glass panels to foreign glazier studios. Among them we should highlight the *pre-modernist Bazin-Latteux*'s atelier. The *Bazin-Latteux* workshop was located at Mesnil-Saint-Firmin (Oise), on the French Picardie region. The company was founded on 1845 by Gabriel Boniface Bazin (1791-1862) as a painting on glass (*peinture sur verre*) atelier. The sons of G. B. Bazin associate with Ludovic Latteux in 1865 and established the *Bazin frères et Latteux* company. In the following years the company is changing its name several times being *Bazin et Latteux* the most common denomination found on the panels. The atelier employed over 60 persons in 1878 and exported a large amount of its production. During the last active years, the

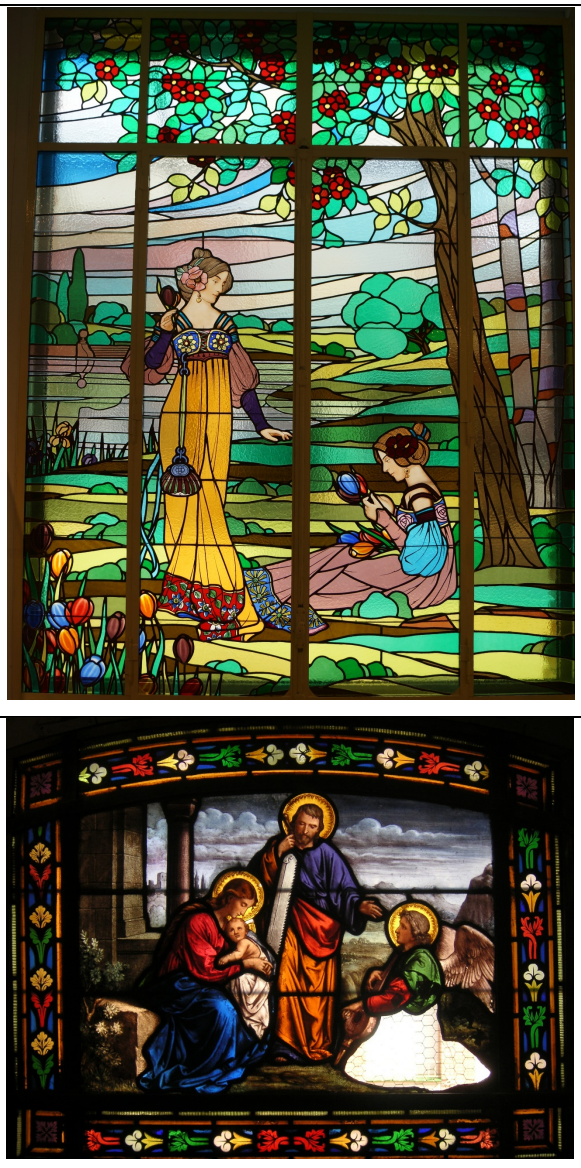

Fig. 1.5. (**top**) a panel from *Les Dames de Cerdanyola* Kept in the *Museu de Cerdanyola* by *Dietrich*. (**bottom**) a panel from the *Acadèmia Mariana de Lleida* by the pre-modernist *Bazin et Latteux* workshop. Pict.: J.M. Bonet workshop.

workshop was owned by L. Latteux and his wife, before it was closed in 1906 [11,12]. The company made the stained glass windows from the *Acadèmia Mariana de Lleida,* designed in 1871 by the architect Pere A. Peña upon the medieval foundation of a 13th century Mercedarian convent (**Fig. 1.5**). This assemblage of stained glass windows is considered *pre-Modernist*.

In the second decade of the 20th century an artistic movement called *Noucentisme* appears as a reaction to *Modernisme*. Consequently, the stained glass makers had to adequate their artistic language to the new aesthetics. New workshops were created, among them *Rigalt, Bulbena & cia*. The workshop was funded in 1923 by Lluís Rigalt i Corbella, son of Antoni Rigalt in association with Ramon Bulbena. Lluís Rigalt studied at the *Escola Llotja de Belles Arts de Barcelona* while training at his father's stained glass workshop. They made stained glasses for important buildings of the city such as *Generalitat de Catalunya* or the *Bishops Palace of Barcelona* [7].

1.3. The Materials

The scientific revolution of the 18th and 19th centuries was responsible for the discovery of new materials and methods of production. In particular, new glass types, colourants and pigments and a new type of enamels and paintings ready-to-be-used were developed and sold in Europe and America. In this section, a summary of the materials used for the production of stained glass through history, including transparent glass, coloured glass, enamels, silver stains and *grisailles* is presented with special attention to the innovations introduced in the *Modernist* period.

1.3.1. Transparent substrate glass

The use of flat transparent glass panels to cover windows and skylights dates back to the first century AD when the Romans began to use clear glass for architectural purposes. However, it is not until the 12th century, when it started to be widely used associated to church buildings during the Gothic period, an architectural style that was characterised by large openings for windows to maximise light. This increase in glass demand is linked to a change in glass-making technology in northern Europe, with a change in raw materials from the classical Mediterranean soda-rich natron or plant ashes glass to potash-rich glass obtained from local wood or fern ashes, known as *forest glass*. *Forest glass* is

characterised by high potassium (as high as 20 %K_2O) and calcium (between 10-25 %CaO), relatively low silica, and moderate concentrations of sodium, magnesium, phosphorus, manganese, aluminium and iron oxides [13]. Allowing for regional variations in the composition and depending on the local resources (high or low MgO and P_2O_5), forest glass continued being used until the first half of the 15th century when a new technological development resulted in a change in composition into a high lime-low alkali glass (HLLA) [13-14]. HLLA glass is characterised by a high lime (~22 %CaO) and low alkali content (~ 4-8 %K_2O, ~ 3 %Na_2O) [14]. The next important change in the glass composition does not happen until the 18th century with the beginning of the industrial revolution [14].

One of the main problems of producing a clear glass is the use of natural materials (sand and plant ashes) which may contain impurities, in particular the most common and abundant is iron oxide. In order to counteract the colour given to the glass by the presence of reduced iron oxide (characteristic deep green colour), oxidising agents were incorporated (manganese oxide, arsenic oxide, antimony oxide, etc..). Still, oxidised iron gives a light yellowish tinge to the glass. The only way to avoid this colouring effect is to remove the impurities. Traditionally this was made by washing the plant ashes to prepare the alkali salts, eliminating the fine clay fraction, using large quartz pebbles instead of fine sand, etc… (the Antonio Neri's treatise *L'Arte Vetraria* published on 1612). However, the colouring effect was not fully removed until synthetic materials started being used in the 19th century. This had a great impact on the development of the glass industry.

The new manufacturing processes associated to the Industrial Revolution required large amounts of new chemical components and, institutions such as the *Académie des sciencies,* made a call to scientists to work on new processes to elaborate raw materials. As a result of this call, the French chemist Nicholas Leblanc invented in 1791 an innovative process to elaborate sodium carbonate or soda ash (Na_2CO_3) [15]. In 1835 the glass industry introduced the Leblanc soda ash in the glass production becoming proud of this innovation [16]. The use of abundant and cheap materials as common salt (NaCl), limestone ($CaCO_3$) and coal was the key for the success of this process (1.1 and 1.2).

$$2NaCl + H_2SO_4 \rightarrow Na_2SO_4 + 2HCl \quad (1.1)$$

$$Na_2SO_4 + CaCO_3 + 2C_{(s)} \rightarrow Na_2CO_3 + CaS + 2CO_2 \quad (1.2)$$

In the first step (1.1), common salt is treated a with sulfuric acid to produce sodium sulphate, also known as salt cake. The second step (1.2) and principal Leblanc's contribution has two parts. First (1.3) there is a carbothermic reaction where the coal, a source of carbon, reduces sulphate to sulphide. Then (1.4), the sodium sulphide reacts with calcite ($CaCO_3$) to produce sodium carbonate and calcium sulphide, a mixture named as black ash. Finally, the soda ash is extracted with water.

$$Na_2SO_4 + 2C_{(s)} \rightarrow Na_2S + 2CO_2 \quad (1.3)$$

$$Na_2S + CaCO_3 \rightarrow Na_2CO_3 + CaS \quad (1.4)$$

Another process to obtain Na_2CO_3, the Solvay process was originally developed by Ernest and Alfred Solvay, sons of a Belgian salt manufacturer. They patented the recipe in 1861 to produce soda ash by using salt, limestone ($CaCO_3$), ammonia and coal [17]. In the first step (1.5), carbon dioxide passes through a concentrated aqueous solution of NaCl and ammonia. The CO_2 necessary for the reaction is obtained from the calcination of limestone (1.6). The sodium bicarbonate precipitates and produce sodium carbonate by calcination (1.7). Finally, the ammonia from (1.8) returns back to the first step for an equilibrium displacement.

$$NaCl + NH_3 + CO_2 + H_2O \rightarrow NaHCO_3 + NH_4Cl \quad (1.5)$$

$$CaCO_3 \rightarrow CO_2 + CaO \quad (1.6)$$

$$2\ NaHCO_3 \rightarrow Na_2CO_3 + H_2O + CO_2 \quad (1.7)$$

$$NH_4Cl + CaO \rightarrow NH_3 + CaCl_2 + H_2O \quad (1.8)$$

As a consequence of this, the transparent glass produced in the 19th century is silica and soda rich (>70 %SiO_2 and >15 %Na_2O) with a low level of impurities. A progressive substitution of Na_2O by CaO to increase the resistance of the glass to weathering in the last decades of the 19th century resulted in the production of transparent glass with a relatively broad composition.

Moreover, according to Dungsworth [16], the glasses of this period could also be divided in two groups depending on the nature of the refining agent used in the glass. Refining agents were added in minor amounts to remove the bubbles in the glass. The process is usually achieved by adding a compound which produces large bubbles which drag the

small bubbles to the surface. The introduction of arsenic oxide (or antimony oxide, although not so common) in low amounts, 0.1-1 wt%, as a refining agent was discovered some few years after the invention of Leblanc salts and is documented in contemporary sources such as the S. Muspratt chemical treatise [18]. The nitrate reduction [19] converts a trivalent oxide (As or Sb) to a pentavalent oxide (1.9), which is easily dissolved in the glass batch.

$$4KNO_3 + 2As_2O_3 \rightarrow 2K_2O + 2As_2O_5 + 4NO + O_2 \quad (1.9)$$

At high temperature, the pentavalent oxide is transformed again into the trivalent oxide producing O_2 (1.10).

$$As_2O_5 \rightarrow As_2O_3 + O_2 \quad (1.10)$$

Around 1870, the addition of arsenic (antimony) oxide is disused and substituted by saltpetre (KNO_3). The thermal decomposition of KNO_3 occurs at 400ºC and producing KNO_2 and O_2 bubbles of [20]. As a result, the K_2O content of the glasses increased.

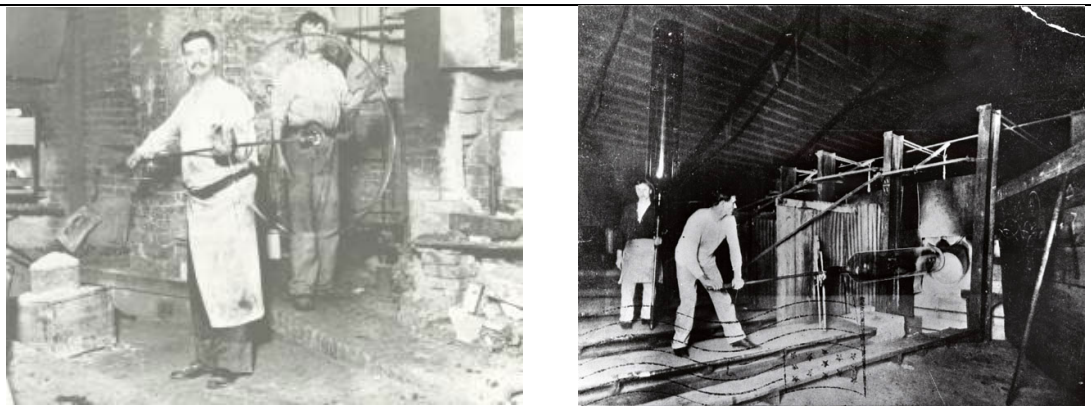

Fig. 1.6. (**Left**) an early 20th century picture showing crown glass being spun at Pilkington's glassworks, St. Helens, UK. Pict.: R. McGrath & A.C. Frost, Glass in Architecture and Decoration, 1937.

(**Right**) a first half of the 20th century picture from a glassworker with a blown cylinder glass at Wellsboro, UK. Pict.: Division of Parks and Forestry Photograph collection, New Jersey: State Archives, Department of State.

In order to produce a flat surface, two main traditional processes were used; among the earliest the so-called *crown* glass was obtained by spinning the blown glass at the end of the rod until flattened into a disk; a second type is the *cylinder* glass, which was made

blowing a glob which was swung out into a cylinder or muff, cut longitudinally and flattened while still hot, probably invented by German glass makers (**Fig. 1.6**). *Crown* glass did not have to be flattened and so had a superior surface finish compared to *cylinder* glass. However, the central swelling or bull's eye of the *crown* glass prevented the production of large panels of glass.

The first drawn sheet glass produced, known as *plate* glass, dates back to the late 17th century. A molten mass of glass was cast over the surface of a table and rolled flat, once cooled the glass was ground and polished to obtain perfectly flat and polished surfaces, a procedure which was extremely expensive. Between 1834 and 1888 the factory Chance and Co. from Birmingham developed a new method to produce flat textured glass. The molten glass is pushed through a set of cylinders on to a flat table (**Fig 1.7**). Most of the textured glass (known and cathedral glass) used nowadays is still produced by this system.

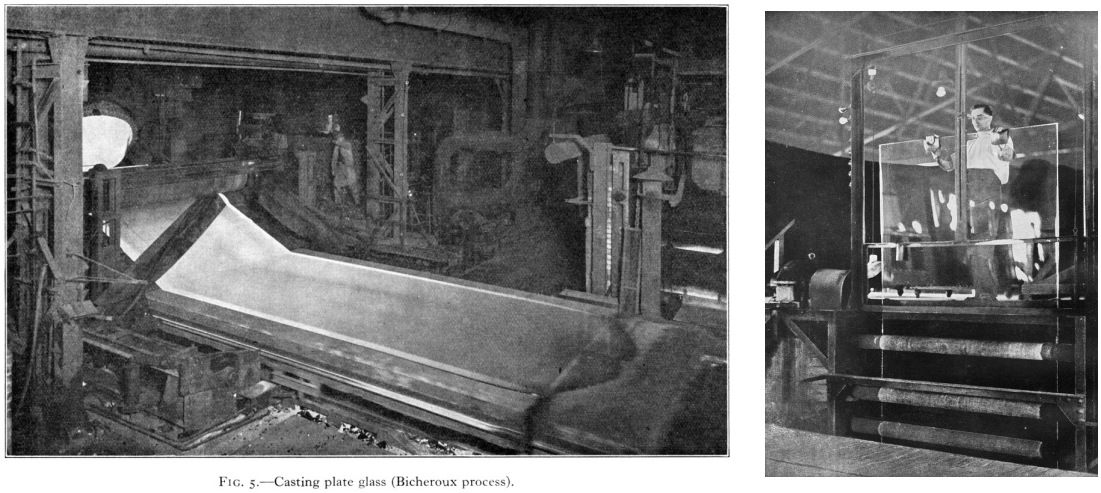

FIG. 5.—Casting plate glass (Bicheroux process).

Fig. 1.7. (**Left**) A turn of the century picture of the drawn sheet glass production. Pict.: Casting plate glass (the Bicheroux Process), The Making of a Sheet of Glass, Royal Institution of Great Britain, 1933.

(**Right**) a 1904 picture of the glass production following the Fourcault method. Pict. Villum window collection, Denmark.

The first method to produce glass continuously was the Fourcault process. It was introduced by Émile Fourcault during the first decade of the 20th century, due to its success, it expanded all over the world. The glass was drawn vertically from a bath of molten glass as shown in **Fig. 1.7**. The glass resulting from this procedure was not homogeneous and showed waviness consequence of the different viscosities resulting from local variations in the chemical composition [21]. Due to the long time that the glass

is kept hot, it shows a tendency to devitrify with the consequent precipitation of small crystals. An attempt to solve this problem was the replacement of part of the calcium oxide by magnesium oxide; as a result of this, the window glasses made after 1930 are MgO richer [16].

1.3.2. Colourants

The colours of the glasses are obtained by the presence/addition of transition metals, fired under oxidising or reducing conditions. The colour given to the glasses is due to the nature (iron, copper, manganese, cobalt, chromium), valence (Fe^{2+}, Fe^{3+}, Cu^{2+}, Cu^{+}, Cu^{o}, Co^{2+}, Cr^{3+}, Cr^{6+}, Mn^{3+} Mn^{2+}), coordination number (four, five, six) and geometrical arrangement (tetrahedral, octahedral...) of the neighbouring atoms [22]. The colour is caused by the absorption of light at specific light wavelengths by the metal ions (**Fig. 1.8**). Iron is the most important colourant as it is the most abundant impurity present in rocks and may produce many colours. Fe^{2+} has a high absorption in the infrared (~1100 nm) with a large tail extending into the red and yellow, and consequently, imparts a blue colour to the glass. Fe^{3+} has some lower absorption bands in the ultraviolet and blue (**Fig. 1.8**), imparting a yellow tinge to the glass. Both are normally present in the glass, the Fe^{2+}/Fe^{3+} ratio being determined by the atmosphere and firing temperature; the higher the temperature the higher the ratio. A reducing firing will provide a blue colour while an oxidising firing will result in a yellow/brown colour. For equivalent amounts of iron, the colouring effect of Fe^{2+} is far more important than that of Fe^{3+}.

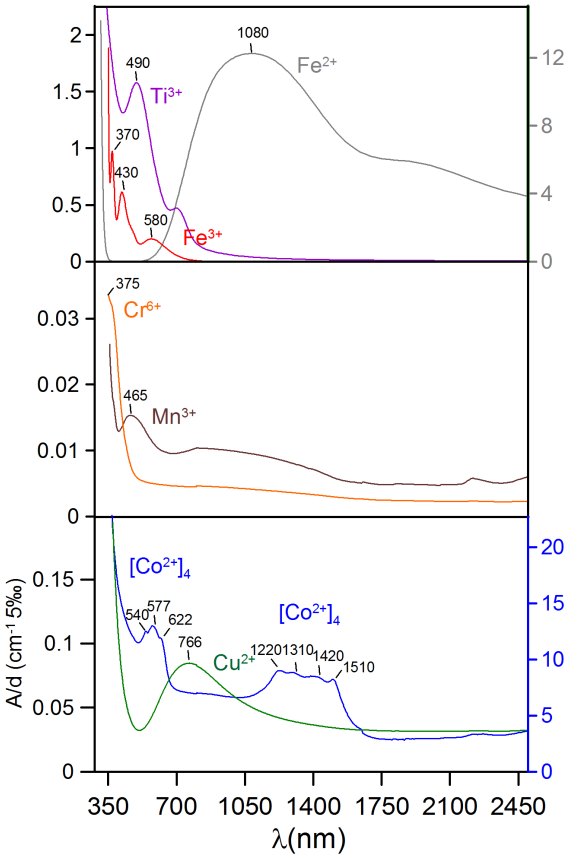

Fig. 1.8. UV-Vis-NIR spectra of the most common glass colourants [23].

As with iron, copper is also capable of imparting a wide range of colours to the glass. Under oxidising conditions, Cu^{2+} and Cu^{+} are both present, and the high broad absorption

of Cu^{2+} in the red with a large tail extending to the yellow (**Fig. 1.8**), taken together with variations in the coordination and nature of the neighbouring atoms, produces a range of colours from turquoise to green. In contrast, firing under reducing conditions may result in the reduction of some of the copper to metallic copper, Cu^{o}, which provides a red to dark-red colour to the glass [22].

Mn^{3+} gives a purplish colour to the glass, black in large concentrations. Nevertheless, the position of the absorption band varies strongly with the composition of the glass, (470 nm for a soda-lime and 520 nm for a potash-lime glass) shifting the colour from more reddish to more bluish. Moreover, trivalent manganese is often in coexistence with Mn^{2+} which imparts a faint yellow or brown colour.

Chromium gives a variety of colours and hues from green to yellow depending on its redox state from Cr^{3+} and Cr^{6+} respectively. Cr^{3+} is responsible of a dark green colour to the glass due to the characteristic absorption bands between 600-700 nm [24] but require of reducing glass melting conditions, and it is often difficult to avoid the presence of some Cr^{6+}. If the glass is fired under oxidizing conditions, Cr^{6+} give a yellow hue to the glass (**Fig. 1.8**) [22].

Finally, cobalt is present as Co^{2+}, but gives a blue colour if linked to four oxygens, tetrahedral coordination (CoO_4), and a pink colour if linked to six oxygens, octahedral coordination (CoO_6). The change from tetrahedral to octahedral coordination due to the loss of potassium is known to be responsible for the faint blue colour of smalt, a cobalt blue potash glass, used as a pigment in paintings [22].

1.3.3. Grisailles

Cennino Cennini in its treatise *Il Libro dell'Arte*, written in the last years of the 14th century, distinguishes between the glass painter and the glazier [25]. Although this is the first text mentioning paints, the use of *grisaille* paints is verified in an early 6th century glass fragment conserved at the Museo Nazionale di Ravenna [26]. In fact, the first known painted decoration on stained glass is a *grisaille* paint and the first known recipe is given in the 10th century treatise by Eraclius [27]. A *grisaille* (**Fig. 1.9**) is a dark and opaque paint applied and fired to be fixed over a substrate glass, to depict designs and shades [28]. There is a specific denomination for the two types of *grisailles* commonly used: the one used to draw lines and contours is known as *grisaille a contourner*, *contour grisaille*;

while the one used to add textures to the original drawing is known as *grisaille a modeler*, or *modelling grisaille*. The most obvious difference between both is the thickness of its application [29] and maybe, the particle size of the pigment particles. The main pigment particles used are iron oxide, haematite particles (Fe_2O_3), but depending on the historical period other elements such as copper, cobalt, zinc, tin or manganese were also incorporated [28]. The first known *grisailles* consisted on a lead rich glass to which iron oxide particles were added. The first compound added to this basic composition described in the Teophilus 12th century treatise is copper oxide (CuO). Copper oxide was added to counteract the red colour given by the iron oxide (haematite) particles, as Cu^{2+} gives a blue/green tinge to the glass. Between the 12th and the 17th centuries the *grisailles* contain decreasing Cu/Fe ratios. Although the lead glass is the main ingredient, since the last third of the 17th century some boron was also added to the glass, probably to reduce the firing temperature.

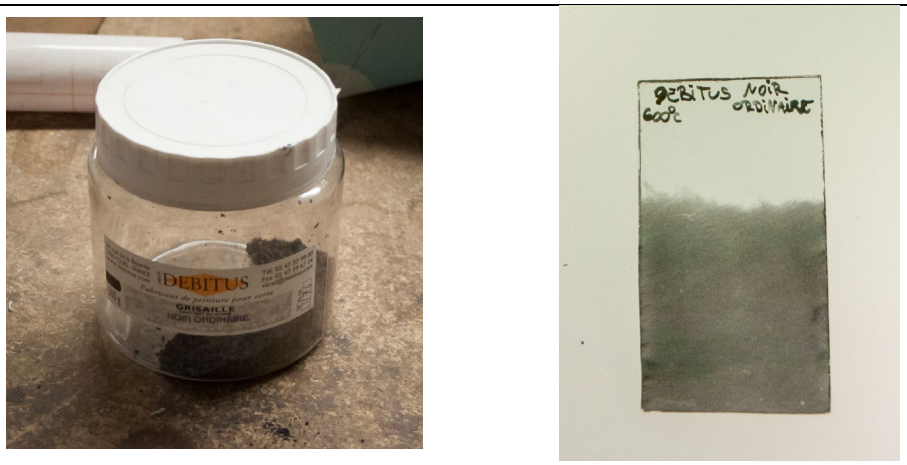

Fig. 1.9. (**Left**) A black *grisaille* powder from *Debitus,* a contemporary company and (**Right**) the *grisaille* obtained from it. Pict.: G. Molina.

In the 19th century, new chromophores such as cobalt, chromium and manganese [28] were also incorporated. Additionally, an organic binder is also often described in the treatises, to give more plasticity to the *grisaille* and help its application.

1.3.4. Silver stains

Silver stains are among the earliest methods for painting designs on glass. They originated in the Levant, either Egypt or Syria as early as the 6th century, although the earliest dated

objects are from the 8th century. Soon *silver stains* started being used to paint designs on glazed ceramics, due to the lustrous metallic effects obtained, they are known as *lustre* decorations. Stained glass continued being produced by the Fatimid and also Byzantine glassworkers (10th –13th centuries AD). It is not until the 13th century that *silver stains* started being used to tinge in yellow the stained glass panels from the European cathedrals [30]. The analysis has shown that in the 15th and 16th century copper salts were added to the silver stains in order to obtain brighter yellow and orange colours [31].

The silver stain or *lustre* (**Fig. 1.10**) is a micrometric layer made of silver (it may contain also copper) metallic nanoparticles lying beneath the glass surface and which may show a large variety of colours (green, yellow, amber, red, brown, white) and iridescent (bluish, purplish) or even metallic-like (golden, coppery, silvery) appearance [30]. It is formed by the reaction between a paint (mainly silver and/or copper salts Ag_2SO_4, AgCl or Ag_2S, $CuFeS_2$ among other dispersed in a clay) applied with a brush over the surface of the glass with the glass in a low-temperature firing. The firing temperature must be set above the *glass transition temperature* but well below the *softening point* of the glass (between 550ºC and 600ºC depending on the glass composition) [32]. After the firing, the paint residue is rubbed off revealing the stain layer beneath. During the firing the silver (Ag^+) and copper (Cu^+ or Cu^{2+}) ions from the paint are exchanged by sodium (Na^+) and potassium (K^+) ions from the glass; diffuse inside the glass and finally, are reduced to the metallic state and coagulate forming small nanoparticles. Redox reactions with the silicate network non-bridging oxygen or with other ions as Fe^{2+}, Sb^{3+}, As^{3+} or Sn^{2+}, present in the glass or added with the silver compound are responsible for the reduction of silver ions

Fig. 1.10. Silver stain, grisaille and blue enamel in the Mourning Virgin, Lautenbach Master. Germany, Upper Rhineland, Strasbourg, about 1480. (The Cloisters Collection, NY). Pict.: T. Pradell.

to the metallic state [31]. An oxygen depleted atmosphere during the firing was also used to help the reduction of silver ions to the metallic state.

1.3.5. Enamels

An enamel is a thin glass layer applied on a substrate glass and fixed by firing. The earliest enamels were those applied over glass objects starting in the late 12th century in the Islamic regions, probably in Syria. An enamel has a main vitreous part to which metal transition ions and/or pigment particles are added to impart colour and also opacity. They were crushed, mixed with water and sometimes an organic binder, applied over the transparent glass, then, fired to a temperature high enough to soften the enamel and fuse it into the substrate glass but not enough to deform or soften the substrate glass [27].

Enamels started being use to paint stained glass in the 16th century. The first treatise giving enamel recipes is the Antonio Neri's *L'Arte Vetraria* published in 1612. The enamel has a vitreous part containing Na_2O, PbO and SnO as fluxing agents [27]. Other contemporary sources specified the use of K_2O instead of Na_2O and SnO. Pierre Le Vieil (1708-1772) on his treatise *L'art de la peinture sur le verre et de vitrerie* (1774) was the first to describe the use of borax ($Na_2H_4B_4O_9 \cdot nH_2O$). B_2O_3 is strong low temperature flux. The incorporation of borax seems to have become more common in the 19th and 20th centuries [27].

Fig. 1.11. 19th portrait of Adolphe Lacroix. Pict.: A Quinet, Paris: BNF, dep. Geographie portrait-187.

Adolphe Lacroix (1833-1915) was at the forefront of developing a new type of enamel, as described in his 1872 treatise "*Des couleurs vitrifiables et de leur employ pour la peinture sur porcelain, faience, vitraux*" [33]. A. Lacroix (**Fig. 1.11**) was born in Paris and studied chemistry at the *laboratoires de Pelouze*, a private laboratory founded by the academic Théophile-Jules Pelouze (1807-1867). In 1855 he founded a laboratory on Faubourg Saint-Denis where he begun producing enamels, ready-to-be-used, which were sold by his laboratory. He received an award for the innovation on the enamels manufacture due to the good quality of the products [34].

Lacroix sold colour enamel powder (**Fig 1.12**) made of crushed glass to which transition metals (cobalt, copper, manganese, iron, etc.) and/or pigment particles were added to produce a wide range of transparent, translucent hues or opaque paints. They could be mixed with water and applied directly with a brush over the transparent substrate glass. In fact, their use helped to improve the artistic quality of the paints and, as a consequence, the materials were highly acclaimed by artists, curators and restorers with the consequent proliferation of enamel manufacture industries [34].

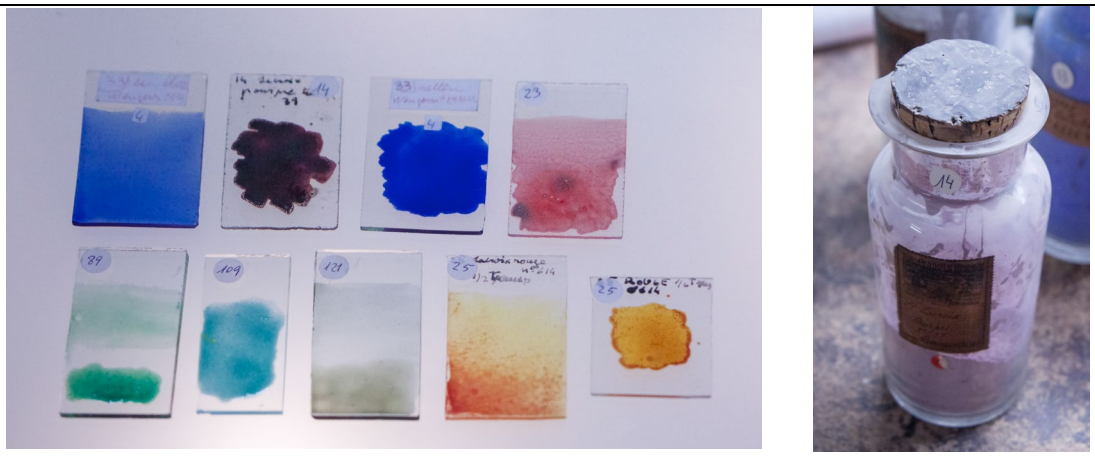

Fig. 1.12. (**Left**) Colour enamels obtained from ready-to-be-used enamels from the *Modernist* period. (**Right**) A purple enamel from Lacroix. Pict.: G. Molina.

Other companies working in the sector were Wenger and L'Hospied, both located in the United Kingdom. Wenger (**Fig. 1.13**) was founded by Albert Francis Wenger (1840-1924) in Etruria, Stoke-on-Trent. In 1874 the company already advertised "crystallised boracic acid, chemically pure, for the manufacture of China, Earthenware, and Enamel Colours"; and, in 1914, the company promoted as "Manufacturers of colours and chemicals for potters, glazed brick manufacturers, glassmakers and enamellers on metal" [35]. The company ceased trading in 1964.

Thompson L'Hospied & Co Ltd was founded near Stourbridge, UK, - a town known for its glass production since the early 1600s - by Charles Herbert Thompson, a chemist with commercial interests in England and France. Thompson is known for the invention in 1895, of the so called *Verre sur Verre* enamelled glass [35].

Fig 1.13. A 1964 picture of the Wenger company in Etruria, Stoke-on-Trent, UK. Pict: B. Bentley, Stoke on Trent City Archives SD1480/134-21.

1.4. Degradation of the enamels and *grisailles*

Almost all the *modernist* stained glasses are kept in their original locations. Consequently, most of this fragile heritage is suffering some degree of deterioration. However, the reasons for the alteration are not always clear and distinguishing between inadequate production processes, particularly aggressive atmospheric conditions and incompatibility among the materials is not always possible. In fact, the analysis of what is left gives only a very partial and limited information.

With regard to inadequate praxis, one of the main issues in the conservation of the decorative layers (enamels and *grisailles*) is the quality of its adherence, and this depends on the firing temperature which relays on the thermodynamic properties of both substrate glass and paints. Incompatibility among some of the materials cannot be withdrawn, because the materials used were often modified by the glass painter, which even for materials in origin stable, could lead to unstable paints. Finally, the *modernist* enamels applied over stained glasses are located on exterior walls due to their functional nature as building's windows, have been exposed to the atmosphere and solar irradiation for many years and appear damaged; cracked, flaked off, discoloured, etc..

Deterioration (**Fig. 1.14**) seems to have affected blue and green enamels in a particular way [36-41]. Specifically, the blue and green enamels produced in the *Modernist* period

(1885-1920) by famous stained glass workshops from Barcelona appear often more deteriorated than other colours, even when found in the same object.

The deterioration of 16th and 17th centuries blue enamels has been attributed to the use of too low firing temperatures for an adequate fixation [27] but also to their chemical composition, as potash rich lead glasses known to have a low stability were used for the production of the enamels [42-43]. Their instability has also been related to the high thermal expansion coefficients of the lead-potash enamels compared to those of the substrate glass [27]. Generally speaking, the difference in the thermal expansion coefficients between the enamels and substrate glass has often been related to the formation of cracks and the subsequent flaking off of the enamels [36-37].

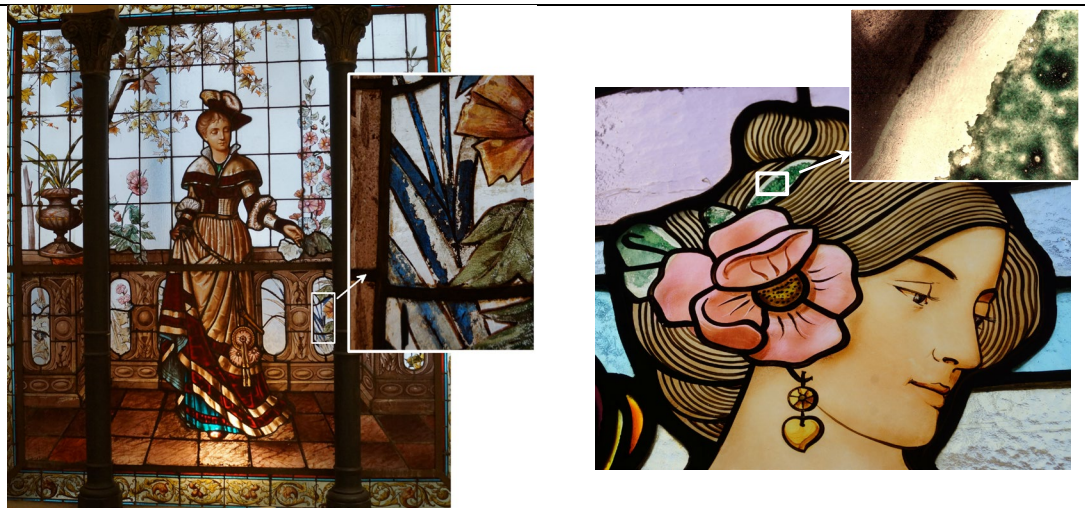

Fig 1.14. (**left**) Blue enamel degradation in a *Rigalt i Granell* stained glass panel from a private house. (**right**) Green enamel degradation in one of the windows from *Les Dames de Cerdanyola* by *Dietrich*. Pict.: J.M. Bonet workshop.

However, the nature of the 16th and 17th century enamels and substrate glass [39] is very different from those of the 18th and in particular of the 19th century. The low stability shown by the enamels in the 18th and 19th century was already commented by Barff. F.S. Barff (1822-1866) was a chemist fellow of the Chemical Society glass in the United Kingdom who owned a company that manufactured stained and invented preservation methods for a range of materials. He related the enamels wash off to the use of lead-borate [38]. Since the second half of the 18th century, lead-borate obtained from a solution of borax and lead nitrate was added in variable proportions to the enamels to reduce the

softening temperature. However, the enamels obtained appeared to be particularly sensible to moisture corrosion, which resulted in the lead and boron leaching and the flacking off of the enamels. F.S. Barff [38] stated that "the action of moisture causes the dissolution of borax" and the loss of the paint. The discolouration of the enamels was associated to the subsequent precipitation of lead carbonate, a white compound [39].

In summary, the proliferation of enamel manufacture industries which incorporated borax or boric acid in the enamels formulation and the variability of the substrate glasses composition has been related to the low stability of the 18th and 19th century glass paints.

To all this, we have to add the effect that UV-solar irradiation has in some of the chromophores, particularly remarkable for manganese tinged glasses, and known to be responsible of their decolouration (solarization) [44].

Grisaille paintings on *modernist* stained glasses seem to deteriorate in a similar way than the enamels [26,28]. The glass panels exposed to weathering usually show a loss of the black contouring drawing layer. This loss has been related to a shortness of fluxing agents in the paint, that attains a powder-like consistency and flakes off [27,36]. Moreover, solar irradiation generates thermal stresses [45-46] due to the differences between the expansion coefficients of the grisaille and glass substrate, which may cause the development of cracks and of the paint detachment [47-49].

1.5. Objectives and Methodology

The aim of the thesis is to determine the materials (substrate glasses, enamels, *grisailles*, *carnations* and silver stains) and painting techniques used in the production of *Modernist* enameled stained glasses from Barcelona. Special emphasis will be devoted to the degradation mechanisms affecting the enamels and *grisailles* with a final target of defining strategies to improve the conservation of the in-situ stained glass.

The study is developed in close collaboration with *J.M. Bonet Vitralls S.L.*, a company set in Barcelona and dedicated to the production and restoration of stained glass since 1923. The company has a hundred years documentation on the stained glass produced in Barcelona, an ample collection of historical materials and a long-term experience in the production and restoration of stained glass, in particular of *Modernist* stained glass. The

collection of historical materials includes enamels, *grisailles* and silver stains, and among them the workshop materials acquired to *Granell & cia* (1923-1931) previously *Rigalt, Granell & cia* (1890-1923) before closing. The materials included a collection of ready-to-be-used enamels from various manufacturing companies such as *Wenger*, *Lacroix* and *L'Hospied*. This historical collection opened a new possibility, the analysis of the materials used by one of the most important workshops from the *Modernist* period in Barcelona. Considering that one of the main difficulties faced while analysing historical samples is the fact that they are a hundred years old and, consequently have, to a greater or lesser extent, been submitted to corrosion, being able to study the original materials from the *Rigalt i Granell* workshop represented a great advantage. To this we have to add the extraordinary value of the experience that a company such as *J.M. Bonet Vitralls S.L.* has in the production of stained glass.

The *first objective* of the thesis is the determination of the nature and compatibility of the various materials used in the production of *Modernist* stained glass, in particular through the study of the materials of the *Rigalt i Granell* workshop.

A *second objective* is to determine the conservation state, the degradation mechanisms and the effect that corrosion has on the enamels and *grisailles*. The extent of the chemical alteration of the enamels and the corrosion products will be determined. Nevertheless, considering that the poor state of conservation of some of the enamels has been related by some scholars to the "creativity" of some glaziers in terms of painting techniques and/or materials used, a *third objective* of the study will be to identify differences in materials, painting and firing techniques and state of conservation of the artistic output of various glazier workshops active at the time and establish their relationship to the conservation state. To this end, we investigated a collection of enamelled glass fragments obtained from windows, skylights, decorative panels and screens covering the entire period and the most important glazier workshops operating in the city of Barcelona, including also some earlier and later enamelled samples. The fragments belong to the collection owned by *J.M. Bonet Vitralls S.L.* from over a hundred years of restoring stained glass from churches, palaces, mansions and private houses designed by the most relevant architects and artists and produced by the most important *Modernist* workshops of Barcelona.

The thesis has four milestones which will be developed in different chapters:

1- Microanalytical investigation of the nature of *Modernist* stained glass (substrate glass, enamels, *grisailles* and silver stains). Analysis of the *Rigalt i Granell* workshop materials. (**Chapter 2**)

2- Determination of firing temperatures of enamels and *grisailles* to the substrate glasses. Determination of the *glass transition temperature* and *softening range* of enamels and *grisailles* and compatibility with the substrate glasses. (**Chapter 3**)

3- Microanalytical investigation of the factors involved in the corrosion of enamels and *grisailles*. Analysis of a series of stained glass fragments produced by the main *Modernist* workshops, *Rigalt i Granell*, *Buxeres i Codorniu*, *Bordalba*, *Amigó*, *Dietrich* and *Maumejan*. Analysis of some *pre-modernist* (by *Bazin et Latteaux*) and a *Noucentist* (probably produced by *Bulbena*) stained glass. (**Chapter 4**)

4- Conclusions of the study and design of a conservation strategy. (**Chapter 5**)

1.6. References

[1] H.C. Gearhart, Teophilus' On Diverse Arts: The Persona of the Artist and the Production of Art in the Twelfth Century, PhD thesis (University of Michigan), 2010.

[2] D. Mackay, El Modernisme: Identitat i modernitat, El Vitrall Modernista, Barcelona: Departament de Cultura de la Generalitat, 1984, 11-17.

[3] J. Vila-Grau, F. Rodon, Els vitrallers de la Barcelona modernista, Barcelona: Edicions Polígrafa, S.A., 1982.

[4] A. Thomas, Le Vitrail a l'Exposition Universelle (Stain glass in the Universal Exhibition), in: L'Art Décorative, París (1900) 179 -187.

[5] M. García-Martín, Vidrieres d'un gran jardí de vidres, Barcelona: Catalana de Gas y Electricidad, S.A., 1981.

[6] M. García-Martín, J. Vila-Grau, F. Rodon, Contrallums, Vitralls de l'Eixample, Exposició del 20 d'abril al 31 de maig de 1983, Casa Elizalde, Valencia 302, Barcelona: Consell Municipal dels districtes IV i VI, 1983.

[7] N. Gil Farré, El taller de vitralls modernista Rigalt, Granell & Cia. (1890-1931), PhD thesis (UB), 2013.

[8] N. Gil Farré, La decoración con vidriera artística en el mueble domestico modernista catalán. Virtuosisme Modernista. Tècniques del moble. Associació per a l'Estudi del Moble i Museu del Disseny de Barcelona (2019) 131-147.

[9] S. Cañellas, N. Gil Farré, La Fábrica de Vidrieras de los Amigó, Cuadernos del Vidrio, Escuela Superior del Vidrio (2015) 42-60.

[10] B. Manauté, La manufacture de vitrail et mosaïque d'art Maumejean - Flambe! Illumine! Embrase!, ed. le festin, 2015.

[11] A. Velasco Gonzàlez, Lux Mariae: un conjunt de vitralls del taller Bazin-Latteaux a l'Acadèmia Mariana de Lleida, Taüll, 19, Secretariat interdiocesà per a la custodia i promoció de l'art sagrat a Catalunya (2006) 10-12.

[12] Y. Devred, J.F. Luneau, Verriers et verrières en Picardie au dix-neuvième siècle, Le vitrail en Picardie et dans le nord de la France aux XIXe et Xxe siècles, Amiens, Encrage (1995) 21-43.

[13] L.W. Adlington, I.C. Freestone, J.J. Kunicki-Goldfinger, T. Ayers, H. Gilderdale Scott, A. Eavis, Regional patterns in medieval European glass composition as a provenancing tool, Journal of Archaeological Science 110 (2019) 1-13.

[14] O. Schalm, K. Janssens, H. Wouters, D. Caluwé, Composition of 12-18th century window glass in Belgium: Non-figurative windows in secular buildings and stained-glass windows in religious buildings, Spectrochimica Acta Part B 62 (2007) 663-668.

[15] J. Rodríguez Guarnizo, D. Rodríguez Barrantes, Los procedimientos clásicos de fabricación de la sosa (Basic procedures of soda fabrication), Ensayos: Revista de la Facultad de Educación de Albacete, Nº. 14 (1999) 293-309.

[16] D. Dungworth, The value of Historic Window Glass, The Historic Environment, Vol. 2 No. 1, June (2011) 21–48.

[17] D.S. Kostick, The origin of the U.S. natural and synthetic soda ash industries, Proceedings of the First International Soda Ash Conference, Vol I, Laramie, Wyoming (1998) 11-35.

[18] S. Muspratt, Chemistry: Theoretical, Practical and Analytical, Glasgow: Mackenzie, 1860.

[19] M. Hujova, M. Vernerová, Influence of fining agents on glass melting: A Review, Part 1, Ceramics-Silikáty 61 (2) (2017) 119-126.

[20] C.M. Kramer, Thermal decomposition of $NaNO_3$ and KNO_3, Proceedings of the Electrochemical Society, PV 1981-9 (1981) 494-505.

[21] M.L. Ferreira Nascimiento, Brief history of the flat glass patent – Sixty years of the float process, World Patent Information, 38 (2014) 50-56.

[22] W.A. Weyl, Coloured glasses, Society of Glass Technology, Sheffield, 2016.

[23] T. Pradell, J. Molera, Ceramic technology. How to characterise ceramic glazes, Archaeological and Anthropological Sciences, 2020 12:189.

[24] O. Villain, G. Calas, L. Galoisy, L. Cormier, J.-L. Hazemann, XANES determination of chromium oxidation states in glasses: comparison with optical absorption spectroscopy, Journal of the American Ceramic Society, 90 (11), Wiley (2007) 3578-3581.

[25] A. Machado, Historical Stained Glass Painting Techniques. Technology and preservation, PhD, Universidade Nova de Lisboa, 2018.

[26] M. Vilarigues, C. Machado, A. Machado, M. Costa, L.C. Alves, I.P. Cardoso, A. Ruivo, Grisailles: Reconstruction and characterization of historical recipes, Int. J. Appl. Glass Sci. (2020) 1-18.

[27] O. Schalm, V. Van der Linden, P. Frederickx, S Luyten, G. Van der Snickt, J. Caen, D. Schryvers, K. Janssens, E. Cornelis, D. Van Dyck and M. Schreiner, Enamels in stained glass Windows: Preparation, chemical composition, microstructure and causes of deterioration, Spectrochimica Acta B, 64 (2009) 812-820.

[28] T. Pradell, S. Murcia, R. Ibáñez, G. Molina, C. Liu, J. Molera, A.J. Shortland, Materials, techniques and conservation of historic stained glass “grissailles”, Int. J. App. Glass Sci., 7 (2016) 41-58.

[29] O. Schalm, K. Janssens, and J. Caen, Characterization of the Main Causes of Deterioration of Grisaille Paint Layers in 19th Century Stained-Glass Windows by J.B. Capronnier, Spectrochimica Acta B, 58 (2003) 589–607.

[30] T. Pradell, Lustre and nanostructures – Ancient technologies revisited, Nanoscience and Cultural Heritage, Springer – Atlantic Press (2016) 3-39.

[31] G. Molina, S. Murcia, J. Molera, C. Roldan, D. Crespo, T. Pradell, Color and dichroism of silver-stained glasses, Journal of Nanoparticle Research, 15(9), 2013.

[32] K.C. Barley, Tests et observations à propos de l'usage du jaune d'argent in: Grisailles, jaune d'argent, sanguine, émail et peinture à froid. Dossier de la Comission Royale des monuments, sites et fouilles, 3, Forum pour la Conservation et la Restauration des Vitraux (1996) 117–121.

[33] A. Lacroix, Des couleurs vitrifiables et de leur employ pour la peinture sur porcelain, faience, vitraux, Chez A. Lacroix, Paris, 1872.

[34] A.F. Lozano Cajamarca, Innovations des techniques verrières au XIXe siècle et leurs applications dans la realization de vitraux, PhD thesis, HDR, Université Pierre et Marie Curie, 2013.

[35] Grace's guide to British Industrial History. https://www.gracesguide.co.uk

[36] G. Van der Snikt, O. Schalm, J. Caen, K. Janessens, M. Schreiner, Blue enamel on sixteenth and seventeenth-century window glass: deterioration, microstructure, composition and preparation, Stud. Conserv. 51(3) (2006) 212–222.

[37] N. Attard-Montalto, A. Shortland, 17th century blue enamel on window glass from the cathedral of Christ Church, Oxford: Investigating its deterioration mechanism, J. Cult. Herit. 16 (2015) 365–371.

[38] F.S. Barff, Silicates, silicides, glass and glass painting, J. Soc. of Arts. 20 (1034) (1872) 841-852.

[39] A. Machado, M. Vilarigues, Blue enamel pigment-Chemical and morphological characterization of its corrosion process. Corros. Sci. 139 (2018) 235–242.

[40] L. Robinet, M. Spring, S. Pagès-Camagna, D. Vantelon, N. Trcera, Investigation of the Discoloration of Smalt Pigment in Historic Paintings by Micro-X-ray Absorption Spectroscopy at the Co K-Edge. Anal. Chem. 83(13) (2011) 5145-5152.

[41] A. Gilchrist, The tears wept by our windows: sever paint loss from stained glass windows of the Mid-Nineteenth Century, Vidimus, 64 (2012).

[42] M. Verità, Modern and ancient glass: nature, composition and deterioration mechanisms, Scienze e Materiali del Patrimonio Culturale, 8, The Materials of Cultural Heritage in their environment (2006) 119-132.

[43] M. Verità, Composition, structure et mechanism de deterioration des grisailles in: Grisailles, jaune d'argent, sanguine, émail et peinture à froid, Dossier de la Comission Royale des monuments, sites et fouilles 3, Forum pour la Conservation et la Restauration des Vitraux (1996) 61-68.

[44] L.F. Day, Windows a book about stained and painted glass, ed. B.T. Batsford, Charles Scribner's Sons, New York, 1909.

[45] T. Palomar, F. Agua, M. Gómez-Heras, Comparative assessment of stained-glass windows materials by infrared thermography, Int. J. Appl. Glass Sci. 9 (2018) 530–539.

[46] T. Palomar, M. Silva, M. Vilarigues, I. Pombo Cardoso and D. Giovannacci, Impact of solar radiation and environmental temperature on Art Nouveau glass windows, Herit. Sci. 7 (2019) 82

[47] N. Attard-Montalto, A. Shortland, 17th century blue enamel on window glass from the cathedral of Christ Church, Oxford: Investigating its deterioration mechanism, J. Cult. Herit. 16 (2015) 365–371.

[48] F. Becherini, A. Bernardi, A. Daneo, F. Geotti-Bianchini, C. Nicola, M. Verita, Thermal stress as a possible cause of paintwork loss in medieval stained glasswindows, Stud. Conserv. 53 (4) (2008) 238–251.

[49] M. Verità, C. Nicola, G. Sommariva, The stained glass windows of the SainteChapelle in Paris: Investigations on the origin of the loss of the painted work, Annales du 16e congrès de l'AIHV, Association Internationale pour l'Histoiredu Verre (AIHV), Imperial College, London, 2003.

Chapter 2

Characterization of the *Rigalt, Granell & cia* workshop materials

Chapter2

Characterization of the *Rigalt, Granell & cia* workshop materials

The *first objective* of the thesis is the determination of the nature and compatibility of the various materials used in the production of *Modernist* stained glass, substrate glasses, enamels, *grisailles* and silver stains.

One of the main difficulties to face while analysing historical samples is the fact that, after a hundred years of being submitted to the action of humidity, pollutant gases, solar irradiation, temperature changes or of chemicals applied for their cleaning, the enamels, *grisailles* and silver stains are changed. This means that their composition and microstructure are different from the original ones. As a consequence, we expect to have difficulties discerning among the original composition/materials and those resulting from the action of time.

The collection of materials from the *Rigalt i Granell* workshop kept by *J.M. Bonet Vitralls S.L.*, (**Fig. 2.1**) and in particular the collection of ready-to-be-used enamels from various manufacturing companies is, therefore, of exceptional value. It opened new possibilities: on the one hand, it is possible to analyse the original enamel powder and, on the other hand, we can replicate the enamels and study them. The enamel powder has been kept inside their original flask away from humidity, atmospheric gases and solar irradiation, and therefore, we expect it to be reasonably well

Fig. 2.1. The collection of materials from *Rigalt i Granell* kept by *J.M. Bonet Vitralls S.L.* Pict.: G. Molina.

preserved. To this we have to add the extraordinary value of the experience that a company such as *J.M. Bonet Vitralls S.L.* has in the production of stained glass which has allowed us to replicate the enamels, *grisaill*es and silver stains following a similar procedure and firing protocol used in the *Modernist* workshops. The study of the enamels, *grisailles* and silver stains obtained will provide not only information on their chemical composition but also on their microstructure, and should allow us to distinguish between the original pigment particles from those obtained from the reaction among the components and resulting from the aging and alteration.

The collection of materials kept by *J.M. Bonet Vitralls S.L.* is very vast, it was therefore necessary to select a representative set. The selection included different colour enamels (blue, green, red, purple and yellow) also various manufacturing companies: *Lacroix*, *Wengers* and *l'Hospied*. A *grisaille*, four *silver stains* and a *flux*, a powder material which could be added at convenience to reduce the firing temperature of the enamels and improve the adherence to the substrate glass were also selected for study.

2.1. Replication of the enamels, *grisaille* and silver stains

A total of two purple (E107 and E14), three red (E23, E25 and E124), four yellow (E3, E4, E106 and E119), three green (E34, E89 and E121) and four blue (E33, E122, E114 and E115) transparent and semi-opaque enamels, four silver stains a *grisaille* (G1) and a *flux* were selected. The enamels were manufactured by different companies, mostly by *Lacroix* except two blue enamels, E33 produced by *Wengers* and E122 by *l'Hospied*.

In order to prepare the replicated enamels, *grisailles* and silver stains (**Fig. 2.2**), the powder was mixed with water and applied with a brush over a substrate glass. As a blown glass was mainly used in the *Modernist* period as substrate glass, a blown glass dated in the 1950s and still used by *J.M. Bonet Vitralls S.L.* was employed in the production of the replicas. The painted glass was first heated to 400ºC for over two hours, kept at this temperature for 30 minutes, then heated at a constant rate of 2.5ºC/min to 590ºC, kept at this temperature for 20 minutes and, finally, left to cool naturally to room temperature (~24 hours). For the silver stains, the residue of the paint remaining after firing was mechanically removed. The firing temperature selected happens to be the maximum temperature advisable to avoid the 1950s blown substrate glass damage. The procedure followed was designed to avoid excess thermal stresses in the substrate glass, thus

avoiding its cracking. A *Modernist* blown glass fragment obtained from casa Amatller, and dated from 1900, was also included in the study.

Selecting

Enamel Powder

Preparation

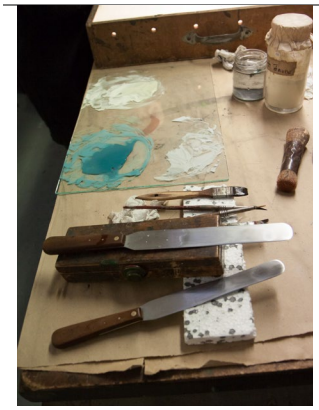

Ready to paint

Painting

Removing excess powder

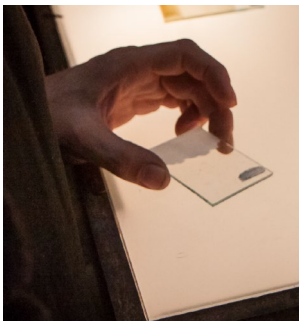

Ready to fire

Firing

Fig. 2.2. From top left to right bottom, production process of the enamels. Pict.: G. Molina.

2.2. Analytical methods

The replica enamels, *grisaille* and silver stains obtained are very thin, typical layer thickness vary between 20 µm and 50 µm. Moreover, micrometric and/or nanometric particles and reaction compounds are present in some of the enamels and *grisaille*. They have also a glass component which we expect to contain both boron and lead and also

metal transition elements added as colourants. Consequently, a combination of microanalytical techniques able to determine the chemical composition and the crystalline compounds present in the paint layers is required to complete their characterisation. The analytical techniques also require of specific sample preparation methods.

Laser Ablation Inductively-Coupled Plasma Mass Spectrometry (LA-ICP-MS) was selected to determine the chemical composition of the replica enamels and the substrate glasses. LA-ICP-MS has the advantage of probing micrometric areas at the same time that determines a broad range of elements including lead and boron and all the metal transition elements even when present in minor or trace amounts. The enamelled glasses were also analysed by Scanning Electron Microscopy (SEM) with an Energy Dispersive Spectroscopy detector (EDS) to determine the composition of the microcrystalline pigment and reaction particles, and by Focus Ion Beam (FIB) to identify the pigment nanoparticles. The crystalline compounds present in the replica enamels were determined by conventional X-ray Diffraction (XRD) and in some cases also by μ-XRD with synchrotron light. Finally, the colour and nature of the colourants was investigated by Ultraviolet Visible and Near Infrared (UV-Vis-NIR) spectroscopy using Diffuse Reflectance and Transmission modes respectively.

Polished cross sections of the replica enamels were prepared (**Fig. 2.3**) embodying a small fragment of the stained glass in a resin which was afterwards polished with a serial of cloths finishing with 1 μm diamond paste. The polished sections were examined both in reflected light with an optical microscope (OM), and after coated with a sputtered carbon layer, in a crossbeam workstation (Zeiss Neon 40) equipped with scanning electron microscopy (SEM) GEMINI (Shottky FE) column with attached EDS (INCAPentaFETx3 detector, 30 mm^2, ATW2 window, resolution 123 eV at the Mn Kα energy line), operated at 20 kV accelerating voltage with 1.1 nm lateral resolution, 20 nA current, 7 mm working distance, and 120 s measuring times. The EDS data was calibrated using mineral standards and verified with glass standards (K299, K93a, SRM612 and K252 from Geller MicroÅnalytical Laboratory, Inc.). The enamel microstructures were studied and recorded in a back-scattered electron (BSE) mode in which the different phases present could be distinguished on the basis of their atomic number contrast. BSE images of the microstructures were obtained at 20 kV acceleration voltage. The FIB was used to polish the surface and to obtain high resolution images of nanoparticles when present in the replica enamels.

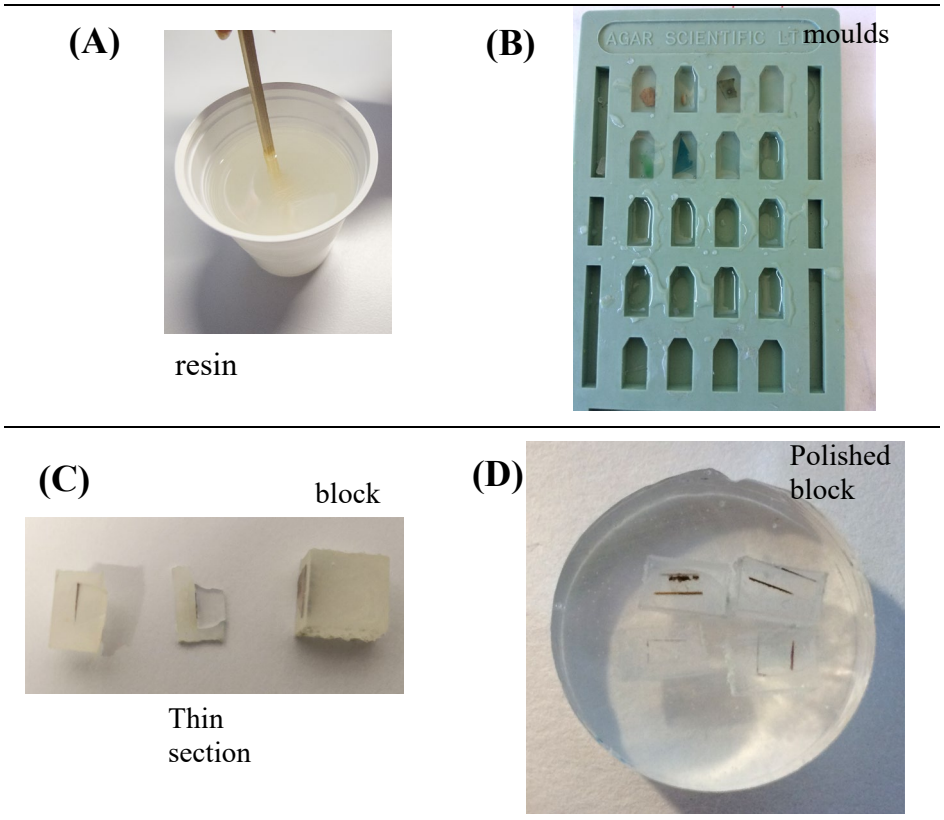

Fig. 2.3. (A) Epoxy resin, **(B)** mould, **(C)** cross section and thin cross section of a block, **(D)** blocks mounted and polished.

The composition of the powders and replica enamels was determined by LA-ICP-MS at the Cranfield Forensic Institute using a direct solid laser ablation sampling system (Q switched Nd:YAG ESI 213 nm laser ablation system, New Wave Research) coupled to a quadrupole ICP-MS (Thermo Scientific XSERIES 2), operating in standard mode. Due to the thinness (20-50 μm) of the replica enamels, it was not possible to perform the analysis on the polished cross sections, and consequently, they were taken directly from the surface of the replica enamels. After placing the samples in the ablation chamber (flushed with He at a rate of 500 $ml \cdot min^{-1}$), the targets were ablated with 20-50 s spot-mode analyses with a spot size of 80 μm on the frontal section of the applied enamel at 10 Hz laser frequency, fluency of ca. 12 J/cm^2 and 20 ms dwell time per amu. Three spot replicates were undertaken per analysis, with 15 sweeps per replicate. Several analyses on the dry gas were carried out in each set to establish the background prior to ablation. A pre-ablation time of 15-20 s was selected in order to remove surface contaminants. Instrumental drift was monitored throughout the analysis by measuring synthetic certified reference glasses (NIST 612 and 610) up to every 9 measurements within each run. To improve the instrument sensitivity, lower background noise, and reduce oxidized species,

the ICP parameters (including RF power, ion lens voltage and sampling position within the plasma, extraction voltage, and gas flow rates) were fine-tuned at the beginning of every set of analysis by continuously ablating on a reference glass (NIST 612) using the same working conditions chosen for the analyses. The internal standard independent (ISI) method was used to calculate the elemental concentration [1]. Within this method the summation of the element oxides is assumed to constitute 100% of the sample. The accuracy was evaluated with respect to Corning Museum of Glass (CMG) [2].

XRD analysis of the powders and replica enamels was performed to determine the presence and nature of crystalline particles. The surface of the enamels was directly analysed using a PANalytical X'Pert PROMPD Alpha1 powder diffractometer with Bragg-Brentano θ/2θ and Cu-Kα radiation. Measuring conditions were 4-100° 2θ, with a step size of 0.017° and measuring time of 150 s.

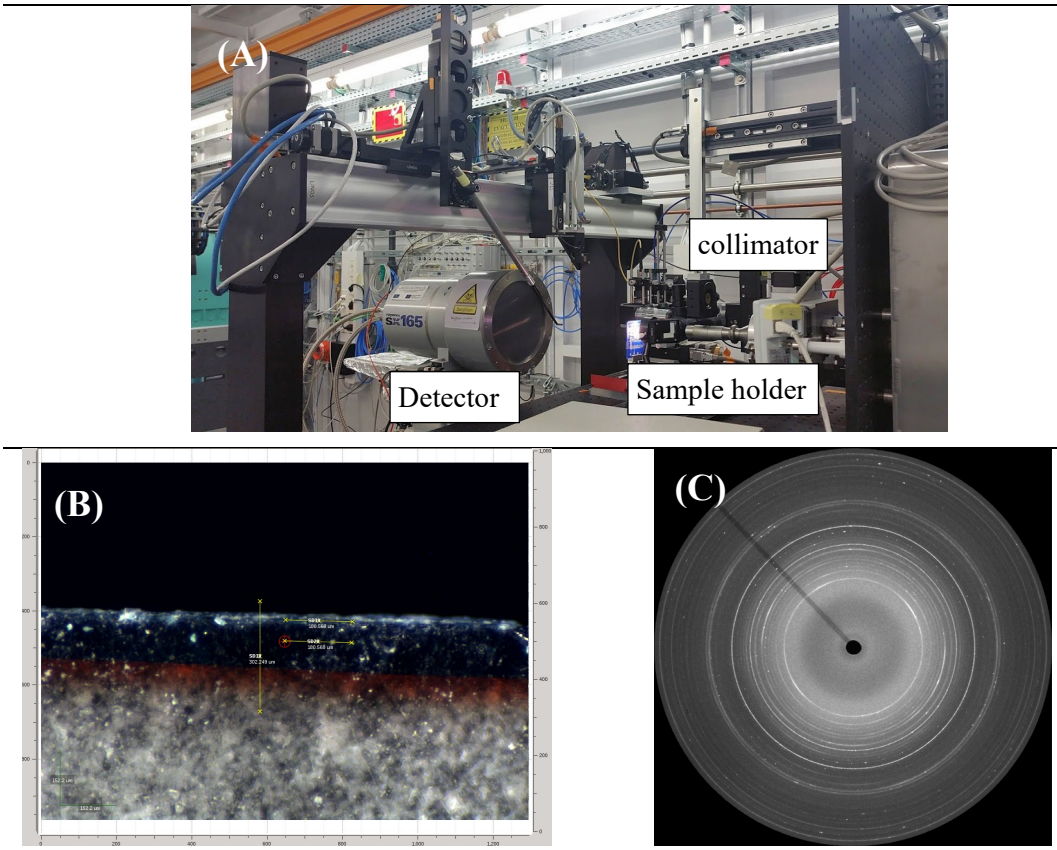

Fig. 2.4. **(A)** MSPD BL04- μ-XRD setup; **(B)** cross section of the enamel in the beamline showing the points analysed; **(C)** 2D μ-XRD image. Pict.: T. Pradell.

Synchrotron X-ray microdiffraction (μ-XRD) data from thin cuts (100 µm thick) of cross sections **(Fig. 2.3C)** of some of the replica enamels were collected in the Materials Science and Powder Diffraction beamline (MSPD BL04), **Fig. 2.4 (A)** [3] at the ALBA Synchrotron Light (Cerdanyola, Spain) of the enamelled glasses in transmission geometry, using 0.4246 Å wavelength (29.2 keV), a 20 × 20 µm^2 spot size, and a CCD camera, SX165 (Rayonix, L.L.C., Evanston, IL) detector. Thanks to the sub-micrometric size of the particles present in the enamels a powder like XRD pattern was mainly obtained, **Fig. 2.4 (C)**. Nevertheless, a small angle rotation (±5º) was applied to avoid intense spots. The 2D images have been integrated using the **d2Dplot** program developed by O. Vallcorba and J. Rius [4]. The XRD data has been identified using the Powder Diffraction File Database (PDF) from the International Centre for Diffraction Data (ICS) [5].

UV-Vis Transmittance and Diffuse Reflectance (with ISR 3100 Ulbricht integrating sphere) measurements of the replica enamels were obtained using a double beam UV-Vis spectrophotometer (Shimadzu 2700) with a spot size of 3 mm x 1 mm recorded between 200 nm and 800 nm; barium sulphate was used as a white standard for the reflectance measurements and calculation of the colour coordinates. NIR transmittance measurements of the replica enamels were obtained using a double beam UV-Vis spectrophotometer (Shimadzu 3600) with a spot size of 8 mm x 1 mm recorded between 800 nm and 3000 nm.

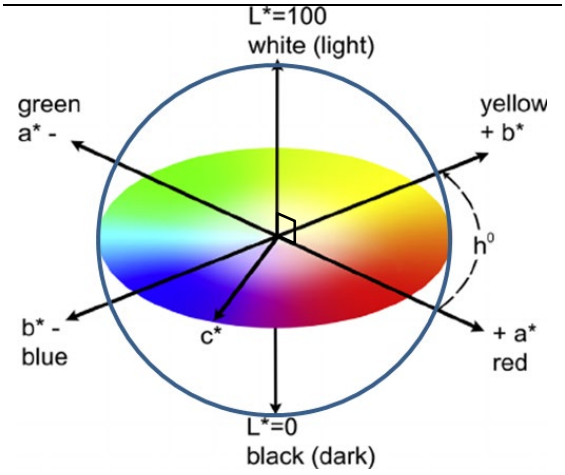

Fig. 2.5. Three-dimensional representation of the CIE *L*a*b** colour space.

The colour coordinates ($L^*a^*b^*$) are calculated from the Diffuse Reflectance UV-Vis spectra defined by the International Commission on Illumination (CIE) in 1976 [6]. L^* corresponds to the lightness and a^* and b^* the colour coordinates. The lightness value, L^*, varies between black at $L^* = 0$, and white at $L^* = 100$, while a* = 0 and b* = 0 correspond to neutral. The a^* axis represents the green–red component, with green in the negative direction and red in the positive direction. The b^* axis represents the blue–yellow component, with blue in the negative direction and yellow in the positive direction. The scaling and limits of the a^* and b^* axes vary between ±100. The $L^*a^*b^*$ values are calculated relative to CIE standard illuminant D50 and $BaSO_4$ is used as white standard. From them chroma c^*, $c^* = \sqrt{a^{*2} + b^{*2}}$; hue h^*, $h^*(°) = \tan^{-1}\left({b^*}/{a^*}\right)$ and the colour saturation s^*, $s^* = \sqrt{L^{*2} + c^{*2}}$ are defined (**Fig. 2.5**).

2.3. The *Rigalt, Granell & cia* workshop enamels, *grisaille* and *flux*

Both the original powders from the *Rigalt, Granell & cia* workshop and the replica enamels produced were analysed. The chemical composition of powders and enamels did not differ appreciably, and we can confirm that the chemical composition of the enamels does not change significantly with firing. The LA-ICP-MS data of the replica enamels is shown in **Table 2.1**. Looking at the data we can see that the enamel glass phase composition is a PbO-B_2O_3-SiO_2-ZnO type to which the pigment particles and/or colourants have been added.

On the other hand, the crystalline particles associated to the pigment particles and colourants show some differences between the original powders and enamels and also among the enamels. A summary of the pigment particles determined by XRD is shown in **Table 2.2**. The XRD data has been identified using the Powder Diffraction File Database (PDF) and the numbers of the cards used for the identification are given in brackets [5]. The presence of some lead carbonate ($PbCO_3$) in the powder is related to the weathering of the glass component after 100 years, and which is decomposed after firing it to obtain the enamel replicas. Other differences among the powder and the replicated enamels are associated to the decomposition and dissolution of some of the crystalline compounds, this will be discussed for each case.

Table 2.1 Chemical composition (typical error 5%) of the replica enamels produced from the raw materials found in the *Rigalt, Granell & cia* workshop and determined by LA-ICP-MS. Sulphur was not measured. T: Transparent, O: Opaque

Color	Sample	Opacity	Manufacturer	wt%																	ppm		
				B_2O_3	**SiO_2**	**ZnO**	**PbO**	Na_2O	MgO	Al_2O_3	K_2O	CaO	Cr_2O_3	MnO	Fe_2O_3	CoO	CuO	SnO_2	Sb_2O_5	Se	Cd	Ni	Ag	Au
Purple	E14	T	Lacroix	21.05	8.64	11.15	53.23	2.09	0.09	0.30	0.18	0.86	0.01	0.01	0.11	0.03	0.00	1.78	0.04				1112	2117
	E107	½ O		19.80	8.93	13.82	52.62	0.91	0.02	0.24	0.26	0.61	0.00	0.00	0.05	0.00	0.00	2.60	0.01				19	82
Red	E23	½ O	Lacroix	16.55	9.25	14.03	40.82	0.78	0.00	0.26	0.08	0.55	0.00	0.00	0.03	0.00	0.00	7.58	0.01	1.95	7.97	19		
	E25	T		12.12	7.86	9.94	62.67	0.40	0.01	0.41	0.18	0.38	3.53	0.00	0.13	0.00	0.00	2.29	0.01					
	E124	T		17.81	7.54	13.69	56.67	1.35	0.16	0.47	0.13	0.73	0.00	1.24	0.08	0.00	0.01	0.03	0.03			10		
Yellow	E3	T	Lacroix	6.97	30.41	0.02	52.97	5.06	0.06	0.27	0.11	2.61	1.25	0.00	0.10	0.00	0.00	0.01	0.03					
	E4	T		16.17	7.23	13.75	59.44	0.95	0.04	0.54	0.18	0.42	0.47	0.64	0.08	0.00	0.01	0.00	0.00					
	E106	½ O		7.87	22.38	4.09	54.61	2.10	0.04	4.80	0.41	0.45	0.01	0.00	0.23	0.00	0.00	0.49	2.41			10		
	E119	½ O		20.35	8.19	13.88	53.40	1.11	0.00	0.23	0.25	0.47	0.52	0.00	0.05	0.00	0.00	1.43	0.01					
Green	E34	½ O	Lacroix	8.13	10.74	1.85	49.82	2.04	0.40	5.92	0.50	0.33	10.84	0.01	0.20	6.47	0.27	0.91	1.23			1269		
	E89	T		16.36	8.49	12.37	53.94	1.73	0.02	0.45	0.21	0.66	0.16	0.01	0.16	0.00	5.32	0.06	0.01			18		
	E121	T		15.24	6.90	13.94	59.23	0.87	0.04	0.52	0.17	0.50	0.37	0.00	0.06	2.01	0.01	0.01	0.07			290		
Blue	E33	T	Wengers	11.07	11.38	9.20	41.87	2.76	0.53	13.89	0.12	0.70	0.02	0.01	0.35	7.67	0.01	0.16	0.05			732		
	E122	T	L'Hospied	3.80	23.18	0.22	71.23	0.15	0.04	0.76	0.04	0.24	0.01	0.00	0.07	0.12	0.01	0.01	0.02			48		
	E114	½ O	Lacroix	15.40	8.67	15.09	57.25	0.64	0.01	1.37	0.27	0.43	0.00	0.00	0.04	0.29	0.00	0.48	0.01			28		
	E115	T		18.25	7.72	14.64	56.47	0.65	0.01	0.46	0.26	0.43	0.00	0.01	0.05	0.84	0.01	0.17	0.01			79		
Grisaille	G1	O	Granell	0.00	19.95	0.04	50.41	0.20	0.03	0.53	0.14	0.08	0.02	6.52	21.87	0.00	0.03	0.00	0.00			97		
Flux	F1	T	Lacroix	9.15	9.15	0.12	80.10	0.07	0.03	0.90	0.04	0.16	0.00	0.00	0.11	0.00	0.00	0.03	0.07			2		
1900 Amatller house	GL1	T	blown glass	0.01	72.5	0.01	0.00	12.1	0.41	0.61	0.22	13.8	0.00	0.01	0.277	0.00	0.00	0.00	0.00			2.9		
1950	GL2	T		0.03	74.5	0.01	0.20	13.4	4.22	0.71	0.14	6.50	0.00	0.00	0.120	0.00	0.00	0.00	0.00			3.9		

Table 2.2 Crystalline compounds determined in the powder and in the replica enamels. The X-ray Diffraction ICDD-PDF numbers used for the identification of the compounds are given in square brackets.

Color	Sample	Opacity	Manufacturer	Powder	Enamel
Purple	E14	T	Lacroix	n.d.	Ag-Au –[FM-3M, a=4.08Å]
	E107	½ O		cassiterite (SnO_2) – [01-071-0652]	cassiterite (SnO_2) – [01-071-0652]
Red	E23	½ O	Lacroix	CdS – [01-071-1545], Cd(S,Se) – [P63mc with a=4.19Å c= 6.82Å] CdSe – [01-088-2346], cassiterite (SnO_2) – [01-071-0652]	CdS– [01-071-1545], Cd(S,Se) – [P63mc with a=4.19Å c= 6.82Å] CdSe -[01-088-2346], cassiterite (SnO_2) – [01-071-0652]
	E25	T		phoenicochroite ($PbO{\cdot}Pb(CrO_4)$) – [01-076-0861] cassiterite (SnO_2) – [01-071-0652], SiO_2 – [01-085-0335], $Na_2B_4O_7{\cdot}H_2O^*$ - [01-086-2215], $Pb(BO_2)_2{\cdot}H_2O^*$ - [00-007-0011]	phoneicochroite ($PbO{\cdot}Pb(CrO_4)$) – [01-076-0861] cassiterite (SnO_2) – [01-071-0652]
	E124	T		n.d.	n.d.
Yellow	E3	T	Lacroix	$Pb_3(CO_3)^*$ -[01-070-2052]	n.d.
	E4	T		phoenicochroite ($PbO{\cdot}Pb(CrO_4)$) – [01-076-0861] SiO_2 – [01-085-0335]	n.d.
	E106	½ O		SiO_2 –[01-085-0335], $Pb_2(Sn,Sb)_2O_7$ –[01-073-1737]	SiO_2 –[01-085-0335], $Pb_2(Sn,Sb)_2O_7$ –[01-073-1737]
	E119	T		crocoite $PbCrO_4$ – [00-008-0209], cassiterite (SnO_2) – [01-071-0652]	n.d.
Green	E34	½ O	Lacroix	$Co(Al,Cr)_2O_4$ –[01-078-0711], $Pb_2(Sn,Sb)_2O_7$ –[01-073-1737] cerussite ($PbCO_3$)* - [01-070-2052]	$Co(Al,Cr)_2O_4$ – [[Fd-3m, a=8.333Å], $Pb_2(Sn,Sb)_2O_7$ –[01-073-1737]
	E89	T		n.d.	n.d.
	E121	T		phoenicochroite ($PbO{\cdot}Pb(CrO_4)$) – [01-076-0861] SiO_2 – [01-085-0335]	n.d.
Blue	E33	T	Wengers	$CoAl_2O_4$ – [01-082-2242], cerussite ($PbCO_3$)* – [01-070-2052]	$CoAl_2O_4$ –[01-082-2242]
	E122	T	L'Hospied	$CoAl_2O_4$ – [01-082-2242], cerussite ($PbCO_3$)* – [01-070-2052]	n.d.
	E114	½ O	Lacroix	cassiterite (SnO_2) – [01-071-0652]	cassiterite (SnO_2) – [01-071-0652], $CoAl_2O_4$ – [01-082-2242]
	E115	T		cassiterite (SnO_2) – [01-071-0652]	cassiterite (SnO_2) – [01-071-0652]
Grisaille	G1	O	Granell	hematite (Fe_2O_3) – [01-072-0469] pyrolusite (MnO_2) – [01-072-1984]	hematite (Fe_2O_3) –[01-072-0469] melanotekite ($Pb_2(Fe,Mn)_2Si_2O_9$) – [01-088-1889] bixbyite ($Fe,Mn)_2O_3$) – [01-071-0636] jacobsite ($FeMn_2O_4$) –[01-075-0035]

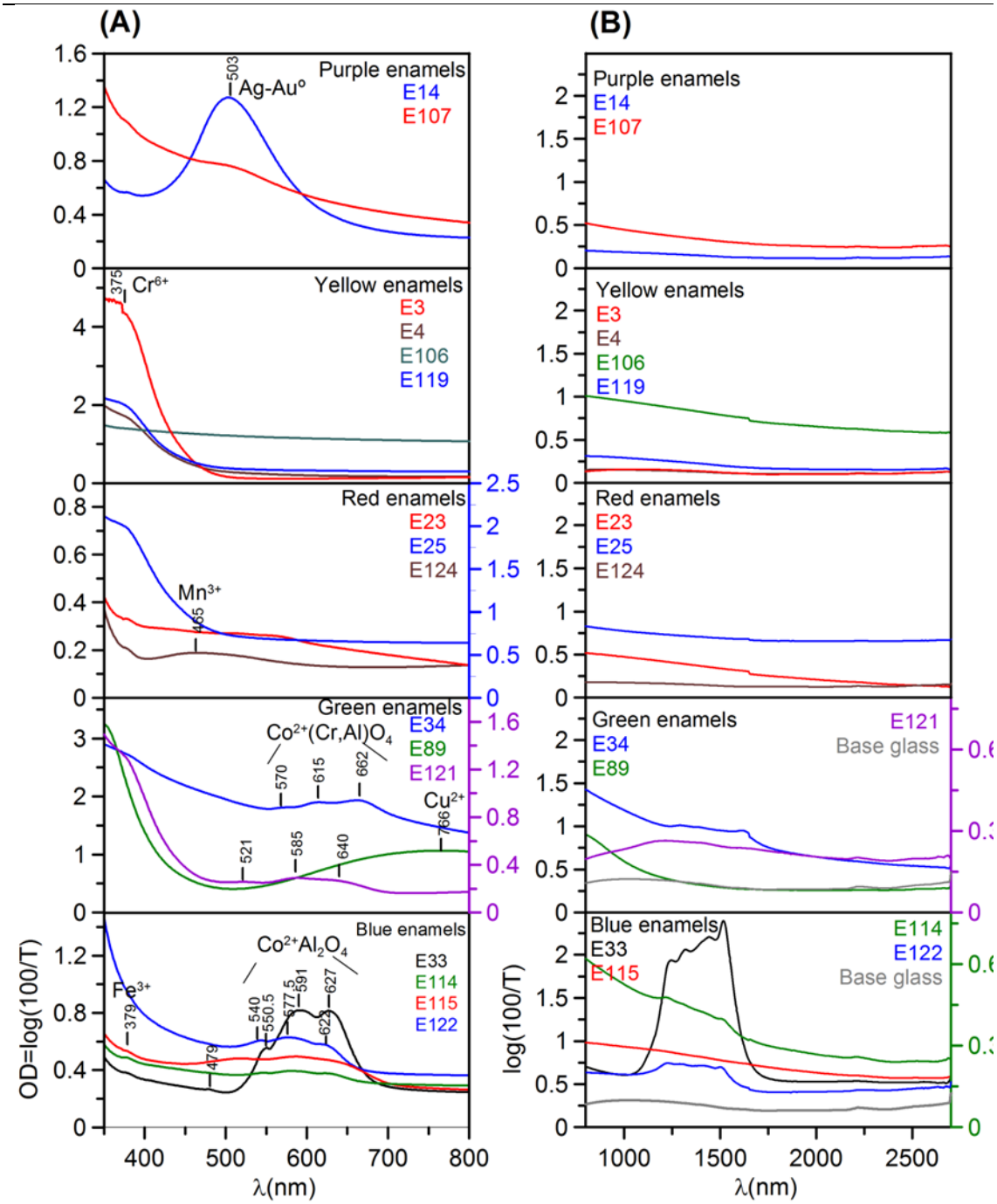

Fig. 2.6. (A) UV-Vis spectra taken in transmission mode -log(1/T)- from the enamels and showing the chromophores, Cr^{6+}, Mn^{3+} and Cu^{2+}, absorption SPR peak of Ag-Au° nanoparticles, ultraviolet absorption of the CdS and (Cd,Se)S nanoparticles and the absorption bands of Co^{2+} Cr^{3+} and Cu^{2+} and cobalt spinel particles. Fe^{3+} absorption bands are also seen but are related to the substrate glass.

(B) NIR Absorption spectra showing the enhanced absorption shown by Co^{2+}, Cr^{3+} and Cu^{2+} and cobalt spinel particles. The absorbance between 1000 nm and 1500 nm of the substrate glass is related to Fe^{2+}.

The colourants were determined by UV-Vis-NIR spectroscopy in Transmission mode taken from the replicated enamels, and the corresponding optical density spectra, OD=log(1/T), are shown in **Fig. 2.6.**

The colour coordinates (*L*a*b**) are calculated from the Diffuse Reflectance UV-Vis spectra using barium sulphate as a white standard, are shown in **Table 2.3** and the CIE colour chart represented in **Fig. 2.7**.

Table 2.3 Lab* colour coordinates calculated from the Diffuse Reflectance spectra obtained of the enamels from the *Rigalt i Granell & cia* workshop.

			*L**	*a**	*b**	*c**	*h**	*s**
Purple	E14	Lacroix	18.8	3.4	5.2	6.2	56.5	31.4
	E107		31.9	2.5	-3.0	4.0	309.6	12.3
Red	E23	Lacroix	36.4	19.3	12.4	22.9	32.8	53.3
	E25		40.1	31.7	23.3	39.4	36.3	70.1
	E124		18.6	1.7	-0.8	1.9	334.6	10.3
Yellow	E3	Lacroix	21.5	-7.8	21.1	22.5	110.3	72.3
	E4		21.1	-0.8	8.3	8.4	95.6	36.8
	E106		19.1	-2.1	8.2	8.4	104.6	40.5
	E119		26.2	-7.5	14.8	16.6	116.9	53.4
Green	E34	Lacroix	31.0	-13.2	-7.0	15.0	208.0	43.5
	E89		24.1	-10.3	1.4	10.4	172.3	39.5
	E121		7.1	-1.6	-0.1	1.6	181.9	22.2
Blue	E33	Wengers	11.9	6.7	-17.8	19.1	290.7	84.8
	E122	Hospied	31.3	-1.6	-5.1	5.4	252.6	16.9
	E114	Lacroix	24.1	-0.3	-19.0	19.0	269.0	61.9
	E115		22.5	5.4	-15.6	16.5	289.2	59.1
Grisaille	G1	Granell	40.4	47.8	48.3	67.9	45.3	85.9

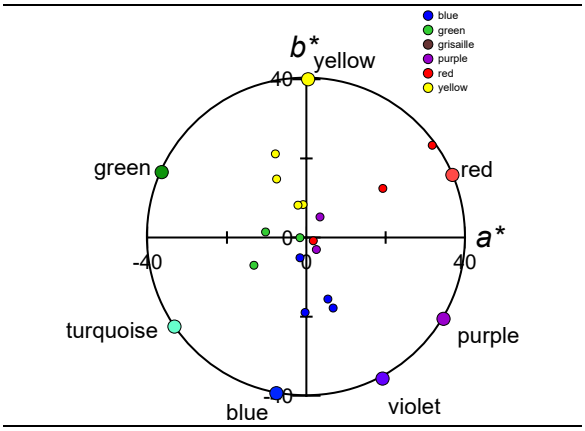

Fig. 2.7. *Lab** colour coordinates of the replicated enamels from *Rigalt, Granell & cia*.

2.3.1 Composition of the glass component of the enamels, flux and grisaille

The enamels are made of a glass mixed with colourants and/or pigment particles. The chemical composition shown in **Table 2.1** that the glass component of all the enamels is a high lead glass, but it also contains as major elements B_2O_3, SiO_2 and ZnO. The amount of MgO, K_2O and CaO is very low (normally well below 0.5%) and may be associated to impurities in the original materials. Although some enamels contain up to 2% Na_2O, their presence may be associated with impurities present in the sand and other glass ingredients (use of borax instead of boron oxide), but also to some degree, to the interaction between the substrate glass (rich in Na_2O and CaO) and the enamel. Finally, transition metals like Cr, Co, Cu and Mn are added as colourants and Al, Mn, Fe, Cr, Sn, Sb, Se and Cd are high only in those enamels where they are present within particulate matter, rather than in the glassy phase. Consequently, we can assume that the original glass component of the enamels is of a *high-lead and zinc borosilicate* type to which pigment particles or transition metal ions were added.

After removing all the elements but PbO, B_2O_3, ZnO and SiO_2, and renormalizing we obtained the composition of the glass component for each of the enamels, flux and *grisaille*. They can be classified into various types shown in **Table 2.4**.

Table 2.4 Chemical compositions of the synthetic enamels determined after the chemical composition of the workshop enamels after subtracting the pigment particles, colourants and impurities.

Type	***Rigalt, Granell & cia.*** **Enamels**	**(%wt)**				**(%mol)**			
		SiO_2	**PbO**	**B_2O_3**	**ZnO**	**SiO_2**	**PbO**	**B_2O_3**	**ZnO**
M1	*grisaille* (Granell)	29	71	0	0	60	40	0	0
M2	*flux* (Lacroix)	8	84	9	0	20	60	20	0
M3	E14, E107, E23, E25, E124, E131, E4, E89, E121, E33, E114, E115	11	58	18	14	20	30	30	20
M4	E106	27	60	9	4	50	30	15	5
M5	E3, E122	24	71	6	0	50	40	10	0
M6	E34	16	69	11	4	35	40	20	5

The *grisaille* is a high lead glass (71% PbO + 29% SiO_2) and the *flux* a high lead-borosilicate glass (84% PbO + 8% SiO_2 + 9% B_2O_3), types M1 and M2 in **Table 2.4** respectively. The third type, M3, correspond to the most abundant type, of composition 58% PbO + 11% SiO_2 + 18% B_2O_3 + 14% ZnO, and includes E14, E107, E23, E25, E124,

E131, E4, E89, E121, E33, E114, E115. Another type with less zinc (4% ZnO) comprises a green (E34) enamel with high lead and higher silica (69% PbO + 16% SiO_2 + 11% B_2O_3) and a yellow (E106) enamel with lower lead and lower silica (60% PbO + 27% SiO_2 + 9% B_2O_3); both contain lead antimonate particles, they have been labelled as M6 and M4. The last type (M5) includes two enamels (E3 and E122) that are B_2O_3 poorer and ZnO free (6% B_2O_3 + 71% PbO + 24% SiO_2). In fact, the valency of chromium in the glass is known to be quite sensitive to the composition of the glass and in particular to the presence of boron [7]; the yellow colouration of E3, with (1.3% Cr_2O_3), indicates the presence of Cr^{6+} and corresponds to the low boron concentration. Finally, E122 is a high lead cobalt blue glass enamel, in this case the cobalt was added in the form of cobalt aluminate particles but, contrarily to the other blue/green enamels, after firing the particles dissolved completely in the enamel.

Borosilicate glasses were invented at the end of the 19th century contemporarily to the invention of our ready-to-be-used enamels. The addition of PbO and/or ZnO to the borosilicate glass produces a low-melting glass which may be used as solder [8]. Boric oxide glasses have a structure formed by BO_3 triangles which is weaker than the tetrahedral structure of SiO_4 silicate glasses. In borosilicate glasses lead has a dual role both as network former and network modifier. Lead borosilicate glasses, like many other borosilicate glasses, show phase separation upon cooling and opaque glasses are often obtained [9-11].

A peculiarity of borate and borosilicate glasses, is the fact that as modifier oxides such as Na_2O, PbO or ZnO are added, the network of trigonal $[BO_3]^{3-}$ units (and tetrahedral $[SiO_4]^{4-}$ units) is not depolymerized by the formation of non-bridging oxygen atoms. Instead, trigonal BO_3 units react with the added modifier oxide and form a $[BO_4]^{4-}$ tetrahedral, which negative charge is balanced by the cation of the modifier oxide. Depending on the type of modifier oxide, a maximum of BO_4 units is reached at MO/B_2O_3 = 0.5, and an equilibrium exists between trigonal and tetrahedral metaborate ($[BO_3]^{3-}$ <=> $[BO_4]^{4-}$) [9-10].

A dense transparent glass with a low softening temperature and a thermal expansion coefficient matching those of the substrate glass while retaining a good resistance to water corrosion is obtained for compositions of 30-40 mol% PbO and B_2O_3:SiO_2 ratios between 2:1 to 2:3 [9-11]; ZnO acts in a similar way to PbO but with a lower effect on the softening temperature and density (ZnO favours the trigonal metaborate over the tetrahedral [12],

and can instead act as glass former). High zinc borosilicate glasses are also obtained with B_2O_3:SiO_2:ZnO = 30:20:50, 30:10:60 and 20:20:60 molar ratios [13]. The progressive depolymerisation produced by the addition of lead increases the thermal expansion coefficient (6-12·10^{-6} K^{-1}) while the incorporation of zinc gives glasses with a lower thermal expansion coefficient (4-5·10^{-6} K^{-1}) [13].

Consequently, lead borosilicate glasses with compositions matching those of our enamels show a low softening temperature and a thermal expansion coefficient matching those of the substrate glass while retaining a high resistance to chemical corrosion and transparency [9-10].

However, upon addition of a higher amount of modifier oxide (PbO) to the lead borosilicate glass, the non-bridging oxygen atoms become dominant, and the known depolymerization of the glass network occurs. In these high lead borosilicate glasses, $[PbO_4]^-$ tetrahedra contribute to glass formation and the borosilicate network is highly depolymerized, most likely consisting of dimers and trimers of the network forming silicates and borates. Consequently, these glasses have a very low softening temperature (~300ºC) and low chemical resistance to water [9-10]. The *flux* is one of this type of lead borosilicate glasses with lower boron and higher lead content than the enamels (B_2O_3:SiO_2:PbO=20:20:60 mol%). The *flux* was added to the enamels by the glazier in order to reduce their softening temperature; this might have been necessary if the substrate glass was unable to stand the firing temperature.

Finally, the grisaille is a high lead glass (40 mol% PbO + 60 mol% SiO_2) without boron to which iron and manganese oxide pigment particles are added. High lead glasses with > 40 mol% PbO show a broken silicate network, PbO cluster can form and change its role from pure modifier to an intermediate glass former [9,14,15]. As a result, the glass network is depolymerized, with the consequent low softening temperature. They are characterised by their high refractive index, high density, low viscous melts and high fragility (a large variation in viscosity with temperature) [9,14].

2.3.2. Pigment particles and colourants

- Purple enamels

Two purple enamels both produced by *A. Lacroix* were selected. Both contain tin and traces of gold and silver (**Table 2.1**).

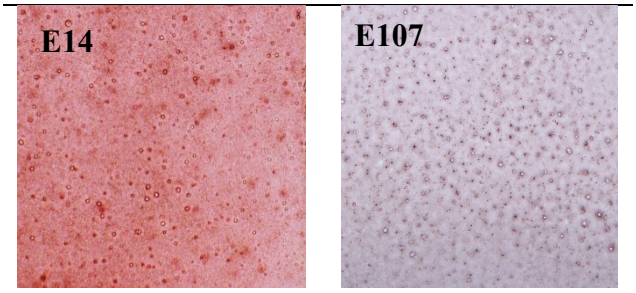

Fig. 2.8. Replicated purple enamels from the *Rigalt, Granell & cia* workshop.

LA-ICP-MS data of the purple enamels (E14 and E107) show that they contain 1112 ppm and 2117 ppm for E14 and only 19 ppm and 82 ppm for E107 of silver and gold respectively and a similar amount of tin (1.78% and 2.60% SnO_2 for each enamel). E14 is obviously red and more transparent (h^* = 56.5º L^* = 18.8%) than E107 which is purple (h^* = 309.6º L^* = 31.9%) (**Fig 2.8**, **Table 2.3**). SEM-BSE images of the cross sections (**Fig. 2.9A** and **B**) show a suspension of small "drops" containing small (≈10 nm) nanoparticles rich in Ag, Au and Sn, and in E107 the presence of small crystallites of cassiterite (SnO_2). The XRD patterns show also the presence of SnO_2 for E107 but not for E14 (**Fig. 2.9A** and **B)**. As a consequence, E14 is transparent while E107 is partly opaque. This suggests that the **red** or **purple** enamels are of the type known as *Purple of Cassius* [7].

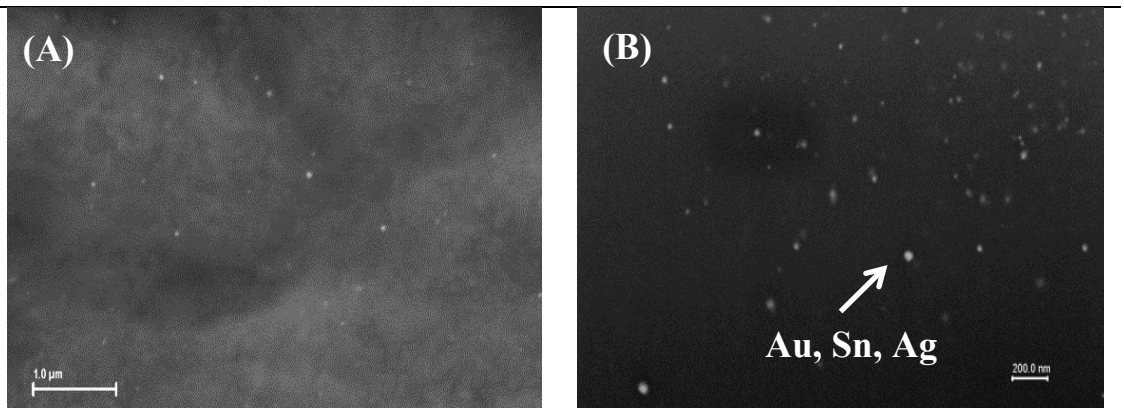

Fig. 2.9. (A) SEM-BSE image from the purple enamel E14 and **(B)** SEM-Inlens image from a FIB polished surface of the E14 purple enamel showing the presence of small nanoparticles containing Au-Ag-Sn of various compositions.

Purple of Cassius is a pigment named after Andreas Cassius of Leyden who described how to produce it in his work *De Auro* [16]. Purple of Cassius is a coprecipitate of gold and stannic acid. It was obtained according to the text adding a solution of stannous chloride ($SnCl_2$) to a solution of gold in *aqua regia* ($AuCl_3$). Sn^{2+} has the reducing agent function for the gold salt (2.1)

$$2Au^{3+} + 3Sn^{2+} \rightarrow 2Au^{o} + 3Sn^{4+} \quad (2.1)$$

At the same time that the Sn^{4+} hydrolysis (2.2) produces stannic acid:

$$Sn^{4+} + 2H_2O \rightarrow H_2SnO_3 \quad (2.2)$$

A purple precipitate with general formula $xH_2SnO_3 \cdot yAu^{o}$ is obtained. A compound containing colloidal gold.

In 1679 Johann Kunckel's edition of the *Ars Vitraria Experimentalis* of the Florentine priest Antonio Neri [16] describes for the first time the production of **red/purple** glass adding an acid solution of gold with salt and tin to the glass batch before firing. The Kunckel's gold red-ruby glass was famous for its beauty, but the high cost of production lead to a decrease of its manufacture. In the 19th century glass makers abandoned the use of gold for the production of red glasses [7].

In fact, the red/purple colour is due to the presence of colloidal gold or gold-silver alloy. Metallic nanoparticles are basically transparent to all visible light wavelengths except specific wavelength for which a collective oscillation of the conduction band electrons resonates with the oscillating electric field of the incident light known as *Surface Plasmon Resonance* (SPR). The SPR wavelength (λ_p) depends on the nature of the metal, size and shape of the nanoparticles and the refraction index of the medium in which the nanoparticles are hold. For the case of gold/gold-silver nanoparticles, the SPR absorption of the yellow-green light results in the red/purple colour of colloidal gold solutions.

The difficulty in producing red/purple glasses is twofold; on the one hand, to dissolve enough gold atoms in the melt and, on the other hand, to avoid the growth of the particles during the cooling. Tin is probably one of the best metallophilic elements in glass; Sn^{2+} in the glass appears highly polarised, $Sn^{2+} \rightarrow Sn^{4+} + Sn^{o}$. Consequently, the oxide (Sn^{4+}) side of the ion links to the glass structure while the metallic (Sn^{o}) links to the metal atoms. Therefore, the addition of tin to the melt increases the solubility of gold. During cooling the stannous ions accumulate around the gold atoms and prevent the growth of the particles stabilising the colloidal subdivision [7].

Both enamels show a single absorption peak, very faint for E107 but pretty intense for E14. The SPR peak for E14 occurs at 503 nm, **Fig. 2.6A**, indicating that the nanoparticles are not pure gold, but an alloy, in fact, a silver-gold alloy [17]. The composition can be calculated assuming a linear relationship between the position of the absorption bands for pure silver and gold nanoparticles. For nanoparticles size of about d≈10 nm in a medium with an index of refraction of about n ≈1.7 (a high lead glass), the silver and gold SPR absorption bands occur at λ_p ≈440 nm and λ_p ≈560 nm respectively. Consequently, the nanoparticles of the enamels have an approximate composition 49 at% Ag/(Ag+Au).

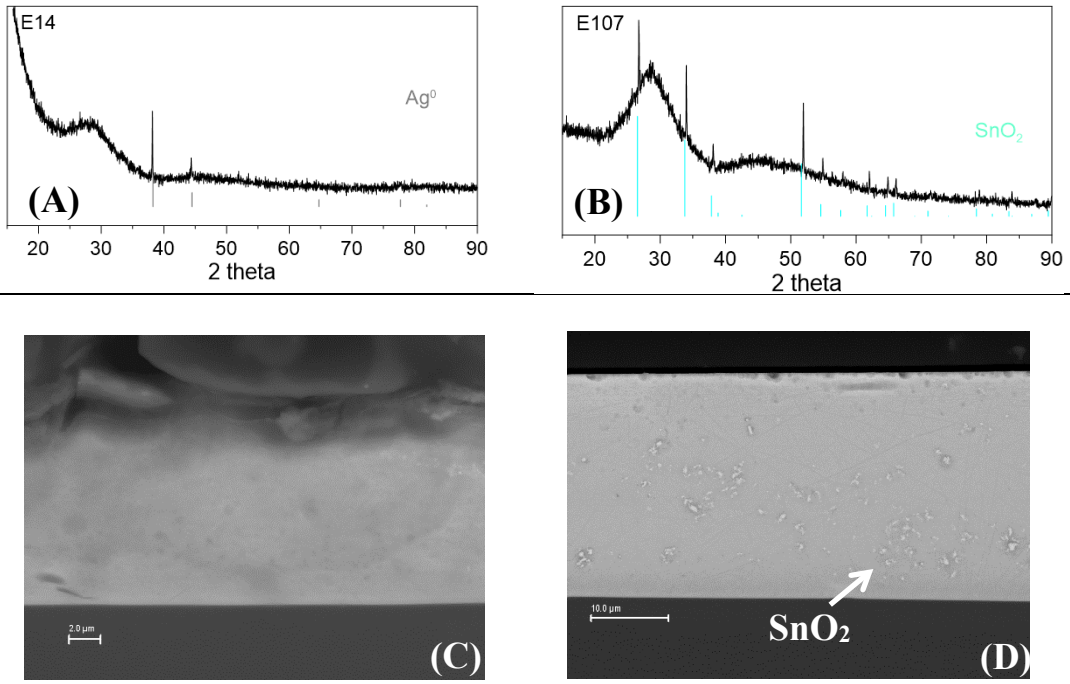

Fig. 2.10. XRD patterns from **(A)** E14 and **(B)** E107 and SEM-BSE images from polished cross sections from **(C)** E14 and **(D)** E107.

Lacroix describes in his treatise the addition of silver to modify the hue of the enamel [18]. Moreover, *Rigalt* described also a mixture of auric chloride and silver chloride in various proportions to the enamel glass [19] in order to obtain a range of purple to red colours. In fact, the colour of the enamel E14 (**Table 2.3**) is actually red rather than purple (h^* = 56.5º). E107 is more opaque, higher lightness (L^* = 31.9) and whiter, lower colour saturation (s^* = 12.3) due to the presence of the cassiterite particles. The enamel is gold richer (4/1 Au/Ag ratio) (**Table 2.1**) and shows a faint SPR peak associated to the gold-silver nanoparticles (**Fig. 2.6A**); the colour (**Table 2.3**) is purple (h^* = 309.6º).

- Red Enamels

Three different types of red enamels all of them produced by *A. Lacroix* were selected: E23, E25 and E124 (**Fig. 2.11**). E25 contains cadmium and selenium, E23 chromium and tin and E121 manganese (**Table 2.1**).

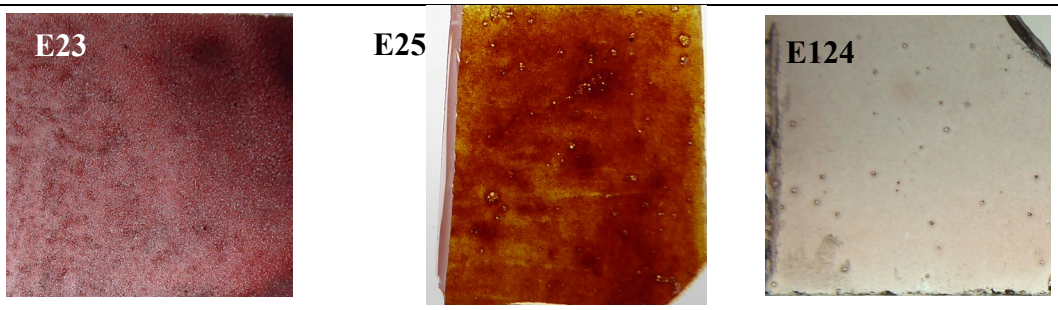

Fig. 2.11. Replicated red enamels from the *Rigalt, Granell & cia* workshop.

LA-ICP-MS data from E23 shows the presence of Cd and Se and the XRD pattern identifies the compound as cadmium sulphide selenide, CdS_xSe_{1-x}, and in lower amounts CdS and CdSe together with cassiterite (**Fig. 2.12A** and **B**). CdS and CdSe form a complete solution, the main phase determined by XRD, CdS_xSe_{1-x}, has a wurtzite structure with lattice parameters (a = b = 4.19Å and c = 6.82Å) matching a composition close to x = 0.79. The colour of CdS_xSe_{1-x} varies from yellow (pure CdS, x = 1), orange (x = 0.81), red (x = 0.65) to brown (x = 0.25) [20].

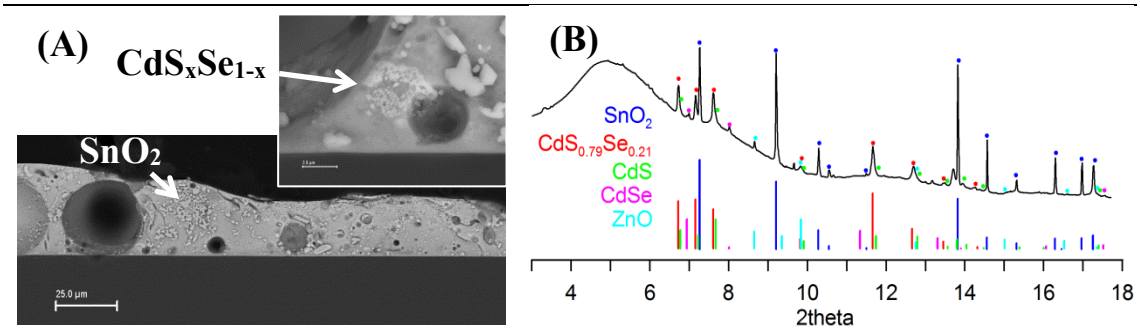

Fig. 2.12. (A) SEM-BSE image and **(B)** µ-XRD pattern from E23 showing the presence of CdS_xSe_{1-x} and, CdS, CdSe, ZnO and SnO_2 particles.

The chemical composition of the cadmium sulphide selenide particles has been confirmed by SEM-EDS. Unfortunately, the S content cannot be accurately determined because of

interference from the lead present in the surrounding glass. Nevertheless, the cadmium and selenium content can be determined, giving 0.29 ± 0.04 Se atoms for each Cd atom, equivalent to x = 0.79. The composition is, therefore adequate to obtain a red opaque colour (h^* = 32.8º, L^* = 36.4%) (**Table 2.3**) at a temperature close to the enamels firing temperature (≈590ºC). Higher firing temperatures favour the formation of crystals richer in Se, and lower firing temperatures produce crystals richer in S [20]. Consequently, the colour may change from red to orange if the firing temperature is too low.

The first to use selenium as a pink glass colourant was the French chemist Téophile-Jules Pelouze in 1865. First attempts to use selenium pink showed a poor reproducibility, low colour saturation and tendency to burn out, which were responsible of the little early interest [7]. Although the first patent of a red selenium containing glass is due Franz Welz in 1892, who added selenium to cadmium sulphide [21], the first publication stating the use of this pigment in glass dates to 1919 [22].

The addition of between 5-10% ZnO is known to favour the precipitation of the cadmium sulpho-selenide particles; zinc is known to stabilise and retain the sulphur ions in the melt avoiding their oxidation, during the cooling the cadmium-selenium sulphide precipitates. However, if ZnO is added in higher amounts the colour faints and disappears [7]. In fact, the presence of zinc oxide and other small unidentified phases are observed in the XRD pattern (**Fig. 2.12B**).

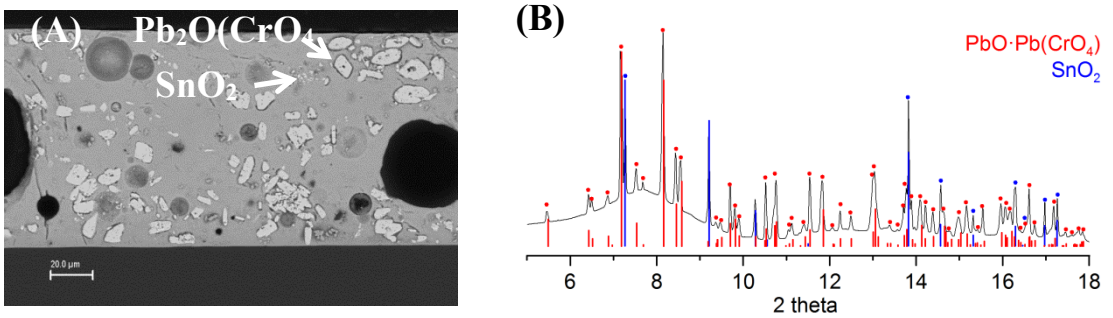

Fig. 2.13. (A) SEM-BSE image and **(B)** µ-XRD pattern from E25 showing the presence of $Pb_2O(CrO_4)$ and SnO_2 particles.

LA-ICP-MS data from E25 show the presence of Cr and higher levels of Pb than the other enamels while the XRD pattern shows the presence of phoneicochroite, $PbO{\cdot}Pb(CrO_4)$, particles (**Fig. 2.13A**), a basic lead chromate which bestows a coral red colour (h^* = 36.3º)

(**Table 2.3**) to the glass. The particles are large and round indicating some degree of dissolution in the glass (**Fig. 2.13B**). Small cassiterite particles which increase the opacity (L^* = 40.1%) (**Table 2.3**) and decrease the colour saturation are also present.

Chromium was discovered in the late 18th century by Louis-Nicolas Vauquelin as a component of a mineral named crocoite, a lead chromate [7]. In the 19th century the use of chromium compounds in the pigment manufacture was extensive, as chromium-based compounds gave striking colours. The synthesis of basic lead chromate ($PbO{\cdot}PbCrO_4$) was also due to L.N. Vauquelin in 1809, who produced it heating a lead chromate in a sodium hydroxide solution [23]. The colour obtained ranges from orange to red increasing the particle size [23-24]. We can see that in the enamel the particles are rather big (**Fig. 2.13A**).

Finally, E124 contains manganese (**Table 2.1**) and shows no crystalline particles (**Fig. 2.14A** and **B**). Consequently, it it is very transparent, low lightness (L^* = 18.6%) compared to the other red enamels and is purplish (h^* = 334.6º) rather than red (**Table 2.3**). The UV-Vis spectra taken in transmission mode shows a wide absorption band at 455 nm (**Fig. 2.6A**) corresponding to the presence of the Mn^{3+} ion [7].

Manganese is one of the oldest known colouring agents used in glasses, the earliest is Egyptian glass dated 1400 BC [7]. Mn^{3+} gives a purplish colour to the glaze, black in large concentrations. Nevertheless, the position of the absorption band varies strongly with the composition of the glass, shifting the colour from more reddish to more bluish. Moreover, trivalent manganese is often in coexistence with Mn^{2+} imparting a faint yellow or brownish colour to the glass [7].

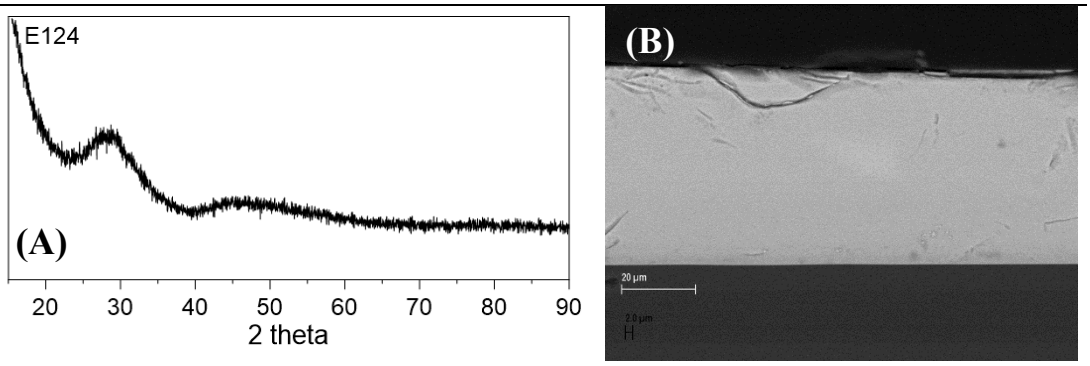

Fig. 2.14. (A) XRD pattern and **(B)** SEM-BSE image from E124 showing the absence of crystalline particles.

- *Yellow enamels*

Four yellow enamels all of them produced by *A. Lacroix* were analysed: E3, E4, E106 and E119 (**Fig. 2.15**). LA-ICP-MS data of the yellow enamels shows that the colour is related to the presence of chromium in E3, E4 and E119 and antimony, in E106. E106 and E119 contained also tin (**Table 2.1**).

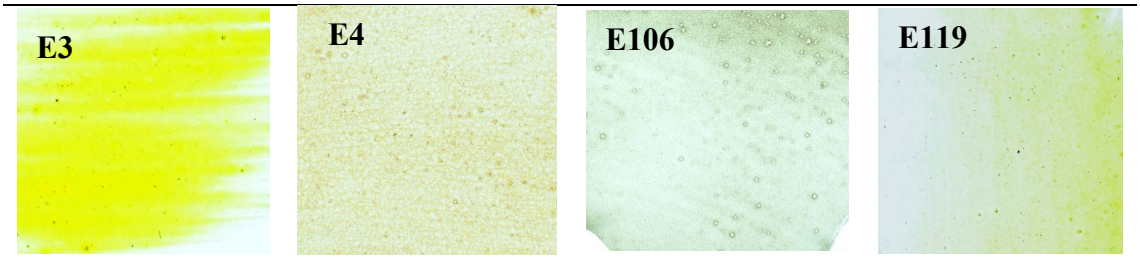

Fig. 2.15. Different colours shown by the yellow replicated enamels from the *Rigalt, Granell & cia* workshop.

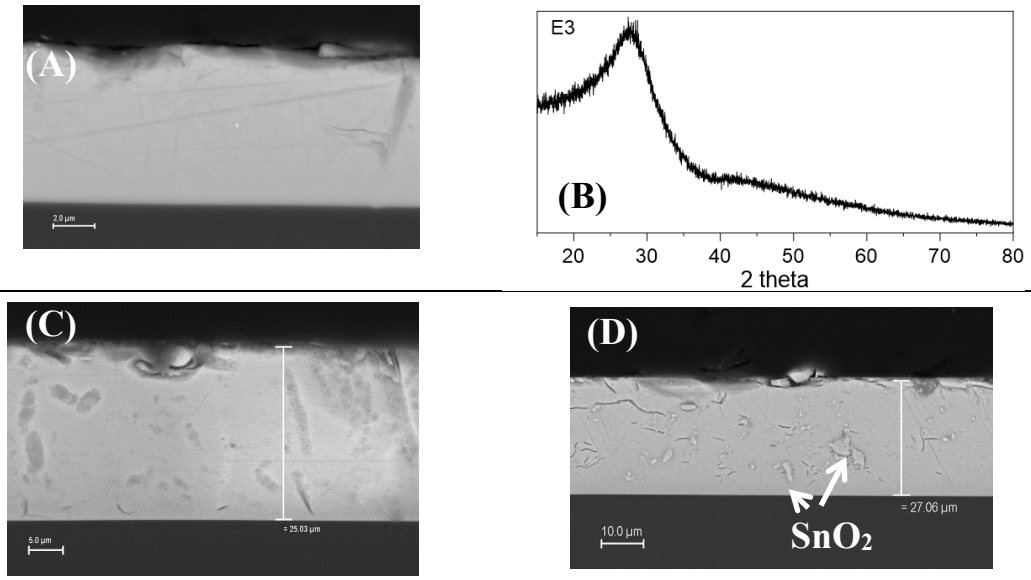

Fig. 2.16. (A) SEM-BSE image and **(B)** XRD pattern from E3 showing the absence of any crystalline particles. SEM-BSE images from **(C)** E4 amorphous and **(D)** E119 which shows the presence of cassiterite particles.

The UV-Vis spectra from E3, E4 and E119, **Fig. 2.6**, show the presence of hexavalent chromium, Cr^{6+}, dissolved in the glass as colourant (**Fig. 2.16A**) [25]. E119 shows also the presence of cassiterite particles that increase the opacity (L^* = 26.2%) and reduce the

colour saturation compared to the other enamels. Hexavalent chromium is responsible for the high absorption in the ultraviolet region extending to the yellow, at 500 nm, (**Fig. 2.6A**) bringing about the yellow-greenish colour shown by the enamels (h^* between 95.6º and 116.9º) (**Table 2.3)**.

The yellow enamel E106, contains antimony, as well as Sn and Fe in smaller amounts. This enamel has lower B_2O_3 and ZnO content than the other enamels. The XRD pattern (**Fig. 2.17B**) shows the presence of particles of lead-antimony oxide with a pyrochlore structure, $Pb_2(Sn,Sb)_2O_7$. The presence of small amounts of tin (iron, zinc, etc…) are known to help the stability of the pyrochlore structure in the glass [26]. The microcrystalline lead antimonate particles are responsible for the broad scattering with a maximum at 500 nm shown in the UV-Vis spectrum, **Fig. 2.6**, and, consequently, of the yellow colour (h^* = 104.6º) of the enamel (**Table 2.3)**.

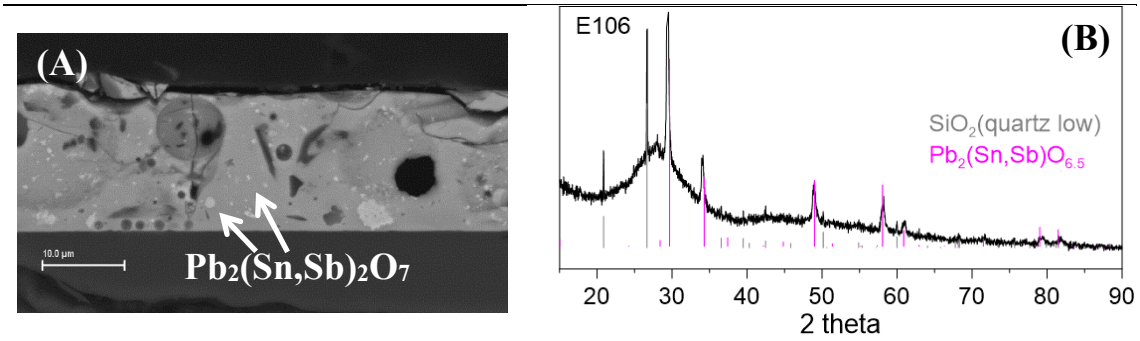

Fig. 2.17. (A) SEM-BSE images from the yellow enamel E106 and **(B)** XRD pattern showing the presence of crystalline particles of $Pb_2(Sn,Sb)_2O_7$.

Lead antimonate has been used as a pigment in glass and glazed objects since the Antiquity in Mesopotamia and Egypt [26]. The earliest use in glass and glazed ceramics in Europe dates back to the Renaissance (late 15th early 16th centuries). The Cipriano Piccolpaso treatise, *Li tre libri dell'arte del Vasaio* gives some of the earliest recipes. The highest popularity in European art dates between 1750 and 1850 when it was known as Naples yellow and was used also in paintings. The pigment is obtained roasting mixtures of lead and antimony oxides [27]. At the end of 19th century was still in use as a colouring agent for enamels.

- Green Enamels

Three different types (**Fig 2.18**) of green enamels produced by *A. Lacroix* were identified. LA-ICP-MS data shows that E34 contains chromium, cobalt, copper and aluminium but also antimony and tin, and minor amounts of iron and trace amounts of nickel, most probably related to the cobalt ore. E89 contains copper and in minor amounts iron and E121, contains cobalt and chromium and also minor amounts of iron and trace amounts of nickel (**Table 2.1)**.

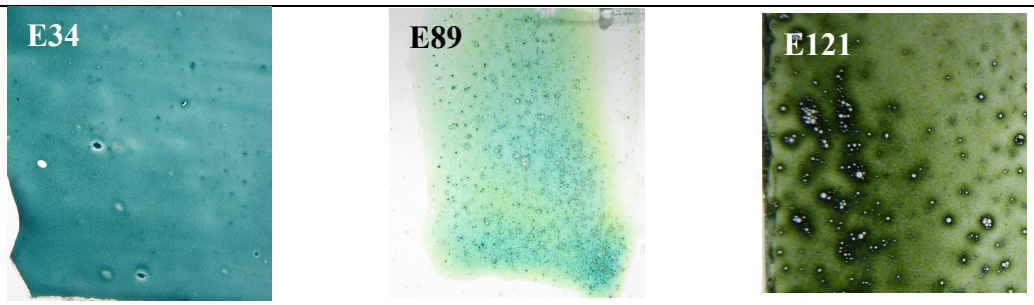

Fig. 2.18. Green replicated enamels from the *Rigalt, Granell & cia* workshop.

The XRD pattern from E34 shows the presence of cochromite particles, an spinel of aluminium cobalt and chromium, $Co(Cr,Al)_2O_4$, together with small yellow particles of lead antimonate with pyrochlore structure, $Pb_2(Sn,Sb)_2O_7$ (**Fig. 2.19)**; like most spinels the composition of the cochromite particles is quite diverse. The particles measured by SEM-EDS showed typical compositions varying between 0.6-0.8 atoms of Al and 1.4-1.2 atoms of Cr (**Fig. 2.19A)**. The UV-Vis spectrum showed the three characteristic absorption peaks of Co^{2+} ions in fourfold coordination at 570 nm, 615 nm and 662 nm (**Fig. 2.6A**) (the triple band is attributed to a Jahn–Teller distortion of the tetrahedral structure), shifted slightly to higher wavelengths compared to a pure cobalt aluminate [28], and which are responsible for the green-bluish colour (h^* = 208.0º) and its relative opacity (L^* = 31.0%) (**Table 2.3)**.

E89 contains copper dissolved in the glass matrix (**Fig. 2.20A**). Cu^{2+} is known to have a large absorption broad band with a maximum at 800 nm (**Fig. 2.6A**) extending to the near infrared (1000 nm) (**Fig. 2.6B**), together with the presence of cuprous ions are responsible for the U-shaped profile of the absorbance with a maximum transmission at about 500 nm, which gives a green colour (h^* = 172.3º) (**Table 2.3)** to the enamel [7]. The enamel

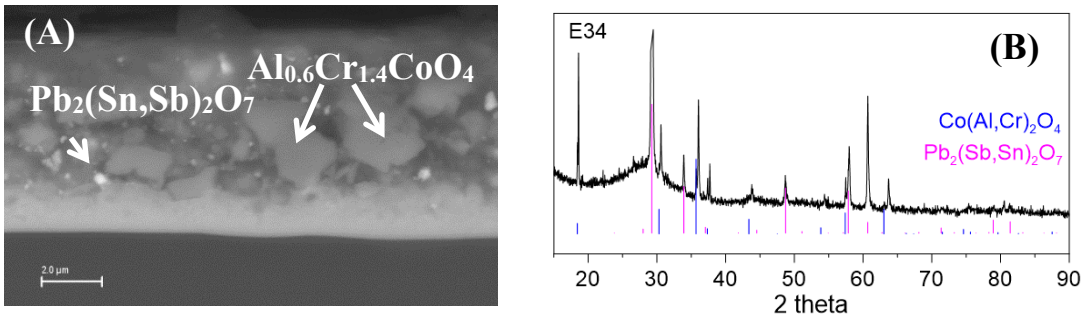

Fig. 2.19. (A) SEM-BSE images **(B)** XRD pattern from the green enamel E34 showing the presence of crystalline particles of $Co(Cr,Al)O_4$ and $Pb_2(Sn,Sb)_2O_7$.

is more transparent (L^* = 24.1%) (**Table 2.3)** because it does not contain pigment particles of any kind.

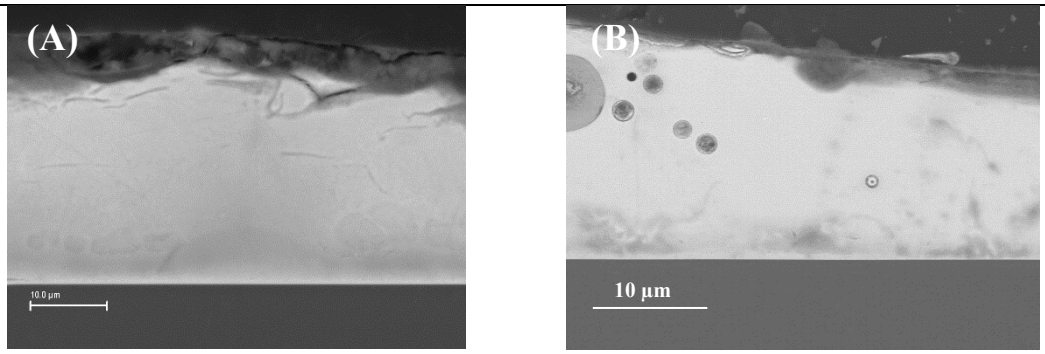

Fig. 2.20. (A) SEM-BSE images from the green enamels E89 and **(B)** E121.

Finally, E121 contains both cobalt and chromium ions dissolved in the glass (**Fig. 2.20B**). Blue (CoO_4) groups in the glass show three characteristic intense absorption peaks in the 500-650 nm range and which exact positions and intensities depend mainly on the composition of the glass; the shoulder at 479 nm is related to transitions between the octahedral and tetrahedral sites. Cr^{3+} is known to give a dark green colour to the glass due to the characteristic absorption bands between 600-700 nm [25], but if the glass is fired under oxidising conditions, it is difficult to avoid the presence of Cr^{6+} [7]; in fact, the presence of lead oxide in the glass exerts a stabilising action on hexavalent chromium [7]. The UV-Vis spectrum (**Fig. 2.6A**) shows that the addition of chromium blue shifts and broadens the triple Co^{2+} absorption band, producing a green (h^* = 181.9º) transparent (L^* = 7.1%) enamel (**Table 2.3)**. Moreover, we can also observe an enhanced absorbance in the NIR range (**Fig. 2.6B**) between 1250 and 1750 nm related also to the blue (CoO_4) groups.

- Blue enamels

Four blue enamels belonging to three companies have been studied (**Fig. 2.21**). The LA-ICP-MS analysis showed that all of them contained cobalt; E122 produced by *L'Hospied*, E33 produced by *Wengers* contained also aluminium and E114 and E115 were produced by *A. Lacroix* contained also tin (**Table 2.1)**.

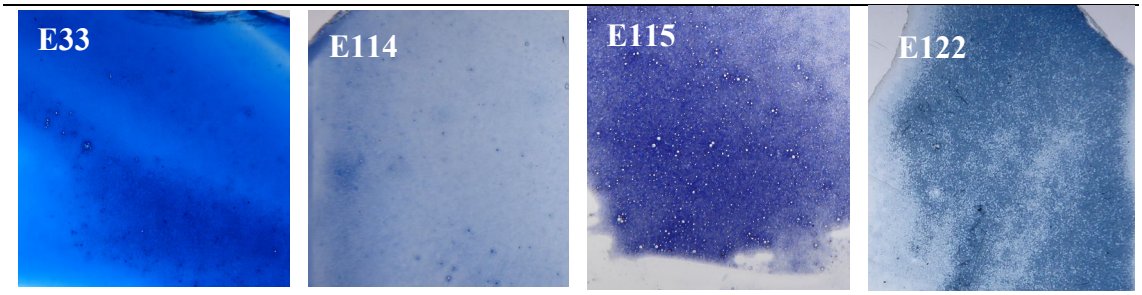

Fig. 2.21. Blue replicated enamels from the *Rigalt, Granell & cia* workshop.

However, although the powders of the enamels E33 and E122 originally contained cobalt aluminate particles with spinel structure, $CoAl_2O_4$, after firing only the replicated enamel E33 had them (**Fig. 2.22A** and **Fig. 2.23A)**. E122 showed some relics of the original particles (**Fig. 2.22C)**, but essentially the cobalt appears dissolved in the glass. In fact, E122 is richer in PbO with very low B_2O_3 and ZnO contents. Cobalt appears also dissolved in the glass in E114 and E115, but they contained cassiterite particles to increase their opacity (L^* = 24.1% and 22.5% respectively) (**Fig. 2.2D** and **Fig 2.23B**, **Table 2.3)**.

All the absorbance spectra show the characteristic triple absorption band of CoO_4 groups (**Fig. 2.6A)** and the peak positions varying with glass compositions from a dark opaque blue of E122 (h^* = 252.6º, L^* = 31.3%) to an intense transparent blue of E33 (h^* = 290.7º, L^* = 11.9%) (**Table 2.3)**. Another important characteristic is the enhanced NIR response of the CoO_4 groups (**Fig. 2.6B),** in the range 1250-1750 nm, which is particularly high in the enamels containing $CoAl_2O_4$ particles [28]; E33 shows an increase in absorption in this region of about 30%. This enhanced NIR absorption is seen in all the cobalt-containing enamels, whether green or blue (**Fig. 2.6B**).

The transparent substrate glass shows also a broad enhanced NIR absorbance in the range 1000-1500 nm (**Fig. 2.6B**) which is related to the presence of Fe^{2+}, well known for its NIR absorption [29]. Nevertheless, the effect is low compared to the absorbance shown

by the other cobalt containing enamels, mainly because the iron content of the substrate glasses of the period is very low (not higher than 0.2%) and part of it is present as Fe^{3+}.

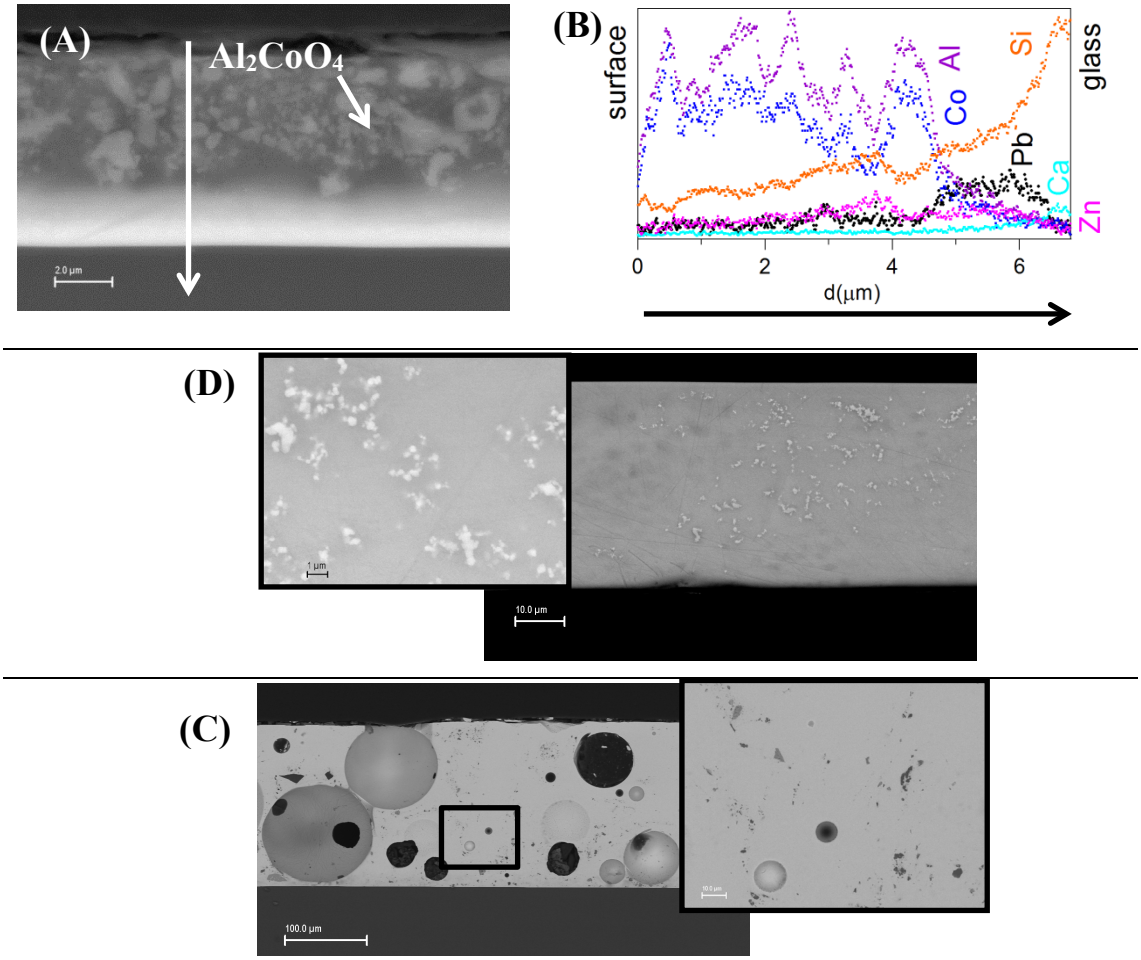

Fig. 2.22. (A) SEM-BSE image and **(B)** and SEM-EDS chemical analysis of the cross section from E33 showing the presence of Al_2CoO_4 particles. SEM-BSE image of a cross section from **(C)** E122 and **(D)** E114.

Another interesting aspect is that the $CoAl_2O_4$ particles have low density (3.8 g/cm^3) compared to the glass. This is why the particles tend to float and accumulate on the surface (**Fig. 2.22A**). An interesting consequence of this is that the enamel shows a layered structure, with a lead rich layer at the enamel-glass interface (~54% PbO and negligible amounts of boron as total SEM-EDS analysis add to 98%) (**Fig. 2.22B**).

This effect can also be seen although to a lesser extent in the green enamel E34 which contains $CoCr_{0.6}Al_{1.4}O_4$ particles (density ~4.7 g/cm^3) with a lead rich interface layer (~48% PbO and negligible amounts of boron), **Figure 2.19A**. It does not occur in enamels with particles of $PbO{\cdot}Pb(CrO_4)$ or CdSSe (density of 5.3 g/cm^3 and 5.1 g/cm^3 respectively) (**Fig. 2.12A** and **2.13A)** or in particle free enamels (**Fig. 2.14B**).

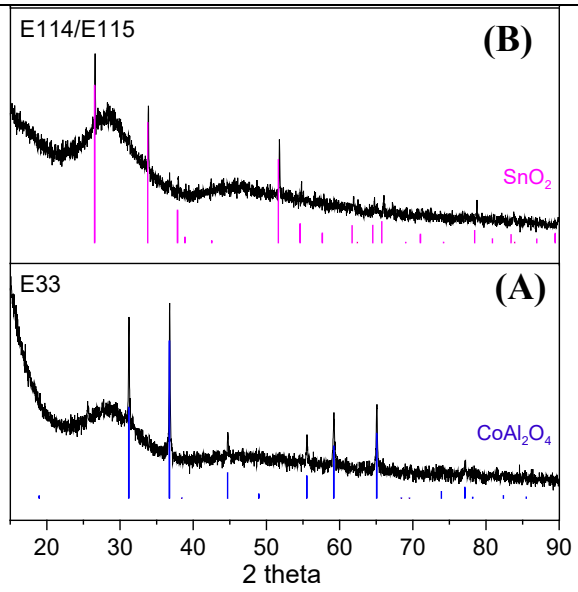

Fig. 2.23. XRD pattern from **(A)** E33 and **(B)** E114.

- Grisaille

The analysed 19th century *grisaille* (G1) is a high lead glass (≈71% PbO) to which iron oxide (haematite, Fe_2O_3) and manganese oxide particles (pyrolusite, MnO_2) are added (**Fig. 2.24**) [30]. Although haematite particles are still the main crystalline compound after firing, the particles react to form bixbyite, $(Fe,Mn)_2O_3$, and jacobsite, Fe_2MnO_4, and with the lead oxide to form melanotekite, $Pb_2(Fe,Mn)_2(Si_2O_7)O_2$ (**Fig. 2.24B** and **C**). Mn^{4+} is reduced, first to Mn^{3+} (in bixbyite and in the lead silicate) and finally to Mn^{2+} (in the spinel structure), although all the structures may accept mixed valences. The colour is opaque dark red (h^* = 45.3º, L^* = 40.4%) (**Table 2.3)**.

As shown in **Fig. 2.24** and opposite to the green and blue enamels, the *grisaille* does not show a layered structure with floating particles as the density of the particles (melanotekite, 5.7 g/cm^3, haematite, 5.3 g/cm^3 and bixbyite 5.1 g/cm^3) is comparable to those of the glass.

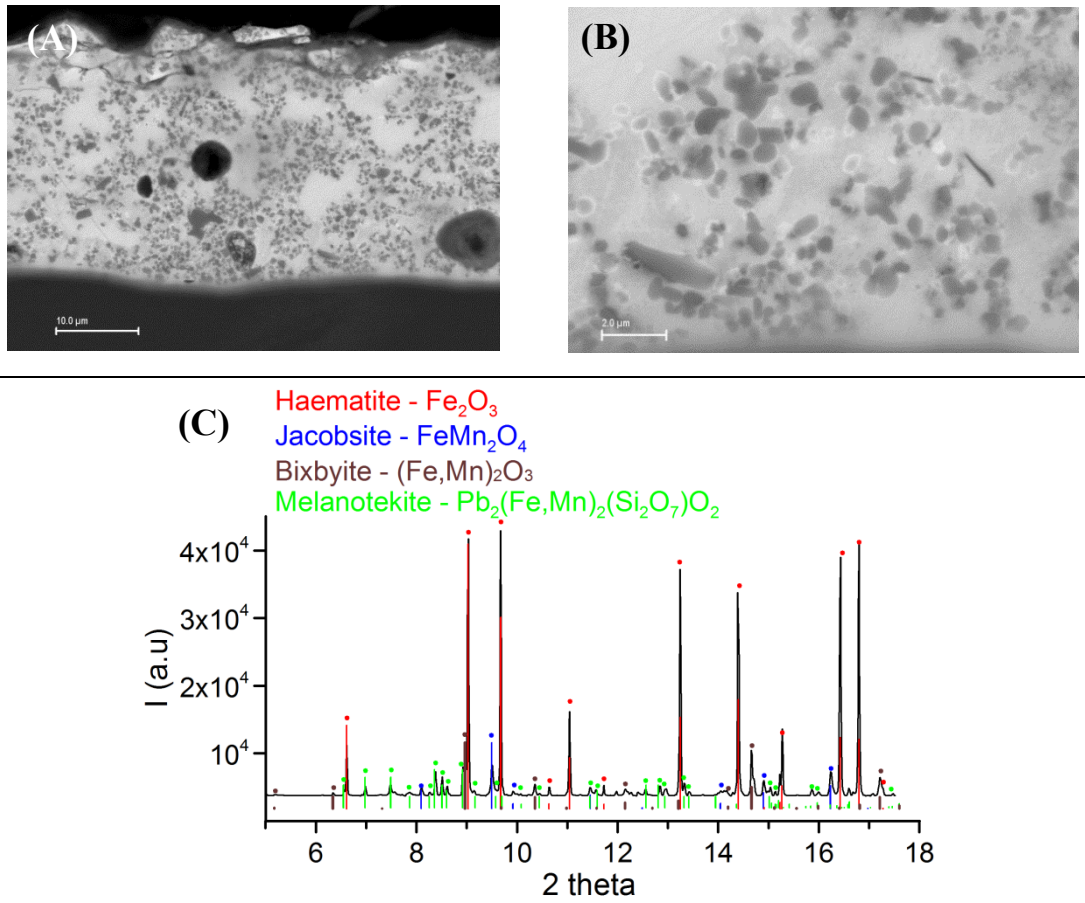

Fig. 2.24. (A) and **(B)** SEM-BSE images and **(C)** µ-XRD pattern from the grisaille G1. Melanotekite is seen as white precipitates around the darker grey iron oxide particles in the SEM-BSE image.

2.4. Silver stains

J.M. Bonet Vitralls S.L. had also a collection of silver stains (see **Fig. 2.25**) from different companies: one of them from *l'Hospied* (E97) and dated from the *Modernist* period, two from *Harshaw-Poulenc-Coiffe* (E39 and E86) of undefined date, but most probably from the 2nd half of the 20th century, and one from Bonet's workshop (E38) also dated from the second half of the 20th century.

As we have described in the **Introduction**, silver stains are not enamels. They consists in a micrometric layer made mainly of silver metallic nanoparticles within the glass surface formed by the reaction between a paint (silver and copper compounds dispersed in a medium) and the glass when fired at a low-temperature, above the *glass transition temperature* but below the *softening point* of the glass, to allow the ionic exchange of

silver/copper ions of the paint (Ag^+, Cu^+) by sodium and/or potassium (Na^+, K^+) ions from the glass. Silver diffuse inside the glass and finally, is reduced to the metallic state and form small metallic silver nanoparticles. The paint is rubbed off after firing, while the silver/copper nanoparticles are kept embodied into the glass surface. Considering the *glass transition temperature* of the *Modernist* period glass, about 575ºC, or slightly lower, the typical firing temperature should be set just below 600ºC, similar to the enamels firing temperature, probably lower than the *grisaille* firing temperature.

Fig. 2.25. Silver stain powders. Pict.: G. Molina.

Consequently, the stain powders before firing have a composition different from the stains themselves. The LA-ICP-MS analysis of the silver stain powders are shown in **Table 2.5** and the XRD patterns in **Fig. 2.26**. We can see that there are two types of silver stains [31], one which contains clay minerals and iron oxide (haematite) (E38 and E39) and a second type which contains sodium nitrate and/or sulphate and copper oxide (E86 and E97). Both incorporate silver either as silver sulphide (E38 and E86) or silver chloride (E39 and E97).

Table 2.5 Silver stains powder chemical composition (sulphur and chlorine were not measured). HPC: Harshaw-Poulenc-Coiffe

Ref.	company	Period	wt%										
			Na_2O	MgO	Al_2O_3	SiO_2	P_2O_5	K_2O	CaO	TiO_2	Fe_2O_3	CuO	Ag_2O
PE38	Bonet	20th c.	1.1	1.25	11.6	44.0	0.36	2.64	0.76	0.64	30.8	0.27	6.05
PE39	HPC	20th c.	0.12	0.61	17.1	46.3	0.48	1.35	0.27	0.79	14.8	0.00	17.9
PE86	HPC	20th c.	4.3	0.03	0.21	1.58	0.02	0.03	0.15	0.01	0.53	41.3	48.7
PE97	L'Hospied	Modernist	19.2	0.01	0.04	0.35	0.00	0.02	0.07	0.01	0.17	69.5	10.1

Sample	ppm														
	B	V	Cr	Mn	Co	Ni	Zn	As	Rb	Sr	Zr	Sn	Sb	Ba	Pb
PE38	319	250	122	493	22	50	551	295	119	71	33	20	50	562	252
PE39	132	121	126	138	16	32	178	41	104	160	111	17	11	812	201
PE86	4	0	1	1	2	29	17	30	0	0	4	15	115	0	9
PE97	111	2	24	18	12	550	440	430	0	2	20	300	2211	23	234

The first type has what we can consider the traditional composition. That is, the silver and copper salts are dispersed in a clay medium enriched with iron oxides. The second type, is a new type, probably invented in the 19th century.

Considering the composition of the two silver stain powders, the following aqueous solutions might have been prepared to obtain E86 and E97.

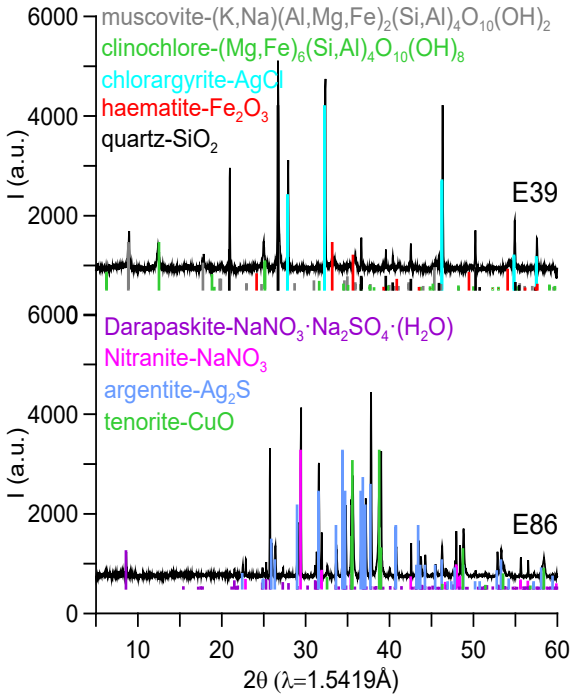

Fig. 2.26. XRD patterns corresponding to the silver stain powders E39 and E86.

To produce E97:

$$AgNO_{3(aq)} + NaCl_{(s)} \rightarrow NaNO_{3(aq)} + AgCl_{(s)} \quad (2.3)$$

The copper oxide was probably added to the precipitate.

To produce E86:

$$2AgNO_{3(aq)} + 3NaOH_{(aq)} + CuSO_{4(s)} \rightarrow 2NaNO_{3(aq)} + NaSO_{4(aq)} + Cu(OH)_{(s)} + AgOH_{(s)} \quad (2.4)$$

After drying, copper hydroxide will be transformed into copper oxide while silver hydroxide into silver sulfide.

After firing the powder residue has to be removed. E38 and E39 leave a red opaque residue (mainly the clay), E86 a black opaque residue (silver sulfide) and E97 a whitish transparent (translucent) residue.

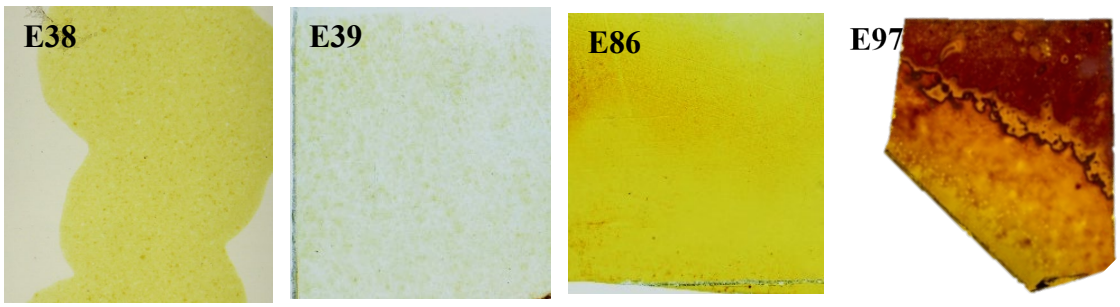

Fig. 2.27. Silver stain layers obtained.

The corresponding silver stains obtained are shown in **Fig. 2.27**. A micrometric (between 20-50 μm thick) layer of the glass incorporates silver and/or copper by ionic exchange, therefore, sodium and/or potassium are removed from the glass. The chemical composition of the silver stain surface (**Table 2.6)** is those of the glass with less sodium and/or potassium and incorporating silver and/or copper. E86 has a composition slightly different because the substrate glass was first attacked with an acid which removed some of the SiO_2 and produced a rough surface. The silver stain layer contains metallic silver nanoparticles while copper appears mainly dissolved in the glass, as is shown in **Fig. 2.28**. Nevertheless, depending on the amount of copper and silver incorporated into the glass (thickness of the paint) and on the firing temperature and atmosphere, metallic copper or cuprite nanoparticles can also precipitate. The X-ray diffraction patterns (**Fig. 2.28**) corresponding to the silver stains show in all the cases the presence of metallic silver, a smaller a broader peak for E38 and E39 than for E86 and E97. In the case of the red area of E97 a small amount of cuprite is also observed. However, although a large amount of copper is present in the powders of E86 and E97, it appears to penetrate into

the glass to a very limited extend. Nevertheless, the presence of copper is known to favour the growth of the silver nanoparticles in the glass. Copper is known to act as a reducing agent for silver, as it is more easily oxidised. In fact, some antimony and tin are also present in larger amounts in E97, they are also known as reducing agents [31].

Table 2.6 Silver stain chemical composition (sulphur and chlorine were not measured).

Ref.	Color	company	wt%											
			Na_2O	MgO	Al_2O_3	SiO_2	P_2O_5	K_2O	CaO	TiO_2	Fe_2O_3	CuO	Ag_2O	PbO
GL2	t	1950 glass	13.4	4.22	0.71	74.5	0.01	0.14	6.50	0.05	0.12	0.00	0.00	0.00
E38	y	Bonet	11.9	4.80	1.11	72.5	0.02	0.42	6.70	0.05	0.10	0.60	1.63	0.11
E39	y	HPC	12.3	4.15	0.70	74.3	0.01	0.30	6.53	0.05	0.14	0.00	1.40	0.02
E86	y	HPC	11.2	3.80	0.90	68.6	0.02	0.56	7.54	0.05	0.17	1.54	4.08	1.41
E97	o/r	L'Hospied	0.42	4.07	0.93	57.3	0.04	0.20	6.42	0.01	0.05	17.6	12.9	0.02

The colours of the silver stains obtained vary depending on various parameters; the composition (silver to copper ratio), the nature of copper compounds (dissolved as Cu^{2+}, Cu^{+}, cuprite nanoparticles or metallic copper nanoparticles), size of the nanoparticles, index of refraction of the glass, particle density and thickness of the layer. In fact, the silver stains studied herewith show different colours, **Fig 2.29.** and different in Transmission than in Reflection.

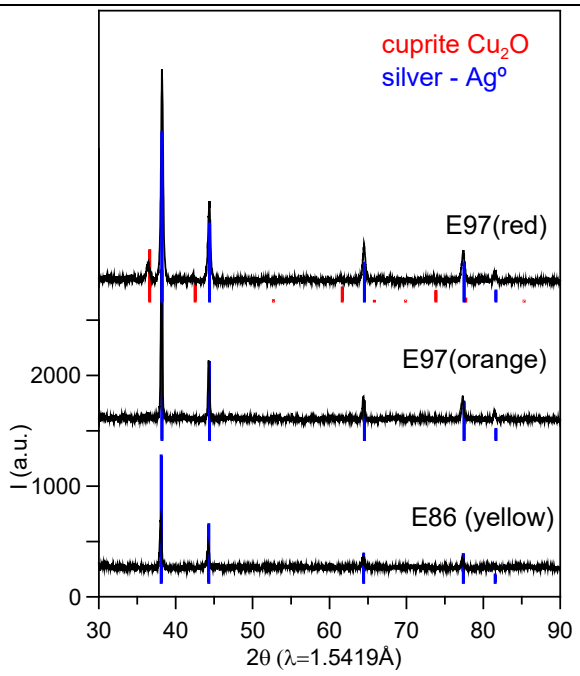

Fig. 2.28. XRD patterns from the silver stain, orange and red stains produced with E86 and E97powders.

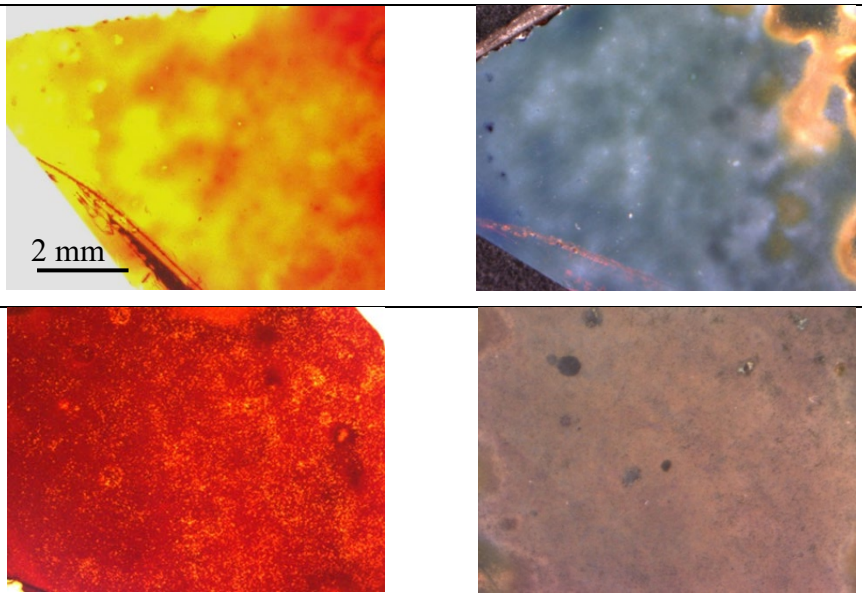

Fig. 2.29. From left to right transmission and reflection OM images from E97 (top) yellow and (bottom) red area.

One of the characteristics of the metallic nanoparticles is the narrow absorption band in the UV-Vis region related to the SPR as we have commented for the purple enamels, the colour of which is due to the presence of gold and gold-silver nanoparticles. In the case of silver stains, the colour will be due to the **absorption** and **scattering,** of the silver nanoparticles (SPR) in a soda-lime glass (refraction index $n_{glass} \sim 1.52$) which depends on the nanoparticles size. The light which is absorbed and scattered disappears from the main beam, it is extinct: **Extinction = Absorption + Scattering**. Due to the scattering, the silver stains may show a different colour in Transmission than in Reflection. The light **transmitted** through the stain is those which is **not extinct**, while the **reflected** light has also some contribution due to the **scattered** light. **Fig. 2.30A** shows the calculated Extinction, Absorption and Scattering cross sections for silver nanoparticles in a glass of $n_{glass} \sim 1.52$ as a function of the nanoparticles size. **Fig. 2.30B** shows the position of the SPR versus the width of the extinction peak and **Fig. 2.30C** the colour coordinates corresponding to the transmission calculated from the Extinction cross section as a function of the silver nanoparticles size. We can see how the colour of the silver stain layer changes from yellow-green to yellow then orange and finally red increasing the size of the silver nanoparticles.

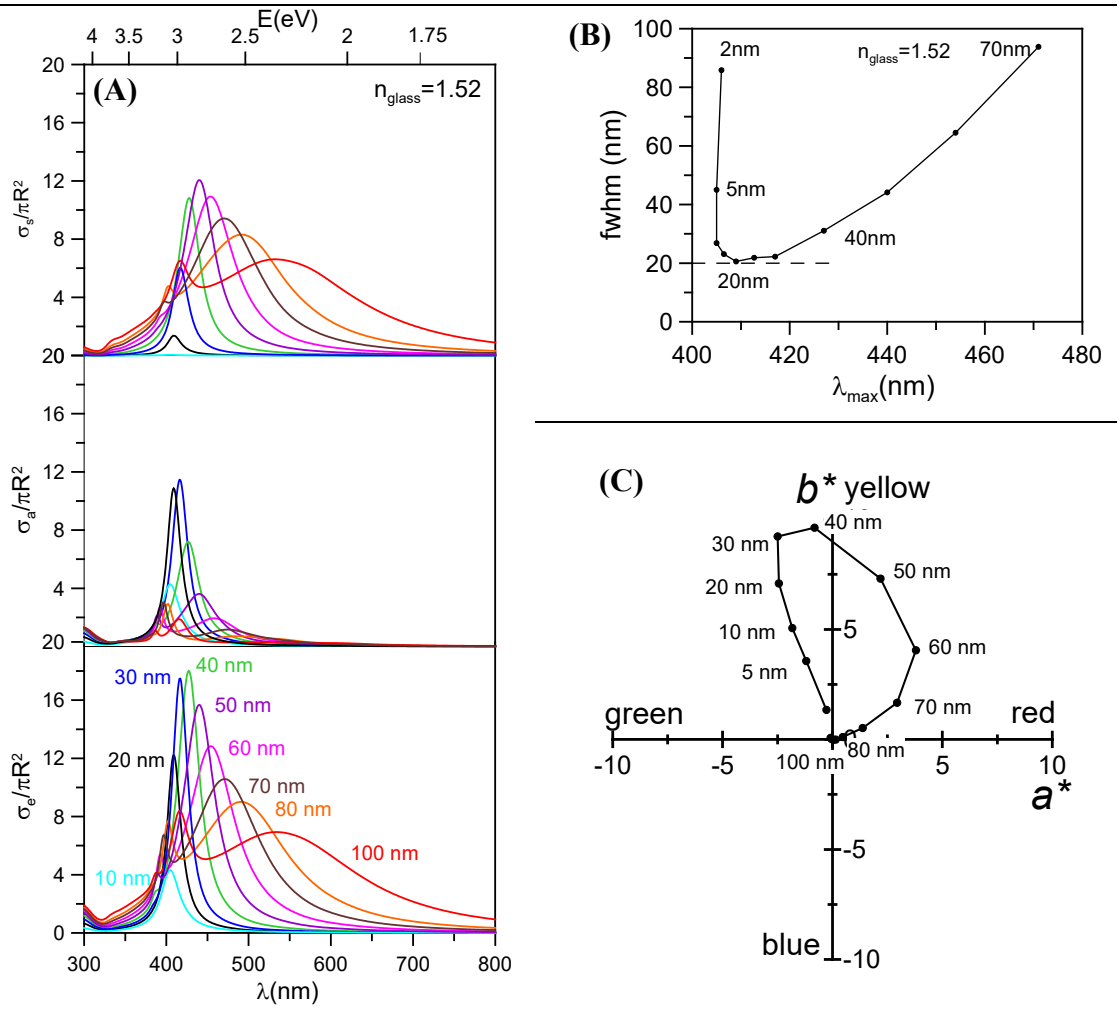

Fig. 2.30. (A) From top to bottom calculated Extinction, Absorption and Scattering cross sections, **(B)** maximum versus full with at half maximum of the Extinction and **(C)** colour coordinates calculated for the transmitted light for silver stains as a function of the silver particle size [32].

The UV-Vis OD (equivalent to Extinction) and the Reflectance spectra corresponding to the silver stains are shown in the **Fig. 2.31**. A large absorption band between 412 nm and 460 nm is observed in all the cases. These peak positions correspond, looking at the calculated data (**Fig. 2.30**), to 10 nm and 40 nm particle sizes respectively. For particle size ≥ 40 nm the scattering becomes more important than the absorption. The stains have a broad peak indicating that they have a distribution of particle sizes. This is the reason why in the Reflectance spectra both absorption and scattering are observed, but absorption dominates for E38, scattering dominates for E86 and E97 while both are similar for E39. For E97(red) the scattering is shifted to very large wavelengths (above 500 nm) which indicates the presence of very large particles (~70-80 nm).

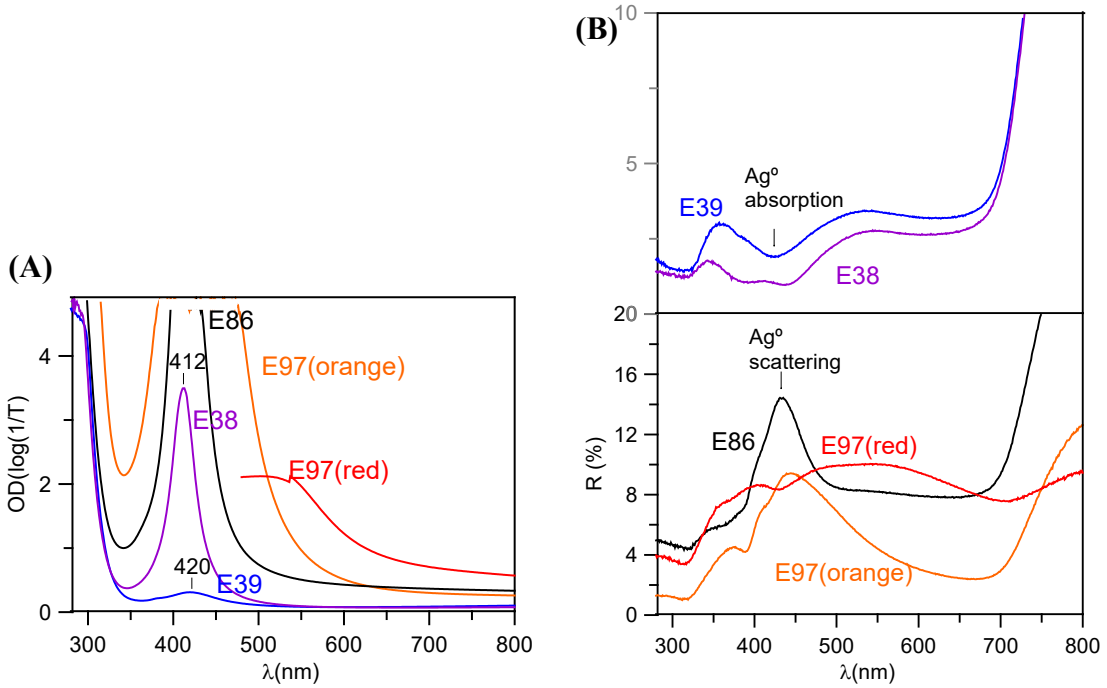

Fig. 2.31. UV-Vis (**A**) Extinction and (**B**) Reflectance spectra corresponding to the silver stains from the *Rigalt, Granell & cia* workshop.

The colour coordinates are calculated from both the transmission and reflection spectra and shown in **Fig. 2.32** and **Fig. 2.33** respectively. In fact, E38 and E39 show the same colour, yellow with a slight green component, in transmission and reflection while E86 is yellow in transmission and violet in reflection, and E97 shows two colours, orange in transmission and blue in reflection and red in transmission and brown in reflection.

(A)

	Reflection					
	*L**	*a**	*b**	*c**	*h**	*s**
E38	20.3	-5.0	12.3	13.2	112	55
E39	21.1	-3.3	6.4	7.2	118	32
E86	19.3	6.5	-7.3	9.8	312	45
E97 red	37.4	-3.2	2.2	3.9	145	10
E97 orange	25.3	-1.6	-17.2	17.3	265	56

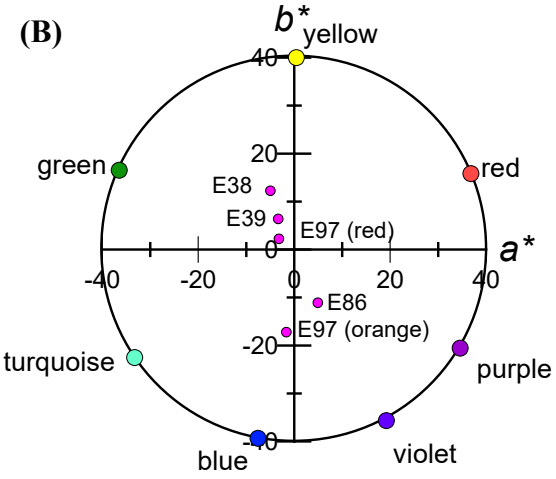

Fig. 2.32. (A) Colour coordinates and (**B**) colour wheel of the silver stains measured in Reflection.

(A)

Transmission						
	*L**	*a**	*b**	*c**	*h**	*s**
E38	90.9	-12.9	50.0	51.6	105	49
E39	92.3	-5.2	15.8	16.6	108	18
E86	61.8	-2.3	67.1	67.2	92	74
E97 red	138.3	34.9	78.0	85.5	66	53
E97 orange	26.0	29.3	21.2	36.2	36	81

(B)

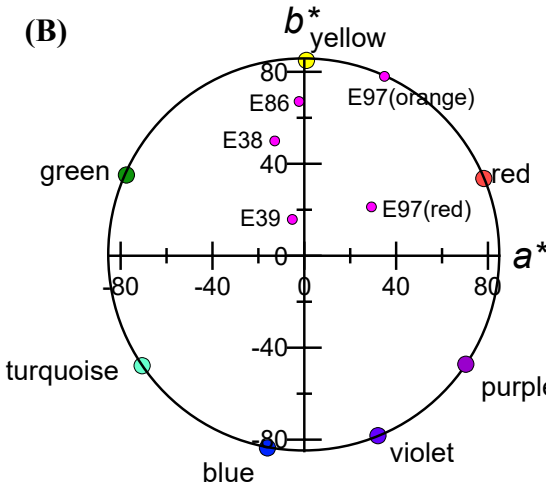

Fig. 2.33. (A) Colour coordinates and (**B**) colour wheel of the silver stains measured in Transmission.

2.5. Conclusions

The study of a collection of the enamels used by one of the most important glazier workshops of the period in Barcelona, *Rigalt, Granell and cia*, has unveiled the nature of these enamels. Using a selection of the raw materials from the *Rigalt & Granell* workshop, blue, green, yellow, purple and red enamels as well as a *grisaille* were obtained and analysed to determine their chemical composition, pigment particles, colourants and microstructure. The enamels are made of a high lead-zinc borosilicate glass, most of them with composition, in mol%, $30PbO+20SiO_2+30B_2O_3+20ZnO$, although some variations exist; they are mixed with a wide variety of colourants and pigment particles. The enamel glass composition range is characterised by a low firing temperature while maintaining a reasonable stability against chemical corrosion, in particular water corrosion.

A glassy compound, *flux*, which apparently was added to the enamels when necessary to improve their adherence to the substrate glass has also been studied. The *flux* is a high lead borosilicate glass, 60 mol% PbO, with 20 mol% B_2O_3, 20 mol% SiO_2 and little ZnO. A composition outside the limits of high-lead borosilicate glass stability.

Finally, the grisaille glassy phase is a typical high lead glass with eutectic composition (40 mol% PbO) characterised by its high refractive index, low viscosity, and a large variation in viscosity with temperature.

The purple pigment is a s tin rich suspension of small “drops” containing small (≈10 nm) gold or gold-silver nanoparticles, commonly known as purple of Cassius.

Different pigments/colourants have been identified in the red enamels, one contains cadmium selenium sulphide particles, a second contains basic lead chromate particles and a third which contains dissolved Mn^{3+} ions.

Three of the yellow enamels contain Cr^{6+} ions and the fourth lead antimony-tin oxide particles with pyrochlore structure.

Different pigments/colourants have been identified in the green enamels, one contains cochromite particles, a spinel of cobalt and chromium, plus lead antimony-tin oxide particles, the second Cu^{2+} ions and the third contains Co^{2+} in tetrahedral coordination (CoO_4) and chromium (Cr^{3+}) ions dissolved in the glass.

All the blue enamels contain cobalt either as particles of a cobalt aluminate with a spinel structure $CoAl_2O_4$ or Co^{2+} in tetrahedral coordination (CoO_4) dissolved in the glass.

In some of the enamels, opacity is increased adding tin oxide, cassiterite, particles.

Silver stains, a 20-50 μm thick surface glass layer with silver nanoparticles, were obtained from different recipes giving rise to diverse nanoparticle sizes and, consequently, colour: light yellow, deep yellow, orange and red. Copper is also present in the layer but mainly as Cu^{+} or Cu^{2+} dissolved in the layer. Only in one of the silver stains cuprite nanoparticles are formed.

The study showed that the presence of some pigment particles with a density lower than that of the enamel glass resulted in the formation of a layered microstructure, with large particles floating closer to the surface while the enamel-substrate glass interface was lead-rich (~54 % PbO and negligible amounts of B_2O_3). This phenomenon was particularly pronounced in the blue and green enamels that contain cobalt and chromium cobalt aluminate particles ($CoAl_2O_4$ and $Co(Cr,Al)_2O_4$), respectively. Moreover, the cobalt ions both in the form of cobalt (chromium) aluminate particles and in solution are in tetrahedral coordination (CoO_4) which is responsible for the characteristic absorption in the red and Near Infrared regions. Other chromophores also show absorption in the NIR range: Cu^{2+} in some green enamels, Fe^{2+} and Mn^{3+}-Mn^{2+} often present in the *grisailles* but also in some purple enamels.

The combination of the layered microstructure and the high absorption in the NIR may be responsible for the enhanced alteration that has been widely described in relation to the blue and green enamels as well as in some *grisailles*. The enhanced absorbance of particles and colour centres in the enamel would be responsible for the increase in the

overall temperature of the enamel submitted to solar irradiation, as well as for the thermal mismatch between pigment particles, enamel glass and substrate glass. Thermal stresses will cause the formation of cracks due to the mismatch in the thermal expansion coefficients, and a faster/greater deterioration of the enamels. The natural corrosion expected to happen in all the enamels due to weathering conditions and cleaning (mainly water corrosion) is expected to be more substantial in the layered enamels, at the same time that solar irradiation increase the thermal induced damage.

2.6. References

[1] B. Gratuze, J. Blet-Lemarquand, J.N. Barrandon, Mass Spectrometry with laser sampling: A new tool to characterize Archaeological materials, J. Radioanal. Nucl. Chem. 247 (2001) 645–656.

[2] A.J. Shortland, N. Rogers, and K. Eremin, Trace Element Discriminants between Egyptian and Mesopotamian Late Bronze Age glasses, J. Archaeol. Sci., 34 (2007) 781–789.

[3] F. Fauth, I. Peral, C. Popescu, M. Knapp, The new material science powder diffraction beamline at ALBA synchrotron, Powder Diffr. 28 (2013) 360–370.

[4] O. Vallcorba & J. Rius. d2Dplot: 2D X-ray diffraction data processing and analysis for through-the-substrate microdiffraction, J. Appl. Cryst. 52 (2019) 478-484.

[5] web site of the International Centre for Diffraction Data, https://www.icdd.com/.

[6] web site http://cie.co.at/.

[7] W.A. Weyl, Coloured glasses, Society of Glass Technology, Sheffield, 2016.

[8] W. Vogel, Glass chemistry, Springer Verlag, Berlin, 1992.

[9] T.S. Petrovskaya, Properties of lead borosilicate glasses: The effect of the structure. Glass Ceram. 54(11–12) (1997) 347–350.

[10] M.P. Brungs, E.R. Cartney, Structure of sodium borosilicate glasses, Phys. Chem. Glasses 16 (1975) 48-52.

[11] D. Möncke, G. Tricot, A. Winterstein-Beckmann, L. Wondraczek, E.I. Kamitsos, On the connectivity of borate tetrahedra in borate and borosilicate glasses, Phys. Chem. Glasses 56(5) (2015) 203-211.

[12] D. Möncke, E.I., Kamitsos, D. Palles, R. Limbach, A. Winterstein-Beckmann, T. Honma, et al., Transition and post-transition metal ions in borate glasses: Borate ligand speciation, cluster formation, and their effect on glass transition and mechanical properties, J. Chem. Phys. 145(12): 124501 (2016)

[13] J.M. Wu, H.L. Huang, Microwave properties of zinc, barium and lead borosilicate glasses, J. Non-Cryst. Solids 260 (1999) 116-124.

[14] S. Kohara, H. Ohno, M. Takata, T. Usuki, H. Morita, K. Suzuya, et al., Lead silicate glasses: Binary network-former glasses with large amounts of free volume, Phys. Rev. B. 82 (2010) 134209.

[15] P.W. Wang, L. Zhang, Structural role of lead in lead silicate glasses derived from XPS spectra. J. Non-Cryst. Solids. 194 (1996) 129-134.

[16] L.B. Hunt, The True Story of Purple of Cassius. The birth of gold-based glass and enamel colours, Gold Bulletin 9 (1976) 134-139.

[17] D. Mahl, J. Diendorf, S. Ristig, C. Greulich, Z.A. Li, M. Farle, M. Köller, M. Epple, Silver, gold, and alloyed silver–gold nanoparticles: characterization and comparative cell-biologic action, J. Nanopart. Res. 14 (2012) 1153-1155.

[18] A. Lacroix, Des couleurs vitrifiables et de leur employ pour la peinture sur porcelain, faience, vitraux (About the glassy colours and their use for the painting on porcelain, faience, stain glass), Chez A. Lacroix, Paris, 1872.

[19] J. Vila-grau, F. Rodon, Els vitrallers de la Barcelona Modernista, Edicions Polígrafa S.A., Barcelona, 1982.

[20] M.W. Murphy, Y.M. Yiu, M.J. Ward, L. Liu, Y. Hu, J.A. Zapien, Y.K. Liu, T.K. Sham, Electronic structure and optical properties of CdSxSe1−x solid solution nanostructures from X-ray absorption near edge structure, X-ray excited optical luminescence, and density functional theory investigations, J. App. Phys. 116 (2014) 193709.

[21] F. Welz, Patent No. 417.676, Unites States, 1892.

[22] F. A. Kirkpatrick, George G. Roberts, Production Of Selenium Red Glass, Journal of the American Ceramic Society, Volume2, Issue11 (1919) 895-904.

[23] H. Kühn and M. Curran, Artists' Pigments: a handbook of their history and characteristics, vol. 1 (1986) 208–211.

[24] V. Otero, L. Carlyle, M. Vilarigues, M.J. Melo, Chrome yellow in nineteenth century art: historic reconstructions of an artists' pigment. RSC Adv., 2(5) (2012) 1798–1805.

[25] O. Villain, G. Calas, L. Galoisy, L. Cormier. XANES determination of chromium oxidation states in glasses: comparison with optical absorption spectroscopy, J. Am. Ceram. Soc. 90(11) (2007) 3578–3581.

[26] G. Molina, G.P. Odin, T. Pradell, A.J. Shortland, M.S. Tite, Production technology and replication of lead antimonate yellow glass from New Kingdom Egypt and the Roman Empire, J. Archaeol. Sci. 41 (2014) 171-184.

[27] I.N.M. Wainwright, J.M. Taylor, R.D. Harley, Lead Antimonate Yellow, Artists Pigments: a handbook of their history and characteristics, vol. 1 (1986) 219–254.

[28] W. Zheng, J. Zou, Synthesis and characterization of blue TiO2/CoAl2O4 complex pigments with good colour and enhanced near-infrared reflectance properties, RSC Advances 5(107) (2015) 87932.

[29] M. Ookawa, T. Sakurai, S. Mogi, T. Yokokawa, Optical spectroscopic study of lead silicate glasses doped heavily with iron oxide. Mater. Trans.-JIM 38 (1997) 220–225.

[30] T. Pradell, G. Molina, S. Murcia, R. Ibañez, C. Liu, J. Molera, A.J. Shortland, Materials, Techniques, and Conservation of Historic Stained Glass "Grisailles", Int. J. Appl. Glass Sci. 7(1) (2016) 41–58.

[31] T. Pradell, Lustre and nanostructures – Ancient technologies revisited, Nanoscience and Cultural Heritage, Springer – Atlantic Press (2016) 3-39.

[32] G. Molina, S. Murcia, J. Molera, C. Roldan, D. Crespo, T. Pradell, Color and dichroism of silver-stained glasses, Journal of Nanoparticle Research, 15(9) (2013).

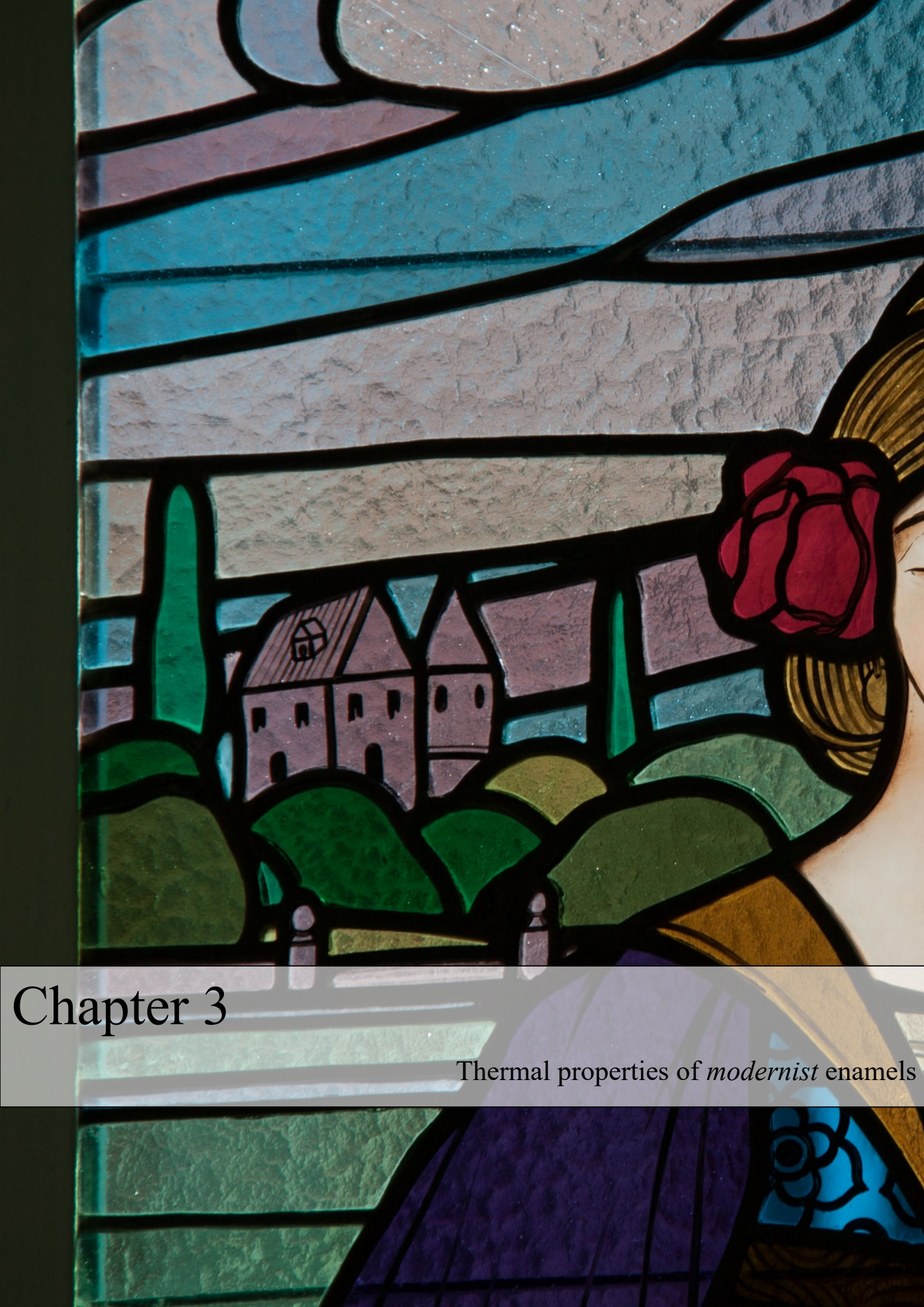

Chapter 3

Thermal properties of *modernist* enamels

Chapter 3

Thermal properties of *modernist* enamels

One of the main issues in the conservation of the paint layers (enamels and *grisailles*) is the quality of their adherence, and this depends directly on the thermodynamic properties of both substrate glass and paint layers. In fact, an adequate firing temperature range is essential for a correct adherence of the paints to the contemporary substrate blown glass. As shown previously, *modernist* enamels and *grisailles* have two different parts. On one hand, the colouring part consisting on transition metals and pigment particles On the other hand, the vitreous part which is constituted by a high lead-zinc borosilicate glass for the enamels and a high lead glass for the *grisailles* determines some of the physical properties of the paints of relevance, such as, the temperature dependence of the viscosity and density. Nevertheless, the first and more important thermal properties are the glass transition, deformation and softening temperatures.

3.1. The glass transition (T_g), deformation (T_d) and softening (T_s) temperatures

A particles system is in a metastable state if a small increase in the potential energy results in a change of its state [1]. An example is the undercooled state obtained when some liquids can be held at temperatures below their freezing point without crystallizing. In the case of our study, one of the most important characteristics or properties of the glasses is the temperature's range in which a cooled metastable melt transforms gradually into a vitreous material [2]. The transition from the undercooled melt (in metastable thermodynamic equilibrium) to the configurationally frozen glassy state is known as *glass transition*. It is determined experimentally as a *glass transition temperature* (T_g), which can be defined as the highest temperature at which the system can no longer reach its equilibrium state within the time scale of the experiment [3]. Above the *glass transition* temperature, the material is still a liquid state, below the glass transition temperature, it becomes solid (glass).

Viscosity is an important property of a fluid, and usually is defined as the resistance of a fluid to a change of shape due to the friction with another material. Above the glass transition temperature, the glass still behaves like a liquid, with a viscosity log(Pa·s)) ~ 12.3.[1] [4]. Below the glass transition temperature, the glass behaves like a solid. Consequently, thermodynamic properties, such as the density, diffusivity, heat capacity among other change abruptly at the *glass transition* temperature (**Fig. 3.1**). The relaxation theory describes the variation of the properties of the glass upon transition from the high viscosity liquid-state to the vitreous solid-state during cooling and the reverse transition during heating. Gustav Tammann was the first academic, late 1920, to work the glass transition temperature (T_g) concept. He proposed to use T_1 and T_2 corresponding to the initial and final points of the heat capacity jump, known as the glass transition range in modern terminology to determine the glass transition temperature. In 1930, William E.S. Turner defined T_g in a more general way, as the temperature at which the properties of glasses jump in the course of uniform heating [2].

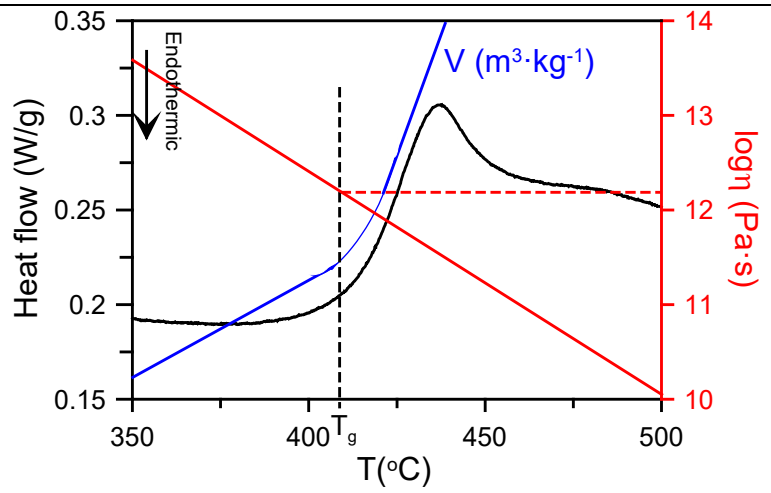

Fig. 3.1. DSC curve of an enamel with a representation of the heat flow and the specific volume, **V,** behaviour at the glass transition temperature, **T_g**.

Among the various physical properties of the glass that change at the *glass transition* temperature, we have to mention the diffusivity. The glass components diffusivity increases by several orders of magnitude above T_g. The adherence of a melt to the substrate glass requires the interdiffusion of the glass components. Consequently, in order

[1] Viscosity units on Si are Pa·s (Pa·s = 1 Kg·m^{-1}·s^{-1}), which is equal to 10 poises (P = 1 g·cm^{-1}·s^{-1}).

to have a good adherence of the molten enamel to the substrate glass, they should be heated above the *glass transition* temperature.

Once a glass is heated above T_g, it behaves like a liquid and all the properties are determined by its viscosity which depends on the temperature. The *glass deformation* point (T_d) is defined as the temperature at which the dilatation of the glass stops in a dilatometer and corresponds to a viscosity of $\log(\eta(Pa \cdot s)) = 10.5$. This point marks the beginning of the so-called *softening range*, which depends on the force applied to the glass. The highest temperature is given by the Littleton *softening point* (T_s) defined as those for which the glass deforms under its own weight: $\log(\eta(Pa \cdot s)) = 6.6$.

The working temperatures, *glass transition* (T_g), *glass deformation* (T_d) and *glass softening* temperatures (T_s) determine the range of firing temperatures necessary to obtain a correct adherence of the paint layers to the substrate glass.

On the one hand, the **enamel** should be fired at a temperature above its *softening point* to obtain a homogeneous continuous glass. On the other hand, the *glass transition* temperature of the **substrate glass** should be reached in order to ensure a good adherence of the enamel, at the same time that the *softening range* of the **substrate glass** should not be reached to avoid its deformation, see **Fig. 3.2**. Consequently, the optimal firing temperature is a compromise between the substrate glass softening and glass transition temperatures and the enamel softening temperature [5]. Moreover, if the viscosity of the enamel is too high during firing, large bubbles may be produced [6-7]. Their large surface/volume ratio is also a handicap to the enamel's preservation. It is therefore convenient to reach a temperature as high as possible (below the softening point of the substrate glass) to ensure the enamel's lowest viscosity. It is obvious that depending on the composition of the substrate glass and the enamel, these restrictions may leave a very narrow temperature range (**Fig. 3.2**).

Problems of adherence of the enamels may be related to the composition of the substrate glass. Changes in the substrate glass composition have been determined along history. The *forest glass* used between the 11th and 15th centuries characterized by high potash and lime [8]; the high lime content low alkali content glass [8-9] used between the 15th and 18th centuries [9]; the silica and soda rich glass of the 19th century with low Al_2O_3, MgO and CaO content [10] and the progressive substitution of Na_2O by CaO and of CaO by MgO at the end of the 19th century. Furthermore, the beginning of the 20th century is

characterized by the start of the production of flat glass by mechanical means that progressively substituted blown glass [11], with the consequent modification of the window glass composition to one better adapted to the needs of the mechanical process. Among all the substrate glasses, the 19th century glasses had the lowest maximum firing temperatures, a fact which has been related to the increase in the fluxing agents added to the *grisailles* which would allow to fire them at a temperature low enough to avoid damaging the substrate glass. [12]

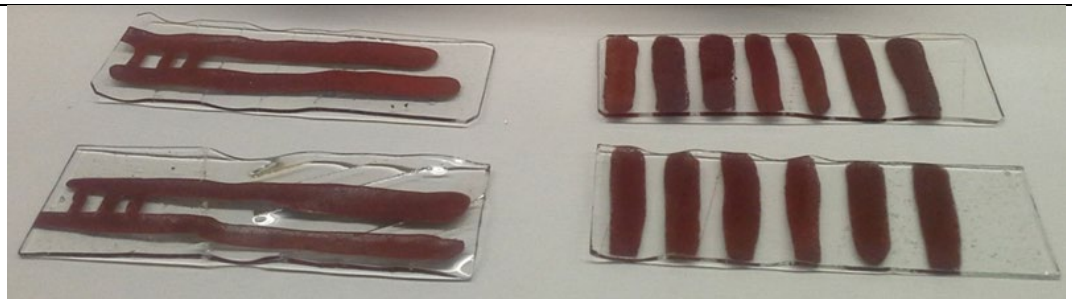

Fig. 3.2. Replicated *grisailles*. The replicas were heated up to 700 ˚C above the softening temperature of the substrate glass, which deformed under its own weight.

In this chapter, the *glass transition* and *softening range* of the enamels, *grisaille* and flux from the Rigalt i Granell workshop and substrate glasses from this period are studied and their suitability determined.

3.2. Experimental

The enamels are constituted by a glass to which colourants and pigment particles were added (**Fig 3.3.**). Nevertheless, the working temperatures of the enamels will be mainly determined by the composition of the glass component. We have seen in the previous chapter that the glass component of the enamels is a high lead and zinc borosilicate glass and a high lead glass for the *grisaille;* the workshop had also a *flux*, a glassy material supposedly used to decrease the firing temperature and increase the adherence of the paints to the substrate glass. The composition of the glass component from enamels, *grisaille* and *flux* found in the *Rigalt, Granell & cia* workshop is determined. The main glass component composition has obtained removing the contribution of the pigment

particles, colourants and impurities and leaving only the glass components SiO_2, PbO, B_2O_3 and ZnO. The results obtained are shown in **Table 3.1**.

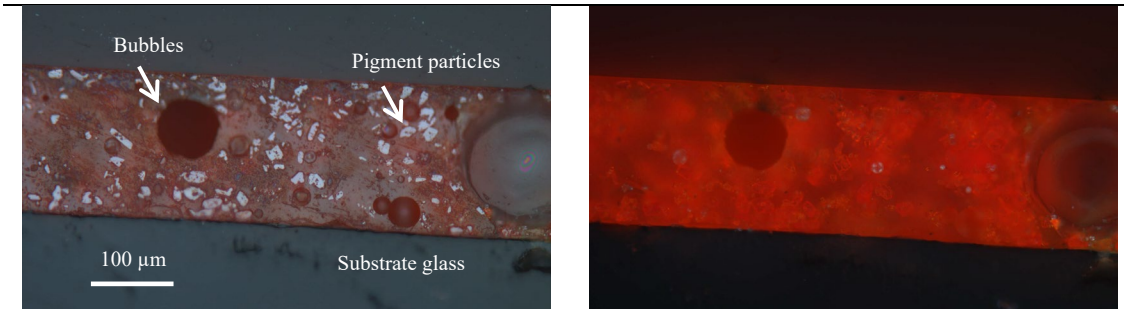

Fig 3.3. (Left) Bright field and (Right) polarized OM image from a cross section of a red enamel over a substrate glass showing the presence of pigment particles and bubbles.

Table 3.1 Chemical composition of the glass component of the workshop enamels determined after subtracting the pigment particles, colourants and impurities.

Company/After	colour	opacity	label	SiO_2	PbO	B_2O_3	ZnO
Lacroix	purple	transparent	E14	12	58	18	13
		opaque	E107	9	57	18	16
Lacroix	red	opaque	E23	13	53	15	19
		transparent	E25	8	68	13	11
		transparent	E124	8	59	19	14
Lacroix	yellow	transparent	E3	34	59	8	0
		transparent	E4	7	62	17	14
		opaque	E106	25	61	9	5
		transparent	E119	9	56	21	14
Lacroix	green	opaque	E34	15	71	12	3
		transparent	E89	9	59	18	14
		transparent	E121	7	62	16	15
Wenger	blue	transparent	E33	15	57	15	13
Lacroix		opaque	E114	9	59	16	16
		transparent	E115	8	58	19	15
L'Hospied		transparent	E122	24	72	4	0
Lacroix	flux	transparent	F1	9	81	9	0
Granell	grisaille	opaque	G1	28	72	0	0

From the data above, four main enamel glass compositions, one for the *flux* and another for the *grisaille* were determined, their chemical composition is given in **Table 3.2**. Based on this, synthetic glasses with the corresponding six compositions have been produced. The synthetic glasses were prepared using commercial reagents (SiO_2, PbO, ZnO and H_3BO_3). For the preparation, 200 g of each mixture was melted in a platinum crucible, then they heated at a rate of 5˚C/min from room temperature to 850˚C in air, and kept at this temperature for 1 h. The glasses were then cast by pouring the liquid over a cold copper surface [13-14]. Polished sections of fragments from the glasses were obtained for their analyses. Different steps of the procedure are shown in **Fig. 3.4**.

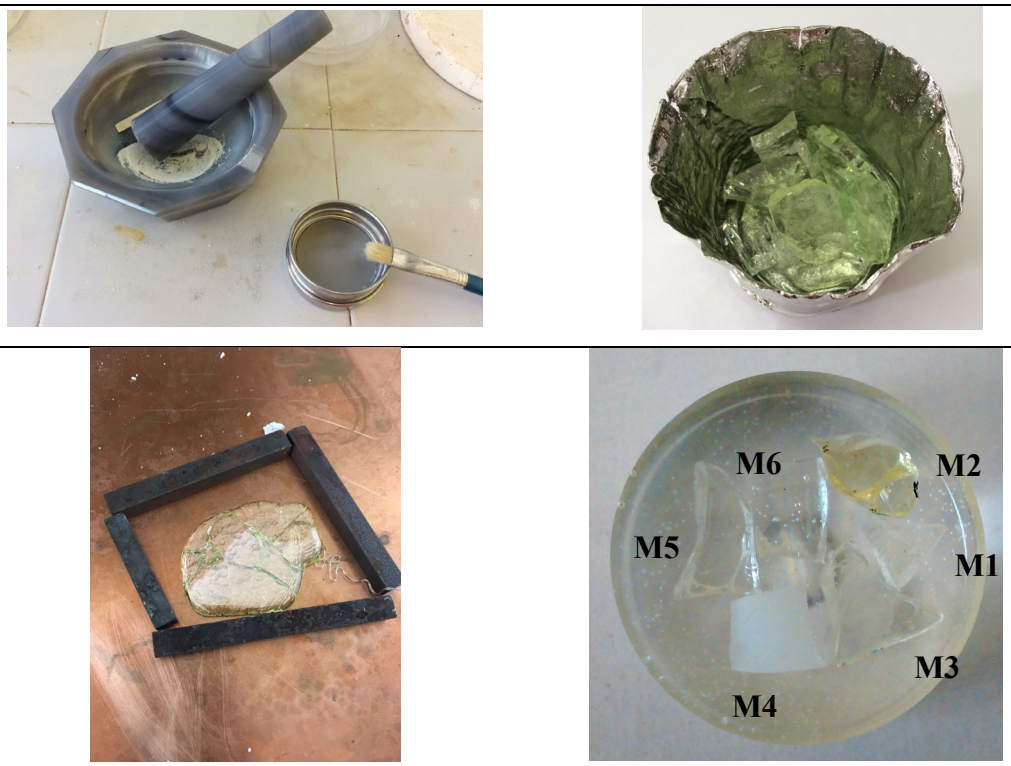

Fig. 3.4. From top-left to bottom-right, preparation of the mixtures, platinum crucible used in the melting, glass obtained pouring the liquid over a cold copper surface and polished cross sections of the synthetic glasses.

Table 3.2 Chem. composition of the synthetic glasses calculated from the workshop enamels glass composition calculated after subtracting the pigment particles, colourants and impurities.

REF.	Rigalt, Granell & cia enamels	colour/ opacity	(%wt)				(%mol)			
			SiO_2	PbO	B_2O_3	ZnO	SiO_2	PbO	B_2O_3	ZnO
M1	*grisaille* (Granell)	transparent	29	71	0	0	60	40	0	0
M2	*flux* (Lacroix)	transparent yellow	8	84	9	0	20	60	20	0
M3	Purple/red/blue/ green/yellow (Lacroix/Wenger)	transparent	11	58	18	14	20	30	30	20
M4	E106 yellow (Lacroix)	white opalescent	27	60	9	4	50	30	15	5
M5	E122 blue (l'Hospied)	transparent	24	71	6	0	50	40	10	0
M6	E34 green (Lacroix)	transparent	16	69	11	4	35	40	20	5

3.3. Analytical methodology

Thermal properties including the *glass transition* temperature and *softening range* were determined by Differential Scanning Calorimetry (DSC) and Hot Stage Microscopy (HST) respectively. The *glass transition* temperature was evaluated for the *Rigalt, Granell & cia* workshop enamels and synthetic glasses while the *softening range* has been evaluated only for the synthetic glasses.

3.3.1. Differential Scanning Calorimetry (DSC)

The glass transition temperature was determined using DSC with a Netzsch F404 Pegasus instrument. The temperature is selected from the intersection of the extensions of two approximately straight lines portions of the thermogram below and above the inflection point (**Fig. 3.5**), which is associated with the onset of the relaxation process [2]. To avoid the effects of thermal memory the sample is submitted to a first heating and cooling process, and only the second heating curve is used to estimate the glass transition temperature.

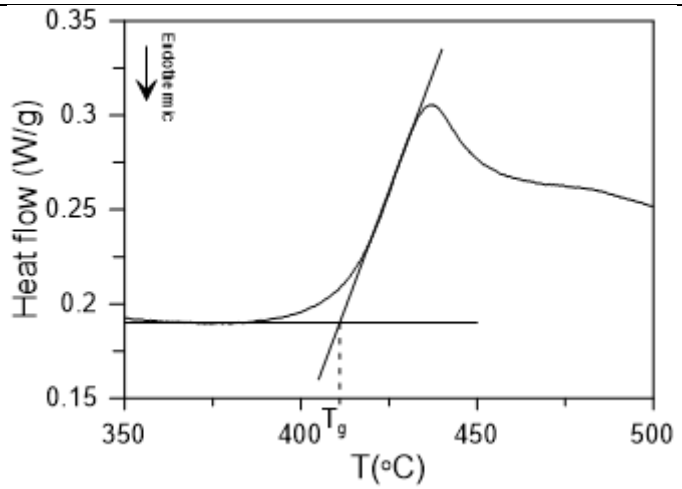

Fig. 3.5. DSC curve showing the intersection of the two straight lines used to determine the onset point corresponding to the *glass transition temperature*.

20 mg of enamel/glass powder were transferred into an alumina pan (Al_2O_3) and heated at 20˚C/min rate from room temperature to 700˚C in air, followed by an isotherm for 30 min before being cooled to 30˚C. Afterwards, the enamel was heated for a second time following the same thermal path [2,15].

3.3.2. Hot Stage Microscopy (HSM)

The behavior of glass viscosity with temperature has been determined only for the synthetic glasses with compositions equivalent to those of the glass component of the *Rigalt, Granell & cia* workshop enamels, *grisaille* and *flux* given in **Table 3.2.**

The temperatures related to fixed viscosity points in the softening range defined for Hot Stage Microscopy (HSM) according to the German rule DIN 51730 27 were determined for the synthetic enamels using the HSM equipment in the *Department de Mineralogia, Petrologia i Geologia Aplicada* of the Geology Faculty, *Universitat de Barcelona* [16]. HSM is a suitable technique to study the behavior of glass viscosity with temperature. [14,17]. The temperatures corresponding to the characteristic viscosity points were determined relative to the geometrical changes (**Fig. 3.6**) of a bloc during heating [16]. The values of the viscosity in log(η(Pa·s)) for the fixed points are: between 8.1 and 9.1 (first shrinkage), between 6.8 and 7.2 (maximum shrinkage), between 5.3 and 5.1 (softening), 4.4 (ball), between 3.1 and 3.6 (half ball) and between 2.4 and 3.1 (flow).

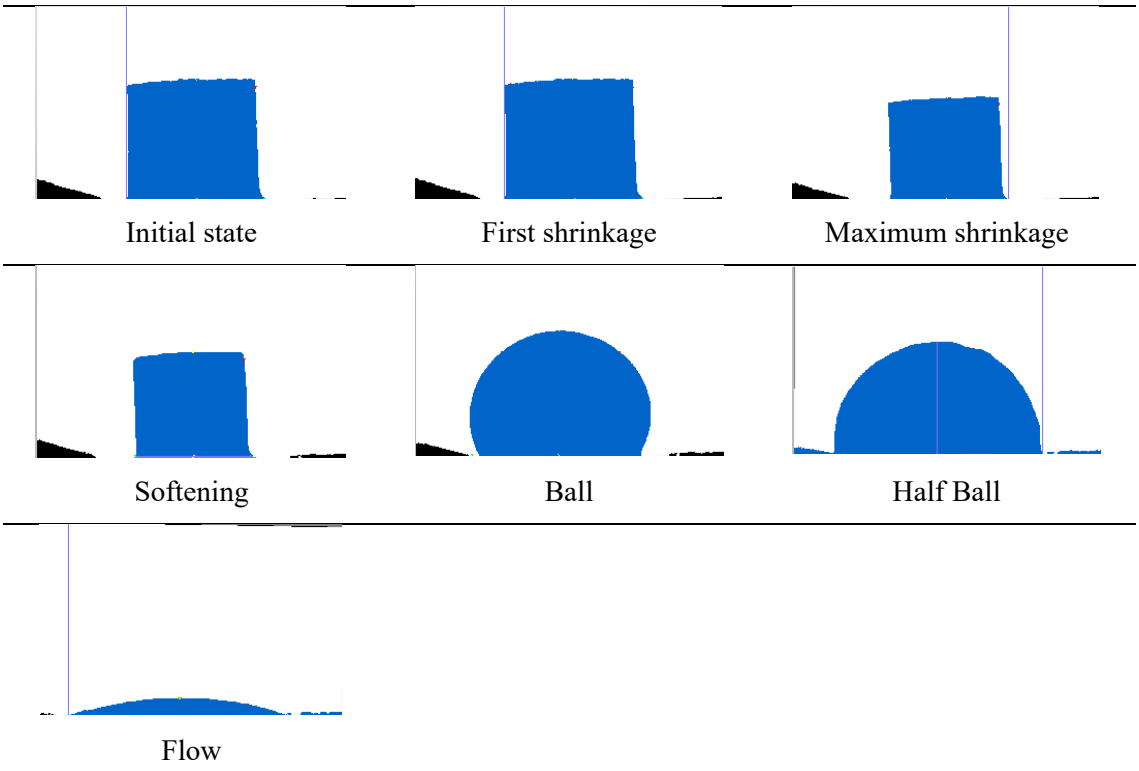

Fig 3.6. From top-left to bottom-right, Geometrical changes of the cylinder probe during heating in the HSM corresponding to given viscosity points.

The synthetic glasses were ground and sieved to obtain a fine (45 µm) powder which was mixed with a 1/20 solution of Elvacite in acetone and pressed into a cylinder (3 mm x 3 mm of diameter) in a uniaxial press. The cylinders were place in a horizontal silicon carbide furnace and heated to 800˚C with a heating rate of 7˚C/min. Pictures of the cylinder were taken every 2 min during the first part of the experiment and every 3s above 500˚C. The pictures were recorded with ProgRes Capture Pro software and the images were analyzed using the Hot-Stage software, developed by the *Departament de Llenguatges i Sistemes Informàtics, Universitat Politècnica de Catalunya*.

3.4. Results

The glass transition temperatures corresponding to the workshop enamels and synthetic glasses determined by Differential Scanning Calorimetry (DSC) are summarized in **Table 3.3**.

All the workshop enamels show a similar behavior (**Fig. 3.7**). In the first heating of the powder enamel (in red in **Fig. 3.7**) a double broad exothermic effect at the glass transition

is observed, which may be related to the heterogeneous nature of the enamel, either due to some phase separation or, more likely, to an incomplete sintering process.

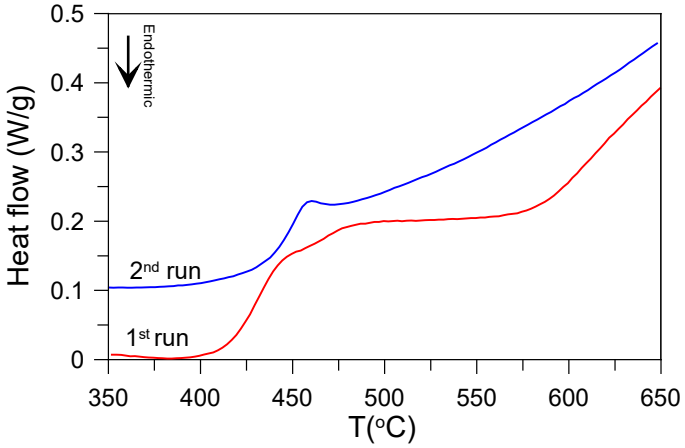

Fig. 3.7. DSC curves obtained for the enamels. The first run shows a double broad exothermic effect which indicates the heterogeneity of the enamel powder, the second run shows a homogeneous glass.

In the second heating (in blue in **Fig. 3.7**) a single exothermic effect at an intermediate temperature is then obtained, indicating that the initial double exothermic process resulted from incomplete sintering rather than the presence of a phase separation. This idea is reinforced by the fact that this phenomenon does not happen for the synthetic glasses, which in the first heating already show a single exothermic effect. The second heating DSC curves corresponding to all the workshop enamels are shown in **Fig. 3.8.**

The glass transition temperature (T_g) determined for most of the studied workshop enamels varies 420-440˚C for the other, in good agreement with those determined for all the synthetic glasses (430-448˚C). Nevertheless, some workshop enamels deviate from this: E3, E25, E89 and E122 have a low glass transition temperature varying between 402-408 ˚C. E3, E89 and E122 are characterized by having transition metals, Cr^{6+}, Co^{2+} and copper (as Cu^{+} and Cu^{2+}) respectively, completely dissolved in the glass and which act as glass modifiers [18]. On the other hand, E25 contains phoneicochroite ($PbO{\cdot}Pb(CrO_4)$) particles. Consequently, an important amount of the lead is kept in the particles the composition of glass component of the enamel is probably lead poorer than initially estimated.

Table 3.3 Glass transition temperatures measured by DSC corresponding to the workshop enamels, *grisaille*, *flux* and also to the synthetic glasses produced with compositions equivalent to the workshop enamel's composition. [1]For the substrate glasses, the *glass transition*, *deformation* and *Littleton softening* temperatures corresponding to log(η(Pa·s)) = 12.5, 10.5 and 6.6 respectively are calculated after [17].

	Company/After	colour		T_g	T_d-T_s
workshop materials	Lacroix	purple	E14	425	
			E107	439	
	Lacroix	red	E23	450	
			E25	407	
			E124	419	
	Lacroix	yellow	E3	402	
			E4	422	
			E106	444	
			E119	430	
	Lacroix	green	E34	438	
			E89	407	
			E121	428	
	Wenger	blue	E33	435	
	Lacroix		E114	441	
			E115	440	
	L'Hospied		E122	408	
	Lacroix	*flux*	F1	306	
	Granell	*grisaille*	G1	435	
Blown glass	1900 Amatller house	transparent	GL1	575[1]	613-744[1]
	1950	transparent	GL2	537[1]	581-733[1]
Synthetic glasses	*grisaille* (Granell)	transparent	M1	420	
	flux (Lacroix)	Transparent yellow	M2	299	
	purple/red/blue/ green/yellow (Lacroix/Wenger)	transparent	M3	448	
	E106 yellow (Lacroix)	white opalescent	M4	442	
	E122 blue (l'Hospied)	transparent	M5	437	
	E34 green (Lacroix)	transparent	M6	432	

The glass transition temperature of the *grisaille* is ~435˚C and of that of the *flux* ~300˚C. The values obtained are in reasonably good agreement with those measured for the corresponding synthetic glasses (~420˚C and ~299˚C) considering that the *grisaille*, some of the iron and manganese oxides react with the lead glass giving rise to the precipitation of melanotekite ($Pb_2(Fe,Mn)_2Si_2O_9$) among other compounds.

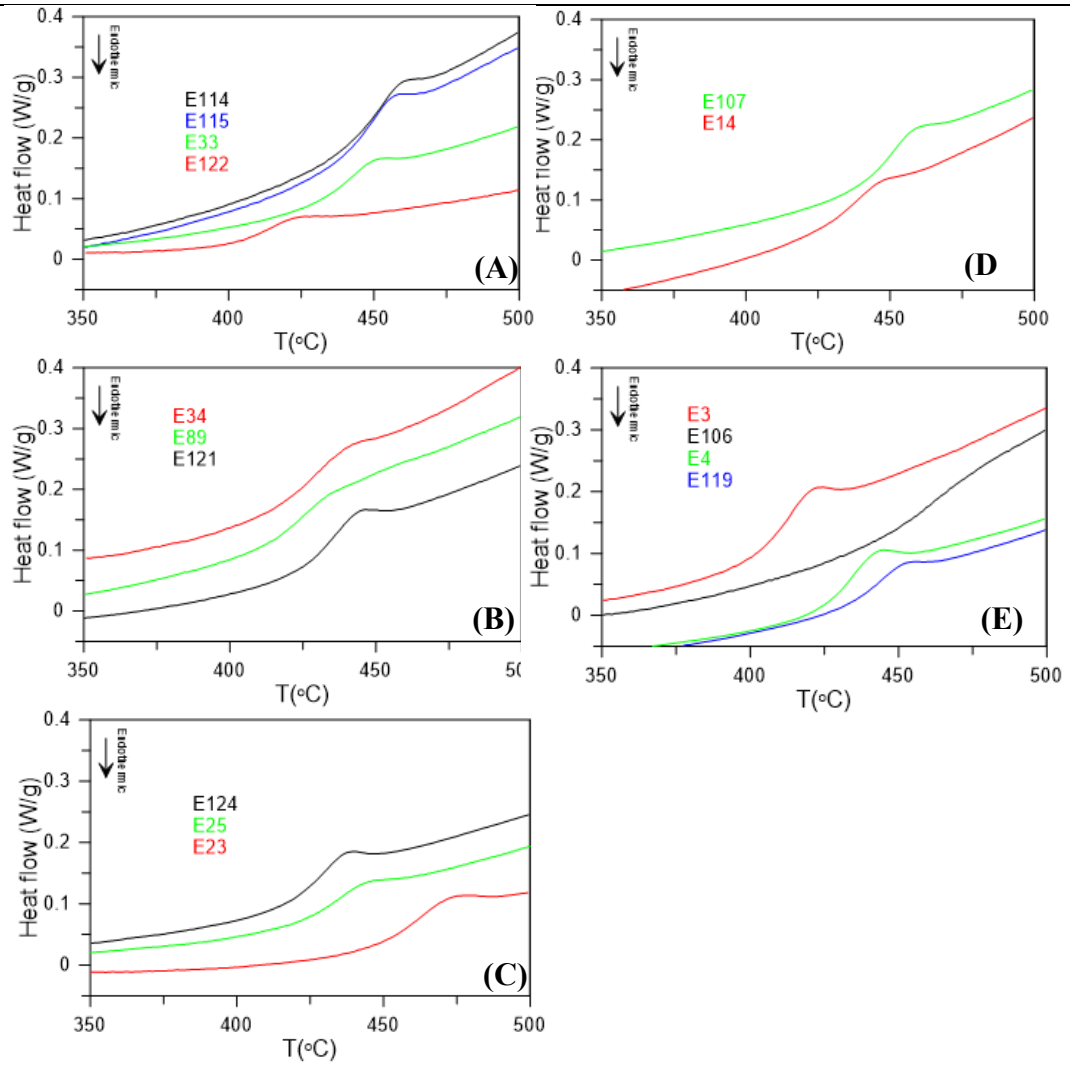

Fig. 3.8. DSC curves obtained after a second run for the **(A)** blue, **(B)** green, **(C)** red, **(D)** purple and **(E)** yellow enamels.

The temperature dependence of the viscosity was determined for the synthetic glasses in terms of the fixed viscosity points defined for HSM, and are summarized in **Table 3.4** [2,19]. The first shrinkage (log(η(Pa·s) = 8.1-9.1) corresponds to a value of the viscosity ten times smaller than those of the deformation point (T_d), while the *softening point* determined (log(η(Pa·s) = 5.1-5.3) corresponds to a viscosity ten times smaller than those of the Littleton softening point (T_d).

Table 3.4 Obtained temperatures (ºC) from the prepared synthetic glasses. The fixed values of the viscosity are after [1]Pascual and [2]Scholze [14,19].

Sample	log(η(Pa·s))	M1	M2	M3	M4	M5	M6
Flow point	2.4[1] – 3.1[2]	816	589	713	923	792	723
Half ball point	3.1 – 3.6	789	515	640	810	701	669
Ball point	4.4 –	763	514	640	704	677	642
Softening point	5.3 – 5.1	686	477	590	617	613	583
Maximum shrinkage point	6.8 – 7.2	650	476	586	597	608	571
First shrinkage point	8.1 – 9.1	600	457	522	512	533	530

The *softening point* of our synthetic glasses is one of the critical temperatures, varying between 583ºC and 617ºC, the highest for the silica richer glasses, and even higher (686ºC) for the glass used for the *grisaille*. In general, the softening temperature increases with increasing SiO_2 content of the lead-zinc borosilicate glasses.

On the other hand, the optimal temperature range for the substrate glass should be higher than the *glass transition* temperature but below the *softening point*. Moreover, it has to be as high as possible to improve the interatomic diffusion and, consequently, the adherence of the enamel to the substrate glass but not as high as to soften it.

Typical 19th century transparent glasses are silica and soda rich (>70% SiO_2 and ~15% Na_2O), by the end of the 19th century, a progressive substitution of Na_2O by CaO to increase the resistance to weathering, of K_2O which was introduced as a finning agent and since the beginning of the 20th century of CaO by MgO to improve the quality of mechanical produced glass have been described. Consequently, the glasses from the Modernist period have a certain chemical variability. They are typically soda rich blown glasses although *cathedral* or vertical drawn sheet glasses were also used. The composition of two typical glasses of the period was measured and are also given in **Table 2.1,** one from the end of the 19th century (GL1) belonging to one of the Modernist houses from the city of Barcelona, Amatller, and a second from the 1950's (GL2).

The *glass transition*, *deformation* and *Littleton softening* temperatures have been evaluated from their composition using the global statistical modelling approach developed by Flugel [20] and are also shown in **Table 3.3**. The *glass transition* temperature is 575ºC and the *softening* range 613-744ºC for the Modernist substrate glass

while they are 537ºC and 581-733ºC respectively for the 1950's blown glass. We can see that the *glass transition* and *deformation temperatures* are very close to the *softening temperature* determined for the enamels (583-617ºC). Consequently, these data indicate a narrow firing temperature range for the Modernist enamels.

The master glazier might have been tempted to add more *flux* (high lead borosilicate glass) to decrease the softening temperature of the enamels in order to soften the enamels without raising the firing temperature to avoid the substrate glass damage. However, in such cases the enamels became lead and boron richer and silica poorer and hence less stable and in particular, had also a lower resistance to water corrosion [21]. This may explain the deterioration of some of the enamels. In fact, the addition of lead borate as *flux* in the enamels was already censured by Barff in the 19th century [22], who indicated that although it was very good *flux*, it was also easily altered by air moisture. Moreover, although the enamels will soften at a lower temperature, this does not guarantee a better adherence of the enamel to the substrate glass if the firing temperature is lower (or too close) than the glass transition temperature of the substrate glass.

Finally, some enamels contain transition metals (copper, chromium, manganese) which are completely dissolved in the glass. We have seen that in this case they act as fluxes and, consequently, reduce the *glass transition temperature* and also the *softening range*. This will produce amorphous enamels with a lower firing temperature.

High lead glasses such as those used in the *grisailles* (40 mol% PbO) have a higher *softening temperature* (686ºC) than the high-lead zinc borosilicate glasses used for the formulation of the enamels, and therefore need a higher firing temperature, in some cases high enough to deform the substrate glass. This has already been related to the addition of boron in the *grisailles* formulation, maybe adding *flux*, and the reason why 19th and 20th century *grisailles* appear more amorphous than Medieval *grisailles* [12]. However, adding boron to the lead rich glass is also known to result in some cases in a liquid phase separation (boron rich-lead rich) which may affect the stability of the *grisaille*. Nevertheless, the *grisailles* contain also manganese and copper, elements which when dissolved in the glass, act as fluxes and consequently reduce their *softening temperature range*.

3.5. Conclusions

The ready-to-be-used enamels from *Lacroix*, *Wenger* and *l'Hospied* studied herewith contain a high-lead zinc borosilicate glass with a composition (B_2O_3:SiO_2 between 2:3 and 2:1 adding between 30 mol% and 40 mol% PbO). Their *softening temperatures* vary between 583ºC and 617ºC. These glass compositions are known to be stable show a good resistance to water corrosion [21].

However, their adherence and, consequently, their stability, depends also on the composition of the substrate glass. The composition of the substrate glasses of the period is quite variable due to the innovations in the raw materials [23-26] and production processes [11]. In particular, substrate glasses of different composition were used in the Catalan Modernist period, and the master glazier had to adapt their enamel compositions to them. Still, they might have had problems with specific enamels/substrate glass pairs; in such cases, they might have added a *flux* to reduce the firing temperature. However, this practice made the enamels less stable and does not guarantee a better adherence to the substrate glass.

High lead glasses such as those used in the *grisailles* (40 mol% PbO) have a higher *softening temperature* (686ºC) than the high-lead zinc borosilicate glasses used for the formulation of the enamels, and therefore need a higher firing temperature, in some cases high enough to deform the substrate glass. This has already been related to the addition of boron in the *grisaille's* formulation, maybe adding some *flux*, and the reason why 19th and 20th century grisailles appear more amorphous than Medieval grisailles [12]. However, adding boron to the lead rich glass is also known to result in some cases in a liquid phase separation (boron rich-lead rich) which may affect their stability.

Finally, some enamels and *grisailles* contain transition metals (copper, chromium, manganese) which are completely dissolved in the glass. We have seen that in this case they act as fluxes and, consequently, reduce the *glass transition temperature* and also the *softening range*. This will produce amorphous enamels/*grisailles* with a lower firing temperature, but only if it is higher than the glass transition temperature of the substrate glass, they will also be better adhered to the substrate glass.

3.6. References

[1] W. Kauzmann, The nature of the glassy state and the behaviour of liquids at low temperatures, Chem. Rev., 43[2], (1948) 219-256.

[2] O.V. Mazurin, Problems of compatibility of the values of glass transition temperatures published in the world literature, Glass Phys. Chem. 33[1] (2007) 22–36.

[3] H.R. Sinning, F. Haessner, Determination of the glass transition temperature of metallic glasses by low frequency internal friction measurements, Journal Of Non-crystalline solids 93 (1987) 53-66.

[4] J.M Fernández Navarro, El vidrio, CESIC, 2003.

[5] W.A. Weyl, Coloured glasses, Society of Glass Technology, Sheffield, 2016.

[6] O. Schalm, V. Van der Linden, P. Frederickx, S. Luyten, G. Van der Snickt, J. Caen, D. Schryvers, et al., Enamels in stained glass Windows: Preparation, chemical composition, microstructure and causes of deterioration. Spectrochim. Acta B 64 (2009) 812-820.

[7] G. Van der Snikt, O. Schalm, J. Caen, K. Janessens, M. Schreiner, Blue enamel on sixteenth and seventeenth-century window glass: deterioration, microstructure, composition and preparation, Stud. Conserv. 51(3) (2006) 212–222.

[8] L.W. Adlington, I.C. Freestone, J.J. Kunicki-Goldfinger, T. Ayers, H. Gilderdale Scott, A. Eavis, Regional patterns in medieval European glass composition as a provenancing tool, Journal of Archaeological Science 110 (2019) 1-13.

[9] O. Schalm, K. Janssens, H. Wouters, D. Caluwé, Composition of 12-18th century window glass in Belgium: Non-figurative windows in secular buildings and stained-glass windows in religious buildings, Spectrochimica Acta Part B 62 (2007) 663-668.

[10] D. Dungworth, The value of Historic window glass, The Historic Environment 2[1] (2011) 21-48.

[11] J. Max Mühlig, Notes on the early development of the Foucault process. The development in Belgium, J. Soc. Glass Tech. 17 (1933) T145-T148.

[12] T. Pradell, S. Murcia, R. Ibáñez, G. Molina, C. Liu, J. Molera, et al., Materials, techniques and conservation of historic stained glass “grissailles”, Int. J. App. Glass Sci., 7: (2016) 41-58

[13] I. B. Kacem, L. Gautron, D. Coillot, D. R. Neuville, Structure and properties of lead silicate glasses and melts, Chemical Geology, Volume 461, (2017), 104-114.

[14] M.J. Pascual, A. Duran, M.O. Prado, A new method for determining fixed viscosity points of glasses, Europ. J. Glass Sci. Tech. B: Phys. Chem. of Glasses, 46[5] (2005) 512-520.

[15] X. Guo, M. Potuzak, J.C. Mauro, D.C. Allan, T.J. Kiczenski, Y. Yue, "Unified approach for determining the enthalpic fictive temperature of glasses with arbitrary thermal history", J. Non-Cryst. Solids 357 (2011) 3230-3236.

[16] M. Garcia-Valles, H. S. Hafez, I. Cruz-Matías, E. Vergés, M. H. Aly, J. Nogués, D. Ayala, S. Martinez, Calculation of viscosity-temperature curves for glass obtained from four wastewater treatment plants in Egypt, J. Therm. Anal. Calorim. 111[1] (2013) 107-114.

[17] F. Montanari, P. Miselli, C. Leonelli, C. Boschetti, J. Henderson, P. Baraldi, Calibration and use of the Heating Microscope for indirect evaluation of the viscosity and meltability of Archaeological glasses, Int. J. App. Glass Sci. 5[2] (2014) 161–177.

[18] Z.Y. Yao, D. Möncke, E.I. Kamitsos, P. Houizot, F. Célarié, T. Rouxel, et al. Structure and mechanical properties of copper–lead and copper–zinc borate glasses. J. Non-Cryst. Solids (2016) 55-68.

[19] H. Scholze, Der Einfluss von Viskositat und Oberflachenspannung auf er-hitzungsmikroskopische Messungen an Glasern (Influence of viscosity and surface tension on Hot Stage Microscopy measurements on glasses). Ber. Dtsch. Keram. Ges. 39; (1962) 63-68.

[20] A. Flügel, Glass viscosity calculation based on a global statistical modelling approach. Europ. J. Glass Sci. Tech. A, 48(1) (2007) 13-30.

[21] T.S. Petrovskaya, Properties of lead borosilicate glasses: The effect of the structure. Glass Ceram., 54(11–12) (1997) 347–350.

[22] F.S. Barff, Silicates, silicides, glass and glass painting, J. Soc. of Arts, 20(1034) (1872) 841-852.

[23] J. Rodríguez Guarnizo, D. Rodríguez Barrantes, Los procedimientos clásicos de fabricación de la sosa (Basic procedures of soda fabrication), Ensayos: Revista de la Facultad de Educación de Albacete, Nº. 14 (1999) 293-309.

[24] D. Dungworth, The value of Historic Window Glass, The Historic Environment, Vol. 2 No. 1, June (2011) 21–48.

[25] C.M. Kramer, Thermal decomposition of $NaNO_3$ and KNO_3, Proceedings of the Electrochemical Society, PV 1981-9 (1981) 494-505.

[26] D.S. Kostick, The origin of the U.S. natural and synthetic soda ash industries, Proceedings of the First International Soda Ash Conference, Vol I, Laramie, Wyoming (1998) 11-35.

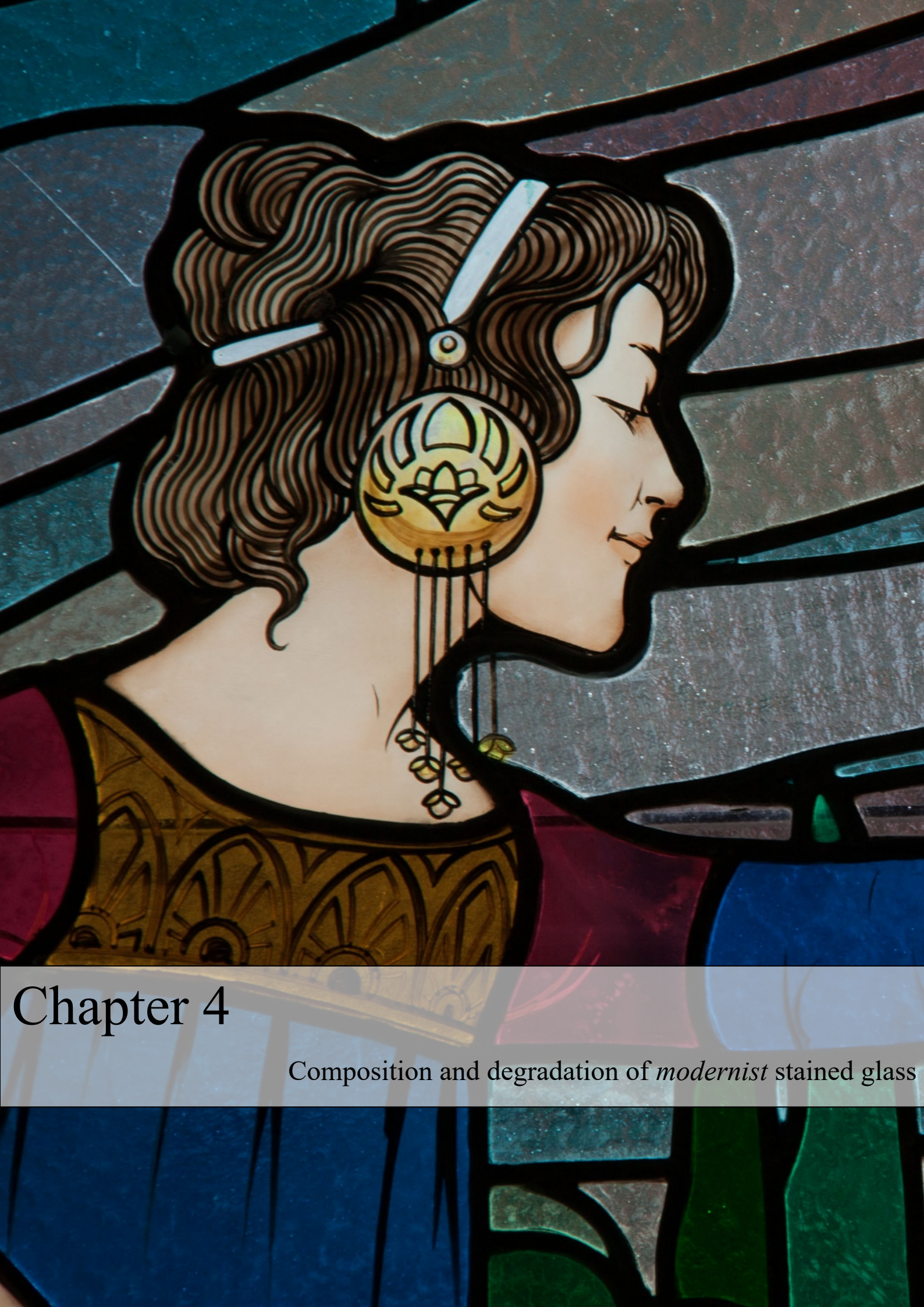

Chapter 4

Composition and degradation of *modernist* stained glass

Chapter 4

Composition and degradation of *modernist* stained glass

The aim of this chapter is to identify differences in materials, painting and firing techniques and state of conservation of the artistic output of the most important active modernist stained glass workshops in Barcelona. We will determine the extent of the chemical alteration of the enamels and identify the corrosion products present, with the aim of establishing the mechanisms of these changes and their relationship to the materials and painting techniques used in the glazier workshops. To this end, we investigated a collection of enamelled glass fragments obtained from windows, skylights, decorative panels and screens covering the entire period and the most important glazier workshops operating in the city of Barcelona, including also some earlier and later enamelled samples.

Table 4.1. List of studied samples of modernist stained glasses fragments from the *J.M. Bonet Vitralls* private collection.

Location	Workshop	Year	Object	Fragments	Substrate glass colour
Academia Mariana (Lleida)	Bazin-Latteaux	1876	window	AMLL1-3	tr
Dames MAC (Cerdanyola)	Dietrich	1888-1910	window	CRD	tr
Cathedral (Palma Mallorca)	Amigó	1889	window	P	am
Private house (Badalona)	Buxeres i Codorniu	1900	decorative panel	BC1-3	tr
Burés house (Barcelona)	Bordalba	1900-1905	skylight	CB	cl
Cama i Escurra house (Barcelona)	Bordalba	1902-1904	lift panel	PG	tr
Church of Sant Jaume (Calaf)	Amigó	1903	window	C1-3	tr
High Court Palace (Barcelona)	Rigalt i Granell	1911-1914	skylight	PJ1-2	tr
				PJ3	tr
North Station (Barcelona)	Maumejean	1910-1912	waiting room	EN	tr
Town hall of the Sants Montjuic District (Barcelona)	Rigalt i Granell	1915	window	SM1-4	y
				SM5	g
Ramon Pla Armengol Foundation (Barcelona)	Bulbena?	1920	window	FARM1-3	tr

The fragments of enamelled glasses belong to the collection of *J.M. Bonet Vitralls S.L.* accummulated from its 100 years of restoration activities. The collection includes glass

fragments from 10 different buildings dated between 1876 and 1920 and produced by some of the most important glazier workshops of the period; *Dietrich*, *Buxeres i Codorniu*, *Bordalba*, *Amigó*, *Maumejan* and *Rigalt i Granell*. We have analysed 13 stained and enamelled fragments from various public and private contexts listed in **Table 4.1** and including also some earlier, pre-modernist stain glass from the French workshop Bazin-Lateaux and later, a *Noucentist* stain glass probably produced by Bulbena) fragments. *Noucentisme* is a style which originated as a reaction to *Modernisme*.

4.1. Analytical methodology

The sample preparation (polished cross sections, thin cross sections) is the same followed for the characterisation on the *Rigalt & Granell* workshop enamels described in **Chapter 2**.

The modernist fragments of the enamelled glasses samples were analysed by LA-ICP-MS in the IRAMAT-CEB at the CNRS, Orléans (France), using a Resonetics M50E excimer laser (ArF, 193 nm) equipped with a S155 ablation cell and a Thermo Fisher Scientific ELEMENT XR mass spectrometer system. The ablations were typically carried out with a 5 mJ energy a 10 Hz pulse frequency in spot-mode and a beam diameter of 100 μm for the base glass. The enamels were typically analysed along the surface due to insufficient thickness with a beam diameter of 50 μm that was occasionally reduced down to 25 μm when saturation of the signal caused by high concentrations transition metals occurred. A pre-ablation time of either 10 s or 20 s depending on the thickness of the sample was followed by 30 s signal acquisition, resulting in 10 mass scans. The ablated material is transported to the plasma torch by an argon/helium flow at an approximate rate of l/min for Ar and 0.65 l/min for He. The ion signals in counts-per-second are recorded for 58 isotopes (from Li to U). Standard Reference Material (NIST SRM610) as well as Corning glasses B, C, and D and APL1 (in-house standard glass) were used for external calibration, while ^{28}Si was used as internal standard. Quantitative concentrations were calculated based on the procedures described by Gratuze [1]. Precision and accuracy are reflected in the repeated measurements of reference glasses Corning A and NIST SRM612. Electron microprobe (EPM, JEOL JXA-8230; JEOL Ltd, Akishima, Tokyo, Japan) was also used to quantify the chemical composition of the substrate glasses. The operating conditions were 20 kV and 15 nA with a focused beam (spot analysis).

Optical Microscopy and Scanning Electron Microscopy (SEM) with an Energy Dispersive Spectroscopy detector (EDS) was used to determine the composition of the microcrystalline pigment and reaction particles, and by Focus Ion Beam (FIB) to identify the pigment nanoparticles. The crystalline compounds present in the replica enamels were determined by μ-XRD with synchrotron light. Finally, the colour and nature of the colourants was investigated by Ultraviolet Visible and Near Infrared (UV-Vis-NIR) spectroscopy using Diffuse Reflectance and Transmission modes respectively. The experimental conditions are the same used in the study of the *Rigalt & Granell* workshop enamels described in **Chapter 2**.

4.2. Enamels, grisailles and stains from *modernist* stained glass

The enamels, *grisailles*, stains and the substrate glasses were analysed. The chemical composition of the substrate glasses was determined by LA-ICP-MS with the exception of sulphur, which was determined by Microprobe. The chemical composition of the substrate glasses was obtained from the polished cross sections of the glasses and is shown in **Table 4.2**. Some of the substrate glasses are coloured, the colourants (metal ions dissolved in the glass) are determined from the chemical elements present in combination with the UV-Vis spectra; the transmission spectra corresponding to the coloured substrate glasses is shown in **Fig. 4.1.**

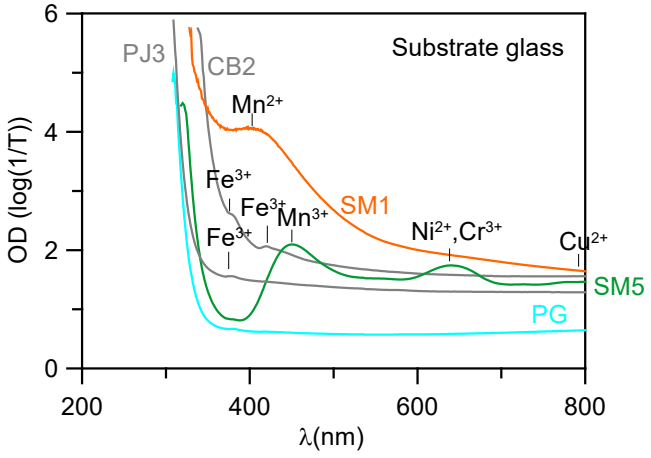

Fig. 4.1. UV-Vis spectra corresponding to differently coloured substrate glasses. In orange and grey, yellow glasses due to the presence of Mn^{2+} and Fe^{3+} respectively; in green a green glass (Mn^{3+} and Ni^{2+} and Cr^{3+}) and in cyan a transparent glass.

Most of the substrates are transparent, except of one amber (P), one yellow (SM1-4), one green (SM5) and one with a yellowish cloudy (CB) appearance. The transparent glasses contain some iron but the colouring effect is counteracted with the addition of small amounts of As or Mn. Higher amounts of Mn^{2+} are present in the amber and yellow glasses and the glass with the cloudy appearance (CB) contains also Sn and Pb which increased the opacity. The green glass contains minor amounts of Cu^{2+}, Ni^{2+} and Cr^{3+}.

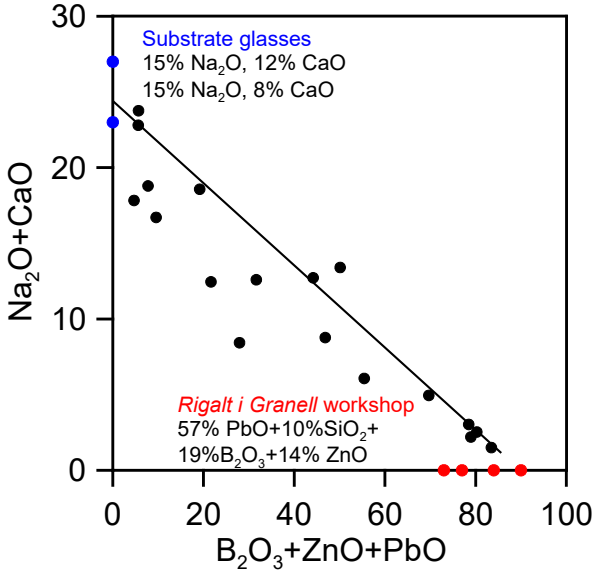

Fig. 4.2. B_2O_3+ZnO+PbO versus Na_2O+CaO contents from the enamels, substrate glass and the main *Rigalt i Granell* workshop enamel types analysed with LA-ICP-MS. The negative correlation observed between them is probably the result of both, corrosion processes, and the analyse of enamel plus some substrate glass.

The chemical composition of the enamels and stains was determined by LA-ICP-MS, but due to the shallow thickness of the enamels the chemical composition was determined scanning the surface instead of over polished cross sections. This method has given very good results for enamels sintered from the collection of raw materials of the *Rigalt i Granell & cia*, which were shown in **chapter 2**. The chemical composition of the enamels is shown in **Table 4.3**. We have to consider that, contrarily to the freshly replicated enamels from the *Rigalt i Granell & cia* workshop, now the enamels are heavily altered and, consequently, are very fragile. They are affected by atmospheric corrosion which is known to produce the depletion of the glass constituents and the incorporation of pollutants, resulting in the formation of a hydrated silica rich glass [2-5]. Moreover, as the corroded enamels are more fragile the substrate glass below is more easily reached

during the laser ablation process. These difficulties are well illustrated in **Fig. 4.2** where the B_2O_3+ZnO+PbO content representing the main ingredients of the *Rigalt i Granell* workshop enamels is compared to the Na_2O+CaO content representing the substrate glasses. The negative correlation is probably the result of both, corrosion processes and the analyse of enamel plus some substrate glass.

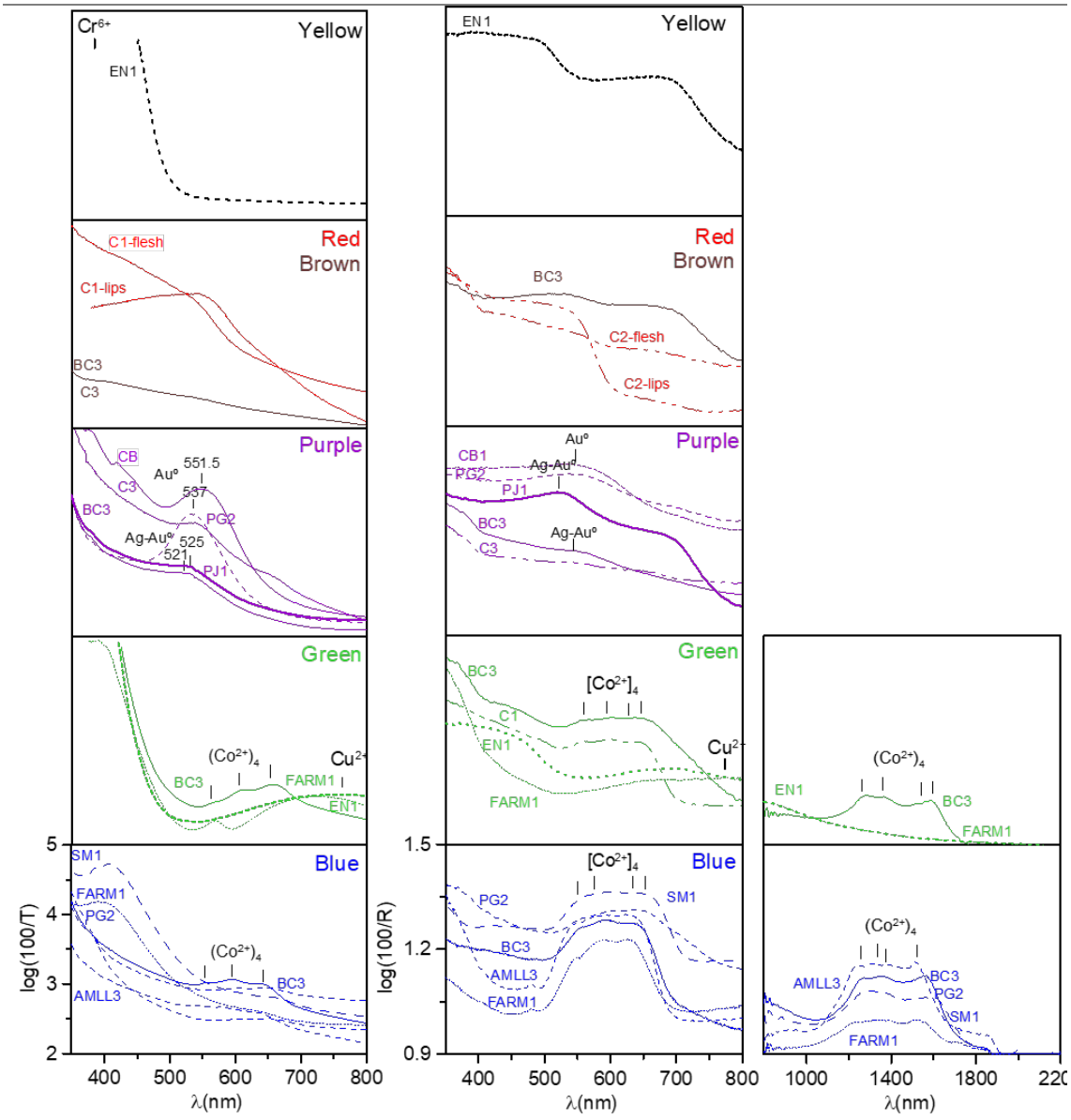

Fig. 4.3. (Left) Optical Density (log(1/T) in transmission of the enamels in the UV-Vis range and (Right) log (1/R) in reflection mode using an Ulbricht sphere of the enamels in UV-Vis-NIR range. Both correspond roughly to Absorption.

The crystalline phases determined by μ-XRD are summarised in **Table 4.4**. The crystalline compounds are classified as pigment particles and reaction compounds originally present in the enamels and those formed due to corrosion. The colourants (metal ions dissolved in the enamel glassy part) determined from the minor and trace chemical elements present in combination with the UV-Vis and NIR spectra are also indicated in **Table 4.4**.

The transmittance is affected by the colour of the substrate glass, for this reason the colour is determined from the spectra measured in reflection mode **Fig. 4.3**. However, as the surface of the enamels is affected by the corrosion which in some cases is very important, the colour has also been calculated from the transmittance data. The Extinction (log (1/T) and Diffuse reflectance of orange and yellow stains, as the red plaque glass are shown in **Fig. 4.4**.

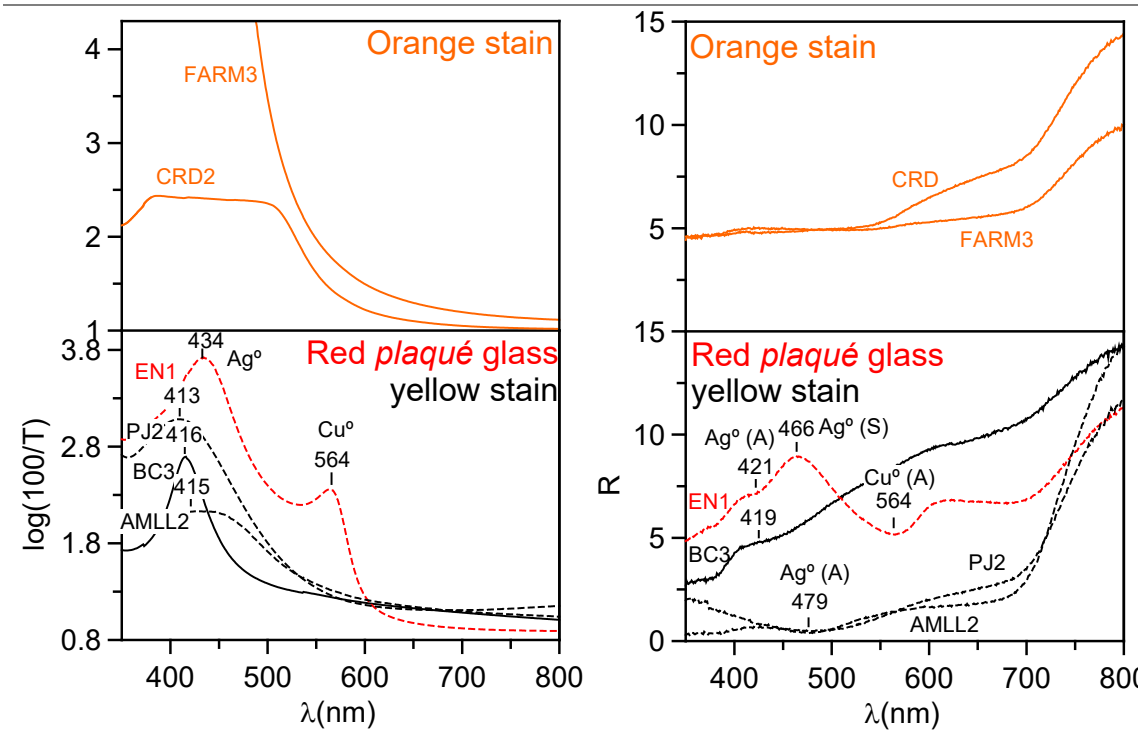

Fig. 4.4. (Left) the Optical Density (log(100/T) which corresponds to the Extinction (Absorption+Scattering) and (Right) total Diffuse Reflectance for the yellow and orange stains as the red *plaqué* glass from the sample EN.

Finally, the *Lab** colour coordinates of the enamels has been calculated from the Diffuse Reflectance and from the Transmittance and they are shown in **Table 4.5**, and the

corresponding colour wheel is also shown on **Fig. 4.5**. The low saturation (s_R* ~ 5-20%) and high lightness (L_R* ~ 22-36%) of the enamels compared to those of freshly made enamels (s* ~ 10-90%, L* ~ 7-30%) (**chapter 2**) is related to the poor preservation state and in particular to the presence of white corrosion products on the surface. The enamels are more opaque and the colour is less saturated than originally.

A detailed analysis of the data will be given for the materials studied from each of the main glazier companies.

Table 4.2. Composition of the substrate glasses. *measured with microprobe. tr: transparent; am: amber; cl: cloudy; y: yellow; g: green.

Fragments	colour	Na_2O	MgO	Al_2O_3	SiO_2	SO_3*	Cl	K_2O	CaO	TiO_2	Fe_2O_3	B	P	Cr	Mn	Co	Ni	Cu	Zn	As	Sr	Zr	Sn	Ba	Pb
AMLL2-3	tr	11.3	0.08	0.85	71.2	1.05	0.08	0.32	15.8	0.03	0.12	5	51	6	49	1	2	4	9	1847	89	19	1	78	150
CRD	tr	12.0	0.45	0.91	71.2	0.21	0.73	0.11	14	0.08	0.19	11	29	13	22	2	3	11	12	3029	182	41	4	32	52
P	am	15.4	0.09	1.42	70.1	0.09	0.41	0.50	11.3	0.03	0.18	8	67	10	3417	2	2	16	8	31	52	27	7	861	6
BC1-3	tr	19.7	0.07	0.69	69.6		0.65	0.24	8.63	0.03	0.05	9	22	7	509	0	7	23	3	1839	41	20	1	41	3
CB	cl	13.2	0.12	1.27	68.1		0.09	0.72	13.1	0.02	0.98	37	96	8	13400	11	2	35	68	337	76	37	1845	542	2181
PG	tr	14.2	0.23	0.28	68.7		0.13	0.07	14.8	0.01	0.25	8	41	6	1786	3	2	958	15	90	176	9	3	8348	49
C1-3	tr	13.8	4.05	0.77	72.5	0.30	0.05	0.36	8.05	0.08	0.12	24	35	6	49	0	1	2	11	487	23	52	1	53	14
PJ1-2	tr	13.8	0.15	0.46	70.0	1.09	0.35	0.13	14.1	0.02	0.20	10	29	5	1810	2	2	48	15	7	120	26	1	4889	45
PJ3	tr	12.9	3.31	1.13	73.7		0.11	0.46	7.82	0.16	0.24	25	62	7	73	1	1	27	19	5	51	270	1	141	10
EN	tr	13.1	0.07	0.38	73.4	0.58	0.13	0.09	12.4	0.02	0.17	20	26	28	26	1	1	309	20	990	47	26	412	39	5
SM1-4	y	14.8	0.06	0.31	68.7	0.13	0.55	0.04	15.1	0.03	0.07	6	39	8	1354	1	3	11	9	5	55	28	0	107	7
SM5	g	18.2	0.08	0.35	69.8	0.07	0.11	0.12	9.96	0.02	0.26	12	23	325	1915	33	2483	3288	74	10	45	22	1	79	8
FARM	tr	17.6	0.07	0.42	68.9		0.09	0.09	12.7	0.03	0.10	24	19	9	92	1	3	11	10	11	53	30	0	36	4

Table 4.3. LA-ICP-MS analysis of the major, minor and trace elements from the colour enamels and stains. bl: blue; g: green, tu: turquoise; br: brown, y: yellow; r: red and p: purple enamels; os: orange stain and ys: yellow stain and rp: red *plaqué* glass.

		wt%																ppm									
Frag	**Colour**	**B_2O_3**	**Na_2O**	**MgO**	**Al_2O_3**	**SiO_2**	**K_2O**	**CaO**	**Cr_2O_3**	**MnO**	**Fe_2O_3**	**CoO**	**CuO**	**ZnO**	**Ag**	**SnO_2**	**PbO**	**Cl**	**P**	**Ti**	**Ni**	**As**	**Sr**	**Zr**	**Sb**	**Ba**	**Au**
AMLL2	ys	0.00	9.35	0.08	0.76	69.3	0.66	16.09	0.00	0.01	0.12	0.00	0.00	0.00	2.78	0.00	0.41	841	197	182	2	1900	96	19	1	88	1
AMLL3	bl	0.05	4.55	0.10	13.8	42.0	0.22	7.90	0.04	0.06	2.44	4.73	0.02	1.01	0.01	0.02	20.6	18485	743	160	1671	999	73	15	100	167	1
CRD	os	0.00	10.1	0.45	0.86	68.5	0.21	14.8	0.00	0.00	0.18	0.00	0.01	0.00	3.66	0.00	0.01	6571	33	498	3	3197	193	44	17	35	0
BC3	ys	0.00	18.2	0.06	0.58	70.2	0.42	8.33	0.00	0.00	0.05	0.00	0.00	0.00	1.35	0.00	0.00	6577	12	154	1	1083	40	19	20	42	0
BC1	bl	5.23	4.87	0.06	3.57	28.3	0.13	1.20	1.79	0.44	1.85	1.62	0.02	8.05	0.00	0.04	42.2	2273	192	139	467	179	132	10	77	2065	41
BC3	g	7.48	6.33	0.06	1.91	26.5	0.18	7.07	2.90	0.09	0.38	1.55	1.61	2.19	0.00	0.02	40.5	4787	256	284	21	980	85	18	149	270	32
BC3	br	0.22	12.50	0.11	1.26	53.2	0.27	6.07	0.02	1.39	5.23	0.01	0.01	0.05	0.00	0.03	18.9	5615	394	221	46	156	63	9	202	445	6601
BC3	p	5.68	6.88	0.15	1.14	29.2	0.26	1.89	0.08	1.41	4.92	0.06	0.01	0.93	0.06	5.62	40.2	4540	157	112	339	226	4823	10	126	741	13
PG1	tu	4.55	5.53	0.09	2.06	32.9	0.07	7.19	2.13	0.24	0.89	1.41	1.92	3.70	0.00	0.04	35.9	4619	150	103	471	68	2879	9	84	3533	48
PG2	p	3.49	6.75	0.16	0.74	41.6	0.26	5.84	0.05	0.89	3.40	0.04	0.05	0.23	0.09	5.95	27.9	13332	155	191	37	73	138	9	180	3843	6715
CB	p	0.07	8.05	0.21	1.17	62.7	0.81	9.78	0.00	1.24	0.94	0.02	0.11	0.11	0.00	8.97	4.50	1409	105	306	42	384	67	39	302	506	9392
C1	r	0.41	11.4	3.43	1.13	63.9	0.46	7.40	0.03	0.58	3.38	0.09	0.01	0.46	0.01	0.02	6.89	971	176	513	359	436	39	53	52	184	11
C3	g	0.63	4.39	1.85	2.28	50.4	0.40	4.04	1.39	0.72	4.37	1.22	0.01	0.25	0.00	0.01	27.1	1296	2366	473	246	509	277	41	71	215	1
C3	p	0.52	9.89	3.27	1.47	64.9	0.55	6.82	0.50	0.03	0.51	0.47	0.01	0.09	0.02	1.05	8.94	2578	1473	505	97	507	34	54	173	74	1002
EN	rp	0.00	12.4	0.06	0.38	75.2	0.22	6.49	0.00	0.00	1.08	0.00	1.21	0.01	0.22	2.16	0.12	3788	77	178	7	83	19	31	7	26	25
EN	g	15.7	1.37	0.02	0.80	15.8	0.15	0.83	0.17	0.01	0.06	0.00	1.63	1.91	0.00	0.04	61.3	525	212	128	2	88	15	11	328	115	0
EN	y	14.5	1.53	0.02	0.50	15	0.10	1.00	1.35	0.00	0.05	0.00	0.01	7.45	0.00	0.01	58.4	496	165	97	1	79	11	8	433	74	0
PJ1	p	0.14	11.0	0.22	0.53	65.8	0.33	12.8	0.03	0.24	0.28	0.02	0.01	0.12	0.09	1.78	5.41	4550	149	147	17	79	122	28	49	4529	1986
PJ2	ys	0.00	11.8	0.14	0.42	68.1	0.23	14.5	0.00	0.23	0.20	0.00	0.01	0.00	3.52	0.00	0.01	3317	27	142	2	7	119	28	1	4946	0
PJ3	ys	0.01	12.3	3.37	1.27	72.5	0.64	7.90	0.00	0.01	0.39	0.00	0.34	0.01	0.69	0.00	0.14	1186	223	1011	2	17	66	279	12	263	22
SM1	bl	0.23	10.5	0.14	3.12	60.2	0.15	12.3	3.83	0.15	0.24	2.88	0.04	0.10	0.00	0.08	5.27	5374	124	190	830	50	54	28	112	97	1
FARM1	bl	17.4	1.04	0.02	2.54	11.0	0.17	0.46	0.00	0.01	0.08	0.54	0.01	4.74	0.01	0.03	61.4	4279	62	56	88	5	13	4	40	114	0
FARM1	g	16.3	2.09	0.04	0.55	8.40	0.09	0.94	0.05	0.04	0.21	0.03	7.52	11.73	0.00	0.06	50.4	13246	86	130	52	129	15	9	313	67	2
FARM3	p	16.6	3.96	0.03	1.17	22.0	0.42	0.99	0.01	0.02	0.07	0.00	0.01	6.28	0.05	0.66	46.8	7204	69	155	4	110	18	11	130	66	754
FARM3	os	0.00	16.4	0.07	0.38	67.5	0.19	13.0	0.00	0.01	0.10	0.00	0.00	0.00	2.14	0.00	0.00	891	21	204	1	12	55	32	0	38	0

Table 4.4. Colourants (col.), pigment particles and alteration compound identified in the enamels, *grisailles* and stains by UV-Vis-NIR and μ-XRD.

Frag.	Colour	Col.	Pigment particles	Alteration compounds
AMLL2	ys		Ag^{o}-[01-087-0597]	-
AMLL3	bl		$(Co,Zn)Al_2O_4$-[Fm-3m-a=8.106Å], Al_2O_3-[00-046-1212]	$PbSO_4$-[01-082-1855]
AMLL3	r		Fe_2O_3-[01-072-0469]	$PbSO_4$-[01-082-1855]
AMLL2	gr		Fe_2O_3-[01-072-0469]	$PbSO_4$-[01-082-1855], $PbCl_2$-[00-026-1150] Pb(OH)Cl-[01-074-2022]
CRD	os		Ag^{o}-[01-087-0597], AgCl-[01-085-1355]	-
BC3	ys		Ag^{o}-[01-087-0597]	-
BC3	bl		$CoCr_2O_3$-[01-080-1668], $(Co,Zn)Al_2O_3$-[Fm-3m-a=8.106Å], Fe_2O_3–[01-072-0469]	Na_2SO_4-[01-070-1541] $NaZn_4(SO_4)(OH)_6Cl{\cdot}6H_2O$-[01-088-1359]
BC3	g	Cu^{+}-Cu^{2+}	$(Cr,Co,Zn)Al_2O_4$-[Fm-3m-a=8.250Å],	
BC3	br		Fe_2O_3–[01-072-0469], MnO_2–[01-072-1984], SiO_2–[01-085-0335], $Pb_2(Fe,Mn)_2Si_2O_9$–[01-088-1889]	-
BC3	p		$(AgAu)^{o}$-[Fm-3m, a=4.08Å]	$PbSO_4$-[01-082-1855], Pb(OH)Cl-[01-074-2022] $SnCl{\cdot}2H_2O{\cdot}2SnCl_3{\cdot}H_2O$-[01-075-2328]
BC3	gr		Fe_2O_3 –[01-072-0469], MnO_2 –[01-072-1984], $Pb_2(Fe,Mn)_2Si_2O_9$–[01-088-1889], SiO_2–[01-085-0335]	-
PG1	tu		$(Cr,Co,Zn)Al_2O_4$-[Fm-3m-a=8.240Å], Fe_2O_3–[01-072-0469], $Pb_2(Fe,Mn)_2Si_2O_9$–[01-088-1889]	$CaSO_4{\cdot}(H_2O)_2$-[01-074-1905]
PG2	p		$(Ag\text{-}Au)^{o}$-[Fm-3m, a=4.08Å], $Pb_2(Fe,Mn)_2Si_2O_9$–[01-088-1889] MnO_2–[01-072-1984]	$PbSO_4$-[01-082-1855] $SnCl{\cdot}2H_2O{\cdot}2SnCl_3{\cdot}H_2O$-[01-075-2328]
PG1	gr		Fe_2O_3–[01-072-0469], $Pb_2(Fe,Mn)_2Si_2O_9$-[01-088-1889] $(Fe,Cu,Mn)_3O_4$-[01-076-2294]	-
CB-2	p		$(AgAu)^{o}$-[Fm-3m, a=4.08Å],SnO_2-[01-071-0652]	SnO_2–[01-071-0652]
C1	flesh	Fe^{3+}	-	-
C1	r		Fe_2O_3-[01-072-0469], $Pb_2(Fe,Mn)_2Si_2O_9$-[01-088-1889]	$CaCO_3$-[01-083-0577]
C3	bl		$FeCrCoO_4$-[Fm-3m, a=8.350Å], Fe_2O_3–[01-072-0469]	$PbSO_4$-[01-082-1855] $Zn_2Fe_2(PO_4)_3{\cdot}2H_2O$-[01-080-1834]
C3	g	Cu^{+}-Cu^{2+}	$(Cr,Co)(Al,Co)_2O_4$-[Fm-3m-a=8.266Å]	
C3	p		Au^{o}-[00-004-0784], $Mg(Cr,Co,Fe,Al)_2O_4$	$CaPb_4Cl(PO_4)_3$-[01-084-0815]
C3	gr		Fe_2O_3-[01-072-0469], $Pb_2(Fe,Mn)_2Si_2O_9$ -[01-088-1889]	$PbSO_4$-[01-082-1855]
EN1	rp		Cu^{o}-[01-085-1326], Ag^{o}-[01-087-0597]	-
EN1	g	Cu^{+}-Cu^{2+},Cr^{3+}	-	
EN1	y	Cr^{6+}	-	
EN1	gr		$(Fe,Cu,Mn)_3O_4$-[01-076-2294]	
PJ2/3	ys		Ag^{o}-[01-087-0597]	-
PJ1	p		$(AgAu)^{o}$-[Fm-3m, a=4.08Å]	$PbSO_4$-[01-082-1855]
PJ3/3	gr		$(Fe,Cu,Mn)_3O_4$-[01-076-2294],$Pb_2(Fe,Mn)_2Si_2O_9$-[01-088-1889]	
SM1	bl		$(Cr,Co)Al_2O_4$-[Fm-3m, a=8.410Å],	$Pb_3(CO_3)_2(OH)_2$-[00-013-0131] $CaCO_3$-[01-083-0577]
SM5	gr		CuO-[01-072-0629], $(Fe,Cu,Mn)_3O_4$-[01-076-2294] $Pb_2(Fe,Mn)_2Si_2O_9$–[01-088-1889]	
SM5	matt gr		CuO-[01-072-0629], $(Fe,Cu,Mn)_3O_4$-[01-076-2294] $Pb_2(Fe,Mn)_2Si_2O_9$–[01-088-1889],SnO_2–[01-071-0652]	
FARM3	os		Ag^{o}-[01-087-0597]	-
FARM1	bl		$CoAl_2O_4$–[01-082-2242]	$CaSO_4{\cdot}(H_2O)_2$-[01-074-1905] $Na_3Pb_2(SO_4)_3Cl$-[01-073-193] $K_2Pb(SO_4)_2$-[00-029-1015] $PbSO_4$-[01-082-1855],Pb(OH)Cl,$PbCl_2$-[00-026-1150]
FARM1	g	Cu^{+}-Cu^{2+}	-	$PbSO_4$-[01-082-1855], Cu_2O-[01-078-2076] $PbCuCl_2(OH)_2$-[01-085-1735]
FARM3	p		$(AgAu)^{o}$-[Fm-3m, a=4.08Å]	$CaSO_4{\cdot}(H_2O)_2$-[01-074-1905] , $PbSO_4$-[01-082-1855]
FARM3	gr		Fe_5CuO_8-[01-076-2294]	$PbSO_4$-[01-082-1855], $Pb_3Cu_2Cl_5(OH)_6$-[01-079-2414]

Table 4.5. Colour coordinates calculated using *Lab** colour space from the Reflectance data measured using the Ulbricht integrating sphere and barium sulphate as white standard and also from the Transmittance data. *L**: lightness, *c**: chroma, *h**: hue and *s*:* saturation.

		Reflectance						***Transmittance***					
Sample	**Colour**	L_R*	a_R*	b_R*	c_R*	h_R*	s_R*	L_T*	a_T*	b_T*	c_T*	h_T*	s_T*
AMLL2	ys	23.4	1.3	3.0	3.2	67	13.6	33.8	0.8	13.5	13.6	86	37.3
AMLL3	bl	36.1	0.4	-10.8	10.8	272	28.6	6.2	-0.1	2.3	2.3	91	34.6
CRD	os	28.4	4.3	3.7	5.7	41	19.7	28.7	17.8	29.4	34.3	59	76.7
BC3	ys	34.8	0.8	6.9	7.0	83	19.6	28.0	-0.6	23.3	23.3	92	63.9
BC3	bl	28.8	-1.5	-3.5	3.8	247	13.2	0.2	-0.1	-0.5	0.5	263	88.5
BC3	br	25.4	0.7	0.2	0.7	16	2.9	33.0	2.0	5.5	5.8	70	17.3
BC3	p	34.3	1.8	3.2	3.7	61	10.8	13.0	1.6	1.9	2.5	49	18.9
BC3	g	25.6	-1.1	1.2	1.6	131	6.4	8.7	-8.6	11.9	14.7	126	85.9
PG2	tu	27.4	-1.9	-0.6	2.0	198	7.4	40.8	-4.3	17.8	18.3	104	41.0
PG2	p	24.3	2.6	-0.1	2.6	358	10.5	9.2	14.6	-1.7	14.6	354	84.8
CB2	p	20.5	3.2	0.7	3.3	13	16.1	6.1	7.6	3.5	8.4	25	81.0
C1	r	27.9	5.3	4.2	6.8	39	23.5	0.8	0.5	0.1	0.5	15	55.9
C3	g	28.7	-1.4	2.1	2.5	123	8.7	0.8	-0.2	0.6	0.6	113	59.2
C3	p	31.3	0.4	0.9	1.0	65	3.2	0.7	0.3	0.3	0.5	48	56.0
C3	flesh	29.9	0.4	1.3	1.4	72	4.7	0.8	0.9	0.9	1.3	43	86.0
EN1	g	31.8	-2.1	5.9	6.3	109	19.4	25.2	-13.2	24.3	27.7	119	74.0
EN1	rp	29.7	4.3	-8.1	9.2	298	29.5	18.5	30.7	25.7	40.0	40	90.8
EN1	y	29.6	-0.2	5.7	5.7	92	19.0	21.3	-0.3	28.3	28.3	91	80.0
PJ1	p	27.7	4.3	1.6	4.6	20	16.3	27.8	4.9	5.5	7.3	49	25.5
PJ2	ys	23.3	2.8	3.0	4.1	47	17.4	23.8	6.6	28.4	29.2	77	77.4
PJ3	ys	30.7	0.3	1.1	1.1	75	3.6	28.8	-0.4	30.6	30.6	91	72.8
SM1	bl	25.9	-1.4	-3.5	3.8	248	14.4	0.8	0.4	1.3	1.3	73	84.9
FARM1	bl	39.8	-1.5	-10.3	10.4	262	25.4	5.3	0.2	5.6	5.6	88	72.8
FARM1	g	34.7	-1.2	1.4	1.8	131	5.3	4.5	-5.0	5.5	7.5	132	85.9
FARM3	p	35.4	-0.7	-1.9	2.0	251	5.7	0.4	1.0	0.8	1.3	36	94.5
FARM3	os	27.0	1.4	0.6	1.5	24	5.5	14.3	17.5	22.5	28.5	52	5.5

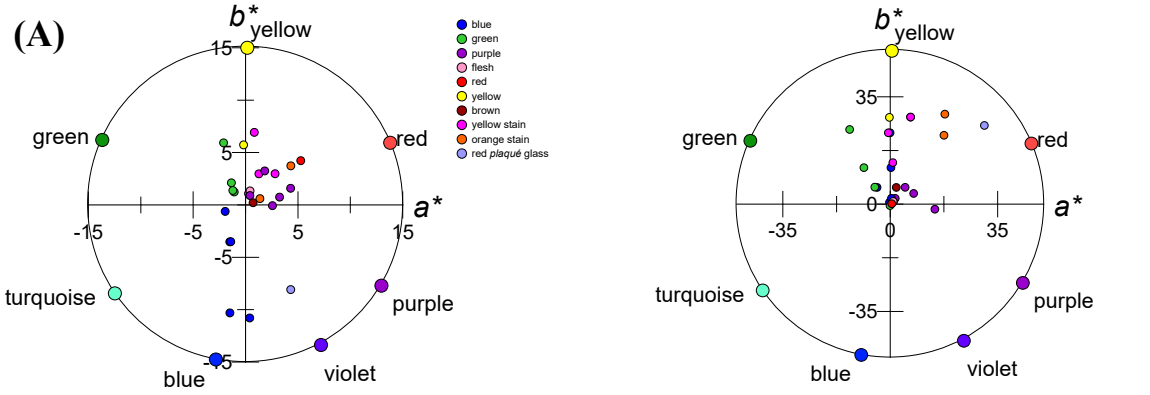

Fig 4.5. *Lab** colour coordinates obtained from the (A) Reflectance and (B) Transmittance.

4.2.1. Rigalt, Granell & cia.

The analysis of these stain glass fragments is particularly important because they can be compared with the materials from the workshop studied in **Chapter 2**. Considering that the composition of the enamels, *grisailles* and stains should not be very different from those determined in **Chapter 2**, their study will give a direct insight on the conservation state of the enamels and what we should expect the composition of the in-situ stained glasses.

Three fragments from a skylight from *High Court Palace* (*Palau de Justicia*, 1908) designed by the architects Domenech Estapà and Enric Sagnier, one consisting of a purple enamel (PJ1) and two more of yellow stain (PJ2-3) obtained during the full restoration of the stained glass carried out in 2009. The fragments are part of a *grisaille* pattern filled two of them with yellow silver (PJ2 and PJ3) stain and the third with a dime purple enamel (PJ1). In some areas the purple enamel is lost. The *grisaille* and purple paint are applied on the internal side of the panels while the yellow silver stain is applied on the opposite side. The skylight is covered by a glass roof, as usual. However, the joints of the glass roof had some leaks for many years until they were fixed during the last restoration campaign when the skylight was completely reinstalled. Since it is quite difficult to reach, dust and dirt deposited and accumulated literally for decades.

The *Town hall of the Sants-Montjuic District*, (*Seu del Districte Sants-Montjuic,* 1914) designed by the architect Jaume Gustà i Bondia and has a large set of windows drawn by the artist Francesc Labarta (1883-1963) and made by the studio of *Rigalt i Granell* in 1914. Several fragments were obtained from after the windows were vandalized during the riots that occurred in May 2014. The violent street demonstrations were sparked by a police operation to evict a squatter's group which from some time occupied a community centre. Some of the demonstrators threw objects at the windows and broke a glass showing the background floral patterns; luckily none of the original faces painted by Labarta were affected. The windows are installed in the main facade of a very busy street with dense traffic. The fragments show grisaille painted motives filled with a mixture of blue and green enamels applied over a yellow cathedral glass (SM1-4) and modelling grisaille over a green glass (SM5). The enamel shows a whitish appearance; the other side of the glass has a matt appearance probably, some sort of enamel or *grisaille* added to reduce the Mediterranean light entering the building. The matt appearance seems to have been obtained by means of an acid attack.

- High court Palace (Palau de Justicia)

The transparent substrate glasses PJ1 and PJ3 are of a soda-lime type with about 15 %Na_2O and 12 %CaO typical of the Modernist period. However, the fragment PJ2 contains lower CaO (~ 8 %CaO) and higher MgO (~3.4 %MgO). The replacement of CaO by MgO could be related to a glass chemistry modification to obtain a more resistant glass, common after 1930 [6], suggesting that the fragment PJ2 might belong to a restauration of the skylight.

Fig. 4.6. Images of the *High court Palace* skylight stained glass samples. (A) PJ1, purple enamel and contour *grisaille;* (B) PJ2 and (C) PJ3 yellow silver stains and contour *grisaille*.

The purple enamel (PJ1) (**Fig. 4.6A**) was found to contain very little lead, boron and zinc (**Table 4.3**) compared to the purple replicated enamels from the *Rigalt i Granell* workshop (**Table 2.1**), but contained about 2000 ppm Au, 1.78 %SnO_2 and Au/Ag ≈ 2, (**Table 4.3**) which corresponds well to the purple enamel replica E14 (**Table 2.1**). Minor amounts of chlorine and traces of phosphorous were also detected by LA-ICP-MS both in the substrate glass and in the enamel. The SEM-BSE images of the cross section confirm the presence of lead sulphate, $PbSO_4$, filling the bubbles and cracks **(Fig. 4.7A**). The enamel has a high silica (45 %SiO_2), low PbO (7 %PbO) and ZnO (0.6 %ZnO) content (**Table 4.3**) and the presence of sulphur (boron cannot be determined by SEM-EDX). The total is very low, confirming the heavy alteration of the enamel chemistry. A lead enriched enamel-substrate glass interface with about 28 %PbO, 7.5 %Na_2O and 6 %CaO, may also be lead depleted assuming that the original composition of the enamel was much higher in lead (**~**53 %PbO) and conforming a structure of three layers (**Fig. 4.7B**). The UV-Vis absorbance spectrum of the purple enamel (**Fig. 4.3)** shows the absorption band associated with Ag-Au^o alloy nanoparticles, as discussed in **Chapter 2**. The colour (h_R* = 20º, s_R* = 16.3%) is magenta-red (**Fig. 4.6A)** and less saturated

than the workshop enamels, most probably to the presence of lead sulphate precipitates which are white.

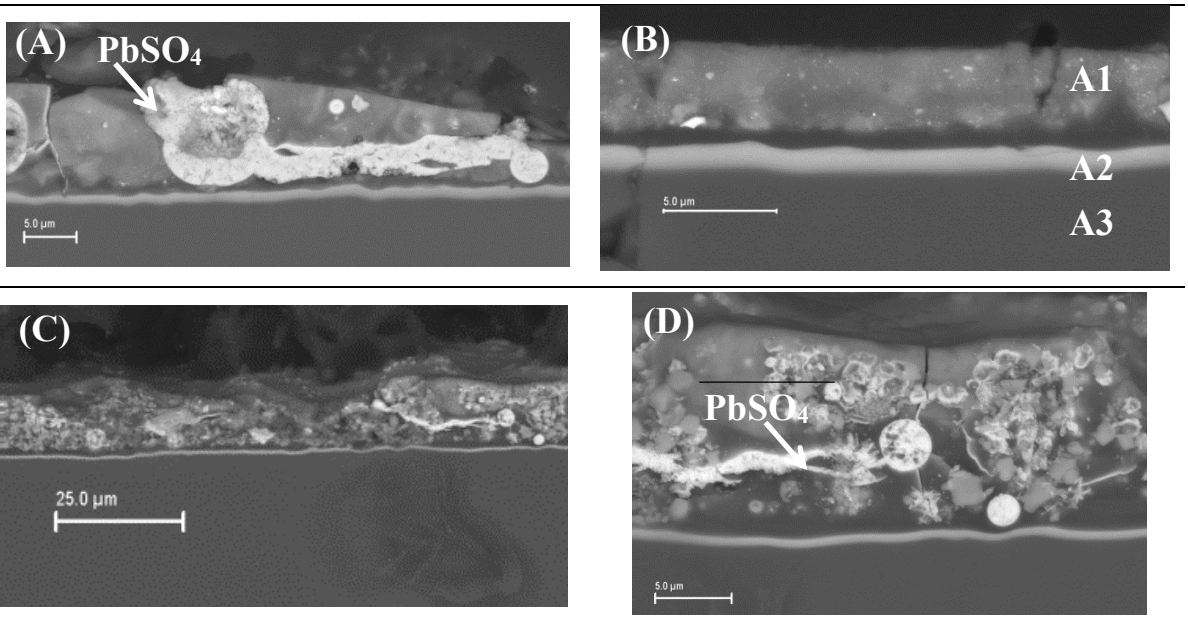

(E)

Wt%	Na_2O	MgO	Al_2O_3	SiO_2	SO_3	Cl	K_2O	CaO	MnO	FeO	ZnO	SnO_2	Ag	Au	PbO	BaO	Total
A1	1.2	0.3	1.5	44.6	1.7	0.2	1.3	1.4		1.0	0.6	14.9	0.5	2.6	7.2		77.7
A2	97.5	0.3	0.5	55.2		0.4	0.5	6.0				1.7			28.0		99.4
A3	13.6	0.2	0.3	68.5	1.0	0.4	0.2	14.2	0.3							0.5	99.1

Fig. 4.7. SEM-BSE images of the purple enamel (PJ1) showing **(A)** the presence of large bubbles and cracks filled with $PbSO_4$, and **(B)** the layered structure: **A1** showing the suspension of gold-silver-tin particles, **A2** corresponding to the reaction of the enamel glass with the substrate glassand **A3** the substrate glass.

(C) and **(D)** SEM-BSE images of the purple enamel mixed with the *grisaille* showing the presence of bubbles and cracks filled with $PbSO_4$.

(E) SEM-EDS analysis of the three layers shown in (B).

The area covered by the *grisaille* shows the same type of alteration, the precipitation of $PbSO_4$ in the cracks and bubbles (**Fig. 4.7C, 4.7D)**. The purple enamel is surrounded by *grisaille* contour lines which are applied on the same side of the substrate glass (**Fig. 4.6A**). The images show how the $PbSO_4$ filling the cracks and around the particles results in the flacking of the grisaille. Although *Lacroix* in his treatise advised of applying the *grisaille* to the other side of the substrate glass to avoid the mixture of enamel and *grisaille*, the application of the enamels on the same side than the contour *grisaille* was not uncommon. *Rigalt* disregarded the advice because of the mismatch between the contour lines and the enamel paint resulting from the

thickness of the substrate glass. *Rigalt* also noted that besides *some difficulties, the result was more satisfactory* [7].

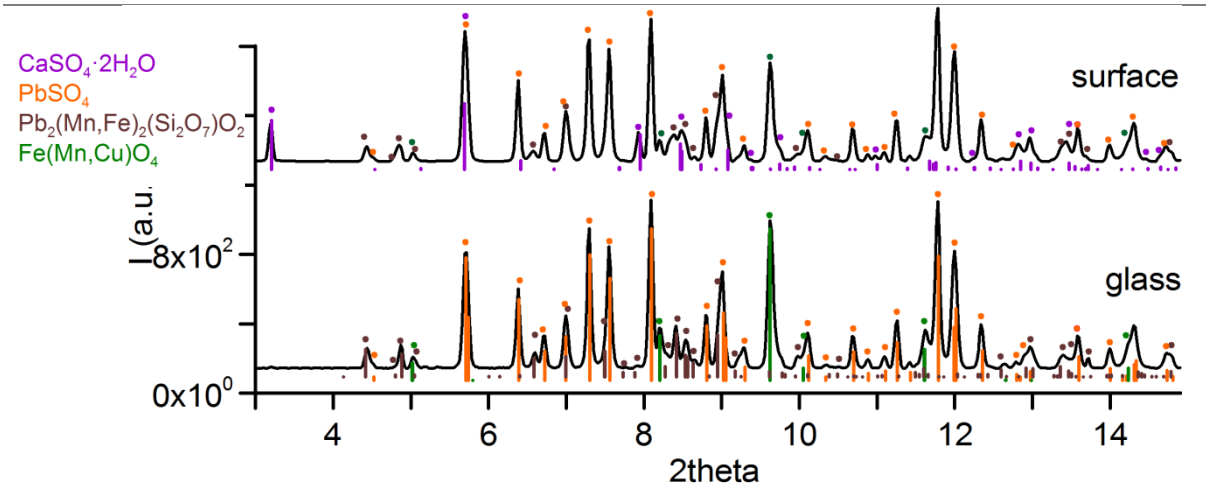

Fig. 4.8. μ-XRD patterns of the grisaille on PJ1 taken near the surface and the substrate glass respectively; $PbSO_4$, $CaSO_4 \cdot 2H_2O$, $FeMn_2O_4$ and $Pb_2(Fe,Mn)_2Si_2O_9$.

The *grisaille* show the presence of iron rich spinel containing manganese and copper ($Fe,(Mn,Cu)O_4$) and iron rich lead silicate ($Pb_2(Fe,Mn)_2(Si_2O_7)O_2$) particles (**Fig. 4.8**) appear mixed with the purple enamel on PJ1. The presence of an iron rich spinel with copper instead of haematite as found in the workshop grisaille must be related to the addition of copper oxide. The addition of copper to the *grisailles* was very common [8]; its main purpose is to reduce the amount of haematite formed to suppress the red hue. Gypsum, $CaSO_4 \cdot 2H_2O$, was also found deposited on the surface.

The fragments PJ2 and PJ3 show a yellow silver stain surrounded by contour grisaille applied on opposite sides of the substrate glass. PJ2 silver is Ag richer (~3.2%) than PJ3 (~0.7%), while PJ3 contains also a small amount of copper, lead and iron. Both stains appear pretty well preserved. Silver stains are obtained by a process in which silver ions are introduced in the substrate glass surface, being easily reduced to the metallic state the silver atoms coalesce and form small (a few to some tens of nm size) metallic nanoparticles. Silver nanoparticles grow into the glass surface causing compressive stress. Moreover, they are not embodied in a glass of a low softening temperature, like the enamels. As a consequence, the silver stained glass surfaces are less prone to corrosion.

Silver nanoparticles absorb and scatter strongly in the blue region of the UV-Vis spectra, PJ2 has the absorption peak around 415 nm related to silver nanoparticles of about 20 nm in a soda-lime glass (**Fig. 4.4),** this causes the typical yellow-greenish colour and the bluish scattering of silver colloidal solutions. Larger sizes tend to red shift the SPR, shifting the colour of the colloids to orange and red [9,10]. In fact the colour of the silver stain of PJ2 is redder and more saturated (h_T* = 77º s_T* = 77.4%, h_R* = 47º and s_R* = 17.4%) than PJ3 (h_T* = 91º and s_T* = 72.8%, h_R* = 75º and s_R* = 3.6%) which accounts for the high amount of silver in PJ2 and also to the different chemical composition of both substrate glasses. It reinforces the possibility that the fragment PJ2 was a later addition.

***- Town hall of Sants-Montjuic District (Seu del Districte Sants-Montjuic*)**

Fig. 4.9. From left to right b fragments SM1 to SM4 showing a blue enamel with modelling *grisaille* over a yellow cathedral glass from the *Town Hall of Sants-Montjuic district* by *Rigalt & Granell*

Some of the fragments studied (SM1-4) showed a blue enamel over a yellow substrate glass (cathedral) with modelling *grisaille* which appears mixed with the enamel in some areas (**Fig. 4.9)**. The blue enamel contains Al, Cr and Co and some Fe which are related to the presence of pigment particles of the type $(Al,Cr)_2CoO_4$ (**Fig. 4.10B** and **4.10C**) like in the *Rigalt i Granell* workshop enamel E34. While E34 also contains also some copper (Cu^{2+} dissolved in the glass), which gives a greenish tinge to the enamel, no copper was detected in SM1-4, which in fact is blue (h_R* = 248º) (**Fig. 4.9A-C)**. Minor amounts of chlorine and traces of phosphorous were identified both in the substrate glass and in the enamel. The enamel shows also a lead enriched enamel-substrate glass interface (~37% PbO). µ-XRD patterns obtained from an area with grisaille and enamel (**Fig. 4.10C**) show from interface to surface the presence of the blue cochromite particles, then the iron rich spinel $(Fe,(Mn,Cu)O_4)$, tenorite (CuO) and melanotekite $(Pb_2(Fe,Mn)_2(Si_2O_7)O_2)$ related to the *grisaille* and calcium carbonate (calcite, $CaCO_3$) and basic lead carbonate (hydrocerussite, $Pb_3(CO_3)_2{\cdot}(OH)_2$) related to pollution and alteration.

Other areas of the surface show the blue enamel particles on top of the *grisaille* particles (**Fig. 4.10D** and **Fig. 4.10E**).

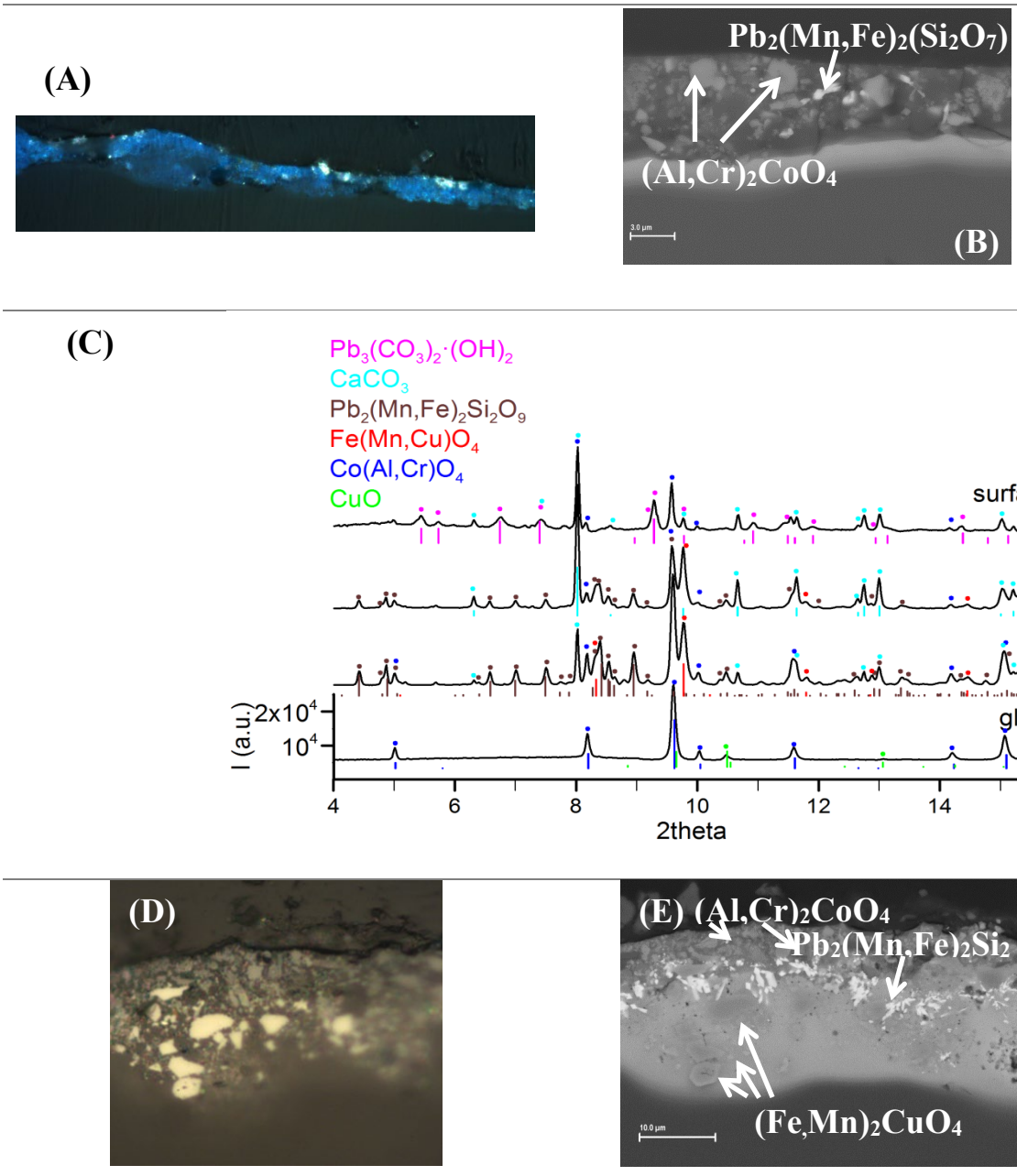

Fig. 4.10. (A) Polarised light optical Microscope image from SM1; **(B)** SEM-BSE image showing the presence of particles of $(Al,Cr)_2CoO_4$ from the blue enamel and of $Pb_2(Mn,Fe)_2Si_2O_9$ from the grisaille and also the enamel-substrate glass interaction layer (A1); **(C)** μ-XRD patterns obtained across the enamel layer SM1 showing the enamel and *grisaille* particles, $(Al,Cr)_2CoO_4$, $(Fe,Mn)_2CuO_4$, CuO and $Pb_2(Fe,Mn)_2Si_2O_9$, and also the presence of $CaCO_3$ and $Pb_2(CO_3)_2(OH)_2$ compounds on the surface. **(D)** Bright field optical Microscope and **(E)** SEM-BSE images from SM3 showing also particles from the *grisaille* and from the blue enamel on the top.

The absorbance measured in transmission mode of the blue enamel (SM1) (**Fig. 4.3A**) is dominated by the colour of the substrate glass, which is yellow, a soda-lime with Mn^{2+} glass shown in **Table 4.2** and **Fig. 4.1**. The Reflectance spectrum of the blue enamel, (**Fig. 4.3B**) shows the triple absorption band between 500 nm and 650 nm and also the large NIR absorption between 1250 nm and 1750 nm related to tetrahedral Co^{2+}. Comparing the historical enamels from the *Rigalt, Granell & cia* workshop with the replica enamels, the former show lower colour saturation (s_R*=14.4%) than the original the *Rigalt i Granell* workshop enamels, most probably related to the presence of lead and calcium carbonate precipitates which are white. The external side of the stained glass shows a whitish matt appearance (**Fig. 4.11**) The whitish colour is due to the application of a lead rich enamel with cassiterite particles well fussed to the substrate glass (**Fig. 4.11B**). The incisions and irregularities of the outer surface probably produced by a mechanical tool or an acid attack give a matt appearance to the surface.

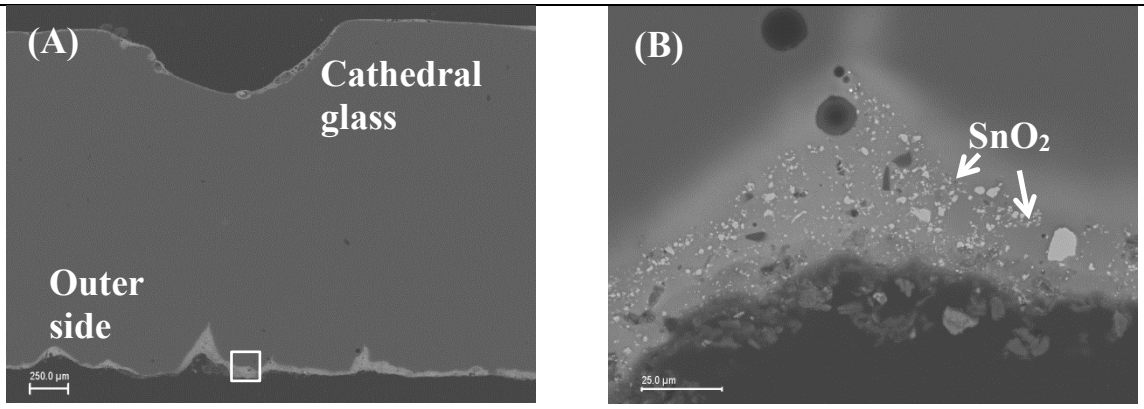

Fig. 4.11. (A) and **(B)** SEM-BSE images from SM1 showing the presence of an enamel layer containing cassiterite particles on the outer side of the glass.

The SM5 glass sample from the *Town Hall of Sants-Montjuic district* has a grisaille over a green substrate blown glass (**Fig 4.12A**). The enamel has reacted strongly with the substrate glass. The microdiffraction patterns of the *grisaille* applied over the substrate glass (**Fig. 4.12C**) shows the presence of an iron rich spinel of $(Cu,Mn,Zn)Fe_2O_4$ and also of an iron rich silicate (pyroxene) probably produced by the reaction of the grisaille compounds with the substrate glass.

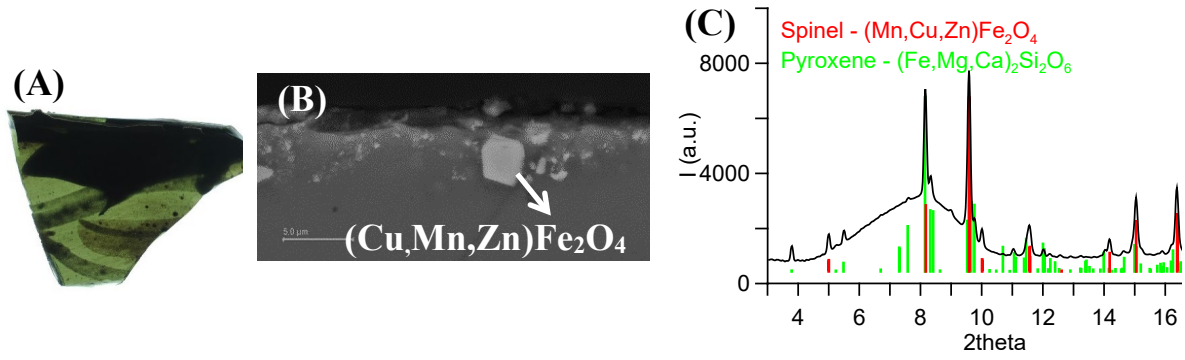

Fig. 4.12. (A) *Grisaille* over a green glass fragment SM5 **(B)** SEM-BSE image and **(C)** μ-XRD pattern showing the presence of particles of $(Cu,Mn,Zn)Fe_2O_4$.

4.2.2. Bordalba

We have also analyzed samples of enameled glasses produced by the *Bordalba* workshop from two private houses in the Barcelona's *Eixample*. They belong to the skylight from the *Bures* house (CB), located near Plaça de Catalunya, at number 30-32 Ausiàs Marc street and to the lift glass panels (PG1 and PG2) from *Cama i Escurra* house, located at number 15 Gran de Gràcia Street. The chemical analyses are shown in **Table 4.3**.

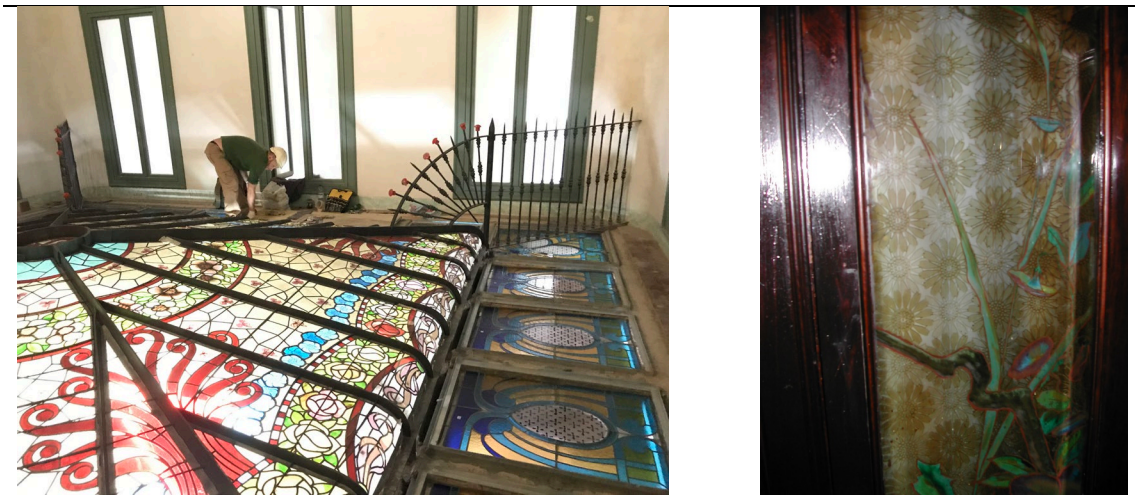

Fig. 4.13. (Left) Detail of the Burés house skylight.
(Right) Enamelled glass panel of the lift from Cama i Escurra house. Pict.: J.M. Bonet workshop.

The *Burés* building was a private residence of the family of Francesc Burés i Borràs in the city of Barcelona and was built in 1900 by the architect Francesc Berenguer i Mestres. The house

has been abandoned for the last 20 years, when investors bought it and reformed it thoroughly to sell luxury apartments. The skylight of the Burés house (**Fig 4.13**) is remarkable for its beauty and design. It was built by Antoni Bordalba and has little enameled glass, mainly a few minor details painted with purple enamel. The purple enamel consists on a thin layer worked with a badger brush and has some pin holes all over the surface. Where the pin holes are absent, it shows a translucid shiny surface.

Cama i Escurra is a Barcelona private house built by the architect Francesc Berenguer in 1902-1904. The building elevator has a couple of stained glass panels attributed to the *Bordalba* workshop (**Fig. 4.13**), because they also made the stain glasses of other Berenguer houses. The stained glass has an acid gravure with floral patterns background and some vegetal grisaille drawn patterns filled with blue, green and purple enamels applied on the same side of the substrate glass.

- Bures house

The *Bures* house skylight (CB) shows some details with a purple enamel surrounded by a contour *grisaille* applied on the same side of a drawn cloudy yellowish glass (**Fig. 4.14A**). The characteristic colour of the substrate glass is due to the presence of chromophores, Fe^{3+} and Mn^{2+} (**Table 4.2**), responsible of the yellowish hue. The chemical analysis also shows a high amount of tin in solution in the substrate glass, probably responsible of the cloudy appearance. **Fig 4.3** shows the UV-Vis spectrum of the substrate glass where the bands at 390 nm and 440 nm are associated to Fe^{3+} and the band at 400 nm associated to Mn^{2+}.

The purple enamel is of a purple of Cassius type (gold nanoparticles suspended in a tin rich glass), which composition is shown in **Table 4.3**. The UV-Vis spectra show the characteristic absorption (surface plasmon resonance, SPR) of the visible light related to the presence of metallic nanoparticles (**Fig. 4.1**). The SPR peak position depends on the size and composition of the nanoparticles [9,11] but also on the refraction index of the glass. Considering that the plasmon peak position for gold particles of about 20 nm size in a glass of refraction index ~ 1.60 is λmax~550 nm [11], the enamel contains mainly gold nanoparticles in good agreement with the LA-ICP-MS analysis (9392 ppm Au and 157 ppm Ag). The microdiffraction pattern shows the presence of metallic gold and cassiterite (SnO_2) (**Fig. 4.14C** and **D**). The colour is red and semi-opaque (h_R* = 13º, h_T* = 25º, s_T* =81.0%, L_T* = 6.1%) due to the presence of cassiterite particles.

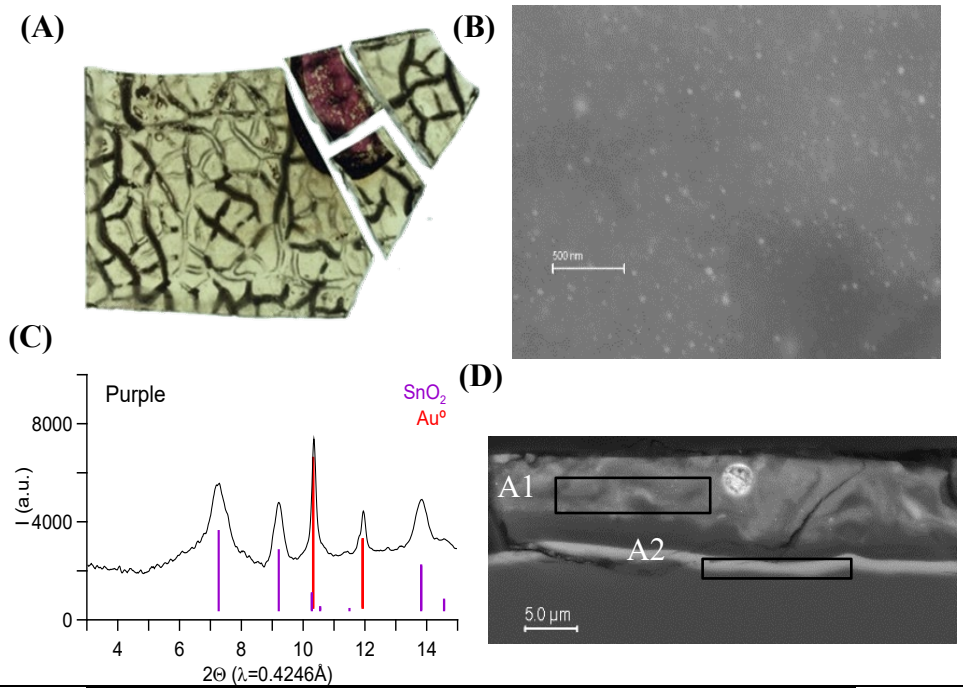

(E)

	Na_2O	MgO	Al_2O_3	SiO_2	SO_3	Cl	K_2O	CaO	MnO	FeO	CuO	SnO_2	Au	PbO	Total
A1	0.7	0.3	1.6	30.4	1.2	0.1	1.1	0.8	0.2	1.4	0.4	34.3	3.7	2.7	78.7
A2	4.2	0.1	1.1	53.6		0.2	0.6	4.0	0.8	0.8		1.0		28.8	94.8

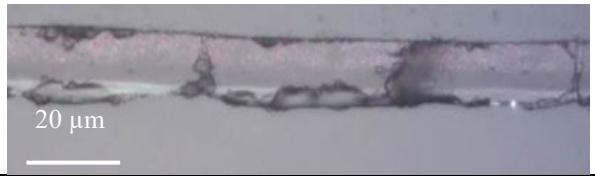

Fig. 4.14. (A) Enameled glass fragment (CB) from the Burés house skylight. **(B)** SEM-BSE image and **(C)** µ-XRD pattern showing the presence of metallic gold nanoparticles and cassiterite (SnO_2). **(D)** SEM-BSE image of the cross section of the enamel showing a layered structure and a lead rich interface. (**E**) SEM-EDS analysis of the areas marked. (**F**) OM bright field image showing the red scattering of the gold nanoparticles and the lack of adherence of the enamel to the substrate glass

The purple enamel appears heavily altered and shows the characteristic layered structure resulting from the loss of lead (**Fig. 4.14D-F**). Although the LA-ICP-MS analysis shows little lead, zinc and boron, the presence of high amount of lead at the enamel-substrate glass interface indicates that originally the enamel was lead rich (**Fig. 4.14D-E)**. The bubble in **Fig. 4.14E** is filled by lead carbonate and cassiterite. Consequently, the loss of lead, and the low total determined by SEM-EDS of the enamel area (**Fig. 4.14D-E)** should be related to the alteration of the enamel and the glass component of the purple enamel is also of a high-lead zinc borosilicate type.

- Cama i Escurra house

The fragment (**Fig. 4.15**) belongs to the lift panels of the *Cama i Escurra* house has *grisaille* drawn patterns filled with turquoise (PG1) and purple (PG2) enamels applied on the same side of the substrate glass (PG). The substrate glass has an acid gravure with floral patterns; a transparent soda lime glass with some iron which contribution to the colour of the glass is counteracted by the addition of minor amounts of manganese (**Table 4.2**).

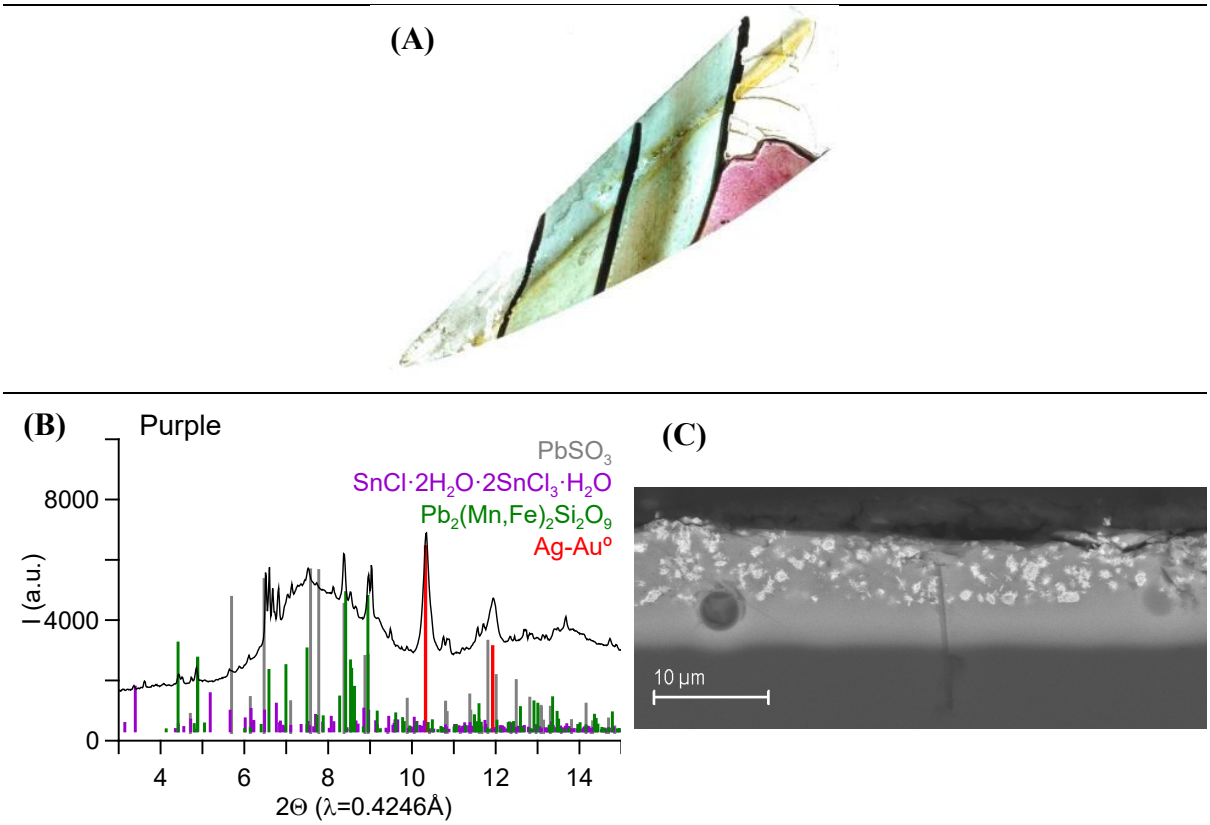

Fig. 4.15. (**A**) Fragment of the stained glass of the Cama i Escurra's lift, *grisaille* patterns filled with turquoise and purple enamels applied on the same side of the substrate glass.

(**B**) µ-XRD pattern and (**C**) SEM-BSE image of a cross section from PG2 showing the purple enamel mixed with grisaille particles (light particles are melanotekite, $Pb_2(Mn,Fe)_2Si_2O_9$).

The purple enamel (PG2) is of *purple of Cassius* type with gold-silver nanoparticles (**Table 4.3** and **Fig. 4.15B** and **C**). The nanoparticles are gold rich (6715 ppm Au and 875 ppm of Ag). The colour is magenta and semi-opaque (h_R* = 358º, h_T* = 354º, s_T* =84.8%, L_T* =9.2%) probably due to the presence of cassiterite.

The chemical composition of the turquoise enamel (PG1) reveals the presence of cobalt, chrome and copper (**Table 4.3**). The microdiffraction pattern and SEM-BSE image shows the presence of some small particles of a spinel of the type cobalt and chromium aluminate containing also some zinc still present on the surface of the enamel, while the copper is dissolved in the glass (**Fig. 4.16A-B**). The presence of a few crystalline particles of melanotekite (**Fig 4.16A-B**), and which should be related to a modelling *grisaille* applied over the enamel surface. The UV-Vis-NIR spectra (**Fig. 4.3**) of the turquoise enamel reveals the characteristic bands of Co^{3+} in tetrahedral coordination and Cu^{2+}, the near infrared region also shows an enhanced absorption of light due to the presence of cobalt and chrome aluminate particles. The colour is turquoise and very transparent (h_R* = 198º, h_T* = 104º, L_T* =40.8%).

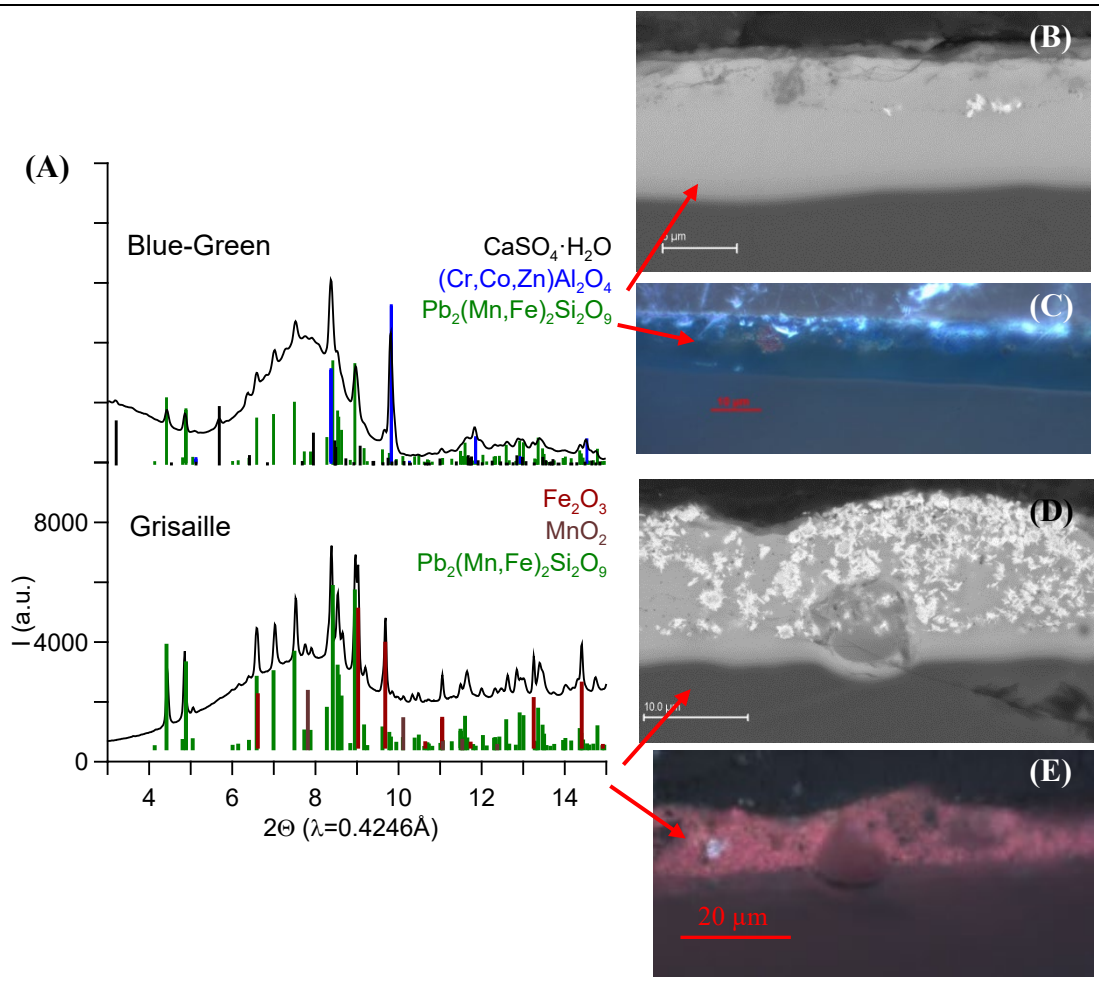

Fig. 4.16. (**A**) Microdiffraction patterns, (**B**) and (**D**) SEM-BSE and (**C**) and (**E**) OM images from cross sections of the turquoise enamel and the contour *grisaille* respectively.

Finally, the contour grisaille contains very small particles of hematite (Fe_2O_3), pyrolusite (MnO_2) with melanotekite ($Pb_2(Mn,Fe)_2Si_2O_9$) growing around them; the copper is dissolved in the glass.

The turquoise enamel (PG1) appears altered only at the surface and the corrosion products identified are mainly precipitates of calcium and sodium sulphate and chloride. The purple enamel appears more altered, with the characteristically layered structure as a result of the lead depletion. It has a lead rich layer, which appears lighter in the SEM-EDS images and precipitates of lead and tin sulphates and hydroxy-chlorides. Although, the enamelled glass was kept in the interior of the buildings and was protected of the weathering, the cleaning of the surfaces may have had some impact.

4.2.3. Buxeres i Codorniu

We have analysed the enamels (BC1 and BC3) from one panel signed by *Buxeres i Codorniu* and produced around the 1900. The panel is located in a private house designed in 1896 by the architect Joan Baptista Pons i Trabal and located in the city of Badalona, close to Barcelona. The fragment is the result of a domestic accident after which all the fragments were kept by the owner for some years. When the windows were finally restored some of the designs appeared incomplete and disconnected. The samples studied belong to an ornamental decoration (**Fig. 4.17**) with blue, brown, purple and green enamels and also a contour *grisaille* all them applied on the same side of the substrate glass; a yellow silver stain was applied on the other side.

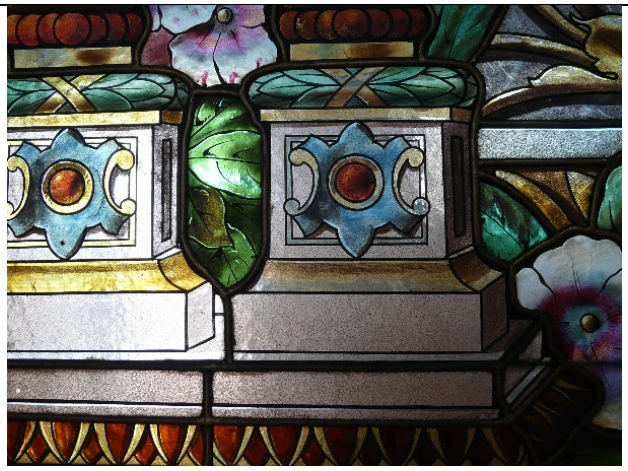

Fig. 4.17. Detail of a stained glass window located at a private house in Badalona made by *Buxeres i Codorniu*. Pict.: J.M. Bonet workshop.

- Private house

The substrate glass reveals that it is a soda lime (high soda with 19.7% Na_2O, with 8.2% CaO and very low MgO concentration) transparent glass of the period (**Table 4.2**) with a relatively high amount of arsenic (0.2% As_2O_5), which could have been added as fining agent [6].

(A)

(B)

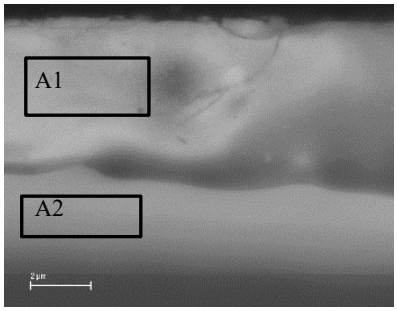

(C)

	Na_2O	Al_2O_3	SiO_2	Cl	K_2O	CaO	ZnO	Ag	SnO_2	Au	PbO	Total
A1	1.0	-	27.4	1.4	0.9	1.5	0.8	0.9	21.6	3.2	26.7	84.0
A2	9.0	0.4	49.6	0.6	0.4	3.1	0.6	-	0.9	-	34.4	98.3

Fig 4.18. (**A**) Fragment (BC3) from a private house in Badalona by *Buxeres i Codorniu*. (**B**) SEM-BSE image showing the layered structure of the purple enamel and (**C**) chemical composition of the different layers.

The blue enamel (**Fig. 4.3**) contains cobalt and chromium. The microdiffraction pattern shows the presence of cobalt and chromium spinel compounds in the form of cobalt chromite or cochromite ($CoCr_2O_4$) and cobalt aluminate $(Co,Zn)Al_2O_4$. The UV-Vis spectra present the characteristic series of absorption peaks between 500 nm and 700 nm and between 1200 nm and 1700 nm, corresponding to $[Co^{2+}]_4$, this is cobalt 2+ in tetrahedral coordination [12]. The colour is pure blue and very opaque (h_T* = 263º, L_T* = 0.2%). The green enamel contains also cobalt and chrome and copper (**Table 4.3**); copper is dissolved in the glassy phase and contains spinel particles ($(Al,Co)Cr_2O_4$) (**Fig. 4.19).** The colour is yellow-green and partly (h_T* = 126º, L_T* = 8.7%). The purple enamel (**Table 4.3**) contains gold, silver and tin, and the microdiffraction pattern (**Fig. 4.19**) and the UV-Vis spectrum (**Fig. 4.3**) indicate the presence of silver-gold alloy nanoparticles. The colour is violet and partly opaque (h_T* = 49º, L_T* = 13.0%). The opacity is related to the addition of modelling *grisaille* to the enamels

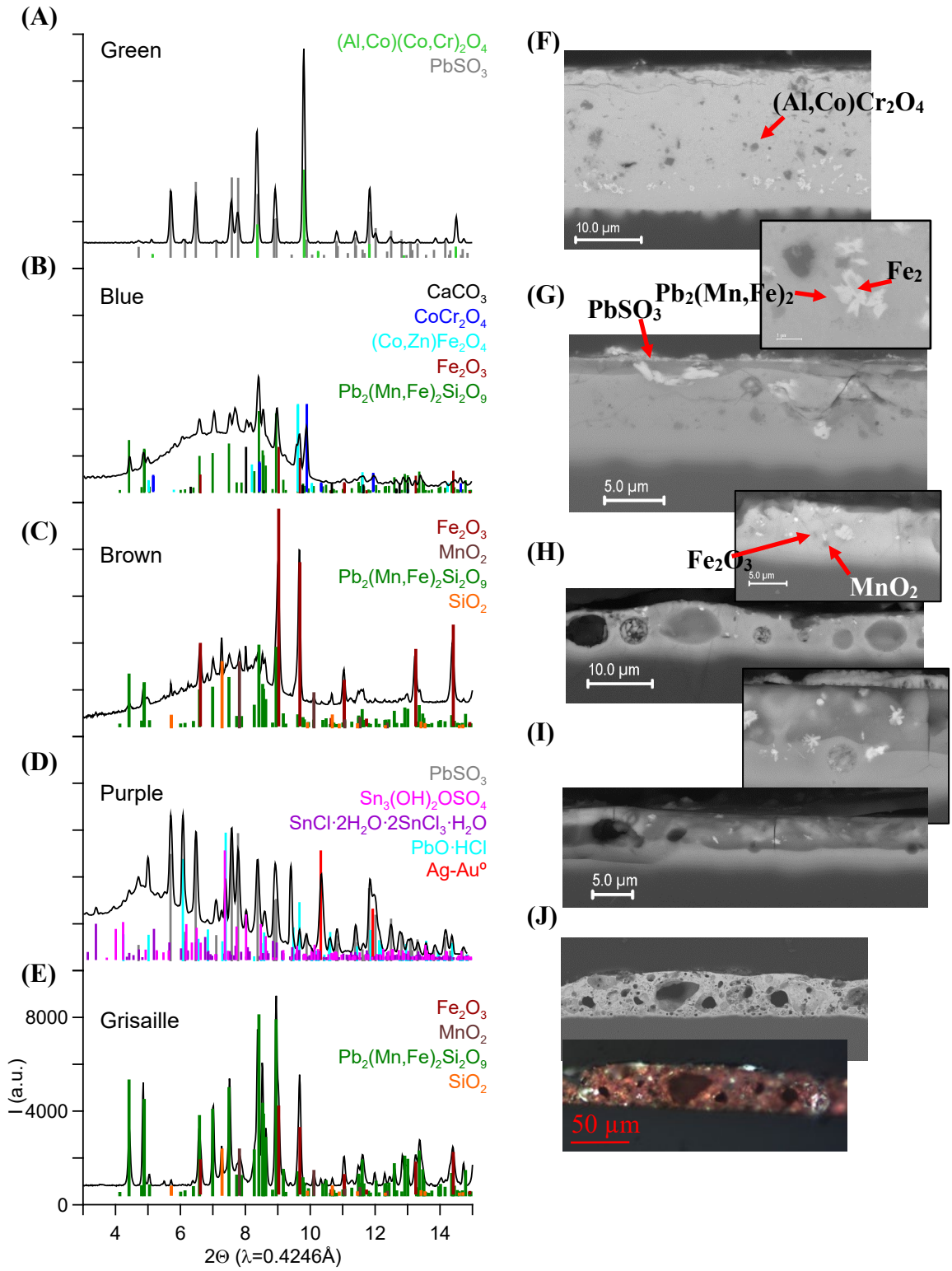

Fig 4.19. (**A-E**) µ-XRD patterns and (**F-J**) SEM-BSE images from selected areas of the different colour enamels.

The brown enamel has a *grisaille* formulation with lead, iron and manganese (**Table 4.3**). The glassy part is a lead glass and has pyrolusite (MnO_2), hematite (Fe_2O_3) and melanotekite ($Pb_2(Mn,Fe)_2Si_2O_9$), as well as some quartz (SiO_2) particles (**Fig. 4.19**). The colour is umber and transparent (h_T* = 70º L_T* = 33.0%). *Grisaille* microdiffraction patterns has the same particles than the brown enamel but in larger amounts, that is the brown enamel is more amorphous. The yellow silver stain shows the presence of silver nanoparticles in the soda lime substrate glass.

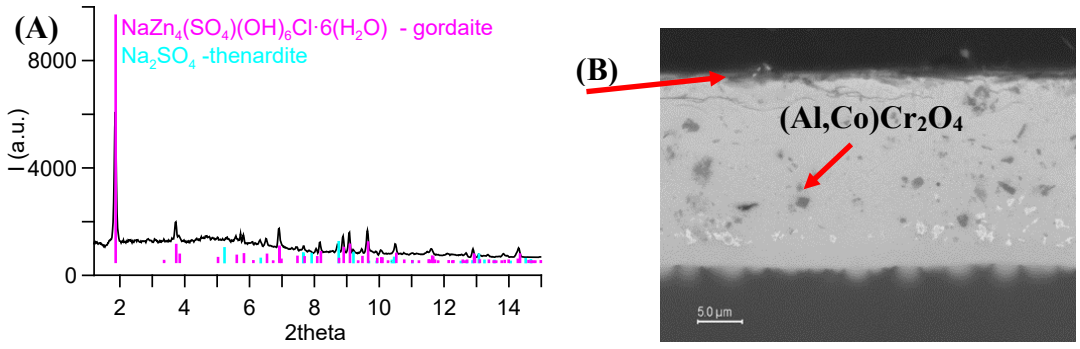

Fig. 4.20. (**A**) Microdiffraction pattern of the surface corrosion products on the green enamel. (**B**) SEM-BSE image of the green enamel showing the presence of cobalt and chrome aluminate particles and the surface alteration.

The enamels are not heavily altered, probably due to their location inside the private building, corrosion affecting only the very surface. Blue and green enamels show precipitates of Na_2SO_4 and $NaZn_4(SO_4)(OH)_6Cl·6H_2O$ on the surface (**Fig. 4.20A**). The purple enamel appears more altered showing a layered structure (**Fig. 4.18B**) lead richer close to the interface enamel-substrate glass. Some corrosion products are precipitated in cracks on over the surface $PbSO_4$, $Pb(OH)Cl$, $SnCl·2H_2O·2SnCl_3·H_2O$ (**Fig. 4.19**). The presence of such corrosion compound could be related to the use of cleaning products containing Cl_2.The brown enamel, the *grisaille* and the silver stain appear unaltered.

4.2.4. Hijos de Eudaldo Ramon Amigó

The *Hijos de Eudaldo Ramon Amigó* workshop was one of the most important pre-modernist and modernist workshops in Barcelona. The stained-glass samples analysed belong to the cathedral of *Palma de Mallorca* (P) and to the parish church of *Sant Jaume de Calaf* (C) and were obtained during their respective restoration works.

The cathedral of Palma de Mallorca is a 13th century religious gothic building which construction was completed in 1630. The *capella de la Santíssima Trinitat* has some windows with enamelled glasses made in 1889 by *Amigó* (**Fig. 4.21**). A fragment of a yellow blown glass with *grisaille* (P) was obtained in the 2017 restoration works of the stained glasses of the cathedral.

The parish church of *Sant Jaume de Calaf* is a late 16th century building which has a set of windows made in 1903 by *Amigó*. Its stained glass windows are very characteristic of the religious work made by this studio with complex geometric patterns surrounding the central figure of a saint standing under a canopy and extensive use of enamels. In addition to the renowned instability of the *Amigó* paints the church was also partly burned during the Spanish civil war adding to the low conservation shown by the enamelled glasses. Moreover, some of the windows were severely damaged by hailstorms, many chips and bits fell from the windows placed 14 meters above the nave ground floor. The fragment of stained glass analysed belongs to a complex painted design including a face, with flesh and red enamels for the skin and lips, green and purple draperies and tracing and modelling *grisailles*. The *grisailles*, red and flesh enamels were painted on the internal side of the glass while the green and purple enamels were painted on the external side. The church keeps some undamaged windows, and although the samples appear very fragmentary, we can assume that all the glasses were painted in a similar way.

4.21. (Left) External view of Palma de Mallorca cathedral showing some of the stained glass panels of the *Santíssima Trinitat* chapel by *Amigó*.

(Right) Detail of the stained glass during the restoration works. Pict.: J.M. Bonet workshop.

- Palma de Mallorca cathedral

An amber coloured glass sample with what is left form a *grisaille* belonging to the *Palma de Mallorca cathedral* by Amigó has been analysed (**Fig. 4.22A**). The amber colour of the substrate glass is due to the presence of chromophores, Mn^{2+} and Fe^{3+} in a soda lime glass (15.5% Na_2O and 11.3% CaO) and (**Table 4.2**). The *grisaille* is very amorphous with large bubbles which indicate a high viscosity (11.5% CaO) (**Fig. 4.22B**), large crystallites of lead-calcium silicate ($CaPbSiO_4$), CuO and $Fe(Mn_{2-x}Cu_x)_2O_4$ are also found (**Fig. 4.22C** and **D**). The SEM-EDS analysis of the glass component of the grisaille:

P1	Na_2O	MgO	SiO_2	K_2O	CaO	CuO	ZnO	PbO	Total
Glass component of the *grissaille*	3.7	0.1	26.1	3.9	0.2	0.3	1.1	55.5	90.3

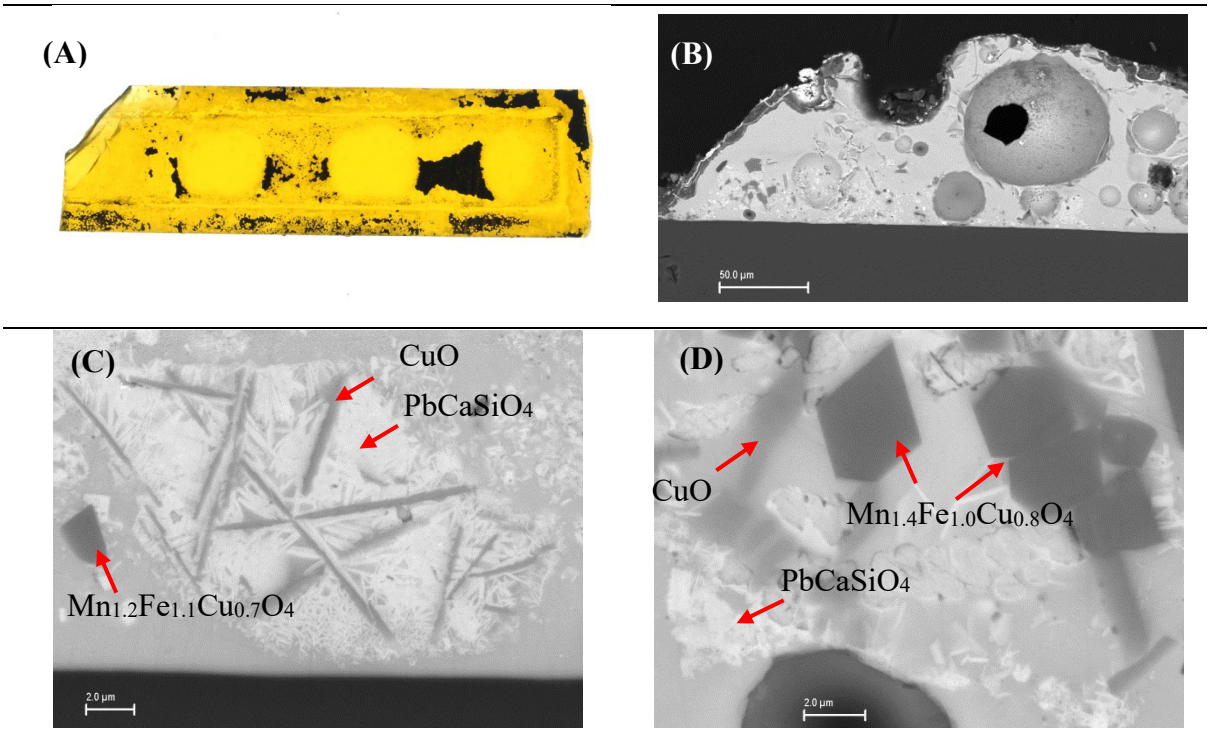

Fig 4.22. (**A**) *Grisaille* on an amber substrate glass from *Palma de Mallorca cathedral* by Amigó (P). (**B**) SEM-BSE image of a cross section of the *grisaille* (**C**) and (**D**) SEM-BSE images of some of the crystals.

It gives a relative low total and contains zinc which together with the amorphous nature of the *grisaille* seems to indicate that a *flux* might have been added. The *grisaille* is not well fused

into the glass-substrate. All this indicates that the *grisaill*e was fired for a long (large crystal precipitates shown in **Fig. 4.22C** and **D**) time but at a low temperature.

- Sant Jaume de Calaf church

The fragments analysed from the Sant Jaume de Calaf church belong to a complex design of a face, painted with *carnation* and red enamels to represent skin and lips (C1) and of green and purple draperies (C3). The substrate glass is a transparent soda lime glass with low amounts of CaO (8.05% Cao) and high amounts of Na_2O (13.8% Na_2O) and MgO (4.05% MgO).

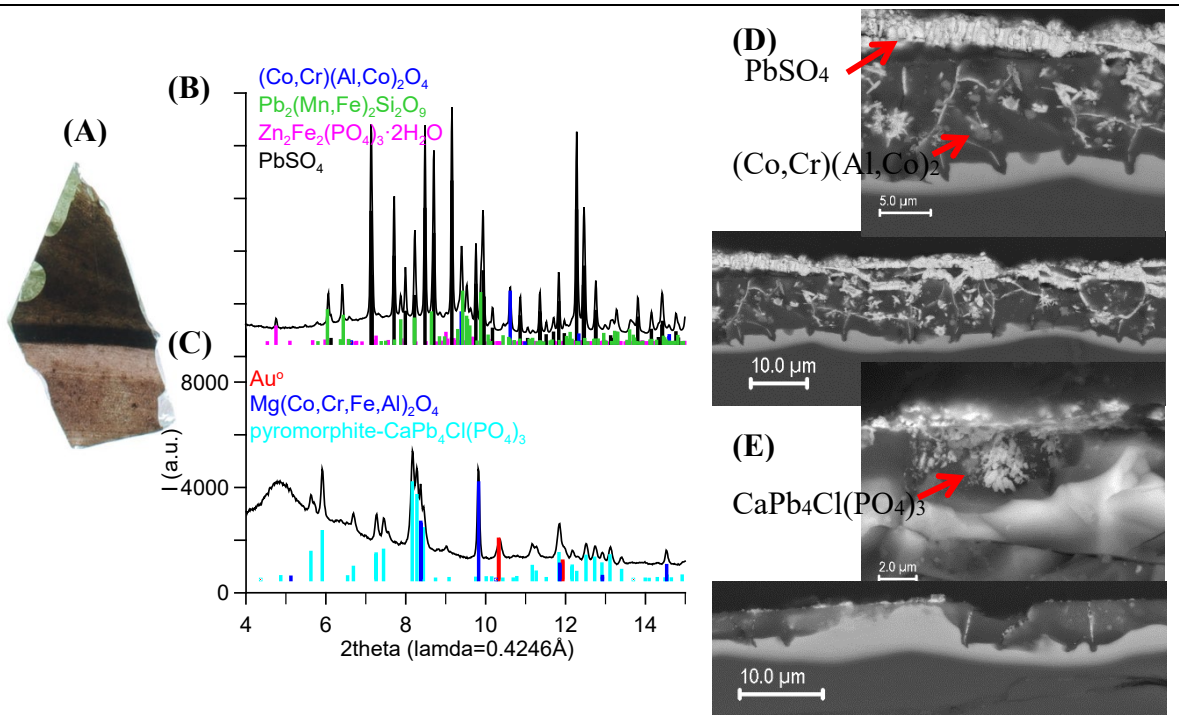

Fig. 4.23. (**A**) C3 sample with green and purple draperies from Sant Jaume de Calaf church. (**B**) and (**C**) microdiffraction patterns and (**D**) and (E), SEM-EDS images from the green and purple enamels respectively.

The chemical analysis (**Table 4.3**) and microdiffraction pattern and SEM-BSE images (**Fig. 4.23**) of the green enamels present on the sample with purple and green draperies (C3) reveals the presence of cobalt, chromium aluminate particles and Cu^{2+} dissolved in the glassy matrix (**Fig. 4.3**) [12]. The colour is olive-green and very opaque (h_T* = 113º, L_T* = 0.8%). The purple enamel is of a *Purple of Cassius* type and contains mainly gold nanoparticles (**Fig. 4.23**). In the green enamel close to the *grisaille* we found some particles of kentrolite and also hematite (Fe_2O_3) associated to the *grisaille*. The colour is dark red and very opaque (h_T* = 48º, L_T* =

0.7%). The green and purple enamels appear heavily altered. The chemical analysis (**Table 4.3**) shows boron, zinc and lead depletion. The presence of pyromorphite ($CaPb_4Cl(PO_4)_3$) and lead zinc phosphate precipitates filling the cracks and bubbles and a layer of mainly lead sulphate growing on the surface. The presence of chlorine and phosphorous could be related to the bird droppings or candles smoke, but considering that the interior of the church was burned during the civil war, it is more likely related to the deposition of ashes. Finally, the thermal stresses induced by the presence of cobalt and copper chromophores and spinel particles may be responsible for the large cracks formed filled with corrosion precipitates in the green and blue enamels (**Fig. 4.23D**). The opacity shown by the enamels should be associated to these precipitates.

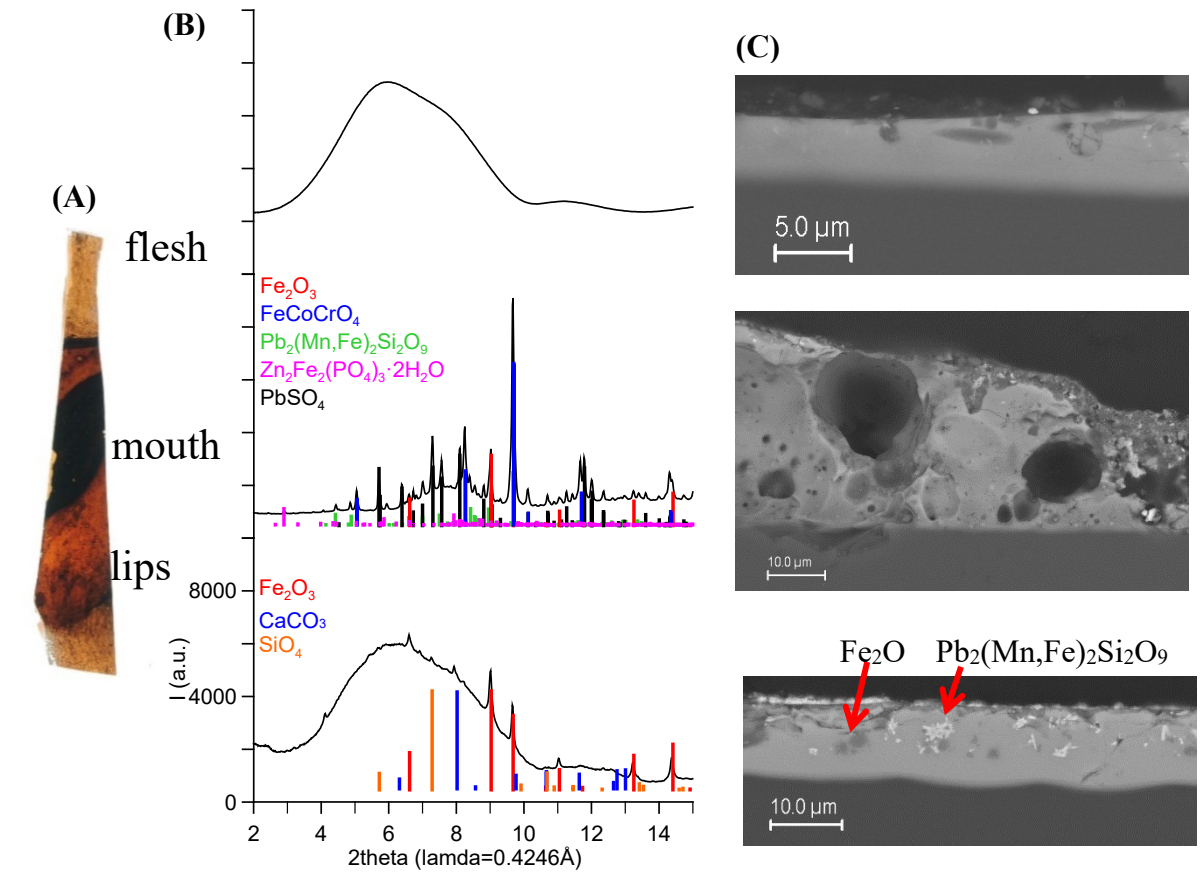

Fig. 4.24. (**A**) C1 sample corresponding the mouth of a panel from Sant Jaume de Calaf church. (**B**) microdiffraction patterns and (**C**) SEM-BSE images corresponding to the flesh, mouth and lips zone respectively.

The *carnation* and red enamel (C1) contain a high lead glass to which iron oxide (Fe_2O_3) particles were added (**Fig. 4.24**). The microdiffraction patterns and SEM-BSE images show

that the flesh enamel is completely amorphous, the lips appear also mainly amorphous but still some undissolved iron oxide particles are present. In fact, the *carnation* and red enamel composition is similar to the *grisaille*, iron oxide and lead glass but without manganese or copper added [8]. The dark colour of the inner part of the mouth is due to the addition of blue cobalt chromium spinel particles. The colour of the *flesh* (h_T* = 43º, L_T* = 0.7%) and lips (h_T* = 15º L_T* = 0.7%,) is red and carmine respectively and very opaque. The *flesh* and red enamels appear well preserved compared to the green and purple enamels and *grisaille* (**Fig. 4.23** and **4.24**).

4.2.5. Maumejean

A fragment of enamelled glass produced by the *Maumejean* workshop for the *Estació del Nord* (EN) has been studied. The original project of the building was developed on 1861 by P. Andrés i Puigdollers, but was during the reform projected by the architect Demetrio Ribes in the first decade of the 20th century when some stained-glass windows were ordered to the workshop. This set of windows was probably made between 1910 and 1915. They show a floral *coupe de fouet* style pattern and were originally placed in the waiting rooms. The fragment has an acid etched copper red plated glass with yellow and green enamels and black tracing grisaille. The train station was closed in 1972 and reopen in 1991 converted into a gym owned by the town hall. The former waiting rooms were transformed into restrooms. The piece appeared badly broken showing a large lacuna area and during a conservation campaign in 1991 a new copy was made. Nevertheless, the enamels appear very well preserved probably due to their location inside the building.

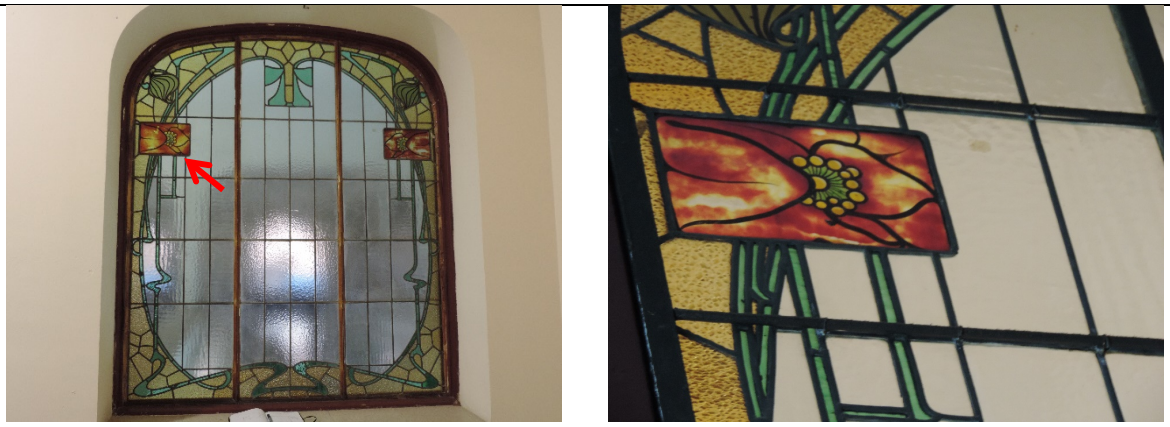

Fig 4.25. (Left) Images of the stained glass in Nord station by *Maumejean*. (Right) Detail of the stained glass where the sample studied belongs. Pict.: J.M. Bonet workshop.

- North station

The yellow and green enamels produced by the *Maumejan* workshop in Barcelona, and found in the *North station* are fully amorphous and show no chemical alteration as shown in **Table 4.3** and **Fig. 4.26**. The *grisaille* is applied on the opposite side of the substrate glass, and appears also mainly unaltered. Both enamels are made of a high lead zinc borosilicate glass with a composition not very different from the enamels replicated from the *Rigalt & Granell* workshop and studied in chapter 2. The yellow enamel shows the characteristic Cr^{6+} UV absorption band and the green enamel also the broad absorption band with a maximum at 800 nm related to Cu^{2+} (**Fig. 4.1**). The colour of the green (h_T* = 119º, L_T* = 25.2%) and of the yellow (h_T* = 91º L_T* = 21.3%,) is yellow-green and yellow respectively and very transparent (**Fig. 4.26**).

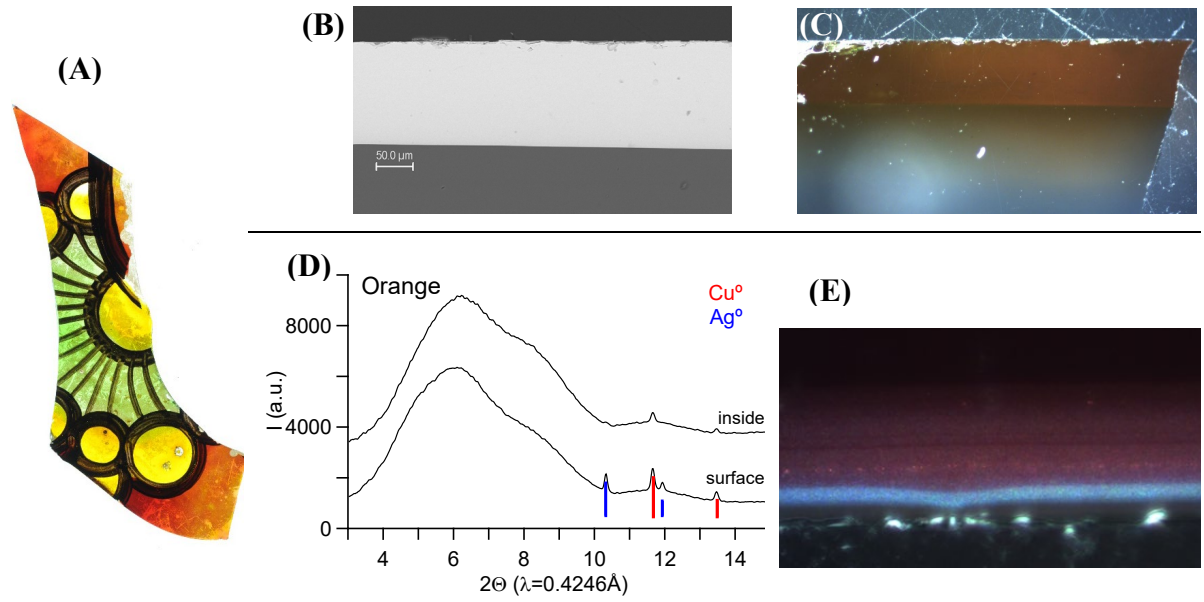

Fig. 4.26. (**A**) Fragment from *North Station* stained glass by *Maumejean*. (**B**) SEM-BSE and (**C**) OM image of the yellow enamel. (**D**) Microdiffraction pattern and (**E**) OM image of the red glass.

The red *plated* glass (EN1) is obtained by soaking the transparent blown glass bubble into a molten red glass before blowing; after cooling, a 25 µm thick layer of red glass stuck over the transparent glass substrate is obtained. The red glass is also of a soda-lime type, but has less lime (6.4% CaO) than the transparent substrate glass (12.4% CaO) (**Table 4.3**). It instead contains 2.2% SnO_2 and 1.1% Fe_2O_3, elements that are known to enhance the solubility of the metals and help their reduction to the metallic state [12]. The corresponding UV-Vis spectrum,

Fig. 4.2, shows an absorption peak at 434 nm related to metallic silver nanoparticles of a typical size of 40 nm [9,10] and a second absorption peak at 564 nm related to metallic copper nanoparticles [9]. A total of 1.0% Cu^o and 0.22% Ag^o is determined (**Table 4.4**). The combination of both metallic silver and copper nanoparticles gives a red colour shown by the glass (**Fig.2.26 D** and **E**). This red glass was removed using an acid prior to the application of the yellow and green enamels. The colour of the red plaque glass (h_T* = 40º, L_T* = 18.5%) is carmine and transparent. Surprisingly, the red glass has a low CaO content (6.4%), in contradiction with data indicating that high lime glasses are more easily acid attacked than low lime glasses and with the high lime content of acid etched historical glasses [13]

The good preservation state is mainly related to the fact that the enamelled glass was part of a panel which has always been indoors. Another aspect of relevance is the grisaille applied on the back side of the glass and opposite to the enamels layer. Nevertheless, the workshop was characterised by its solid technique although the stained glass studied is very modest.

Fig. 4.27. (Left) *Les Dames de Cerdanyola* by Dietrich. (Right) Fragmented piece of the original stained glass during the 2013 restoration (CRD) belongs. Pict.: J.M. Bonet workshop.

4.2.6. Ludwig Dietrich

We have analysed a small fragment of an orange stain/enamel on a transparent glass (CRD) from one of the window panels of the famous *Les Dames de Cerdanyola* (*Museu d'Art de Cerdanyola*, (1888-1910). The stained glass windows were made by *Ludwig Dietrich von*

Bearn (1860-1935), an Alsatian stained-glass maker established in Barcelona in 1900, and is one of the most important works of art of the Modernism. The sample was obtained during the 2013 restoration; the original piece was heavily fragmented.

- Les Dames de Cerdanyola

The chemical and microdiffraction analysis indicates that the layer is in fact a silver stain (**Fig 4.28B**). The colour is orange-red due to the presence of a broad distribution of silver nanoparticles, the UV-Vis spectra (**Fig. 4.4**) shows an extremely intense and broad peak with a tail extending to 600 nm, indicating the presence of particles of 60 to 70 nm [10]. Microdiffraction patterns (**Fig 4.28A**) shows some unusual bands for a silver stain related to the presence of AgCl particles. The production of silver stains [12] involves a silver compound, in this case AgCl dispersed in a medium which is applied over the glass surface. Silver is incorporated by ionic exchange and diffusion into the glass surface. Chlorine as Cl_2 is eliminated from the paint and is responsible for the bubbled appearance of the surface (**Fig 4.28C**). The paint was not removed after the firing accounting for the presence of silver chloride. The paint layer was not removed and silver chloride determined (**Fig 4.28A**). Silver nanoparticles growth are incorporated into the sodium depleted glass surface causing a compressive stress. As a consequence, the silver stained glass surface is less prone to corrosion.

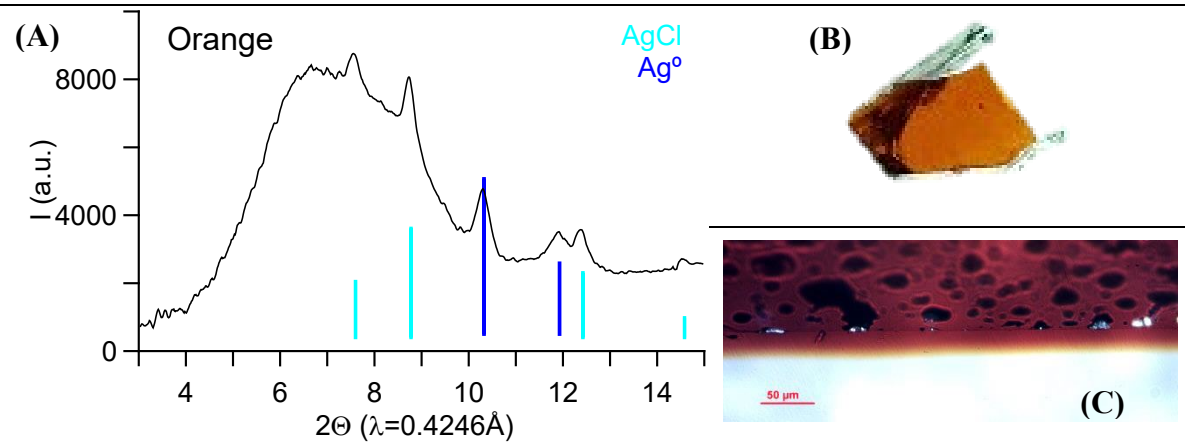

Fig. 4.28. (**A**) Microdiffraction pattern of a fragment from *Les Dames de Cerdanyola* stained glass by *Dietrich*. (B) CRD sample and (C) OM image of the orange stained surface.

4.2.7. Bazin & Latteux

Some pre-modernist stained glass fragments produced by the *Bazin & Latteux* atelier in 1876 for the *Acadèmia Mariana de Lleida* (AMLL) have also been analysed. The *Acadèmia Mariana* is an 1871 building designed by the architect Pere A. Peña upon the medieval foundation of a 13th century Mercedarian convent. During the last years of the 19th century it was remodelled twice. It owns some examples of stained glass produced by the *Bazin Latteux* workshop on 1876; the *Lux Mariae* scenes. Different fragments belonging to the Virgin Mary clothes in blue and brown enamel on the one side and grisaille and yellow stain on the other side.

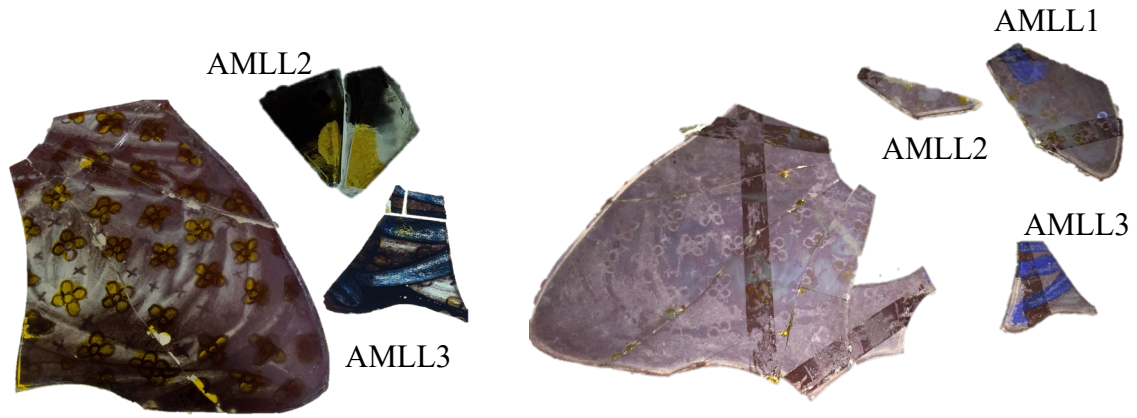

Fig. 4.29. Fragments of the stained glass made by the Bazin & Latteux atelier for the *Acadèmia Mariana de Lleida.*

- Acadèmia Mariana de Lleida

We have analysed two fragments, one from a drapery with blue and red enamels, contour and volume *grisailles* and yellow stain (AMLL3) and another from a yellow stain flower filling a *grisaille* contour (AMLL2), from *Academia Mariana* (Lleida) by the *Bazin-Latteux* workshop.

The substrate glass is of a soda lime type (**Table 4.2**). The chemical composition (**Table 4.3**) together with the μ-XRD patterns (**Fig. 4.30**) have revealed spinel phases of cobalt, zinc and aluminium (cobalt aluminate, $(Co,Zn)Al_2O_4$) (**Fig. 4.30A** and **4.30F**). The UV-Vis spectrum shows a series of absorption peaks between 500 nm and 700 nm and between 1200 nm and 1700 nm on the near infrared zone, corresponding to tetrahedral cobalt II. The red enamel and *grisaille* contain hematite (Fe_2O_3). The blue enamel is applied in some areas over the iron oxide particles, which makes the blue enamel very opaque (L_T* = 6.2%), the colour is a cobalt blue

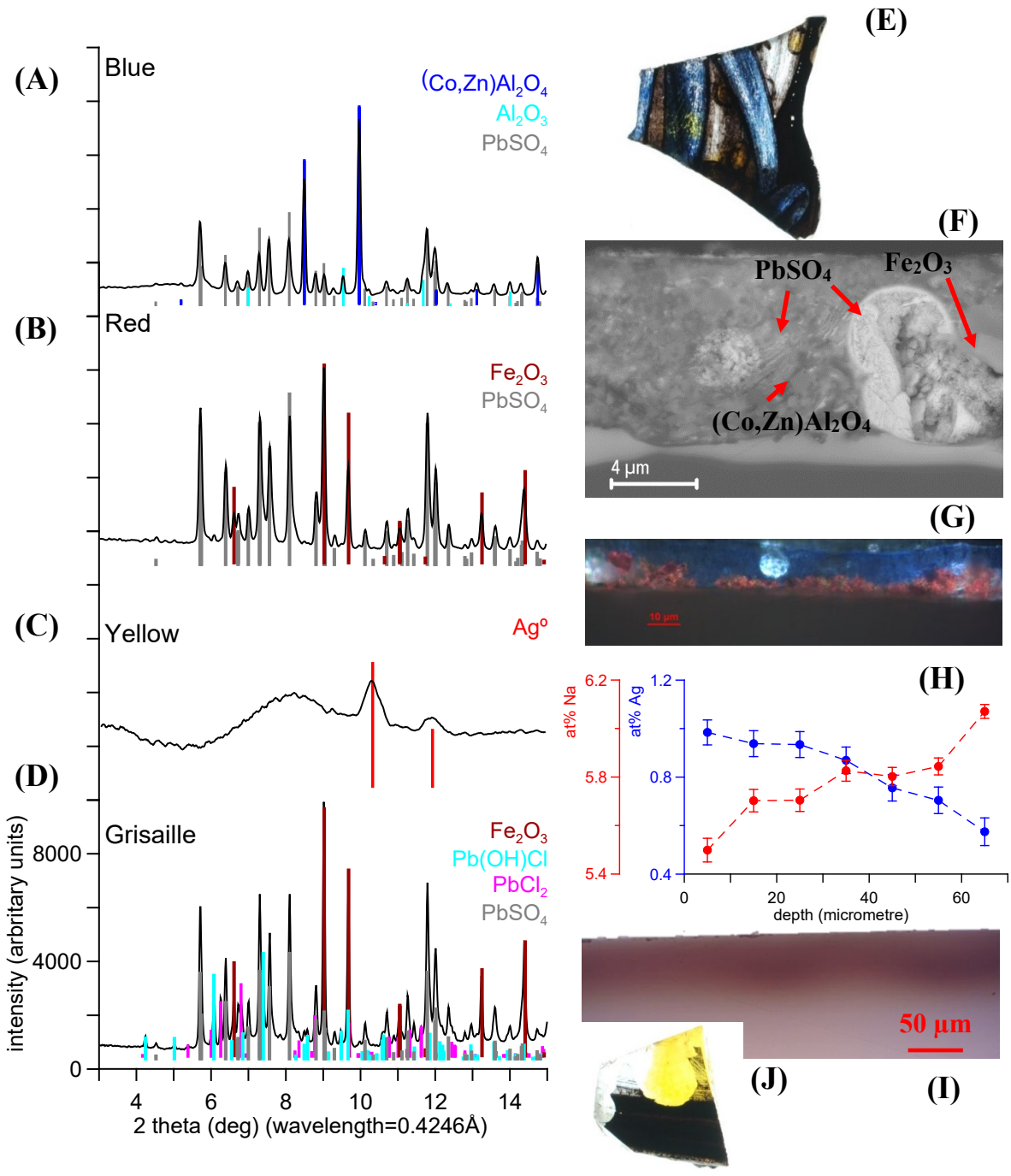

Fig. 4.30. (**A-D**) µ-XRD patterns from selected areas of the different colour enamels from the glass fragments from *Academia Mariana (Lleida)* by Bazin-Latteaux.

(**E**) Fragment AMLL3 showing the blue and red enamels, contour and volume grisailles and yellow stain; (**F**) SEM-BSE and (**G**) OM images of a cross section of the blue enamel.

(**H**) sodium (red) and silver (blue) profile from a cross section of the yellow stain; (**I**) OM image of the cross section of the yellow stain; (**J**) Fragment AMLL2 showing the contour grisaille and yellow stain.

(h_R* = 272º). The yellow stain (AMLL2 in **Fig. 4.30J**) µ-XRD pattern shows the presence of silver nanoparticles, **Fig. 4.30C**; the layer is very thick, 50-100 µm, **Fig. 4.30I**. **Fig. 4.30H** demonstrates that the silver ions of the precursor mixture are exchanged by the sodium ions from the glass**.** The stain is deep yellow and very transparent (h_T* = 86º; L_T* = 33.8%). The observation of an area of the silver stain which was covered by the lead string, showed the silver paint used showed de presence of clay.

The chemical composition of the enamels is heavily affected due to corrosion. **Fig. 4.30F** shows how the enamel is lead depleted, and the presence of lead corrosion compounds filling the bubbles and precipitates around the pigment particles**.** Microdiffraction patterns show the presence of lead sulphate and hydroxy chloride.

4.2.8. Rigalt, Bulbena & cia

Finally, stained-glass fragment from the principal door of the building of the *Fundació Pla-Armengol*, Barcelona, dated from 1920 has also been analysed. The stained glass has a vegetal pattern drawn with *grisaille* and filled with blue, green and purple enamels and silver stain on a cathedral glass. Although the authorship of the stained glass is not known, the *Noucentist* style connects it probably to the *Bulbena* workshop. The stained-glass was on the exterior side of the door and shows a thick white corrosion layer over the enamels.

Fig 4.31. (Left) Door of the *Pla Armengol Foundatin* with a stained glass made by most probably by the *Rigalt & Bulbena* workshop. (Right) Detail of the stained glass. Pict.: J.M. Bonet workshop.

- Pla Armengol Foundation

The fragment analysed belongs to the *Ramon Pla Armengol Foundation* building in Barcelona. The enamels are mainly amorphous (with the exception of some areas of the blue enamel) and very thick, between 50 μm and 150 μm, compared to the Modernist enamels, with the exception of the enamels from *Maumejan*. They are of also of a lead zinc borosilicate type.

The chemical analysis and microdiffraction pattern (**Table 4.3** and **Fig. 4.32**) of the blue enamel shows in some areas the presence of large cobalt aluminate ($CoAl_2O_4$) particles. However, they are not very homogeneous and in some other areas, the enamel is also mainly amorphous and the blue particles are very small. The UV-Vis spectra show also the absorption peaks between 500 nm and 700 nm and between 1200 nm and 1700 nm on the NIR region, corresponding to cobalt II in tetrahedral coordination. The green enamels contain copper II dissolved in the glassy matrix (**Fig 4.32**), with a large and broad absorption peak at 800 nm (**Fig. 4.3**).

The purple enamel is of a *Purple of Cassius* type with gold-silver metallic nanoparticles. The orange stain is due to silver nanoparticles (**Fig. 4.33**). The *grisaille* shows iron copper oxide particles into a high lead glass.

The surface of the enamels appears heavily altered but they are very thick and inside they appear mainly unaltered and, in the overall, their chemical composition is also little affected by corrosion (**Table 4.3**). The corrosion products formed (**Fig. 4.32** and **4.33**) are mainly lead sulphates, chlorides and hydroxy chlorides while sodium and calcium sulphates appear also precipitated on the surface, most probably related to the use of inadequate cleaning products. In fact, those areas of the blue enamels showing large cobalt aluminate particles appear more corroded, the corrosion affecting mainly the cobalt aluminate particles. The grisaille which contains also larger particles shows cracks and bubbles filled with corrosion products. On the contrary those enamels which are more amorphous appear better preserved. The orange stains are not corroded.

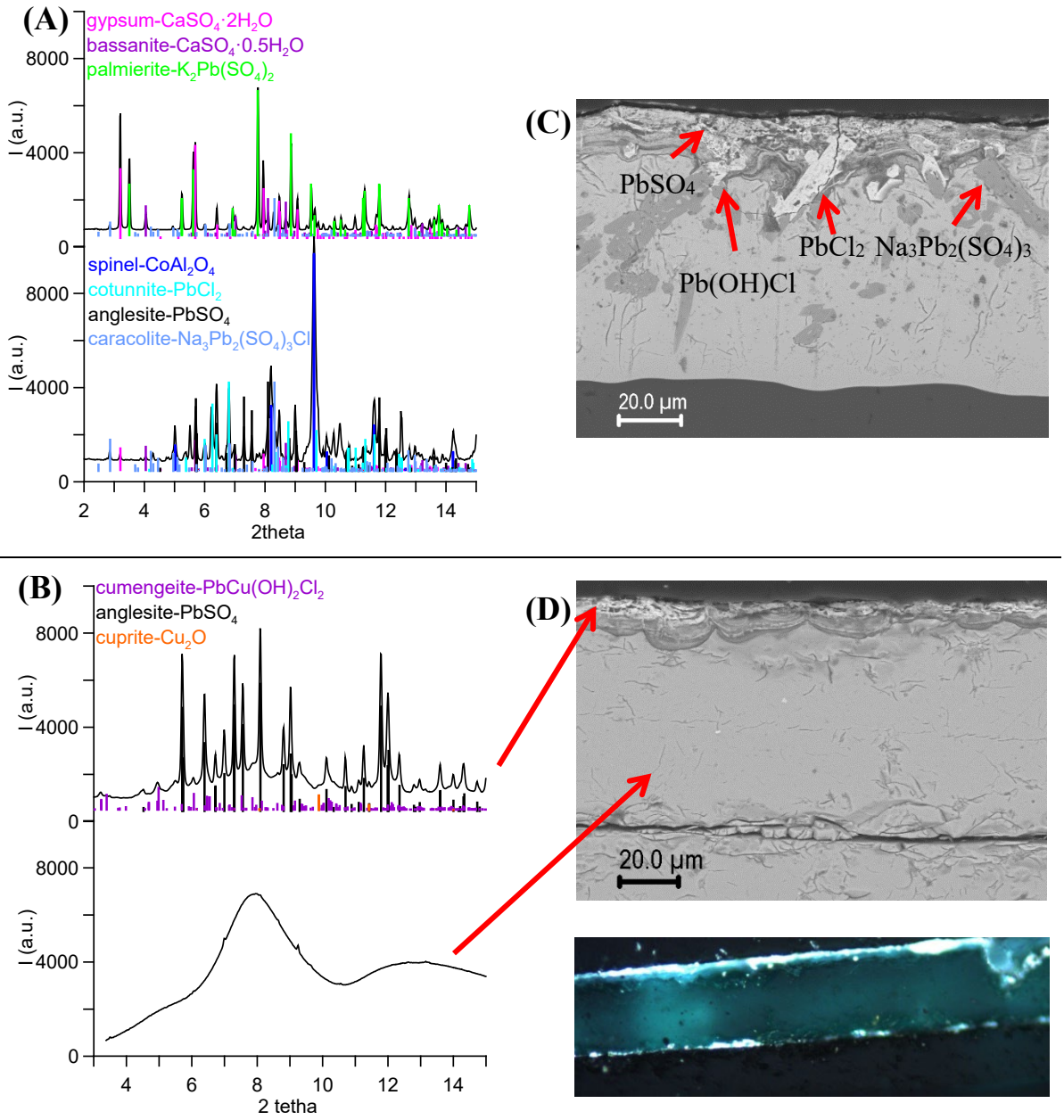

Fig. 4.32. (**A**) Microdiffraction patterns and (**C**) SEM-BSE images from a cross section of the blue enamel. (**B**) Microdiffraction pattern and (**D**) SEM-BSE and OM images from a cross section of the green enamel.

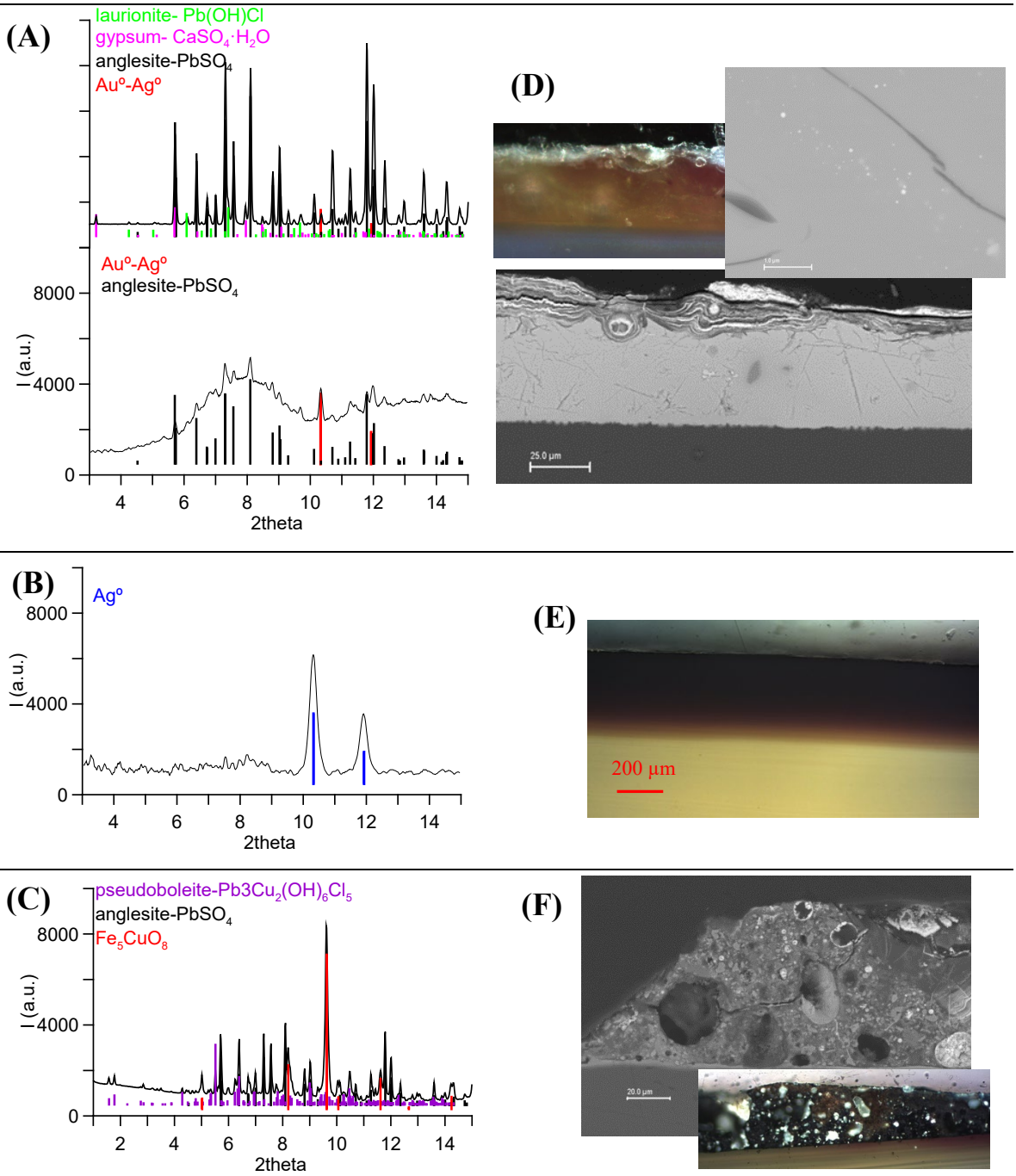

Fig 4.33. (**A**), (**B**) and (**C**) microdiffraction and (**D**), (**E**) and (**F**), SEM-EDS and OM images of the purple enamel, orange stain and grisaille respectively.

4.3. Discussion

Determining the original composition of the enamels has been found to be very difficult because of the poor state of preservation of most of them, but some observations can be made. The enamels that appear reasonably well preserved such as the green and yellow enamels from the *North station* (EN) by *Maumejan*, the blue, green and purple enamels by *Buxeras i*

Codorniu (BC) and the turquoise enamel from *Cama i Escurra* by *Bordalba* (PG) are all of a lead-zinc borosilicate type (**Table 4.3**). These findings are consistent with our results of the powder enamels study from the *Rigalt i Granell* workshop and shown in **chapter 2**. Removing the pigment particles and colourants added, most of the enamels preserved by *J.M. Bonet Vitralls S.L.* share the same composition of the glass compound, a lead-zinc borosilicate (in wt%, 57PbO+10SiO_2+19B_2O_3+14ZnO) with some variations (**Table 2.4**).

In order to verify the degree of alteration of the stained glasses, the fragments studied belonging to the *Rigalt i Granell* workshop are of vital importance as we can compare their composition and microstructure with those obtained from the materials from workshop. The two fragments studied which were produced by the *Rigalt i Granell* workshop, one from the *High Court Palace* (PJ), and one from the *Town hall of the Sants-Montjuic District* (SM) show very low amounts of B_2O_3, PbO and ZnO appear enriched in SiO_2, CaO and Na_2O (**Table 4.3**). Precipitates of lead and calcium sulphate or carbonate are formed within the cracks, bubbles (**Fig. 4.30F** and **Fig. 4.14D**), and they appear forming thick layers on the surface of the enamels only in those enamels showing great lead losses (**Fig. 4.19H**, **Fig. 4.23D** and **E**). Lead sulphate (anglesite, $PbSO_4$) and calcium sulphate dihydrate (gypsum, $CaSO_4 \cdot 2H_2O$) are found in PJ1, while basic lead carbonate (hydrocerussite, $Pb_3(CO_3)_2 \cdot (OH)_2$) and calcium carbonate (calcite, $CaCO_3$) are found in SM1. The difference between the crystalline precipitates between both is related rather to the atmosphere of the environment, the industrial pollutants in the former and a suburb district in the latter. Lead leaching from the enamel in presence of humidity and of atmospheric gases/pollutants (SO_2 and CO_2) results in the subsequent precipitation of lead and calcium sulphates and carbonates [14]. Consequently, the corrosion is humidity-dependent as water provides the medium for the dissolution of the glass and dissolution/deposition of atmospheric gases. Humidity is in any case the principal activator of the whole corrosion process, it is not necessary to have a very humid environment to initiate the process. Minor amounts of chlorine and traces of phosphorous were also detected by LA-ICP-MS. The presence of chlorine is related to the proximity to the sea shore and the presence of phosphorous to bird droppings.

Aqueous corrosion in soda and soda-lime borosilicate glasses is based in a glass dissolution-silica precipitation reaction which involves a complex process. The process is controlled by a diffusion-controlled ion exchange front, involving the inward diffusion of H^+ (and K^+ and Ca^{2+}) coupled to an outward diffusion of Na^+ (and Ca^{2+}) and B. The surface altered layer formed is composed of a so called ‘hydrated glass’ depleted in alkaline elements and an amorphous layer

of porous, silica-rich material (often called 'gel'), and, in some cases, by precipitates of secondary insoluble phases [2-3]. In a lead glass, neutral and acidic media corrosion involves also an interdiffusion controlled lead leaching and silica dissolution and reprecipitation [4-5]. Boron is highly soluble while on the contrary, calcium and lead carbonates or sulphates are highly insoluble.

SO_2 enters the liquid phase by gaseous transport, while SO_4^{2-} enters from deposited atmospheric particles dissolved in rain water. Carbon dioxide is an abundant atmospheric gas, and dissolved in water produces carbonates and basic carbonates where more aggressive competing ions are not present. Nevertheless, organic acid vapours common in urban atmospheres and in rain water are also highly aggressive [14]. Atmospheric nitrate aerosol particles or NO_2 gases are likely to produce nitric acid in rain water, which although being highly aggressive are not expected to produce solid precipitates as both lead and calcium nitrates are highly soluble.

The kinetics of reaction of the glass surface have been determined in the literature for historical glasses [15] and in particular for potash-lime silicate [16], lead-potash silicate [16], soda and soda-lime borosilicate [2-3] and lead-silicate glasses [4-5] in laboratory corroding conditions. Leached depths for K^+ and Ca^{2+} vary between 1.1 and 1.2 μm for exposure times of up to six years, and syngenite ($K_2SO_4 \cdot CaSO_4 \cdot H_2O$) and gypsum ($CaSO_4 \cdot 2H_2O$) are formed in sheltered conditions [16]. Alkaline leaching and formation of lead carbonate precipitates was determined in lead-potash silicate enamels after 2 months of exposure. For lead-silicate glasses typical leached thicknesses of 1-2 μm [4-5] are found after only 162 h exposure although interdiffusion is expected to slow down the process in long term corrosion [3]. Considering the thickness of our enamels (10-50 μm) the corrosion layer might build up in a relatively short period (months to few years) after a continuous exposure. Dry and humid periods and temperature variations will determine the speed of degradation of the glass surface.

Taking this into account, the presence of detectable amounts of boron and zinc of the green and purple enamels from the *church of Calaf* (C) by the *Amigó* workshop, the purple enamel from *Burés house* by *Bordalba* (CB) and all the enamels from the *Ramon Armengol Foundation* (FARM) suggests that they may have also been of a lead-zinc borosilicate type.

In contrast, the blue enamel from *Academia Mariana* by the French workshop *Bazin-Latteux* (which does not belong to the Modernist Catalan workshops) contains too little B_2O_3 (0.05%) compared to the PbO (22.6%), which suggests the use of a high lead glass instead (**Table 4.3**).

The presence of zinc is in this case related to the blue pigment, a cobalt-zinc aluminate, and not to the glass compound.

With regard to the *grisailles*, *carnations* (C1) and some red (C1) and brown (BC3) enamels contain a high lead glass to which iron oxide and/or manganese oxide particles (and reaction compounds such as kentrolite) were added. Copper oxide has also been added to most of the contour *grisailles* to reduce the red hue of haematite. Generally speaking the contour *grisailles* contain more and larger particles and are applied thickly, whereas modelling *grisailles* contain small particles around which kentrolite crystallises. Zn is not identified in any of the *grisailles* by SEM-EDX suggesting that the lead-zinc borosilicate glass was not used in good agreement with the contour *grisaille* found in the *Rigalt i Granell* workshop. It cannot be discarded that some *flux* (high lead borosilicate glass) might have been added in small amounts to reduce the viscosity and reduce the softening temperature. If so, it must have been in small amounts, as the presence of large bubbles suggest a high viscosity melt. A higher firing temperature (~700ºC) is required for the high lead glass compared to the lead borosilicate used for the enamels (~600ºC) (**Table 3.4**). Contour *grisailles* are usually fired in a separated firing before the enamels and were therefore traditionally applied on the unpainted side of the glass. However, Catalan glazier masters preferred to apply them on the same side as the enamel to avoid any misfit between contour lines and colour filling, and sometimes *grisailles* are applied on both sides of the glass substrate. Modelling *grisaille*, on the other hand, that is applied over or mixed with a colour enamel modifies the chemistry of the enamel and both are fired together, probably to a temperature adequate for the *grisaille* and therefore, higher than that expected for the enamel. Enhanced reactivity and/or increased solubility of the pigment particles is expected (see **Fig. 4.19F**, **G** and **H** and **Fig. 15B**), becoming more amorphous.

Two types of painting techniques can be distinguished: a first type with simple designs limited by a thick contour *grisaille* (CRD, BC, PG, CB, EN, PJ and FARM), and transparent enamels, with none (CB, EN, PJ and FARM) or little modelling *grisaille* applied (BC, PG); the second type shows more complex designs often including human figures (AMLL, C and SM), they are more opaque with extensive modelling *grisaille* mixed with the enamels and even various colour enamels appear mixed (C). Interestingly, the first type of enamel tends to be better preserved than the second type, probably because mixing of *grisaille* and enamel and/or various colour enamels modifies the paint chemistry and may thus produce a material of reduced stability.

Accordingly, all the blue and green enamels and *grisailles* of the second painting technique appear heavily altered, see the enamels made by *Bazin-Latteaux* (**Fig. 4.30F**), *Amigó* (**Fig. 4.23D and E**) and *Rigalt i Granell* (**Fig. 4.7** and **Fig. 4.10**). The whole enamel appears lead depleted and shows the presence of large cracks and bubbles a filled with lead sulphate precipitates which may also form a thick layer on the surface. The green and blue enamels of the first type appear instead well preserved (BC, PG, EN and the green enamel of FARM) showing corrosion compounds only at the surface (**Fig. 4.19G** and **H** and **Fig. 4.18B**). Nevertheless, the ones containing pigment particles appear more altered than those that do not; in fact, the large pigment particles from the blue FARM enamel appear altered (**Fig. 4.32C**), while the corrosion in the green FARM enamel which is fully amorphous is limited to the surface (**Fig. 4.32D**). This is consistent with the data obtained in **chapter 2** indicating that the presence of pigment particles, in particular those *floating* near the surface (in particular cobalt spinel compounds) facilitate alterations. The enamels containing pigment particles with a lower density than the glassy matrix show a typical layered structure with the particles floating in a lead poorer glass over a lead rich enamel-substrate glassreaction layer. The leakage of lead seems to affect the stability of these enamels more drastically and rapidly advancing the surface flaking. This affects particularly to the blue and green enamels and *grisailles* and may explain why they are more prone to degradation with respect to other colour enamels. To this we had to add the greater absorption in the near infrared region of the blue cobalt colour centres (CoO_4) an effect which is more dramatic when the enamel contains cobalt aluminate particles. We have seen an enhanced NIR absorbance for Cu^{2+} which would affect the green enamels and also for Fe^{2+} and Mn^{2+}-Mn^{3+}. The differences in the thermal expansion coefficients between particles/enamel glass and between the enamel and the substrate glass are expected to give rise to the formation of cracks. In fact, some recent studies using Infrared Thermography have shown that dark enamels and *grisailles* show an increase of the temperature 40% higher than those of the transparent glass [17,18] and about 20% higher than other colour enamels.

All the purple enamels (**Fig. 4.19D**, **Fig. 4.14D, Fig. 4.23E** and **Fig. 4.7**) independent of whether they were kept indoors or not, appear heavily altered. They are lead depleted (**Fig. 4.19I**, **Fig. 4.14D** and **E**) and show cracks, bubbles (**Fig. 4.14D**, **Fig. 4.23E** and **Fig. 4.7**) and also corrosion compounds (**Fig. 4.19I**, **Fig. 4.14D**, **Fig. 4.23C** and **4.23E** and **Fig. 4.7**). The purple enamels contain a colloidal solution of coprecipitated gold or silver-gold and tin, some are particularly tin rich (5-9 %SnO_2). The reason why tin is added is because Sn^{2+} is a *metallophyllic* ion, a name suggested by Weyl [12]. Sn^{2+} is highly polarised which results in a

disproportioning of Sn^{2+} into Sn^{4+} + Sn^{o}, the metallic particles bind to the metallic side while Sn^{4+} binds to the glass. This is the reason why SnO_2 particles are not formed and the gold or silver-gold particles do not aggregate, resulting in a colloidal suspension of gold particles in a tin rich glass while the interface between the enamel and the substrate glass is gold and tin free. The leakage of lead and boron is limited to the tin-gold area (see for example, **Fig. 4.14D** and **E**) similarly to what happens with the blue and green enamels containing pigment particles.

The *carnations, flesh*, red and brown enamels appear well preserved while only the *grisailles* kept indoors appear reasonably well preserved (**Fig. 4.24**). This could be related to the fact that the *grisailles* contain larger particles while the *carnations* are more amorphous (**Fig. 4.24**).

Finally, the alteration of the enamels and *grisailles* has been related to what might be considered wrong practices: the use of a poorly cleaned base glass, accidental insufficient heat treatment (this is clearly the case of the *grisaille* from the cathedral of Palma de Mallorca, P1, by Amigó), inadequate mixing of compounds or the use of thick paint layers. The first would evidently decrease the adherence of the enamel to the substrate while the second may result in a more unstable enamel composition. In view of our data, the third point is not so obvious. The enamels from the north station (EN) by *Maumejan* were thickly applied, 50-150 μm thick, and, nonetheless appear uncorroded. The enamels belonging to the *Armengol Foundation* (FARM), with a typical thickness of 80-150 μm, all have a thick altered surface (**Fig. 4.32**) and, the blue particles of the enamel appear more extensively corroded (**Fig. 4.32A** and **4.32C**). Both are of the first painting type, the *Maumejan*'s enamels were kept indoors and they are fully amorphous while the *Armengol Foundation's* enamels belong to a humid north facing door and some contain large pigment particles. Hence, atmospheric corrosion (water, pollutants and solar irradiation) and the presence of pigment particles rather than the thickness of the layer are responsible for the alteration.

We can conclude that amorphous enamels are more stable than those containing pigment particles. In particular enamels where the pigment particles are *suspended* near the surface are less stable and more susceptible to weathering, humidity and pollution. But seems to affect also the purple enamels containing a colloidal solution of metallic gold nanoparticles. Blue and green enamels containing cobalt spinel particles are additionally severely affected by solar irradiation due to the high absorption of infrared light of the cobalt blue colour centres which results in thermal stresses in the enamels and the subsequent formation of cracks.

Modernist workshops such as *Amigó* and *Rigalt i Granell* that considered to be more unconventional, produce complex designs, the use of more opaque enamels with pigment particles, modelling *grisaille* and enamel mixtures, and the regular application of contour *grisailles* on both sides of the substrate glass, have indeed shown produce enamels with a reduced stability.

4.4. Conclusions

Our study has shown that the enamels produced by some of the most prestigious glazier workshops in Barcelona during the Catalan Modernist period consisted of a lead-zinc borosilicate glass mixed with a large variety of pigment particles and colourants. Brown and red enamels had a similar composition similar to carnations and modelling *grisailles*, namely a high lead glass with iron and manganese oxide particles and more vitrified than the contour *grisailles*. The contour *grisailles* also contained copper oxide, and displayed larger particles and bubbles.

The exposure to humidity, pollutant gases and solar irradiation is the main cause of corrosion of the painted surfaces. Nevertheless, our results show that the chemical composition and microstructure of the enamels are heavily altered independently of their colour and composition. However, some differences found in the microstructures may explain the reason why blue and green enamels may show flaking and losses more often than the other coloured enamels. The enamels containing pigment particles with a lower density than the glassy matrix show a typical layered structure with the particles floating in a lead poorer glass over a lead rich enamel-substrate glassreaction layer. This layered microstructure is found in the green and blue enamels that contain cobalt aluminate spinel pigment particles but also in purple enamels containing a colloidal suspension of gold nanoparticles, and is not found in any of the other enamels where the particles are denser, or contain transition metal ions dissolved in the glass. The leakage of lead will affect the stability of these enamels more drastically and rapidly advancing the surface flaking. Similarly, the contour *grisailles* containing large particles and bubbles are less stable than carnation and modelling *grisailles* which are more amorphous. Another source of instability is the greater absorption in the near infrared region of Fe^{2+}, Co^{2+} or Cu^{2+} ions but in particular those present in spinel particles. This enhanced absorbance will produce an increase in the overall temperature of the enamel and also a thermal mismatch between particles, enamel glass and base glass. The differences in the thermal expansion

coefficients between particles/enamel glass and between the enamel and the substrate glass are expected to give rise to the formation of cracks.

Modernist workshops such as *Amigó* and *Rigalt i Granell* that considered to be more unconventional, produce complex designs, the use of more opaque enamels with pigment particles, modelling *grisaille* and enamel mixtures, and the regular application of contour *grisailles* on both sides of the substrate glass, have indeed shown produce enamels with a reduced stability. The use of more opaque enamels must have been particularly important for the Modernist stain glass companies which were producing stained glass for buildings placed in Mediterranean areas characterised by the pronounced solar irradiation. The use of more opaque enamels, of painting both sides of the glass or treating the glass surfaces with acid to reduce the light entering the buildings is distinctive of the Catalan stain glass companies.

4.5. References

[1] B. Gratuze, J. Blet-Lemarquand, J.N. Barrandon, Mass Spectrometry with laser sampling: A new tool to characterize Archaeological materials, J. Radioanal. Nucl. Chem. 247 (2001) 645–656.

[2] T. Geisler, T.J. Nagel, M.R. Kilburn, A. Janssen, J.P. Icenhauer, R.O.C. Fonseca, M. Grange, A.A. Nemchin, The mechanism of borosilicate glass corrosion revisited, Geochim. Cosmochim. Acta 158 (2015) 112–129.

[3] C. Lenting, O. Plümper, M. Kilburn, P. Guagliardo, M. Klinkenberg, T. Geisler, Towards a unifying mechanistic model for silicate glass corrosion, NPJ Materials Degradation 2(1) 28 (2018).

[4] S. Wood, J.R. Blachere, Corrosion of Lead Glasses in Acid Media: I, Leaching Kinetics. J. Amer. Ceram. Soc. 61(7-8) (1978) 287–292.

[5] S. Wood, J.R. Blachere, Corrosion of Lead Glasses in Acid Media: II, Concentration profile measurements, J. Amer. Ceram. Soc. 61(7-8) (1978) 292–297.

[6] D. Dungworth, The value of Historic Window Glass, The Historic Environment, Vol. 2 No. 1, June, 2011, 21–48.

[7] J. Vila-grau, F. Rodon, Els vitrallers de la Barcelona Modernista, Edicions Polígrafa S.A., Barcelona, 1982, pp. 178-180.

[8] T. Pradell, S. Murcia, R. Ibáñez, G. Molina, C. Liu, J. Molera, A.J. Shortland, Materials, techniques and conservation of historic stained glass "grissailles", Int. J. App. Glass Sci., 7, 2016, 41-58.

[9] U. Kreibig, M. Vollmer. Optical properties of metal clusters. Springer, Berlin (1995)

[10] G. Molina, S. Murcia, J.Molera, C. Roldan, D. Crespo, T.Pradell, Color and dichroism of silver-stained glasses, J. Nanopart. Res. 15 (2013) 1932-1945.

[11] D. Mahl, J. Diendorf, S. Ristig, C. Greulich, Z.A. Li, M. Farle, M. Köller, M. Epple, Silver, gold, and alloyed silver–gold nanoparticles: characterization and comparative cell-biologic action, J. Nanopart. Res. 14 (2012) 1153-1155.

[12] W.A. Weyl, Coloured glasses, Society of Glass Technology, Sheffield (2016).

[13] L. Pilosi, S. Barack and M. Wypsky, Early acid-etching of stained glass. Le citrail et les traités du Moyen âge à nos purs. Actes du XXIIIe colloque international du Corpus Vitrearum, Torus 3-7 juillet 2006) ed. Karine Boulanger and Michel Hérold. (2006) 97-109.

[14] T.E. Graedel, Chemical mechanisms for the atmospheric corrosion of lead, J. Electrochem. Soc. 141(4) (1994) 922-927.

[15] J. Sterpenich, G. Libourel, Using stained glass windows to understand the durability of toxic waste matrices, Chem. Geol. 174 (2001) 181–193.

[16] M. Melcher, M. Schreiner, Evaluation procedure for leaching studies on naturally weathered potash-lime-silica glasses with medieval composition by scanning electron microscopy, J. Non-Crystall. Sol. 351(14-15) (2001) 1210–1225.

[17] T. Palomar, F. Agua, M. Gómez-Heras, Comparative assessment of stained-glass windows materials by infrared thermography, Int. J. Appl. Glass Sci. 9 (2018) 530–539.

[18] T. Palomar, M. Silva, M. Vilarigues, I. Pombo Cardoso and D. Giovannacci, Impact of solar radiation and environmental temperature on Art Nouveau glass windows, Herit. Sci. 7 (2019) 82

Chapter 5

Conclusions. Design of a conservation strategy

Chapter 5

Conclusions

Design of a conservation strategy

A collection of enamels, grisaille and silver stains used by one of the most important glazier companies of the *Modernist* period in Barcelona, *Rigalt & Granell & cia*, was studied. Using a selection of the original materials from *Rigalt & Granell & cia*, blue, green, yellow, purple and red enamels, a *grisaille* and silver stains were obtained and analysed to determine their chemical composition, glass component, pigment particles, colourants and microstructure. Glasses with a composition matching those of the glass component of the enamels and *grisaille* were produced. From them the firing temperatures adequate to fix the enamels to contemporary substrate glasses were determined. Finally, a collection of kept in-place stained glass fragments from the most important glazier companies from the *Modernist* period in Barcelona was analysed to determine their conservation state and identify the corrosion mechanisms. Among the collection of in-situ kept stained glass, the analysis of those belonging to *Rigalt, Granell & cia* was particularly relevant. The altered paints could be compared to the unaltered replicated paints obtained from the original materials of the workshop and consequently, their study has been crucial to determine the degree of alteration of the paints, as well as to identify the corrosion mechanisms. Finally, the reasons for the low stability shown by some enamels (blue and green) compared to others were revealed.

The ready-to-be-used enamels found in the *Rigalt & Granell & cia*, belong to different companies: *Lacroix*, *Wenger* and *l'Hospied*. They are made of a lead-zinc borosilicate glass with a composition between 2:3 and 2:1 B_2O_3:SiO_2 molar ratio and 30-40 mol% PbO which is characterised by a low firing temperature while maintaining a reasonable

stability against chemical corrosion, in particular water corrosion. The glass is mixed with a wide variety of colourants and pigment particles to obtain the different colours.

The *glass transition temperature* and *softening range* of the glass component of the enamels and *grisaille* and also of the most common substrate glasses used in the period were determined. The softening temperature of the enamels glass component varies between 583ºC and 617ºC for the different types identified. The *glass transition*, *deformation* and *softening temperature* of the soda-lime contemporary blown glass used as substrate glass are 575ºC, 613ºC and 744ºC, respectively, which leaves a relatively narrow firing temperature range for the enamels, ~ 600ºC.

A glassy compound, *flux*, which apparently was added to the enamels when necessary to reduce the firing temperature and improve their adherence to the substrate glass was also studied. The *flux* is a high lead borosilicate glass (in mol% $60PbO+20SiO_2+20B_2O_3$) with a low *softening temperature*, 477ºC, but with a composition outside the limits of lead borosilicate glass stability.

The composition of the substrate glasses varied along the period mainly due to the innovation in the production processes. Substrate glasses of different composition were used in the *Modernist* period. They might have had problems with specific enamels/substrate glass pairs and a *flux* might have been added to reduce the firing temperature. However, this practice made the enamels less stable, and although the enamel will soften at a lower temperature, the adherence to the glass substrate is not necessarily improved.

The *grisaille* glassy phase is a typical high lead glass with eutectic composition (40 mol% PbO) characterised by its high refractive index, low viscosity at the softening point and a large variation in viscosity with temperature. It also has a high *softening temperature* (686ºC) which would require a high firing temperature. This has already been related to the addition of boron in the *grisaille* formulation, maybe using the *flux*, and the reason why 19th and 20th century grisailles appear more amorphous than Medieval *grisailles*. However, adding boron to the lead rich glass is also known to result in some cases in a liquid phase separation (boron rich-lead rich) which may affect the stability of the *grisaille*.

Many enamels and *grisailles* contain transition metals (copper, manganese, cobalt, chromium) completely dissolved in the glass. In this case they act as fluxes and,

consequently, reduce the *glass transition temperature* and also the *softening range*. This will produce amorphous enamels/*grisailles* with a lower firing temperature, closer to the maximum firing temperature adequate for the substrate glasses.

A large variety of pigment particles and colourants were identified:

- The purple pigment is a tin rich suspension of small "drops" of gold or gold-silver nanoparticles (≈10 nm), commonly known as purple of Cassius.
- Different pigments/colourants have been identified in the red enamels, one contains cadmium selenium sulphide particles, a second contains basic lead chromate particles and a third which contains dissolved Mn^{3+} ions.
- Three of the yellow enamels contain Cr^{6+} ions and the fourth lead antimony-tin oxide particles with pyrochlore structure.
- Different pigments/colourants have been identified in the green enamels, one contains cochromite particles, a spinel of cobalt and chromium together with yellow lead antimony-tin oxide particles with a pyrochlore structure, the second contains Cu^{2+} ions and the third tetrahedrally linked Co^{2+} and chromium (Cr^{3+}) ions.
- All the blue enamels contain cobalt either as particles of cobalt aluminate with a spinel structure or as tetrahedrally linked Co^{2+} ions.
- The opacity of some of the enamels is increased adding SnO_2 particles.
- Different silver stain recipes produce different colours: light yellow, deep yellow, orange and red. Although increasing the firing temperature/time also changes the colour to redder hues. Moreover, different paint thickness also increases the amount of silver and copper exchanged and thus, modifies the colour. The different colours are due to the precipitation of silver nanoparticles of different sizes (varying from a few to some tens of nm). Copper is also present in some of the stains as Cu^{+} or Cu^{2+} dissolved in the glass. Only in one of the silver stains Cu_2O nanoparticles are formed.

The study showed that the presence of some pigment particles with a density lower than that of the enamel glass resulted in the formation of a layered microstructure, with a lead poorer surface layer containing pigment particles over a lead rich layer (~54 % PbO and negligible amounts of B_2O_3) near the substrate glass. This phenomenon was particularly pronounced in the blue and green enamels that contain cobalt and cobalt-chromium

aluminate spinel particles. Nevertheless, it also affects the purple enamels which show a cloudy gold-tin rich and lead poorer external layer.

The cobalt ions either present in the spinel blue pigment particles or as tetrahedrally linked Co^{2+} in the glass are responsible for an enhanced absorption in the red and in the Near Infrared regions. Other chromophores such as Cu^{2+}, Fe^{2+} and Mn^{3+}-Mn^{2+} also absorb in the NIR range. They are present in some green and purple enamels and also in the *grisailles*. This enhanced absorbance in the NIR range of particles and ions would be responsible for the increase in the overall temperature of the enamel submitted to solar irradiation, as well as for the thermal mismatch between pigment particles, enamel glass and substrate glass. Thermal stresses will cause the formation of cracks due to the mismatch in the thermal expansion coefficients, and a faster/greater deterioration of the enamels. Consequently, it could account for the specific enhanced corrosion shown by some blue and green enamels and some *grisailles*.

The study of the in-situ kept stained glasses, and in particular those produced by *Rigalt, Granell & cia* which could be compared to the unaltered materials, has revealed that the whole thickness of the enamels appears affected by atmospheric corrosion. The enamels show important lead, boron and zinc losses and the formation of a hydrated silica-rich fragile glass with a low chemical stability. Subsequently corrosion products, mainly of insoluble lead, sodium and calcium carbonates and sulphates, are formed in the cracks around the particles and inside the bubbles and forming layers on the surface in those more heavily corroded enamels, a white crust responsible for the low colour saturation and increased opacity of some of the enamels.

The analysis of the enamels produced by the most prestigious glazier workshops demonstrated that they were using enamels similar to those from *Rigalt, Granell & cia*, that is, a lead-zinc borosilicate glass mixed with a large variety of pigment particles and colourants. With the exception of some brown and red enamels which had a composition similar to the *grisaille*, namely a high lead glass with iron and manganese oxide particles, and which were produced following the same procedure, but which appeared more vitrified than the *grisaille*. The contour *grisailles* contained also copper oxide and displayed large particles and bubbles. This type of enamels was not used by *pre-Modernist* French *Bazin et Lateaux* company.

Exposure to humidity, pollutant gases and solar irradiation was found to be the main cause of corrosion of the painted surfaces. In particular the layered microstructure generated in some of the enamels appeared to be more prone to alteration. The enamels containing pigment particles concentrated near the surface (blue and green enamels containing cobalt spinel compounds and purple enamels containing a co-precipitate of gold and tin) appeared more corroded than enamels that were completely amorphous. Similarly, the contour *grisailles* containing large particles and bubbles were more affected the carnation and modelling *grisailles* which are more amorphous.

The combination of the layered microstructure and the high absorption in the NIR may be responsible for the enhanced alteration that has been widely described in relation to the blue and green enamels as well as in some *grisailles*. The natural corrosion expected to happen in all the enamels due to weathering conditions and cleaning (mainly water corrosion) is more substantial in the layered enamels, at the same time that solar irradiation increase the thermal induced damage. Consequently, in order to improve the conservation of the enamelled window glass, a protection from humidity and atmospheric gasses should also be accompanied by a filter of infrared light, of particular importance in Mediterranean climates.

Some practices followed by the glazier companies may also be responsible for the reduced stability of some of the paint layers:

- The addition of a lead-rich borosilicate *flux* to the enamels in order reduce the softening temperature modifies the composition of the enamels and consequently also their stability. Moreover, as the adherence to the substrate glass depends also on the glass transition temperature of the substrate glass, the corresponding decrease in the firing temperature does not guarantee an improvement of the adherence.
- The application of the enamels and *grisaille* on the same side of the substrate glass, and the mixture of *grisaille* and colour enamels to enhance the opacity reducing the effect of the intense solar radiation (which was desirable to reduce the transmission of light in buildings with Mediterranean climate) and to give some artistic effects, modifies the chemical composition of the glass component of the paints and might decrease the stability of the paints in particular to water corrosion. This practice is common in the Modernist local companies but was less

common in central Europe. In particular the stained glass fragment studied in this thesis and produced by the French company *Maumejean* established in Barcelona does not follow this practice. Nevertheless, some of the works from the *Maumejean* workshop in Barcelona (Glass windows from the "hall of lost steps" in the High court Palace from Barcelona among other[1]) may have also incorporated paints on the other side of the glasses.

- A low firing temperature has been determined to be the main cause of alteration in a heavily damaged *grisaille* by Amigó. Firing the paints to a low temperature or for a too short time is also a main reason for the low stability of some paints.
- The use of enamels containing large pigment particles rather than being completely amorphous appears to be another source of enhanced instability. The presence of pigment particles produces more opaque paints, reducing the light entering the buildings but also increasing the colour richness of the paints. This is a characteristic that was sought by most of the local companies.

It is important to notice that the International Conservation Guidelines[2] when describing the need of a protective glazing system are not specific enough concerning the protection against IR irradiation as they are on other risks (water condensation, etc):

"The installation of a protective glazing system is a crucial part of the preventive conservation of architectural stained glass, which is vulnerable to both mechanical and environmental damage. The principal aims of a protective glazing system are to relieve the stained glass of its function as a weather shield, to protect it against mechanical and atmospheric damage, and to prevent condensation on the surface of the stained glass. Every window installation is unique, and therefore the design of its protective glazing must take into account the particular preservation needs of the stained glass and its architectural setting, as well as the physical and aesthetic impact on the building"

Our study has shown the importance of incorporating a protection against IR, of outmost importance for painted stained glass submitted to intense solar radiation.

[1] Jordi Bonet's personal information
[2] http://www.cvma.ac.uk/CVConservationGuidelines2004.pdf

The concern raised regarding the decay shown by the modernist enamelled glass has led the path to a long-term study and to this thesis. The results obtained have unveiled relevant information on the causes of deterioration and laid a path for the future conservation of this cultural heritage. The success of this study underlines the importance of preserving the historical workshop materials, developing a strategic sampling of materials, keeping craftsmanship knowledge which, together with the strength of cross-field collaboration helped to improve the current state of knowledge.

Bibliography

Bibliography

L.W. Adlington, I.C. Freestone, J.J. Kunicki-Goldfinger, T. Ayers, H. Gilderdale Scott, A. Eavis, Regional patterns in medieval European glass composition as a provenancing tool, Journal of Archaeological Science 110 (2019) 1-13.

N. Attard-Montalto, A. Shortland, 17th century blue enamel on window glass from the cathedral of Christ Church, Oxford: Investigating its deterioration mechanism, J. Cult. Herit. 16 (2015) 365–371.

F.S. Barff, Silicates, silicides, glass and glass painting, J. Soc. of Arts. 20 (1034) (1872) 841-852.

K.C. Barley, Tests et observations à propos de l'usage du jaune d'argent in: Grisailles, jaune d'argent, sanguine, émail et peinture à froid. Dossier de la Comission Royale des monuments, sites et fouilles, 3, Forum pour la Conservation et la Restauration des Vitraux, 1996, 117–121.

F. Becherini, A. Bernardi, A. Daneo, F. Geotti-Bianchini, C. Nicola, M. Verita, Thermal stress as a possible cause of paintwork loss in medieval stained glasswindows, Stud. Conserv. 53 (4) (2008) 238–251.

M.P. Brungs, E.R. Cartney, Structure of sodium borosilicate glasses, Phys. Chem. Glasses 16 (1975) 48-52.

S. Cañellas, N. Gil Farré, La Fábrica de Vidrieras de los Amigó, Cuadernos del Vidrio, Escuela Superior del Vidrio, 2015, 42-60.

L.F. Day, Windows a book about stained and painted glass, ed. B.T. Batsford, Charles Scribner's Sons, New York, 1909.

Y. Devred, J.F. Luneau, Verriers et verrières en Picardie au dix-neuvième siècle, Le vitrail en Picardie et dans le nord de la France aux XIXe et Xxe siècles, Amiens, Encrage, 1995, 21-43.

D. Dungworth, The value of Historic Window Glass, The Historic Environment, Vol. 2 No. 1, June, 2011, 21–48.

F. Fauth, I. Peral, C. Popescu, M. Knapp, The new material science powder diffraction beamline at ALBA synchrotron, Powder Diffr. 28, 2013, 360–370.

J.M Fernández Navarro, El vidrio, CESIC, 2003.

M.L. Ferreira Nascimiento, Brief history of the flat glass patent – Sixty years of the float process, World Patent Information, 38, 2014, 50-56.

A. Flügel, Glass viscosity calculation based on a global statistical modelling approach. Europ. J. Glass Sci. Tech. A, 48(1) (2007) 13-30.

M. García-Martín, Vidrieres d'un gran jardí de vidres, Barcelona: Catalana de Gas y Electricidad, S.A., 1981.

M. García-Martín, J. Vila-Grau, F. Rodon, Contrallums, Vitralls de l'Eixample, Exposició del 20 d'abril al 31 de maig de 1983, Casa Elizalde, Valencia 302, Barcelona: Consell Municipal dels districtes IV i VI, 1983.

M. Garcia-Valles, H. S. Hafez, I. Cruz-Matías, E. Vergés, M. H. Aly, J. Nogués, D. Ayala, S. Martinez, Calculation of viscosity-temperature curves for glass obtained from four wastewater treatment plants in Egypt, J. Therm. Anal. Calorim. 111[1] (2013) 107-114.

H.C. Gearhart, Teophilus' On Diverse Arts: The Persona of the Artist and the Production of Art in the Twelfth Century, PhD thesis (University of Michigan), 2010.

T. Geisler, T.J. Nagel, M.R. Kilburn, A. Janssen, J.P. Icenhauer, R.O.C. Fonseca, M. Grange, A.A. Nemchin, The mechanism of borosilicate glass corrosion revisited, Geochim. Cosmochim. Acta 158 (2015) 112–129.

N. Gil Farré, El taller de vitralls modernista Rigalt, Granell & Cia. (1890-1931), PhD thesis (UB), 2013.

N. Gil Farré, La decoración con vidriera artística en el mueble domestico modernista catalán. Virtuosisme Modernista. Tècniques del moble. Associació per a l'Estudi del Moble i Museu del Disseny de Barcelona, 2019, 131-147.

A. Gilchrist, The tears wept by our windows: sever paint loss from stained glass windows of the Mid-Nineteenth Century, Vidimus, 64 (2012).

Grace's guide to British Industrial History. https://www.gracesguide.co.uk

T.E. Graedel, Chemical mechanisms for the atmospheric corrosion of lead, J. Electrochem. Soc. 141(4) (1994) 922-927.

B. Gratuze, J. Blet-Lemarquand, J.N. Barrandon, Mass Spectrometry with laser sampling: A new tool to characterize Archaeological materials, J. Radioanal. Nucl. Chem. 247 (2001) 645–656.

X. Guo, M. Potuzak, J.C. Mauro, D.C. Allan, T.J. Kiczenski, Y. Yue, "Unified approach for determining the enthalpic fictive temperature of glasses with arbitrary thermal history", J. Non-Cryst. Solids 357 (2011), 3230-3236.

M. Hujova, M. Vernerová, Influence of fining agents on glass melting: A Review, Part 1, Ceramics-Silikáty 61 (2), 2017, 119-126.

L. B. Hunt, The True Story of Purple of Cassius. The birth of gold-based glass and enamel colours, Gold Bulletin 9, 1976, 134-139.

I. B. Kacem, L. Gautron, D. Coillot, D. R. Neuville, Structure and properties of lead silicate glasses and melts, Chemical Geology, Volume 461, (2017), 104-114.

W. Kauzmann, The nature of the glassy state and the behaviour of liquids at low temperatures, Chem. Rev., 43[2], (1948) 219-256.

F. A. Kirkpatrick, George G. Roberts, Production Of Selenium Red Glass, Journal of the American Ceramic Society, Volume2, Issue11 (1919) 895-904.

S. Kohara, H. Ohno, M. Takata, T. Usuki, H. Morita, K. Suzuya, et al., Lead silicate glasses: Binary network-former glasses with large amounts of free volume, Phys. Rev. B. 82 (2010) 134209.

D.S. Kostick, The origin of the U.S. natural and synthetic soda ash industries, Proceedings of the First International Soda Ash Conference, Vol I, Laramie, Wyoming, 1998, 11-35.

C.M. Kramer, Thermal decomposition of $NaNO_3$ and KNO_3, Proceedings of the Electrochemical Society, PV 1981-9, 1981, 494-505.

U. Kreibig, M. Vollmer. Optical properties of metal clusters. Springer, Berlin (1995).

H. Kühn and M. Curran, Artists' Pigments: a handbook of their history and characteristics, vol. 1 (1986) 208–211.

A. Lacroix, Des couleurs vitrifiables et de leur employ pour la peinture sur porcelain, faience, vitraux, Chez A. Lacroix, Paris, 1872.

C. Lenting, O. Plümper, M. Kilburn, P. Guagliardo, M. Klinkenberg, T. Geisler, Towards a unifying mechanistic model for silicate glass corrosion, NPJ Materials Degradation 2(1) 28 (2018).

A.F. Lozano Cajamarca, Innovations des techniques verrières au XIXe siècle et leurs applications dans la realization de vitraux, PhD thesis, HDR, Université Pierre et Marie Curie, 2013.

A. Machado, Historical Stained Glass Painting Techniques. Technology and preservation, PhD, Universidade Nova de Lisboa, 2018.

A. Machado, M. Vilarigues, Blue enamel pigment-Chemical and morphological characterization of its corrosion process. Corros. Sci. 139 (2018) 235–242.

D. Mackay, El Modernisme: Identitat i modernitat, El Vitrall Modernista, Barcelona: Departament de Cultura de la Generalitat, 1984, 11-17.

D. Mahl, J. Diendorf, S. Ristig, C. Greulich, Z.A. Li, M. Farle, M. Köller, M. Epple, Silver, gold, and alloyed silver–gold nanoparticles: characterization and comparative cell-biologic action, J. Nanopart. Res. 14 (2012) 1153-1155.

B. Manauté, La manufacture de vitrail et mosaïque d'art Maumejean - Flambe! Illumine! Embrase!, ed. le festin, 2015.

J. Max Mühlig, Notes on the early development of the Foucault process. The development in Belgium, J. Soc. Glass Tech. 17 (1933) T145-T148.

O.V. Mazurin, Problems of compatibility of the values of glass transition temperatures published in the world literature, Glass Phys. Chem. 33[1], (2007), 22–36.

M. Melcher, M. Schreiner, Evaluation procedure for leaching studies on naturally weathered potash-lime-silica glasses with medieval composition by scanning electron microscopy, J. Non-Crystall. Sol. 351(14-15) (2001) 1210–1225.

G. Molina, S. Murcia, J. Molera, C. Roldan, D. Crespo, T. Pradell, Color and dichroism of silver-stained glasses, Journal of Nanoparticle Research, 15(9), 2013.

G. Molina, G.P. Odin, T. Pradell, A.J. Shortland, M.S. Tite, Production technology and replication of lead antimonate yellow glass from New Kingdom Egypt and the Roman Empire, J. Archaeol. Sci. 41 (2014) 171-184.

D. Möncke, G. Tricot, A. Winterstein-Beckmann, L. Wondraczek, E.I. Kamitsos, On the connectivity of borate tetrahedra in borate and borosilicate glasses, Phys. Chem. Glasses 56(5) (2015) 203-211.

Möncke D, Kamitsos EI, Palles D, Limbach R, Winterstein-Beckmann A, Honma T, et al., Transition and post-transition metal ions in borate glasses: Borate ligand speciation, cluster formation, and their effect on glass transition and mechanical properties, J. Chem. Phys. 2016, 145(12): 124501.

F. Montanari, P. Miselli, C. Leonelli, C. Boschetti, J. Henderson, P. Baraldi, Calibration and use of the Heating Microscope for indirect evaluation of the viscosity and meltability of Archaeological glasses, Int. J. App. Glass Sci. 5[2] (2014) 161–177.

M.W. Murphy, Y.M. Yiu, M.J. Ward, L. Liu, Y. Hu, J.A. Zapien, Y.K. Liu, T.K. Sham, Electronic structure and optical properties of CdSxSe1−x solid solution nanostructures from X-ray absorption near edge structure, X-ray excited optical luminescence, and density functional theory investigations, J. App. Phys. 116 (2014) 193709.

S. Muspratt, Chemistry: Theoretical, Practical and Analytical, Glasgow: Mackenzie, 1860.

M. Okawa, T. Sakurai, S. Mogi, T. Yokokawa, Optical spectroscopic study of lead silicate glasses doped heavily with iron oxide. Mater. Trans.-JIM 38 (1997) 220–225.

V. Otero, L. Carlyle, M. Vilarigues, M.J. Melo, Chrome yellow in nineteenth century art: historic reconstructions of an artists' pigment. RSC Adv., 2(5) (2012) 1798–1805.

T. Palomar, F. Agua, M. Gómez-Heras, Comparative assessment of stained-glass windows materials by infrared thermography, Int. J. Appl. Glass Sci. 9 (2018) 530–539.

T. Palomar, M. Silva, M. Vilarigues, I. Pombo Cardoso and D. Giovannacci, Impact of solar radiation and environmental temperature on Art Nouveau glass windows, Herit. Sci. 7 (2019) 82.

M.J. Pascual, A. Duran, M.O. Prado, A new method for determining fixed viscosity points of glasses, Europ. J. Glass Sci. Tech. B: Phys. Chem. of Glasses, 46[5] (2005) 512-520.

Petrovskaya TS. Properties of lead borosilicate glasses: The effect of the structure. Glass Ceram. 54(11–12) (1997) 347–350.

T. Pradell, S. Murcia, R. Ibáñez, G. Molina, C. Liu, J. Molera, A.J. Shortland, Materials, techniques and conservation of historic stained glass "grissailles", Int. J. App. Glass Sci., 7, 2016, 41-58.

T. Pradell, Lustre and nanostructures – Ancient technologies revisited, Nanoscience and Cultural Heritage, Springer – Atlantic Press, 2016, 3-39.

T. Pradell, J. Molera, Ceramic technology. How to characterise ceramic glazes, Archaeological and Anthropological Sciences, 2020 12:189.

L. Robinet, M. Spring, S. Pagès-Camagna, D. Vantelon, N. Trcera, Investigation of the Discoloration of Smalt Pigment in Historic Paintings by Micro-X-ray Absorption Spectroscopy at the Co K-Edge. Anal. Chem. 83(13) (2011) 5145-5152.

J. Rodríguez Guarnizo, D. Rodríguez Barrantes, Los procedimientos clásicos de fabricación de la sosa (Basic procedures of soda fabrication), Ensayos: Revista de la Facultad de Educación de Albacete, Nº. 14, 1999, 293-309.

O. Schalm, K. Janssens, and J. Caen, Characterization of the Main Causes of Deterioration of Grisaille Paint Layers in 19th Century Stained-Glass Windows by J.B. Capronnier, Spectrochimica Acta B, 58, 2003, 589–607.

O. Schalm, K. Janssens, H. Wouters, D. Caluwé, Composition of 12-18th century window glass in Belgium: Non-figurative windows in secular buildings and stained-glass windows in religious buildings, Spectrochimica Acta Part B 62 (2007) 663-668.

O. Schalm, V. Van der Linden, P. Frederickx, S Luyten, G. Van der Snickt, J. Caen, D. Schryvers, K. Janssens, E. Cornelis, D. Van Dyck and M. Schreiner, Enamels in stained glass Windows: Preparation, chemical composition, microstructure and causes of deterioration, Spectrochimica Acta B, 64, 2009, 812-820.

H. Scholze, Der Einfluss von Viskositat und Oberflachenspannung auf er-hitzungsmikroskopische Messungen an Glasern (Influence of viscosity and surface tension on Hot Stage Microscopy measurements on glasses). Ber. Dtsch. Keram. Ges. 39; (1962) 63-68.

A.J. Shortland, N. Rogers, and K. Eremin, Trace Element Discriminants between Egyptian and Mesopotamian Late Bronze Age glasses, J. Archaeol. Sci., 34, 2007, 781–789.

H.R. Sinning, F. Haessner, Determination of the glass transition temperature of metallic glasses by low frequency internal friction measurements, Journal Of Non-crystalline solids 93 (1987), 53-66.

J. Sterpenich, G. Libourel, Using stained glass windows to understand the durability of toxic waste matrices, Chem. Geol. 174 (2001) 181–193.

A. Thomas, Le Vitrail a l'Exposition Universelle (Stain glass in the Universal Exhibition), in: L'Art Décorative, París, 1900, 179 -187.

O. Vallcorba & J. Rius. d2Dplot: 2D X-ray diffraction data processing and analysis for through-the-substrate microdiffraction, J. Appl. Cryst. 2019, 52, 478-484.

G. Van der Snikt, O. Schalm, J. Caen, K. Janessens, M. Schreiner, Blue enamel on sixteenth and seventeenth-century window glass: deterioration, microstructure, composition and preparation, Stud. Conserv. 51(3) (2006) 212–222.

A. Velasco Gonzàlez, Lux Mariae: un conjunt de vitralls del taller Bazin-Latteaux a l'Acadèmia Mariana de Lleida, Taüll, 19, Secretariat interdiocesà per a la custodia i promoció de l'art sagrat a Catalunya, 2006, 10-12.

M. Verità, Composition, structure et mechanism de deterioration des grisailles in: Grisailles, jaune d'argent, sanguine, émail et peinture à froid, Dossier de la Comission Royale des monuments, sites et fouilles 3, Forum pour la Conservation et la Restauration des Vitraux, 1996, 61-68.

M. Verità, C. Nicola, G. Sommariva, The stained glass windows of the SainteChapelle in Paris: Investigations on the origin of the loss of the painted work, Annales du 16e congrès de l'AIHV, Association Internationale pour l'Histoiredu Verre (AIHV), Imperial College, London, 2003.

M. Verità, Modern and ancient glass: nature, composition and deterioration mechanisms, Scienze e Materiali del Patrimonio Culturale, 8, The Materials of Cultural Heritage in their environment, 2006, 119-132.

J. Vila-Grau, F. Rodon, Els vitrallers de la Barcelona modernista, Barcelona: Edicions Polígrafa, S.A., 1982.

M. Vilarigues, C. Machado, A. Machado, M. Costa, L.C. Alves, I.P. Cardoso, A. Ruivo, Grisailles: Reconstruction and characterization of historical recipes, Int. J. Appl. Glass Sci., 2020, 1-18.

O. Villain, G. Calas, L. Galoisy, L. Cormier, J.-L. Hazemann, XANES determination of chromium oxidation states in glasses: comparison with optical absorption spectroscopy, Journal of the American Ceramic Society, Wiley, 2007, 90 (11), 3578-3581.

W. Vogel, Glass chemistry, Springer Verlag, Berlin, 1992.

I.N.M. Wainwright, J.M. Taylor, R.D. Harley, Lead Antimonate Yellow, Artists Pigments: a handbook of their history and characteristics, vol. 1 (1986) 219–254.

P.W. Wang, L. Zhang, Structural role of lead in lead silicate glasses derived from XPS spectra. J. Non-Cryst. Solids. 194, (1996), 129-134.

web site of the International Centre for Diffraction Data, https://www.icdd.com/.

web site http://cie.co.at/.

F. Welz, Patent No. 417.676, Unites States, 1892.

W.A. Weyl, Coloured glasses, Society of Glass Technology, Sheffield, 2016.

S. Wood, J.R. Blachere, Corrosion of Lead Glasses in Acid Media: I, Leaching Kinetics. J. Amer. Ceram. Soc. 61(7-8) (1978) 287–292.

S. Wood, J.R. Blachere, Corrosion of Lead Glasses in Acid Media: II, Concentration profile measurements, J. Amer. Ceram. Soc. 61(7-8) (1978) 292–297.

J.M. Wu, H.L. Huang, Microwave properties of zinc, barium and lead borosilicate glasses, J. Non-Cryst. Solids 260 (1999) 116-124.

Z.Y. Yao, D. Möncke, E.I. Kamitsos, P. Houizot, F. Célarié, T. Rouxel, et al. Structure and mechanical properties of copper–lead and copper–zinc borate glasses. J. Non-Cryst. Solids. (2016) 55-68.

W. Zheng, J. Zou, Synthesis and characterization of blue TiO2/CoAl2O4 complex pigments with good colour and enhanced near-infrared reflectance properties, RSC Advances 5(107) (2015) 87932.